Metabolite profiling associated with productive recombinant CHO cell culture

A thesis submitted to the University of Manchester for the degree of Doctor of Philosophy in the Faculty of Science and Engineering

2016

Chompoonuth Porncharoennop

School of Chemical Engineering and Analytical Sciences

Table of Contents

Word count: 65,950

List of Figures

List of Tables

Abstract

Abstract for a PhD thesis submitted in September 2016 at the University of Manchester by Chompoonuth Porncharoennop titled “Metabolite profiling associated with productive recombinant CHO cell culture”

A positive correlation between the flux of TCA cycle and productivity of Chinese Hamster Ovary (CHO) cells has been reported. Earlier work in this laboratory revealed that supplementation with nutrients that enter the TCA cycle (combination of glucose (Glc), pyruvate (Py), aspartate (Asp), asparagine (Asn) and glutamate (Glu)) significantly increased maximum viable cell density and antibody production of recombinant CHO cells. Increased amounts of extracellular citrate was associated with feeding conditions. It was hypothesized that increased flux through the TCA cycle and related metabolism was linked to enhanced growth and/or productivity of CHO cells. Therefore, the aim of this thesis is to clarify these relationships to provide routes to improve the efficiency of CHO cells by nutrient supplementation and metabolic engineering.

The relationship between growth, antibody production and metabolite profiles of CHO-LB01 cells was examined in response to individual supplementation with Asn, Asp, Glu, Py and β-hydroxybutyrate (HB). Feeding HB significantly increased antibody titre while Asn feeding increased maximum cell density but led to earlier cell death. Both nutrients increased the amounts of TCA cycle intermediates and decreased the amounts of lactate, glycerol, sorbitol and amino acids. Moreover, oxygen consumption rate was increased in the presence of Asn or HB. This finding inferred that increased production of the TCA cycle intermediates in cells fed Asn or HB correlated with enhanced flux of the TCA cycle leading to enhanced oxidative metabolism. Combination of Asn or HB with Glc further improved cell growth, increased antibody titre and enhanced metabolic responses to feeds (TCA cycle intermediates). Based on these results, inhibition of sorbitol production using chemical reagent (EPBC) and siRNA designed against *Akr1b1* and overexpression of malate dehydrogenase II (MDH II) were undertaken in order to increased flow of carbon atoms to TCA cycle and/or increased flux in the TCA cycle, respectively. Inhibition of sorbitol production was achieved in the presence of EBPC but there was no improvement of cell culture performance and accumulation of TCA cycle intermediates remained the same. CHO cells transfected with exogenous *Mdh2* did not show improved cell culture performance. Whilst stable clones exhibited variable MDH II expression at protein level (and antibody titre), overexpression of exogenous MDH II could not be confirmed by Western blot. One CHO-MDH II clone showed greater antibody titre and exhibited similar metabolite profiling with cells fed Asn or HB. This contrasted to the majority of clones that were low producers. Comparison by RNA-Seq transcriptomic profiling of high- and low-producing CHO-MDH II clones showed that the majority of differentially expressed genes were genes related to cytoskeleton-related element and cell signaling pathways. Overall, these results confirmed the relationship between increased the amount of TCA cycle intermediates and increased antibody production. Increased amount of TCA cycle intermediates could result in increased the flow of TCA cycle lead to enhance energy and antibody production. In addition, this work represents the first study on addition of HB offers a simple effective strategy to increase antibody production.

Declaration

No portion of this work referred to in the thesis has been submitted in support of an application for another degree or qualification of this or any other university or other institute of learning.

Copyright statement

I. The author of this thesis (including any appendices and/or schedules to this thesis) owns certain copyright or related rights in it (the "Copyright") and she has given The University of Manchester certain rights to use such Copyright, including for administrative purposes.

ii. Copies of this thesis, either in full or in extracts and whether in hard or electronic copy, may be made only in accordance with the Copyright, Designs and Patents Act 1988 (as amended) and regulations issued under it or, where appropriate, in accordance with licensing agreements which the University has from time to time. This page must form part of any such copies made.

iii. The ownership of certain Copyright, patents, designs, trade marks and other intellectual property (the "Intellectual Property") and any reproductions of copyright works in the thesis, for example graphs and tables ("Reproductions"), which may be described in this thesis, may not be owned by the author and may be owned by third parties. Such Intellectual Property and Reproductions cannot and must not be made available for use without the prior written permission of the owner(s) of the relevant Intellectual Property and/or Reproductions.

iv. Further information on the conditions under which disclosure, publication and commercialisation of this thesis, the Copyright and any Intellectual Property and/or Reproductions described in it may take place is available in the University IP Policy (see http://documents.manchester.ac.uk/DocuInfo.aspx?DocID=487), in any relevant Thesis restriction declarations deposited in the University Library, The University Library's regulations (see http://www.manchester.ac.uk/library/aboutus/regulations) and in The University's policy on Presentation of Theses.

Acknowledgements

I would like to thank to my supervisor Professor Alan Dickson who gave me, a poor English language international student, a precious opportunity to study here and guide me to develop my knowledge and open my perspective in every steps of my Ph.D. Moreover, his motivation and patience during writing up period was invaluable to me.

I am thankful to past and present members of the Dickson lab for support and friendship. Their kindness makes me relieve from homesick and feel comfortable, in particular Hirra who always help and support me in everything and every time I want her help. I would like to acknowledge the help of Dr. Mark Elvin for help with GC-MS, the Genomic Technologies Facility for processing RNA-Seq and Dr. Leo Zeef for performing Bioinformatics analysis on my RNA-Seq data.

Thanks to all my Thai's friends in UK and Thailand who always keep contact and cheer me up.

Importantly, I would like to thank to my family who have always missed me and given me unconditional love and support throughout my Ph.D steps. Many thank to my husband, Sitthichai Ruchayosyothin who stay beside me in every moments of this route.

I would also like to acknowledge the Royal Thai Government for the funding of my Ph.D.

THANK YOU and THANK YOU again from my heart, KHOB KHUN Ka.

Abbreviations list

ADH - alanine dehydrogenase
Akr1b1 - aldose reductase
AR - aldose reductase
ARSs - aminoacyl-tRNA synthetases
Asn - asparagine
Asp - aspartate
ATP – adenosine triphosphate
B2m - β-2 microglobulin
bp - base pairs
Cdk - cyclin-dependent kinase
cDNA - complementary DNA
CHO - Chinese hamster ovary
Cs - citrate synthase
d.d. - double distilled
DHAP - dihydroxyacetone phosphate
DHFR - dihydrofolate reductase
DMSO - dimethyl sulfoxide
DNA - deoxyribonucleic acid
dNTP - deoxyribonucleotide triphosphate
DNase I - deoxyribonuclease I
EBPC - 2,5-Dihydro-4-hydroxy-5-oxo-1-(phenylmethyl)-1H-pyrrole-3-carboxylic acid ethyl ester (AR inhibitor)
ELISA - enzyme-linked immunosorbent assay
EPO - erythropoietin
ER - endoplasmic reticulum
Erk2 - extracellular regulated kinase 2 (MAP Kinase 2)
FDR - false discovery rate
G3PDH - glycerol-3-phosphate dehydrogenase
GC-MS - gas chromatography-mass spectrometry
gDNA - genomic DNA
GK - glycerokinase
Glc - glucose
Glu- glutamate
Glud1 - glutamate dehydrogenase 1
GS - glutamate synthetase
HB - β-hydroxybutyrate

IgG - Immunoglobulin G

IgH - IgG heavy chain

IgL - IgG light chain

IPA - ingenuity pathway analysis

αKG - α-ketoglutarate

LDH - lactase dehydrogenase

Ldha - lactase dehydrogenase a

LDH-A - lactase dehydrogenase A

mAb - monoclonal antibody

Mdh2 - malate dehydrogenase 2

MDH II - malate dehydrogenase 2

MFA - metabolic flux analysis

MOX - methoxyamine hydrochloride

MSX - methionine sulfoximine

Ogdh - 2-oxoglutarate dehydrogenase (α-ketoglutarate dehydrogenase)

PBS - phosphate buffer saline

PC - pyruvate carboxylase

PCR - polymerase chain reaction

PDH - pyruvate dehydrogenase

Pdha1 - pyruvate dehydrogenase alpha 1

PDHK - pyruvate dehydrogenase kinase

PI - propidium iodide

Py - pyruvate

qRT-PCR - quantitative real-time polymerase chain reaction

Rh123 - rhodamine 123

RNA - ribonucleic acid

SDS – sodium dodecylsulphate

siRNA - small interfering RNA

Slc25a11 - solute carrier family 25 member 11 (mitochondrial carrier oxoglutarate carrier)

Slc25a11 - solute carrier family 25 member 11 (aspartate/glutamate carrier, mitochondrial carrier, aralar)

TEMED - tetramethylethylenediamine

Ta - annealing temperature

TMB - tetramethylbenzidine

UPR - unfolded protein response

w/v - weight/volume

w/w - weight/weight

CHAPTER 1

Introduction

1.1 Biopharmaceuticals

In recent years, the number of biopharmaceuticals used for therapeutic applications has increased dramatically. The first biopharmaceutical was recombinant human insulin, Humulin™, produced in 1982 by using a bacterial expression system for treatment of diabetes mellitus. A wide range of biopharmaceuticals are available such as hormones, clotting factors, cytokines, growth factors and enzymes (Walsh, 2010). The rapid growth in the number of biopharmaceuticals is due to two reasons: a rapid increase in understanding of disease processes and the development of new technologies to produce biologically active molecules.

1.1.1 Growth of the biopharmaceuticals market

The total number of approved biopharmaceuticals marketed in the United States and/or Europe stands at 212 in 2014 (Walsh, 2014). During Jan 2010 until July 2014 in which 54 biopharmaceutical were approved, 17 were monoclonal antibodies (mAbs), 9 were hormones, 8 were blood-related proteins, 6 were enzymes, 4 were vaccines, fusion proteins and granulocyte-colony stimulating factors, 1 was interferon and one was a gene therapy-based product (Walsh, 2014). Based on these data, it can be seen that mAbs were the most booming biopharmaceuticals product during 2010-2014. Moreover, mAbs which reached about $63 billion sale, made up six of top ten product sales in 2013 (Walsh, 2014). Up until November 2014, approximately 47 mAbs have been sold in United States and Europe (Ecker et al., 2015).

The development of a biopharmaceutical is a time-consuming business. The average time from beginning of clinical study to the first approval was 8.3 years. In addition, it is a risky business because a positive result after clinical study is not guaranteed and products can be withdrawn due to safety or commercial reasons at any phase of the

process (Reichert, 2014). Up until 2014, 34 biopharmaceuticals products have been withdrawn from both the US and EU market (Walsh, 2014). However, success rate could be higher from accumulated knowledge and development of technologies in the future.

1.1.2 Monoclonal antibodies (mAb)

Antibodies, also called immunoglobulins (Ig), are glycoproteins produced by the immune system to detect harmful substances. Antibodies are grouped into five major isotypes: IgA, IgD, IgE, IgG, and IgM. IgG is the most abundant antibody comprising two identical heavy chains and two identical light chains connected by disulfide bond to form Y-shape (Figure 1.1). Each heavy chain and light chain has two regions, the constant region and the variable region. The constant region is identical in all antibodies of the same isotype. The variable regions of each heavy and light chain come close together to form the antigen binding site, referred to as the fragment antigen binding domain (Fab) while the fragment crystallizable (Fc) domain which is responsible for effector function is composed of two constant domains of heavy chains. Heavy chain and light chain mRNA are individually targeted to the endoplasmic recticulum (ER) membrane and their polypeptide chains are co-translationally translocated before the translation of their polypeptides is completed. Afterwards, antibody folding and assembly processes are initiated in the ER (Bergman and Kuehl, 1979).

mAb which is typically of IgG isotype is one type of antibody that is capable of attaching to a specific protein produced by cells. Each mAb recognizes a specific epitope of an antigen. Therefore, different mAbs have to be made to target several types of cancer, inflammatory diseases, infectious diseases and autoimmune diseases (Nishimiya, 2014). Nowadays, mAb is a powerful tool of human therapeutics and many mAbs are already available on the market as mentioned in Section 1.1.1. The clinical and

commercial success of mAbs has led to the need for large-scale production and development of mAb production process.

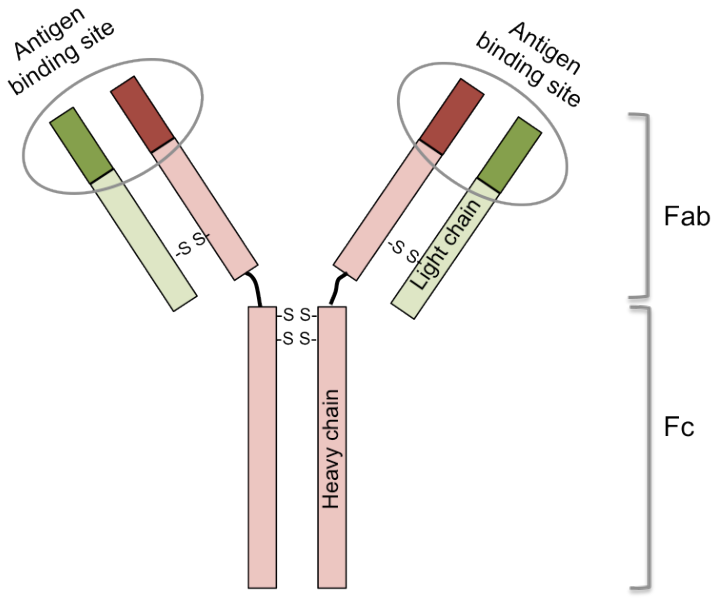

Figure 1.1 Antibody structure

An antibody structure is composed of heavy (red) and light (green) chains linked by disulfide bonds (-S-S). Variable regions are found at the amino terminal ends of the heavy (dark red) and light (dark green) chains, which form fragment antigen binding domain (Fab). The fragment crystallizable (Fc) domain which interacts with Fc receptors and with some proteins in the complement system allowing antibodies to activate the immune system is composed of two constant domains of heavy chains
(adapted from Steinmeyer and McCormick, 2008)

1.1.3 Platforms for biopharmaceutical production

Several host expression systems are used for the production of biopharmaceuticals including bacteria, yeast, plants and mammalian cells. There is no single system that is optimal for all products. For the production of biopharmaceuticals that will be used for human treatment, the most important concern is safety and a focus on the generation of products with consistent characteristics. The majority of therapeutic proteins have been produced in either mammalian cells (e.g.for mAb) or in *Escherichia coli* (*E. coli*) (e.g. for insulin) (Walsh, 2014).

Up until 2006, there are 18 monoclonal antibodies approved for therapeutic use. Ten are manufactured in Chinese hamster ovary (CHO) cell lines and 8 are made in murine lymphoid cells (including NS0 and Sp2/0-Ag 14) (Birch and Racher, 2006, Walsh, 2014). It can be seen that within mammalian expression platforms, CHO cell-based systems remain the most commonly used expression system. Other mammalian-based production cells include mouse myeloma cell lines NS0 and Sp2/0, mouse fibroblast cells, human embryonic kidney 293 cells, baby hamster kidney cells, and human retina-derived PerC6 cells (Datta et al., 2013).

CHO cells are valuable tools for production of recombinant proteins because they produce proteins with human-like glycosylation patterns. CHO cells are considered safe (as they do not propagate most human pathogenic viruses), allow easy transfer of foreign DNA into their genome and grow relatively quickly (doubling time around 14 to 22 hours) and robustly. Therefore, CHO cells have become the workhorse for industrial manufacture of biopharmaceuticals (Kim et al., 2012, Wurm and Hacker, 2011, Xu et al., 2011). All biopharmaceutical products produced in CHO cells until 2012 are showed in Table 1.1 (Datta et al., 2013). It has been estimated that CHO cells produce over 70% of the therapeutic proteins in a global market valued at US $30 billion in annual sales (Datta et al., 2013, Walsh, 2010, Jayapal et al., 2007).

Table 1.1 Biopharmaceutical products manufactured in CHO cells (Datta et al., 2013)

Tradename	Product category	Biological importance	FDA approval year
Zaltrap	Recombinant fusion protein	Colon cancer drug	2012
Eylea	Recombinant fusion protein	Wet (neovascular) age-related macular degeneration (AMD)	2011
Actemra	Antibodies	Treatment of rheumatoid arthritis (RA)	2010
Prolia	Antibodies	Osteoporosis in post menstrual women	2010
Recothrom	Blood factors, anticoagulants	Coagulation Factor	2008
Arcalyst	Recombinant fusion protein	Cryopyrin-Associated Periodic Syndromes	2008
Xyntha	Blood factors, anticoagulants	Hemophilia A	2008
Herceptin	Antibodies	A single agent for treatment of HER2-overexpressing node-negative and node-positive breast cancer	2008
VectibixTM	Antibodies	Antineoplastic, metastatic colorectal cancer	2006
MYOZYME®	Enzymes	Enzyme Replacement Therapy, Pompe disease	2006
Orencia	Others	Treatment of adults with moderate to severe rheumatoid arthritis	2005
Naglazyme	Enzymes	Mucopolysaccharidosis VI	2005
Luveris	Hormones	Luteinizing hormone for treatment of infertility	2004
Avastin	Antibodies	Treatment of first-line metastatic colon or rectum cancer	2004
Aldurazyme	Enzymes	Mucopolysaccharidosis I	2003
Amevive	Immunosuppressive dimeric fusion protein	Chronic plaque psoriasis	2003
Advate	Blood factors, anticoagulants	Hemophilia A	2003
Xolair	Antibodies	Asthma treatment	2003
Raptiva	Antibodies	Treatment of plaque psoriasis	2003
Fabrazyme	Enzymes	Recombinant human alpha galactosidase A for treatment of Fabry disease	2003
Rebif	Interferons	Glycosylated interferon beta-1a for treatment of multiple sclerosis	2002
Humira	Antibodies	Human IgG1 monoclonal antibody	2002
Zevalin	Antibodies	Therapeutic radiopharmaceutical for treatment of non-Hodgkin's lymphoma	2002
Aranesp	EPO and colony-stimulating factors	2nd generation recombinant form of erythropoetin for treatment of anemia	2001
MabCampath	Antibodies	Treatment of chronic lymphocytic leukaemia	2001

Table 1.1 (Cont.) Biopharmaceutical products manufactured in CHO cells

Tradename	Product category	Biological importance	FDA approval year
Cathlo Activase	Blood factors, anticoagulants	Tissue-plasminogen activator (t-PA) for treatment of acute myocardial infarction	2001
Ovidrel		Recombinant human chorionic gonadotropin, r-hCG	2000
ReFacto	Blood factors, anticoagulants	Hemophilia A	2000
TNKase	Blood factors, anticoagulants	Tissue plasminogen activator for treatment of myocardial infarction	2000
Thyrogen	Hormones	Thyroid cancer	1998
Enbrel	Antibodies	A tumor necrosis factor antagonist	1998
Follistim	Hormones	Follicle stimulating hormone for treatment of infertility	1997
Benefix	Blood factors, anticoagulants	Hemophilia B	1997
Gonal-F	Hormones	Follicle stimulating hormone for treatment of anovulation and superovulation	1997
Rituxan	Antibodies	Treatment of patients suffering from B-cell non-Hodgkins lymphoma	1997
Avonex	Interferons	Glycosylated interferon beta-1 for treatment of multiple sclerosis	1996
Cerezyme	Enzymes	Beta-glucocerebrosidase	1994
Bioclate	Blood factors, anticoagulants	Hemophilia A	1993
Pulmozyme	rhDNase	Cystic fibrosis	1993
Recombinate	Blood factors, anticoagulants	Hemophilia A	1992
Procrit	EPO and colony-stimulating factors	Erythropoetin	1990
Epogen	EPO and colony-stimulating factors	Erythropoetin	1989
Activase	Blood factors, anticoagulants	Tissue-plasminogen activator (t-PA) for treatment of acute myocardial infarction	1987

1.2 CHO cell production platforms

1.2.1 History of CHO cells

The original CHO cell line was established in 1958 from the cultured ovarian cells of a female inbred Chinese Hamster (Tjio and Puck, 1958). The Chinese Hamster was chosen as a model cell line to study the genetic effects of different treatments because of its relatively small chromosome content (typically 22) compared with Human cells (46). In addition, CHO cells were attractive for the creation of recombinant cell lines for many reasons as mentioned in Section 1.1.3 (Tjio and Puck, 1958).

The mutation frequency of CHO cells has resulted in the generation of several lines of CHO cell lines used for the production of biopharmaceuticals. These include CHO-K1, CHO- DUKX (or DXB11) and CHO-DG44. The CHO-K1 was generated from the original CHO cell line by single cell cloning (Kao and Puck, 1968) after which chemical mutagenesis of CHO-K1 produced CHO-DXB11 with a deletion of one DHFR allele and an inactivating mutation in the second allele (Urlaub and Chasin, 1980). A few years later, CHO-DG44, in which both DHFR alleles were deleted, was produced from a different starting population of cells by ionizing radiation mutagenesis (Urlaub et al., 1983). CHO-S cell line was derived as a separate clone from the original CHO cell line (Ahn and Antoniewicz, 2011, Danna et al., 1997) (Figure 1.2).

In order to have a detailed understanding of, and to open routes for improvement of, the properties of CHO cells, genomic sequencing of CHO cells has been conducted with the initial genome sequencing of CHO-K1 cells (Xu et al., 2011). The CHO-K1 genome size was estimated to be 2.6 Gb. The final gene set comprises 24,383 predicted genes, 29,291 transcripts and 416 non- coding RNAs. Many of predicted genes have homologs in human (19,711), mouse (20,612) and rat (21,229). It has been concluded that the

CHO-K1 genome is more similar to the rodent genomes than to the human genome (Hammond et al., 2011, Wlaschin et al., 2005, Xu et al., 2011). To access the genomic sequence data, the online resource for Chinese hamster genome database www.CHOgenome.org has been generated. In addition to genomic sequence, this website also provide bioinformatics tools for the CHO community (Hammond et al., 2012, Kremkow et al., 2015). Several studies have found genomic variation of CHO-K1, CHO-S and CHO-DG44 lineages and each cell line has a unique set of mutations. They also found that mutations rapidly accumulate during development of production cell lines (such as adaptation and clonal selection process) or during time in culture (Lewis et al., 2013, Wurm and Hacker, 2011, Derouazi et al., 2006, Worton et al., 1977). In addition to genomic diversification, change in DNA-methylation pattern also found in CHO cells during adaptation to different media and clonal selection process lead to change in phenotype (Feichtinger et al., 2016)

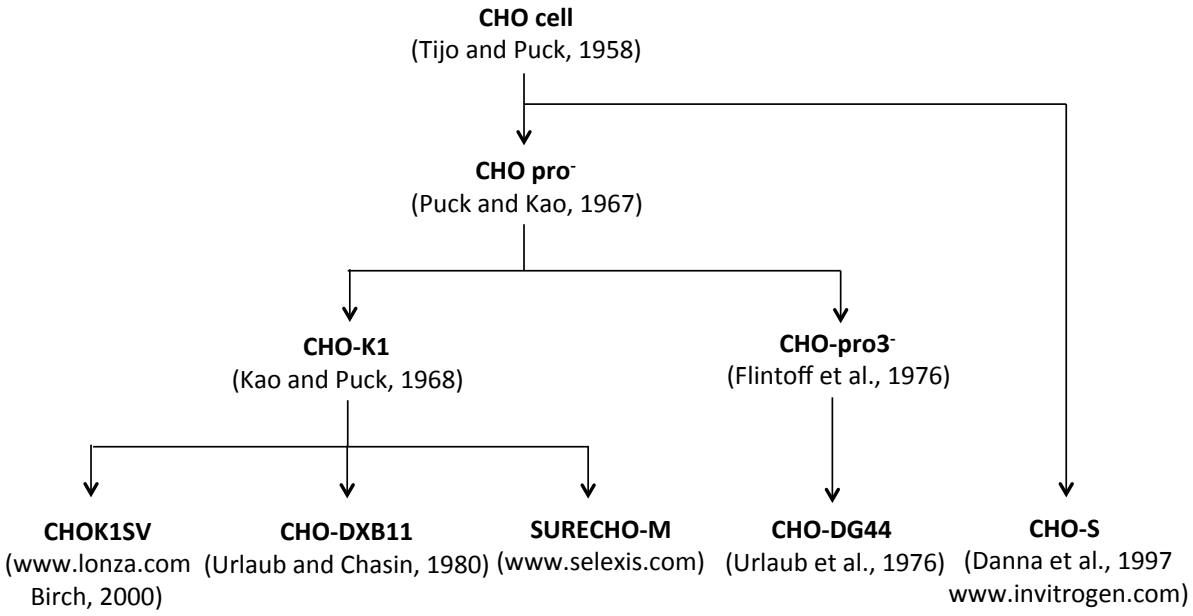

Figure 1.2 CHO cell lineages

The original CHO cell line isolated by Tijo and Puck (1958) was treated by single cell cloning and/or to generate a series of CHO cells with different phenotypes (Section 1.2.1).

1.2.2 Generation of recombinant CHO cell lines expression system

The expression vector systems most frequently used for the production of therapeutic monoclonal antibodies are the glutamine synthetase (GS) gene expression system and dihydrofolate reductase (DHFR) gene expression system (Birch and Racher, 2006).

1.2.2.1 The dihydrofolate reductase (DHFR) expression system

The DHFR system uses the *dhfr* gene as a selection and amplification system. DHFR enzyme is involved in nucleotide metabolism and catalyzes the conversion of dihydrofolate to tetrahydrofolate (Wurm, 2004). The expression vector normally contains a strong viral promoter, the target gene and dhfr selection gene. The transfected cells which have taken up the vector are selected by culture in medium lacking hypoxanthine and thymidine (H/T). Furthermore, this system promotes gene amplification in response to increasing concentrations of methotrexate (MTX), an inhibitor of DHFR enzyme (Figure 1.3). Transfected cells containing the dhfr gene have to increase their capacity for DHFR synthesis in order to survive (Butler, 2005, Wurm, 2004). This system requires around 6 months to achieve a high level of expression (Dorai and Moore, 1987). This system is routinely used with CHO cells deficient in the endogenous DHFR activity ($DHFR^-$) such as CHO-DXB11 and DG44 (Birch and Racher, 2006).

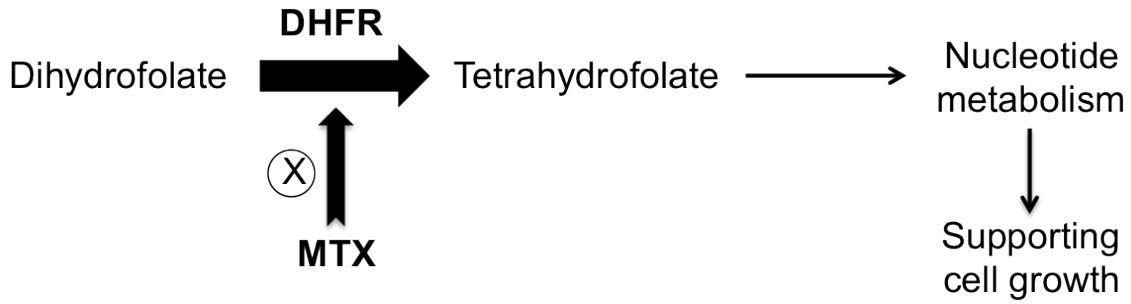

Figure 1.3 Dihydrofolate reductase amplification reaction

Dihydrofolate reductase (DHFR) catalyses the conversion of dihydrofolate into tetrahydrolate. The activity of DHFR is inhibited by methotrexate (MTX) allowing amplification of cells with a high copy number of DHFR and the associated gene of interest (Barnes et al., 2000).

1.2.2.2 The glutamine synthetase (GS) expression system

The GS system was developed by Celltech, and subsequently by Lonza Biologics. This system is based on the GS enzyme, which synthesizes glutamine from the condensation of glutamate and ammonia (Figure 1.4). In the absence of glutamine in the growth medium, the GS enzyme is essential for the survival of mammalian cells in culture. Therefore, in this system the transfected cells are selected in a glutamine-free media (Barnes et al., 2000). For CHO cells, that express sufficient GS to survive without exogenous glutamine, methionine sulfoximine (MSX, an inhibitor of glutamine synthetase) is added at the concentration of 10-100 mM (25 mM) to inhibit endogenous GS activity. Under such conditions only cell which have taken up transfected GS can survive (Butler, 2005). The advantage of this system is that high-producer clones can be achieved in around three months which is half the time that takes for the DHFR expression system (Bebbington et al., 1992). The common GS system uses are the CHO-K1 strain or a derivative of the CHO-K1, CHOK1SV (Birch and Racher, 2006). Recently, second generation of CHO GS system was created by several companies such as Horizon Discovery (GS null CHO K1 cell line), Sigma Aldrich (CHOZN GS$^{-/-}$)

and Lonza (GS Xceed™). In this system both alleles of the endogenous glutamine synthetase gene were knocked out, leading to a requirement for exogenous glutamine. They claimed that this system can generate cell lines faster than the original GS system.

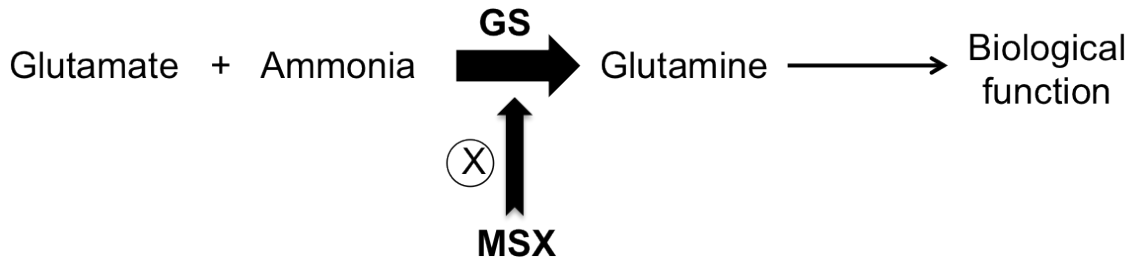

Figure 1.4 Glutamine synthetase amplification reaction
Glutamine synthetase (GS) catalyses the conversion of glutamate and ammonia to glutamine. In CHO cells methionine sulphoximine (MSX) inhibits GS activity lead to amplifying transfected cells with a high copy number of GS and the gene of interest (Adapted from Barnes et al., 2000).

1.2.3 Factors that impact recombinant protein productivity of CHO cells

Due to improvements in expression technology (Section 1.2.2), optimization of media composition and nutrient feeding (Section 1.5.1) and cell engineering technology (Section 1.5.2), recombinant product yields have improved dramatically in recent years with routine antibody yields exceeding 3 g/L (Birch and Racher, 2006, Gilbert et al., 2013, Wurm, 2004). However, further process enhancement is still necessary to decrease production costs, especially for “difficult to expression” products and novel non-antibody products (Johari et al., 2015, Pybus et al., 2014). There are many factors that influence the transgene expression in CHO cells. High productive cell lines result from using a host cell line that has the desired characteristics, an appropriate expression system and cell culture process (Birch and Racher, 2006).

1.2.3.1 Host cell lines

Each cell line has a unique intrinsic capability to function as a cell factory for recombinant protein production (O'Callaghan et al., 2010). Different rates of recombinant protein production may be associated with varying intrinsic functional capacity of transcription, translation, post translation or metabolism (Dinnis et al., 2006, O'Callaghan et al., 2010). In addition, phenotypic heterogeneity which is an inherent property of cell populations and can arise from a variety of factors, including culture conditions, *de novo* epigenetic or genetic changes during subculture can cause uncertain outcome (O'Callaghan et al., 2015). O' Callaghan et al. (2015) suggested that screening of parental populations to remove the large proportion of genetic variants that would never achieve high productivity might be one strategy to improve manufacturing platform. Several researchers have tried to apply 'omics' technology to identify marker transcripts or proteins that correlated with high productive cells (Section 1.4).

1.2.3.2 Expression systems

The expression titre of recombinant proteins is mainly determined by the expression system and the site of integration into the chromosome.

To achieve high levels of gene expression, GS and DHFR vectors usually have been used to drive expression of transgenes. Increased transcription of transgene was generally by gene amplification. Gene amplification is usually achieved by linking transgenes to an amplifiable gene (GS or DHFR, Section 1.2.2) (Birch and Racher, 2006). In addition, the vectors have also included favourable RNA processing signals such as polyA tail, 5' and 3' untranslated region, presence of an intron to encourage export from the nucleus and a splice site to remove this intron. Moreover, codon usage can be optimised for the target cell type to increase mRNA processing and improve

secretion. Furthermore, signal sequences can be added to target the polypeptides to the correct part of the secretory pathway (Birch and Racher, 2006).

The site of integration of the expression vector is a random event and has a major effect on the transcription rate of transgene (position effect) (Wurm, 2004). Integration of the expression vector in the heterochromatin may result in silencing or low level expression of the transgene. However, integration into the more transcriptionally active euchromatin still may not result in optimal transgene expression due to the influence of neighboring condensed chromatin (Wurm, 2004). Moreover, high expression of transgenes may be silenced by histone deacetylation or DNA methylation (Datta et al., 2013). To targeting transgenes into active region of the genome, one approach is to use site specific recombination of the transgenes by designing expression vectors containing a specific targeting sequence that will direct the vector to integrate by homologous recombination into a particular active site (Birch and Racher, 2006, Wurm, 2004). In addition, new mammalian gene expression technologies have been developed to improve protein expression such as Ubiquitous Chromatin Opening Element (UCOE®) (EMD Millipore Corporation) and scaffold/matrix attachment regions (S/MARs). UCOE® technology uses small DNA elements which isolated from around house-keeping genes to create a transcriptionally active open chromatin environment around an integrated transgene to prevents transgene silencing and gives stable and high-level transgene expression regardless of the chromosomal integration site (Betts and Dickson, 2015, Betts and Dickson, 2016). S/MARs are based on matrix-attachment sequences that enable chromatin near these sequences to be accessible to transcription factors. These sequences are flanked on expression vector to generate higher and more stable expression by minimizing gene silencing (Allen et al., 2000, Chang et al., 2014, Girod and Mermod, 2003).

1.2.3.3 Cell culture process

In addition to host cell lines and expression system, extrinsic factors such as media components, nutrient feeding and cell culture condition also influence cell growth and productivity of CHO cell (Datta et al., 2013).

Several media optimization and supplementation of nutrients have been performed in order to enhance cell growth and/or recombinant protein productivity of CHO cells based on an understanding of cells nutritional requirements. This understanding is often based on analysis of design of experiment (DOE) screening, nutrient depletion or metabolic profiling followed by supplementation of the relevant nutrients in the medium. The detail for media and nutrient optimization strategies in CHO cells will be described in Section 1.5.1. Besides media and feed, physical environment of cell culture (such as pH, dissolved oxygen concentration and temperature) is another factor that impacts on productivity of CHO cells. Therefore, these parameters must be controlled and carefully monitored in bioreactor to ensure adequate condition of CHO cell culture.

In summary**,** there are many factors that influence recombinant protein expression in CHO cells. One of the most important factors is the application of metabolism regulation which can modify the metabolic pathways and the overall cellular physiology to improve cell growth and the recombinant protein expression (Section 1.5.2.1). Metabolism of CHO cells will be described in next section.

1.3 Overview of metabolism of CHO cells

Generally CHO cellular metabolism is characterized by high rates of use glucose (when compared with insect and hybridoma cell) (Neermann and Wagner, 1996) and glutamine (when compared with other amino acids in CHO cells) (Templeton et al., 2013, Quek et

al., 2010, Ahn and Antoniewicz, 2011). This leads to high rates of production of lactate and ammonia as the major waste products of glucose and glutamine metabolism, respectively (Ahn and Antoniewicz, 2012, Boghigian et al., 2010, Xie and Wang, 1994, Zhang, 2009).

Glucose and glutamine are the major energy sources for CHO cell culture. Glucose is the most important nutrient for cell culture as both energy and carbon source. Glucose is utilized either through the pentose phosphate pathway to provide nucleotides and reducing power for biosynthesis or through the glycolysis pathway and the subsequent TCA cycle to provide metabolic intermediates and energy for the growth and survival of cell (Butler and Jenkins, 1989, Kurano et al., 1990). Glutamine can be utilized as a major source of energy and a biosynthetic precursor for cell growth that is required as a carbon source for the TCA cycle and as nitrogen source for the synthesis of purine, pyrimidine and amino acids (Zielke et al., 1984). The majority of glutamine was metabolized via glutaminolysis which is the conversion of glutamate to pyruvate via TCA cycle, malate-aspartate shuttle (MAS), and malic enzyme in CHO cells. As a result of utilization of glucose and glutamine, lactate and ammonia are excreted into the culture media as by-products.

Accumulation of lactate in cell culture media can cause changes to pH and osmolality leading to inhibitory effects on cell growth and productivity (Glacken et al., 1986). It has been reported that lactate concentrations lower than 20 mM do not affect cell growth or productivity but lactate concentrations of 20-40 mM have been stated to have a negative effect on productivity and above 40 mM lactate inhibits cell growth (Wagner, 1997). However, a shift from lactate production to consumption has been observed during culture for many kinds of CHO cells (Dean and Reddy, 2013, Ma et al., 2009).

In case of ammonia, the impact of its accumulation is stronger in cell culture than lactate (Reitzer et al., 1979). High ammonia concentration has been reported to dramatically decrease cell growth rate, limit maximum cell density, impair productivity (Hayter et al., 1991, Reitzer et al., 1979) and also have impact on protein glycosylation (Xu et al., 2014). Concentrations of ammonia above 5 mM are toxic for cells (Hayter et al., 1991). Toxicity of ammonia has been shown to depend on pH but the precise mechanism in cells is not clear (Schneider et al., 1996). In order to decrease the accumulation of lactate and ammonia, several approaches have been made as described in Section 1.5.

1.3.1 Metabolic pathway distinctions in exponential and stationary phases of CHO cell batch culture

From the comparison of nutrient uptake and product formation rates between exponential and stationary/decline phases of CHO cells, high rates of glucose consumption and lactate production are observed in exponential phase and when glucose was depleted cells entered a stationary phase (Ahn and Antoniewicz, 2011, Wilkens et al., 2011, Templeton et al., 2013) and lactate was consumed in order to replenish the flow of the TCA cycle (Altamirano et al., 2006a, Quek et al., 2010, Selvarasu et al., 2012, Sengupta et al., 2011, Wilkens et al., 2011, Martinez et al., 2013). Similar to lactate, alanine has been shown to accumulate during the exponential phase of cell culture and be consumed in stationary/decline phases (Li et al., 2012, Luo et al., 2012). The biphasic response may occur because, after the depletion of glucose, not enough pyruvate was produced to supply energy metabolism so lactate and alanine are used for pyruvate synthesis in order to maintain carbon precursor flow into the TCA cycle (Figure 1.5) (Li et al., 2012, Wilkens et al., 2011). In addition, when lactate was entirely depleted towards the end of the non-growth phase, ammonia production increased, which may propose a relationship between lactate depletion and increased amino acid catabolism (Li et al., 2012).

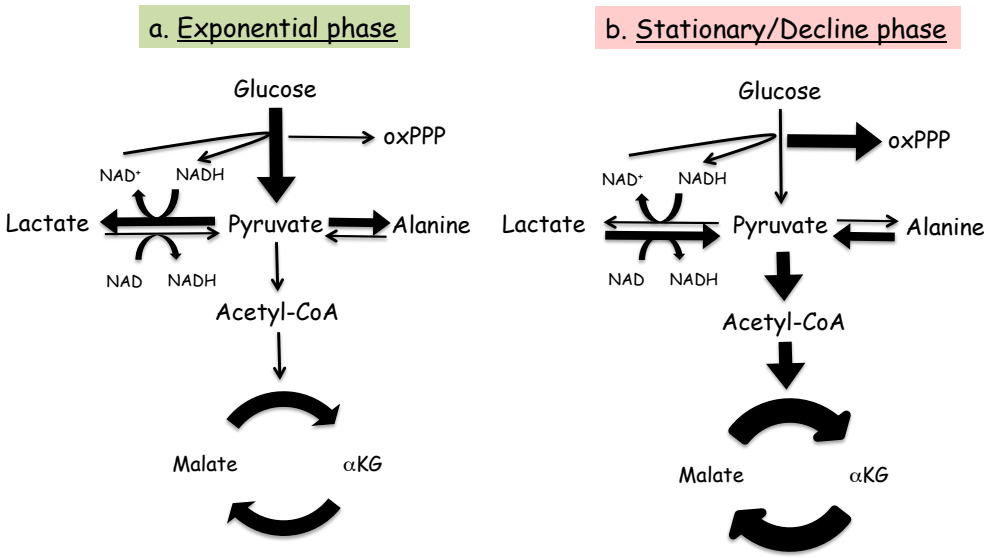

Figure 1.5 Comparison of the metabolic pathways trends in (a) exponential and (b) stationary/decline phases of CHO cell culture.

The size of arrows means the rate of the flux in metabolic pathway. This information is based on the papers of Ahn and Antoniewicz (2011), Camila et al. (2011), Sengupta et al., (2011) and Templeton et al., (2013). (oxPPP = oxidative pentose phosphate pathway, αKG = α-ketoglutarate)

In terms of metabolic flux analysis, defined by isotopic tracer, a difference of central metabolic flux has been observed between exponential and stationary phase (Figure 1.5). In exponential phase, high glycolysis flux, high lactate production, negligible flux of oxPPP and significant anapleurotic flux from glutamate to α-ketoglutarate (αKG) was found. In contrast, decreased flux of glycolysis, increased lactate consumption, significant oxPPP flux, and decreased rate of anapleurosis were observed in stationary phase (Ahn and Antoniewicz, 2011, Sengupta et al., 2011, Templeton et al., 2013). However, different conclusions were drawn in terms of the flux of the TCA cycle. Sengupta et al. (2011), Templeton et al. (2013) and Wilkens (2011) found that TCA cycle flux reached the peak at stationary phase. In addition, a correlation was observed between the fluxes of the TCA cycle and oxPPP. When TCA cycle flux was increased, oxPPP flux was also increased. Both fluxes increased during non-growth phase (Templeton et al., 2013). Increasing oxPPP flux during stationary phase could be an adaptive response to suppress oxidative stress that occurs from high mitochondrial

activity (Figure 1.5) (Sengupta et al., 2011, Templeton et al., 2013). On the other hand, Ahn and Antoniewicz (2011) found that the TCA flux in stationary phase was similar to the flux in the exponential phase because the labeling of metabolites in TCA cycle at both phases was similar of CHO-K1 in fed-batch culture over a period of six days.

1.3.2 The important of maintenance of redox state toward cell survival

NAD^+ and NADH are important for the regulation of pathways in the metabolism, acting as cofactors in glycolysis in the lactate/pyruvate conversion and other reactions (Wilkens et al., 2011). Additionally, recent studies have revealed that cellular signaling pathways (such as cell death and calcium homeostasis) are regulated by the intracellular redox state (Tait and Green, 2012, Ying, 2008). NADH is produced through glycolysis and other oxidative reactions. The total amount of, and balance between, NAD^+ and NADH is strongly regulated in the cells. Unbalanced NADH/NAD^+ ratio might be a cause of early cell death (Dawson, 1979, Ying, 2008). The levels of cytosolic NADH can be regulated by the lactase dehydrogenase (LDH) catalyzed pyruvate-lactate conversion and two mitochondrial shuttle systems, the malate-aspartate shuttle (MAS) (Section 1.3.2.1) and the glycerol-phosphate shuttle (GPS) (Section 1.3.2.2). When the activity of glycolysis is high, cells need to regenerate NAD^+ in order to maintain the redox state in the cytoplasm through the conversion of pyruvate to lactate by LDH (Wilkens et al., 2011). In case of lactate consumption generating more NADH, two mitochondrial shuttle systems are required to shuttle cytosolic NADH into mitochondria (Lovatt et al., 2007). In addition, increased flow of NADH from cytosol to mitochondria by these two mitochondrial shuttle systems was also found when the amount of NADH produced within the mitochondria is not sufficient to meet the demand (Nolan and Lee, 2011). Furthermore, since the TCA cycle and the electron transport chain require NAD^+ and NADH, respectively, an optimal NADH/NAD^+ ratio is needed for efficient mitochondrial metabolism (Stein and Imai, 2012).

1.3.2.1 Malate-aspartate shuttle (MAS)

The MAS system transfers NADH from the cytosol to the mitochondria mediated by two membrane carriers and two enzymes (Figure 1.6). In the cytosol, malate dehydrogenase (MDH I) catalyses the reaction of oxaloacetate and NADH to produce malate and NAD^+. Afterward, the malate-αKG antiporter imports malate from the cytosol into the mitochondrial matrix and exports αKG from the matrix into the cytosol. After malate reaches the mitochondrial matrix, it is converted by mitochondrial malate dehydrogenase (MDH II) into oxaloacetate generating NADH. Then, oxaloacetate is converted into aspartate by mitochondrial aspartate aminotransferase with conversion of glutamate into αKG. Next, the glutamate-aspartate antiporter imports glutamate from the cytosol into the matrix and exports aspartate from the matrix to the cytosol. Once in the cytosol, aspartate is converted by cytosolic aspartate aminotransferase to oxaloacetate and the cycle is restarted. The NAD in the cytosol can be reduced again by another round of glycolysis and the NADH in the matrix can be used for the electron transport chain. Since NADH is regenerated inside the mitochondrial matrix, 3 ATP molecules are formed for each cytosolic NADH by this system (Barron et al., 1998, Lanoue and Williams.Jr, 1971). In addition, key metabolite reactants of this shuttle (malate and oxaloacetate) also participate in reactions of the TCA cycle. Thus, it is possible that activation of this shuttle might alter the availability of these metabolites resulted in change the activity of the TCA cycle by extension and mitochondrial energy production (Barron et al., 1998).

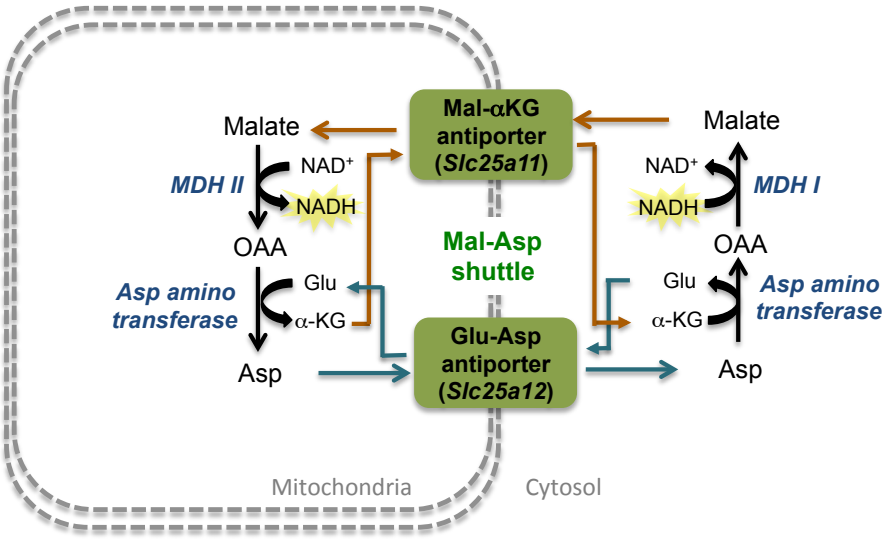

Figure 1.6 Malate-aspartate shuttle

MAS transfers NADH from the cytosol to the mitochondria mediated by two membrane carriers (Mal-αKG and Glu-Asp antiporter) and two enzymes (MDH and Asp aminotransferase) (Mal = malate, αKG = α-ketoglutarate, Glu = glutamate, Asp = aspartate, OAA = oxaloacetate, MDH I = cytoplasmic malate dehydrogenase, MDH II = mitochondrial malate dehydrogenase) (Berg et al., 2002).

1.3.2.2 Glycerol-phosphate shuttle (GPS)

NAD^+ can be produced from the conversion of dihydroxyacetone phosphate (glycolytic intermediate) to glycerol-3-phosphate by cytosolic glycerol-3-phosphate dehydrogenase (G3PDH) (Figure 1.7). Afterwards, glycerol-3-phosphate is converted back to dihydroxyacetone phosphate on the outer surface of the inner mitochondria by FAD dependent-mitochondrial G3PDH or is converted to glycerol by glycerol 3-phosphatase. When cytosolic NADH transported into mitochondria by this shuttle system, 2 ATP are formed per NADH. Therefore, GPS has a lower energy yield compared to MAS (Orr et al., 2014). Moreover, it has been reported that GPS activity is insufficient to compensate for an impaired MAS functioning or in conditions of high cytosolic NADH levels in vascular smooth muscle because increased $NADH/NAD^+$ ratio was still observed in

inhibition of MAS condition by amino-oxyacetic acid which is an inhibitor of aspartate aminotransferase (Barron et al., 1998).

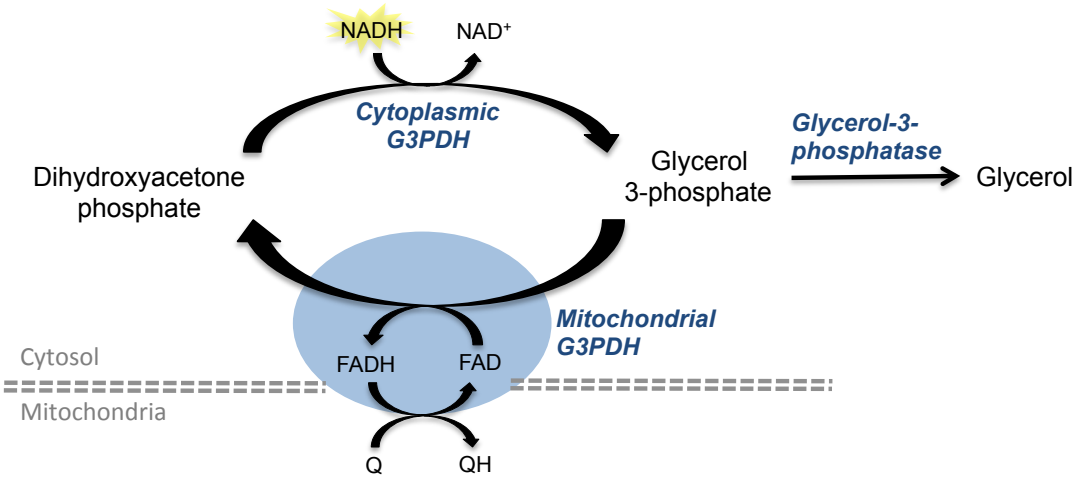

Figure 1.7 Glycerol-phosphate shuttle

GPS regenerates NAD+ from NADH by conversion of dihydroxyacetone phosphate to glycerol 3-phosphate via cytosolic G3PDH. In reverse path, glycerol 3-phosphate converted back to dihydroxyacetone phosphate by mitochondrial G3PDH coupled with reducing FAD to FADH (G3PDH = glycerol-3-phosphate dehydrogenase) (Berg et al., 2002).

1.3.3 The characterization of TCA cycle in CHO cells

CHO cells have been suggested to have a partially truncated TCA cycle (Figure 1.8) (Lu et al., 2003, Ma et al., 2009, Sellick et al., 2011, Sengupta et al., 2011) due to two main reasons. First, activities of enzymes that connect intermediates of glycolysis and the TCA cycle, phosphoenolpyruvate carboxykinase (PEPCK), pyruvate carboxylase (PC) and pyruvate dehydrogenase (PDH), have low activity in CHO cells because no activity of these enzymes could be detected by spectrophotometric assay (Neermann and Wagner, 1996). It has been concluded that most of the glucose carbons flow to lactate via lactate dehydrogenase (LDH) with low activity of PC hampering the flow of carbon into the TCA cycle (Neermann and Wagner, 1996). Secondly, the majority of citrate may

be preferentially exported to the cytoplasm for lipid formation (Coleman and Lavietes, 1981). This hypothesis correlates with the result by Ma et al. (2009) who found the accumulation of citrate outside mitochondria. Therefore, from a combination of two effects, it might be concluded that the TCA cycle is restricted at the point of citrate. As a result, the production of αKG from citrate has been shown to be limited (Coleman and Lavietes, 1981, Lu et al., 2003, Ma et al., 2009, Sellick et al., 2011, Sengupta et al., 2011). For maintenance of αKG to fulfill the cycle, αKG can be derived from glutamate or glutamine deamination through glutamate (Godia and Cairo, 2006, Zhang et al., 2006). Moreover, because of the high rate of glutamine consumption and the anapleurotic reaction of αKG incorporated into the cycle, the flux from αKG to malate is higher than the flux from citrate to αKG. As a result, the flux in each part of the TCA cycle in CHO cells is not equal (Lu et al., 2005, Godia and Cairo, 2006) (Figure 1.8).

1.3.4 The relationship between protein production and metabolism in CHO cells

Biosynthesis of protein is associated with a high energetic cost (Martinez et al., 2013). Recruitment and release of tRNAs and peptide bond formation require approximately 3-4 ATP per peptide bond (Klein et al., 2015). Schmidt (1999) reported that protein synthesis in animal cells consumed 20–25% of total cellular energy.

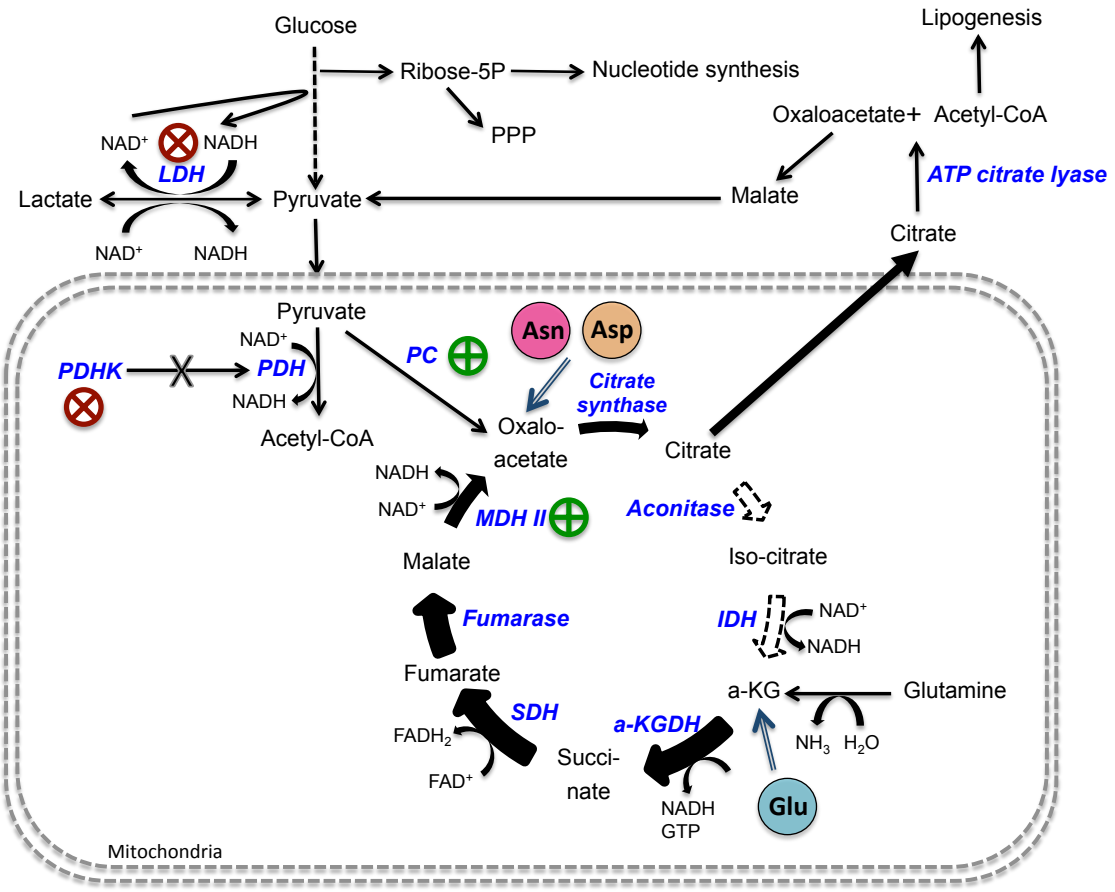

Figure 1.8 Overview of central metabolism of CHO cells.

CHO cells have a partially truncated TCA cycle at the point of citrate (dashed arrows) and the flux from αKG to malate (big arrows) is higher than the flux from citrate to αKG. Several enzymes in the metabolism were engineered by suppression (⊗) or overexpression (⊕) to improve the efficiency of CHO cell for recombinant protein production (Section 1.5.2.1). From nutrient feeding experiment (Section 1.5.1.2), the nutrients enter metabolic pathway via oxaloacetate (Asn and Asp) and αKG (Glu) that were shown in double line arrows (⇐). This information is based on the papers of Coleman and Lavietes (1981), Lu et al. (2003), Lu et al. (2005), Godia and Cairo (2006), Ma et al. (2009), Sellick et al. (2011), Sengupta et al. (2011). (LDH = lactate dehydrogenase, PDH = pyruvate dehydrogenase, PDHK = pyruvate dehydrogenase kinase, PC = pyruvate carboxylate and MDH II= malate dehydrogenase II, IDH = isocitrate dehydrogenase, α-KGDH = α-ketoglutarate dehydrogenase, SDH = succinate dehydrogenase, PPP = pentose phosphate pathway, Asn = asparagine, Asp = aspartate and Glu = glutamate)

As for the relationship between recombinant protein production and cell metabolism, conflicting views have been reported. Hayter et al. (1991) determined that the specific protein production rate was highest during the initial period of exponential growth of CHO-K1 cells in stirred batch culture. In contrast, Fussenegger et al. (1997) established a cytostatic production phase of CHO-K1 by overexpression of the tumor suppressor genes (p21, p27, or p53175P). Their results showed that recombinant protein production was greatest when the cells were switched to decreased proliferation. This might be because cellular resources can be diverted directly to protein synthesis without supply to biomass production. However, an ideal cell culture production process would combine rapid growth until the desired cell density was reached followed by a production phase with little or no proliferation (Fusseneger et al., 1997). Dean and Reddy (2013) found that the majority of protein production of high performer CHO cells (DHFR expression system) occurred during the last three days of the fed-batch culture when the growth was minimal. Templeton et al. (2013) found that antibody production of CHO cells (DHFR expression system) was minimal at early exponential phase but production rate increased during stationary phase when biomass production decreased. The cells transitioned from growth phase to protein production phase when lactate metabolism switched from production to consumption. In addition, increased antibody production at stationary phase was closely correlated with increased TCA cycle and oxPPP flux while a highly glycolytic metabolism state correlated with increased cell growth at exponential phase (Templeton et al., 2013)

Overall, in order to improve the productivity of CHO cells based on metabolic information, optimization of culture medium composition is a common approach undertaken by researchers (Section 1.5.1). In addition, the enzymes in TCA cycle and related enzymes that link between glycolysis and TCA cycle have been targeted for metabolic engineering to improve the metabolism of CHO cells as shown in Section 1.5.2.1.

1.4 Omics-based analysis of recombinant protein production in CHO cells

Omics technologies involve the measurement of large numbers of parameters at a particular functional level; gene (genomics), RNA (transcriptomics), protein (proteomics) and metabolites (metabolomics). Mammalian cells consist of 20,000-25,000 protein-coding genes and the number of transcripts are much larger (> 100,000) due to alternative splicing and transcription of noncoding sequences lead to generation of up to 1 million proteins. Almost 8000 metabolites have been compiled in the human metabolome database (HMDB, version 2.5, http://www.hmdb.ca/) but the number of metabolites present in individual cell lines is assumed to be much lower (Dietmair et al., 2012b, Lay et al., 2006).

Omics play an important role in CHO cell engineering by providing the cellular basis for high productivity and how individual mechanisms within a cell contribute to the overall phenotype. To successfully generate high productive cells, better understanding of these cellular systems is necessary (Datta et al., 2013, Dietmair et al., 2012b).

1.4.1 Transcriptomics

Transcriptomics is the study of the complete set of mRNA that is produced by the genome under specific physiological in a specific cell (Kildegaard et al., 2013, McGettigan, 2013). Comparison of transcriptomes allows the identification of genes that are differentially expressed in distinct cells or different conditions.

The powerful tools for transcriptome analysis have been DNA microarrays, quantitative real-time PCR (qRT- PCR) and RNA sequencing (RNA-seq) (Datta et al., 2013). In the past decade, DNA microarrays is the most frequently used analytical tools for transcriptomics. In recent years, with rapid advances in DNA sequencing technology

RNA-seq is replacing microarrays as the primary tool for gene expression studies (Liu et al., 2014, Vishwanathan et al., 2015). RNA-seq measures gene transcription by qualifying and quantitating tens of thousands of mRNA transcripts simultaneously at a high resolution and with a wide dynamic range, thereby overcoming limitations of fluorescence intensity-based expression arrays (Wang et al., 2009). Applying transcriptomic analysis to CHO cells has demonstrated the correlation of gene expression pattern with their performance during different condition as described below.

To gain a better understanding of apoptosis signaling, Wong et al. (2006) compared the transcript profiles of CHO cells producing IFN-γ at different time points in bioreactor studies using DNA microarray. During exponential phase where cells have high viability, most pro-apoptotic genes were down-regulated. In contrast, several early pro-apoptotic signaling genes were up-regulated when cells decreased viability and late pro-apoptotic effector genes (such as caspases and DNases) were upregulated in later stage of viability loss. These genes were selected as potential target to generate CHO cells resistant to apoptosis in the future.

Low temperature culture has been shown to enhance the specific productivity in CHO cells. Yee et al. (2009) investigated transcriptomics profiles of low temperature cultivation of hybridoma (MAK) cells and recombinant antibody-producing CHO cells using species-specific cDNA microarrays. At low temperature (33°C), increased productivity was observed in CHO cells but not in MAK cells. Additionally, downregulation of genes related to oxidative phosphorylation and ribosomal genes were observed only in MAK cells whilst genes related to protein trafficking genes and cytoskeleton elements were up-regulated only in CHO cells. This suggested that intracellular protein transport and cytoskeletal elements might contribute to increased specific productivity of CHO cells. Another strategy frequently used to increase the product titre is addition of sodium butyrate (NaBu) and application of hyperosmotic stress. Gatti et al. (2007) compared transcript profiles of CHO cells and mouse

hybridoma cells in response to NaBu using species-specific DNA microarrays. The results showed that butyrate treatment, for both CHO cells and mouse hydridoma cells, had an effect on genes related to histone modification, chaperones, lipid metabolism and protein processing. Shen et al. (2010) investigated the effect of hyperosmolarity on the mRNA profile of a CHO cell line producing an Fc-fusion-protein. Using proprietary CHO microarrays, it was found that genes related to metabolism, transcriptional regulation, transporters, and signaling pathway were involved in response to osmotic stress.

In order to eliminate the effect of environmental changes of an extrinsic modifier of specific productivity, many researchers have compared transcriptomics profile of high and low producer CHO cells which is an intrinsic property of cells using DNA microarray or RNA-Seq techniques. Conflicting results have been reported. Clarke et al. (2011), Doolan et al. (2008) and Harreither et al. (2015) found up-regulation of genes related to unfold protein response (UPR), protein processing in ER and golgi, vesicle-mediated transport and secretion process in high producer CHO cells. In addition, down-regulation of genes involved in cholesterol biosynthesis, fatty acid metabolism and ribosomal proteins were also observed in high specific productivity cells. In contrast, Ley et al. (2015) found no differential expression of genes related to protein translocation, protein folding, protein glycosylation or vesicular transport between high and low producer cells. Together, it can be seen that, in general, up-regulation of genes related to UPR, protein processing, vesicular transport and secretion seem to be a feature of high productive CHO cells. However, conflicting view was also observed. This might be due to differences in CHO cells types and cell culture condition.

Transcriptomics technology have also been applied in the study of phenotypic variability of CHO cells. Vishwanathan et al. (2015) focused on comparison of the gene expression pattern of enzymes in energy metabolism and glycosylation in six CHO cell lines and Chinese hamster tissues using RNA-Seq. The six CHO cell lines exhibited differences in

gene expression from each other along with differences in growth, metabolism, and N-glycosylation patterns. CHO cell lines also expressed distinct isozymes of genes related to metabolism, that contrasted with the pattern of expression in Chinese hamster tissues. They suggested that accumulation of mutations in the intergenic regions and other epigenetic events might play an important role in the variability of gene expression and the diversity of the behavior of CHO cells in culture.

1.4.2 Proteomics

Examining the transcriptome can provide insight into regulation of cellular processes but mRNA levels are not necessarily directly correlated with the protein expression levels for their protein products. Therefore proteomics analysis, which is the study of entire proteins expressed by a genome, can provide additional understanding of changes in cell physiology on expression of recombinant protein or changes in culture conditions (Datta et al., 2013).

Several techniques have been employed for proteomics analysis in CHO cells including two-dimensional polyacrylamide gel electrophoresis (2D-PAGE), traditional Western blotting, two-dimensional difference in gel electrophoresis (2D-DIGE) and MS-based techniques (Carlage et al., 2009, Doolan et al., 2010, Meleady, 2007). Many proteomics approaches have been applied to identify proteins that are potentially associated with metabolic shift and elevated product titre of CHO cells

Pascoe et al. (2007) investigated the metabolic shift of two mAb-producing CHO DUKX cell lines displaying different lactate metabolism during fed-batch bioreactor cultures using 2D-PAGE and LC-MS/MS techniques. The majority of differentially expressed proteins were protein related to glycolytic, structural, cell growth and protein processing. Carlage et al. (2009) compared proteomic profiling between high producing CHO cells

which were transfected with the apoptosis inhibitor *Bcl- XL* gene and low producing CHO cells which was not transfected with *Bcl-XL* gene using LC-MS. The data showed that a set of proteins related to translation processes (eukaryotic translation initiation factor 3 and ribosome 40S) and the molecular chaperone BiP were up-regulated in the high producer cell line. This may indicate the UPR due to ER stress as a result of recombinant protein expression. In addition, several proteins involved in regulation of the cell cycle were differentially expressed, reflecting a difference in the control of the cell cycle between low- and high-producing cells. Furthermore, proteomics analysis was applied in many CHO cells culture condition such as NaBu addition (Van Dyk et al., 2003), dimethyl sulfoxide addition (Li et al., 2006) and hyperosmotic stress (Lee et al., 2003).

In order to gain better understanding of genes and proteins that contribute to higher productive CHO cells, proteomics analysis have been combined with transcriptomics approach. Doolan et al. (2010) focused on identification of key genes and proteins regulating the growth of CHO cells. A combination of transcriptomics and proteomics profiling of fast and slow growth rate CHO mAb-secreting cell lines revealed the overlap of 21 genes and proteins associated with the high cell growth rate phenotype. Among 21 candidates, five of them (valosin-containing protein (VCP), heat shock 27 kDa protein 1 (HSPB1), immunoglobulin heavy chain binding protein (HSPA5), enolase 1 (ENO1) and actin-related protein (ACTR1A)) were selected for further functional validation by gene knockdown and overexpression. Altered VCP expression had a significant impact on CHO cell proliferation, indicating that VCP may play an important role in the regulation of CHO cell growth. Baik et al. (2006) examined transcriptomics and proteomics profiling of CHO cells expressing erythropoietin in response to low culture temperature. Transcriptomic analysis showed that genes related to metabolism, transport and signaling pathways were altered in this condition. Of nine differentially expressed proteins identified by proteomic analysis, the correlation was detected between protein and mRNA expression patterns of four proteins (protein disulfide isomerase, nucleoside

diphosphate kinase B, thiol-disulfide oxidoreductase, phosphoglycerate kinase and heat shock cognate 71 kDa protein). Nissom et al. (2006) compared transcriptomics and proteomics profiling between high and low producer CHO DHFR cells. A general lack of correlation between transcript and protein was observed in that study. However, they found that genes and proteins involved in opening up and condensing chromatin were up- and down-regulated, respectively. In addition, dowregulation of genes and proteins that promote cell growth were also observed in high producer cell.

1.4.3 Metabolomics

Metabolomics is a qualitative and quantitative analysis of metabolites (such as sugar, amino acids, nucleosides and fatty acids) within cells and in culture medium (Datta et al., 2013, Khoo and Al-Rubeai, 2009, Oldiges et al., 2007). Metabolomics can be subdivided into (1) target analysis, aiming at quantitative analysis of substrate and/or product metabolites of a target protein; (2) metabolic profiling, focusing at the quantification of metabolites in preselected metabolic pathways or a linked group of metabolites (e.g. sugars, sugar phosphates, lipids, organic acids); (3) metabolomics, aiming for overview of whole-cell metabolic patterns (Fiehn, 2002).

A variety of analytical techniques have been used for metabolite analysis including enzymatic assays, gas chromatography (GC), nuclear magnetic resonance (NMR), high-performance liquid chromatograpgy (HPLC), gas chromatography-mass spectrometry (GC-MS) and liquid chromatography-mass spectrometry (LC-MS). The data comparison between each technique is shown in Table 1.2. GC-MS, LC-MS and NMR techniques are the most frequently used analytical tools for metabolomics (Oldiges et al., 2007, Rochfort, 2005). However, currently there is no one method that can claim to separate, detect, and identify all metabolites, since no single technique is comprehensive, selective and sensitive enough to measure them all (Baidoo et al., 2012). Many

metabolomics approaches have been used to identify key intracellular mechanisms that relate to cell growth, productivity and metabolic shift of CHO cells.

Table 1.2 The comparison of techniques for metabolite quantification (Baidoo et al., 2012, Roux et al., 2011)

Technique	Sensitivity	Advantages	Disadvantages
Enzymatic assays	low	- low cost	- require large amounts of samples
NMR	low	- highly robust technique - no prior seperative method - possibility to detect the structure of unknown metabolites	- expensive - require large amount of samples - long analysis time
GC-MS	high	- highly robust technique - short analysis time	- sample could be derivatized or volatile
LC-MS	very high	- no requirement to derivatize the samples - versatile - possibility to detect many xenobiotics	- require good preparation sample

Selvarasu et al. (2012) combined extra- and intra-cellular metabomics analysis and in silico modeling approach to understand intracellular behaviors of CHO cell lines expressing IgG in relation to cell growth and death. These data showed that decreased in the intracellular GSH pool and glycerophospholipid pathway fluxes in stationary phase might associate with growth limitation. Dean and Reddy (2013) compared change in central metabolism that accompany growth and antibody production between high and low performer cell using isotopomer labeling and biochemical method. They observed that mainly fraction of lactate was derived from glutamine and pyruvate not from glucose during exponential phase. This result is contrary with previous research which glucose has been reported to be the main source to produce lactate (Ahn and Antoniewicz, 2011, Deshpande et al., 2009). In addition, during exponential phase, asparagine and glutamine were utilized to replenish the TCA cycle and glucose was used to replenish

the TCA cycle during stationary phase. Furthermore, they found that high performer cell obtained greater fraction of its TCA cycle intermediates from glucose than low performer cell. This suggested that high performer cell might be a result of more active TCA cycle flux in order to maintain high requirement of ATP for high antibody production. Luo et al. (2012) and Martinez et al. (2013) studied metabolite profile to understand lactate metabolism shift in CHO cell. Luo et al. (2012) found that lactate production phenotype of CHO DUK-XB11 cell producing antibody showed inefficient energy metabolism because glucose was converted to sorbitol, pyruvate, lactate and other glycolytic intermediates. This might be due to lack of ability of pyruvate and acetyl-CoA to channel into the TCA cycle. Martinez et al. (2013) found that, in exponential phase, glucose consumption and lactate production rates were high. The majority of acetyl-CoA was used for fatty acid and steroid production. In stationary phase, glucose was depleted and the cells started to consume lactate. In addition, the majority of acetyl-CoA was oxidized in the TCA cycle.

In addition, change of metabolism related to different medium and nutrient feeding have also been examined using metabolomics approach. Lu et al. (2005) investigated metabolism of CHO cells producing erythropoietin at low glucose concentration by the determination of intracellular metabolites, including ATP, organic acids, and amino acids. The result revealed decreased of intracellular ATP concentration at low concentration of glucose. This suggested that the low energy production might be the reason for the growth limitation at low glucose concentration. Additionally, the specific consumption rates of the majority of amino acids were increased at low concentration of glucose indicating that these amino acids were mainly utilized in cellular catabolism instead of building block for protein synthesis in glucose limitation. However, there was no significant difference in the intracellular concentrations of organic acids with the decrease in the glucose concentration. Dietmair et al. (2012a) examined extra- and intra-cellular metabolite profile of CHO cell line CB515 producing human growth hormone cultivated in three different media (CHO-S-SFMII (SFM), HyQ SFM4CHO

(HyQ), and CD CHO). They found that cells in SFM medium grew as fast as cells in HyQ in exponential phase, but entered stationary phase at a lower cell density. Cells in CD CHO grew significantly slower. The results from intracellular metabolite profiles showed that concentration of nucleotides (dCTP, CTP, GTP, ATP, and NAD), which act as building block for the synthesis of RNA or DNA, and UDP-glucuronic acid (UDP-glcA), which are used for the production of proteoglycans, were higher in HyQ and SFM cultures than in CD CHO in exponential phase. This suggested that nucleotide and UDP-glcA might associate with the differences in growth rates of the cells. Sellick et al. (2015) investigated extra- and intra-cellular metabolite profile of CHO K1SV cells in response to supplementation with CHO CD EfficientFeeds^{TM} A or B to identify key metabolites associated with increased cell culture performance. Supplementation with CHO CD EfficientFeeds^{TM} A or B resulted in increased cell growth, specific productivity and product titre accompany with decreased lactate production and increased intracellular amount of citrate, succinate, fumarate and malate. Citrate and malate were involved in mitochondrial-cytosolic shuttle system (fatty acid biosynthesis and redox/amino acid interconversions). They suggested that mitochondrial function and efficiency could be a major reason to enhance cell growth and protein production in CHO cells.

In addition to using GC-MS, LC-MS or NMR techniques as analytical tools for metabolomics, subsequently, data analysis of metabolic behavior may be enhanced by using flux-based methods such as metabolic flux analysis (MFA). MFA is a useful tool based on the principle of mass conservation within a stoichiometric network of cellular metabolism, allowing the estimation of intracellular fluxes under assumed metabolic steady state given measurable rates of nutrient consumption and by-product accumulation (Stephanopoulos et al., 1998).

MFA has recently been used in CHO cells for a variety of application. Quek et al. (2010) applied MFA to estimate fluxes in a large-scale model for CHO cell metabolism, which was used to compare metabolism of CHO cells and hybridoma cells. The rates through glycolysis and TCA cycle of CHO cells were higher than hybridoma cells, when cultured in similar growth media and at similar growth rate. This difference could reflect glutamine limitation in the hybridoma culture shifting the cells to a more efficient metabolism, while glutamine and glucose were not limiting in the CHO batch culture. Xing et al. (2011) used data from MFA in different concentrations of medium components to optimize the amino acid composition of CHO cell culture media. The result showed that methionine, tryptophan, asparagine and serine were limiting while alanine, arginine, glutamine and glycine were in excess at the semi-steady states. Sengupta et al. (2011) used MFA to examine fed-batch culture of GS-CHO SF18 cell producing antibody in late non-growth phase. Almost all of the consumed glucose was channeled to pentose phosphate pathway with a high NADPH production. Since there was no biomass formation during this period, high NADPH might be produced in order to counteract oxidative stress. Moreover, the majority of pyruvate produced from glycolysis was entered the TCA cycle with no lactate production. Ahn and Antoniewicz (2011) applied MFA to compare flux maps between exponential and stationary phases of fed-batch culture of CHO-K1 host cells. At exponential phase, high flux of glycolysis from glucose to lactate and anaplerosis from pyruvate to oxaloacetate and from glutamate to αKG were observed. At stationary phase, flux of glycolysis and net lactate uptake was decreased while pentose phosphate pathway flux was significantly increased. The TCA cycle flux were similar at both exponential and stationary phase. Templeton et al. (2013) performed MFA to investigate cell metabolism throughout four phases (early exponential, late exponential, stationary and decline phase) of high productive CHO cell producing antibody. They found that peak specific growth rate was associated with high lactate production and minimal TCA cycle. Lactate metabolism switched from production to consumption when the culture transitioned from peak growth to peak antibody production as the cells entered stationary phase. During the peak antibody production

phase, energy was mainly generated through the TCA cycle and oxidative phosphorylation.

Together, it can be seen that there were a variation of results of metabolomics profiling of CHO cells. However, it seems to be that most of the observations point out that the connection between glycolysis and the TCA cycle could be an important part related to enhance recombinant protein production in CHO cells.

Since the metabolites are downstream of transcriptome and proteome, they will provide valuable information about the regulatory or catalytic properties of a gene product (Oldiges et al., 2007) (445). Ryan and Robards (2006) suggested that “metabolomics may provide the most functional information of the omics technologies as changes in the transcriptome and proteome do not always result in altered biochemical phenotypes”. Therefore, several researchers have tried to understand the metabolism of CHO cells, as described in this section and Section 1.3, in order to help in development of culture media (Section 1.5.1.1), designing feeding regimes (Section 1.5.1.2) and identify potential metabolic engineering targets (Section 1.5.2.1). However, combination of metabolomics data with the other omics technologies will contribute to obtain greater understanding of a biological system and implicate potential candidates for further CHO cells engineering (Oldiges et al., 2007).

1.5 Approaches undertaken to improve the efficiency of CHO cell factories

Improving the rate of recombinant protein production in CHO cells is an important consideration in controlling the cost of biopharmaceuticals. Continuous efforts have been devoted to improving the utility of CHO cells as hosts for commercial recombinant protein production, with respect to enhancing protein yield and quality. Two main approaches have been applied in order to increase the productivity of CHO cells - optimization the composition of culture medium (Section 1.5.1) and cell engineering (Section 1.5.2),

1.5.1 Medium optimization

Medium composition, with associated development of an appropriate feed strategy, is crucial because these strategies enable improvement to culture longevity and, potentially, product yield in CHO cells. The main goal of medium development is to support cell growth having a robust process with high viable cell density, high product titre and high product quality (Klein et al., 2015). In order to achieve high titre, the cells require a base medium to support the early stages of culture followed by nutrient feeds to replace limiting nutrients and to extend the period of protein production (Sellick et al., 2015). Many researchers have tried to optimize the composition of culture medium to gain the most suitable conditions for recombinant protein production yield in CHO cells.

1.5.1.1 Substitution of glucose and glutamine

Since high consumption rate of glucose and glutamine have been found in CHO cells lead to high accumulation of lactate and ammonia (Section 1.3). Many attempts have been made to use the nutrients which are able to slow metabolic rates in order to decrease lactate and ammonia accumulation.

Altamirano et al. (2000) replaced glucose and glutamine with galactose and glutamate (that were more slowly metabolized). Use of galactose rather than glucose resulted in decreased quantities of lactate production in medium of CHO TF 70R cells (GS expression system) but this was accompanied by a lower rate of cell growth. Genzel et al. (2005) replaced glutamine with pyruvate in order to decrease ammonia accumulation. As a result, cell growth was improved in adherent MDCK, BHK21 and CHO-K1 cells. For MDCK cells, replacement of glutamine with pyruvate decreased ammonia and lactate production, decreased use of serine, cysteine and methionine and increased use of leucine and isoleucine. Altamirano et al. (2006a) cultured CHO TF 70R cells in batch culture containing glutamate, galactose and glucose. The results showed that cell growth was increased compared with cells that were cultured in medium containing only glutamate and galactose. In addition, it was observed that, after glucose depletion, galactose and lactate were consumed. Thus, it was concluded that cells consumed glucose in the first phase and then used galactose in a second phase to continue growing with the simultaneous consumption of the endogenous lactate.

1.5.1.2 Nutrient supplementation

In addition to changes in the availability of primary nutrients, optimization of feed composition and regimens also allows for improved central carbon metabolism and cell culture performance.

Hansen and Emborg (1994a) examined the effect of addition of three different asparagine concentrations (0.05, 2.55 amd 7.55 mM) to CHO TF70 cells producing tissue-type plasminogen activator (tPA). Increased asparagine concentration caused increased production of ammonia, glycine and alanine and decreased tPA production which resulted from ammonia inhibition. Chen and Harcum (2005) supplied various amino acids to CHO CRL-9606 cells culture under ammonium stress. They found that

addition of threonine, proline and glycine individually improved cell growth and t-PA production but proline was slightly less effective than glycine and threonine. Furthermore, these additions also decreased lactate and ammonia production. Altamirano et al. (2006b) examined the effect of supplementation with vitamins, lipids and amino acids of CHO TF70R cells producing t-PA. The results showed that addition of some vitamins and lipids improved cell and t-PA concentration. Proline and serine supplementation also had a positive effect on cell growth but further improvement of cell growth and t-PA production was observed when asparagine was added with proline and serine. However, these supplementations did not change lactate and ammonia production. Crowell et al. (2007) found that nine amino acids (cysteine, isoleucine, leucine, tryptophan, valine, asparagine, aspartic acid, glutamate, and glutamine) were depleted to low levels during culture of CHO cells producing recombinant human erythropoietin (rHuEPO). Therefore, double the original amount of these amino acids was added to cell culture medium to generate enriched amino acid mediums. As a result, rHuEPO production was increased suggesting that amino acid availability was rate limiting. Li et al. (2012) showed that feeding lactate or pyruvate decreased the amount of ammonia produced throughout culture, linked to decreased amino acid catabolism while feeding had no effect on cell growth and productivity in CHO DUKB11 cells (DHFR expression system). Sellick et al. (2011) found that aspartate, asparagine, glutamate, and pyruvate were depleted at the beginning of the stationary phase of CHO-LB01 cells producing antibody. Thus, they investigated the result of feeding aspartate, asparagine, glutamate, and pyruvate to CHO-LB01 cells (Figure 1.8). The nutrients resulted in extended exponential growth for an extra day, increased cell density and enhanced antibody production by 75% but the cells died more quickly than unfed cells. This was caused by the depletion of glucose, pyruvate and several amino acids. When glucose was added in combination with aspartate, asparagine, glutamate, and pyruvate, it had no further effect on maximum cell numbers but stationary phase was extended by one day and antibody yield was improved by 25% compared with the cultures fed with amino acids and pyruvate alone. Xing et al. (2011) attempted to optimize the amino acid

composition of culture medium based on the result of MFA. The MFA results showed that methionine, tryptophan, asparagine and serine were limiting while alanine, arginine, glutamine and glycine were in excess at the semi-steady states. From these results, the limiting amino acids were increased in culture medium while those in excess were decreased to obtain a balanced amino acid composition in culture medium. Consequently, the modified medium generated less lactate and ammonia and increased cell density and protein production. Gilbert et al. (2013) individually supplemented the culture of CHO-DG44 with TCA cycle intermediates (αKG and citrate). As a result, lactate and ammonia production were decreased but cell growth and recombinant protein production profile were not reported. Kishishita et al. (2015) supplemented three amino acids (serine, cysteine and tyrosine) that were consumed in significant amounts during cell culture. In the presence of these nutrients, cell viability and antibody production were enhanced in CHO DUK-XB11 cells.

1.5.2 Cell engineering

In addition to optimization of the interaction between cells and their cell culture environment, cell engineering is a technique that has been used to improve the efficiency of CHO cells. Based on the background knowledge of metabolism (Section 1.3) and omics analysis (Section 1.4) in CHO cells, various genetic engineering strategies have been employed to increase metabolic efficiency (Section 1.5.2.1), enhance protein processing capacity (Section 1.5.2.2) and delay apoptosis (Section 1.5.2.3).

1.5.2.1 Metabolic engineering

Improving central carbon metabolism has been a common objective for researchers in the field of cell culture for many years. Specific metabolic pathways can be optimized by over-expression or down-regulation of key enzymes such as LDH, PDHK, PC and MDH in order to decrease lactate accumulation and/or increase the flow of pyruvate to the TCA cycle. From previous research, many target genes in metabolic pathways have been engineered in attempts to improve bioprocess performance of CHO cells as described below (Figure 1.8).

One direct strategy to decrease lactate production was knockdown of the lactate dehydrogenase A (LDH-A) gene by antisense mRNA technology (Jeong et al., 2001) or siRNA (Kim and Lee, 2007a, Zhou et al., 2011). These approaches successfully decreased lactate accumulation but did not achieve any improvement in recombinant protein productivity and/or cell growth. However, when the expression of LDH-A and pyruvate dehydrogenase kinase (PDHK) were simultaneously suppressed in CHO DUKB11 cells using a single shRNA targeting vector, lactate production decreased and the specific production of antibody increased without significant impact on cell growth or product quality. It was speculated that when the activity of PDHK was suppressed, increased pyruvate dehydrogenase activity was able to cause higher pyruvate entry into mitochondria. As a result, the cell had a greater efficiency of TCA cycle activity (and energy production), leading to increased antibody production (Zhou et al., 2011). However, it has been reported that a complete knockout of LDH-A using zinc-finger nuclease-mediated genome editing technology in a PDHK1, 2, and 3 knockdown DUXB11 CHO cell line is lethal (Yip et al., 2014).

PC which was shown to have a very low activity in CHO cells (Section 1.3.3) has been over-expressed to enhance the flow of pyruvate into oxaloacetate in the TCA cycle in

CHO cells. It has been reported that over-expression of yeast PC and decreased culture temperature from 37 to 33°C had an additive effect on specific productivity of CHO-K1-hGM-CSF cells (Bollati Fogolin et al., 2004). CHO cells over-expressing yeast PC displayed a metabolic shift toward lactate consumption and prolonged exponential growth phase led to increase product titre (Toussaint et al., 2016). Additionally, the result of over-expression of human PC in CHO-DG44 cells demonstrated significantly decreased lactate formation and improved cell viability at the end of adherent batch cultures (Kim and Lee, 2007b).

Malate dehydrogenase II (MDH II), defined as a bottleneck in the TCA cycle (Chong et al., 2010, Kim et al., 2012, Selvarasu et al., 2012, Wilkens and Gerdtzen, 2015), has been over-expressed in CHO cells. MDH II over-expression in mAb-secreting CHO cells has been demonstrated to increase intracellular ATP and NADH, improve integral viable cell number by 1.9-fold and recombinant protein production by 1.2-fold (Chong et al., 2010). However, over-expression of MDH II in IgG-producing CHO DP12 cells was reported to decrease cell growth and recombinant protein production (Wilkens and Gerdtzen, 2015).

In order to decrease the accumulation of ammonia, carbamoyl phosphate synthetase I (CPSI) and ornithine transcarbamoylase (OTC) which catalyze the first and second steps of the urea cycle in the liver were over-expressed in CHO dhfr$^-$ cells. Both the expression of CPS I and OTC can decrease the accumulation of ammonia in the culture media (Park et al., 2000). In extension of previous study, the establishment of CHO cells expressing the first three, first four, or all five enzymes of the urea cycle was undertaken by introducing argininosuccinate synthetase (AS), argininosuccinate lyase (AL), or AS, AL, and arginase (Arg) genes into CPSI and OTC-expressing CHO cells. CHO cells expressing the first three enzymes exhibited decreased ammonia accumulation and similar growth rates to cells expressing the first two enzymes whereas the cells expressing the first four enzymes showed improved ammonia removing abilities and a

higher viable cell concentration. Unexpectedly, the cells expressing the enzymes from all five steps showed a lower ammonia concentration and lower cell viability (Chung et al., 2003).

In addition to the enzymes in metabolic pathways, transporter genes have been selected as targets for engineering. Over-expression of the fructose-specific transporter (GLUT5) in CHO cells gave cells the ability to grow using fructose as the main carbon source. Selected GLUT5-expressing clones exhibited dramatically decreased glucose consumption and lactate production rates and increased cell density (Wlaschin and Hu, 2007). Likewise, enhanced cell density and antibody yield was found in IgG-producing CHO DP12 cells over-expressing GLUT5 (Wilkens and Gerdtzen, 2015). Additionally, over-expression of mitochondrial aspartate-glutamate carrier (ARALAR1) in non-recombinant CHO-S cells was reported to decrease lactate accumulation by promoting a metabolic switch to lactate consumption. This result suggested that MAS could be a key factor to promote metabolic shift (Zagari et al., 2013).

1.5.2.2 Posttranslational engineering

In many cases recombinant protein production is probably limited downstream of transcription as mentioned in Section 1.4.1. Therefore, several researchers have made an attempt to modify the translational or secretory pathways where antibody production is considered limited at folding and assembly reactions (Birch and Racher, 2006).

The protein folding machinery is utilized in the early stage of protein secretion. It consists of many chaperones and co-factors. Several ER chaperones have been targeted for cell engineering. Over-expression of binding immunoglobulin protein (Bip), which interacts with polypeptide folding intermediates transiting the secretory compartment, resulted in decreased stress in the ER but generated limited effect on

transgene production in CHO cells (Dorner et al., 1992, Morris et al., 1997). Protein disulfide isomerase (PDI) catalyzes disulfide bond exchange and also functions as an ER-resident molecular chaperone. The impact of over-expression of PDI in CHO cells was varied depended on the kind of transgene (Borth et al., 2005, Davis et al., 2000, Hayes et al., 2010, Mohan et al., 2007). Similar to PDI, coupled over-expression of PDI and endoplasmic reticulum oxidoreductase (ERO1a/b), which is a helper protein of PDI, in recombinant CHO cells producing antibody enhanced antibody yield in transient expression but did not show significant effect in stable expression (Mohan and Lee, 2010).

The unfold protein response (UPR) pathway is an adaptive pathway that helps cells cope with an increased load of unfolded proteins. This pathway is induced by accumulation of misfolded proteins (Schroder and Kaufman, 2005b, Schroder and Kaufman, 2005a). X-box binding protein 1 (XBP1) is a key regulator of the cellular secretory pathway and UPR. Transient and stable overexpression of XBP1 resulted in enhanced protein titre in CHO cells (Becker et al., 2008, Tigges and Fussenegger, 2006). Overexpression of both XBP-1S and ERO1-La in CHO-S cells was reported to increase antibody yield up to 6 fold (Cain et al., 2013). Additionally, it has been demonstrated that in transient transfection systems overexpression of XBP-1S improved protein titre whereas it had no effect on protein productivity of stable cell lines where it did not exhibit any secretory bottleneck (Ku et al., 2008, Ku et al., 2010). To improve the production of recombinant human antithrombin III (AT-III) in CHO cells, overexpression of growth arrest and DNA damage inducible protein 34 (GADD34), which is a transcription factor involved in the UPR, and activating transcription factor 4 (ATF4) was undertaken in CHO 13D-35D cells. This resulted in significantly enhanced production of recombinant AT-III (Ohya et al., 2008, Omasa et al., 2008). Over-expression of transcription factor C/EBP homologous protein (CHOP) alone or in combination with other proteins (such as chaperones or UPR genes) significantly enhanced antibody production in CHO-K1 cells (Nishimiya et al., 2013).

In addition to the protein folding machinery and UPR pathway, protein secretion is one of major step in post-translational steps. Soluble NSF receptors (SNAREs) are known to regulate exocytosis by mediating fusion of secretory vesicles to the plasma membrane. The ectopic and stable expression of synaptosome-associated protein of 23 kDa (SNAP-23) and vesicle-associated membrane protein 8 (VAMP8), which are members of SNAREs, increased human placental secreted alkaline phosphatase and antibody production in various cells including CHO cells (Peng et al., 2011).

1.5.2.3 Apoptosis engineering

Apoptosis is the main mechanism of cell death in mammalian cell culture and can be triggered by a variety of factors such as nutrient, oxygen, or growth factor deprivation, or accumulation of metabolic byproducts. Limiting or delaying apoptosis has the potential to increase viable cell densities, thereby increasing product titers (Dietmair et al., 2012b). In order to develop robust CHO cells, a variety of apoptotic regulatory genes have over-expressed (or down-regulated in the case of caspase and pro-apoptotic genes).

The Bcl-2 family is the best characterized protein family involved in the regulation of apoptotic cell death consisting of anti-apoptotic and pro-apoptotic members. Bcl-2 and Bcl-XL are anti-apoptotic (Tsujimoto, 1998). Overexpression of Bcl-2 or Bcl-XL was able to limit apoptotic death leading to enhanced cellular lifespan and recombinant protein production and alteration of lactate metabolism (Chiang and Sisk, 2005, Kim et al., 2009, Mastrangelo et al., 2000a, Mastrangelo et al., 2000b, Templeton et al., 2014, Tey et al., 2000, Zustiak et al., 2014). Additionally, enhanced recombinant protein production was achieved by addition of NaBu to Bcl-2 overexpressing CHO cells (Kim and Lee, 2001, Sung and Lee, 2005). In addition to CHO cell engineering via engineering of Bcl-2 family proteins, viable cell density can be improved by overexpression of other anti-

apoptotic genes (such as E1B-19K, XIAP, Crm and Aven) (Dorai et al., 2009, Figueroa et al., 2007, Sauerwald et al., 2002, Sauerwald et al., 2003).

Caspase-3 is the most intensively studied effector caspase and is a key protease in apoptosis cascade. In order to suppress apoptosis, attempts have been made to downregulate Caspase-3 using siRNA strategy. Kim and Lee (2002) reported that suppression of caspase-3 by antisense RNA extended culture longevity of NaBu-induced CHO cells but antibody yield was not increased. However, Sung et al. (2005) demonstrated that down-regulation of caspase-3 in CHO cells did not effectively inhibit NaBu-induced apoptotic cell death because there was compensation by caspase-7 to induce apoptosis. Afterwards, Sung et al. (2007) was successful in extending culture longevity by co-down-regulation of caspase-3 and caspase-7 and this approach enhanced recombinant protein production in CHO cells. Furthermore, Yun et al. (2007) reported that inhibition of caspase-8 and -9 enhanced cell viability in CHO cells. In addition to caspase, pro-apoptotic genes such as Bax and Bak have also been targeted for engineering. Down-regulation of Bax and Bak using shRNA vectors (Lim et al., 2006) or elimination of Bax and Bak using zinc-finger nuclease-mediated gene disruption (Cost et al., 2010) increase cell viability and improve recombinant protein production in CHO cells.

In summary, traditional genetic engineering strategies have been applied to enhance specific productivity by targeting individual genes or specific pathways. These strategies can increase in specific productivity. However, a dramatic increase in specific productivity may require engineering of multiple genes or pathways at global levels (Loh et al., 2014) .

1.6 Summary and objectives

Based on previous research, it can be seen that several strategies have been used to increase productivity of CHO cells. Development of medium and nutrient supplementation and cell engineering have been shown to affect cell growth and product yield of CHO cells. However, the fundamental understanding of metabolic changes at molecular level is limited. Moreover, distinct cell lines and cell culture conditions also provide the potential for differential impact on cell culture performance.

In this study, CHO-LB01 cells (developed by Lonza Biologics) was used as the model recombinant cell line. CHO-LB01 was generated by transfection of the host cell line CHOK1SV (utilizing the GS expression system) with GS vector encoding the gene for IgG4 antibody heavy chain and light chain. This cell line is cultured in CD OptiCHO^{TM} medium (Sellick et al., 2011).

A positive correlation between the flux of TCA cycle and productivity of CHO cells has been reported (Section 1.3.4). Therefore, it was hypothesised that when the flux of TCA cycle and related metabolism is increased, the efficiency of CHO-LB01 cells for recombinant protein production should be enhanced. Prior to direct testing of the hypothesis, it was necessary to understand the metabolite profile of CHO-LB01 cells in CD OptiCHO^{TM} medium supplemented with several nutrients based on the work of Sellick et al. (2011) (Section 1.5.1.2). This information highlighted metabolic targets offering potential for modified nutrient supplementation and metabolic engineering. Thus, the aim of this thesis was to improve the metabolism of CHO-LB01 cells, especially in the efficiency of the TCA cycle, based on previous basic knowledge and further experiments in order to improve the productivity of CHO-LB01 cells by nutrient supplementation or metabolic engineering.

Therefore the specific objectives of this research are defined as follows:

1) Study cell growth, productivity and metabolite profile of CHO-LB01 cells supplemented with several nutrients to examine changes in metabolites associated with growth and productivity (Chapter 3).

2) Enhance cell growth and/or recombinant protein production by modification of nutrient supplementation of CHO-LB01 cells (Chapter 4).

3) Identify target genes and examine the consequence of metabolic engineering on the efficiency of recombinant protein production and growth in CHO-LB01 cells (Chapter 5).

4) Investigate transcriptomic profiles associated with enhanced productivity of CHO-LB01 cells (Chapter 6).

CHAPTER 2

Material and Methods

2.1 Materials and equipment

2.1.1 Sources of chemicals, reagents, and equipment

A list of all reagents and equipment used in this study are provided in Appendix 1.

2.1.2 Preparation of solutions

All solutions are made up in MilliQ water (dd. H_2O) unless mentioned otherwise. Solutions were stored at room temperature unless stated otherwise.

2.1.3 pH measurement

pH was measured by using a digital Corning pH meter 120 with a glass electrode. The pH was adjusted using hydrochloric acid or sodium hydroxide as appropriate.

2.2 Cell culture

2.2.1 Cell maintenance and culture

CHO-LB01 cells (provided by Lonza Biologics) used in this study were generated by transfection of the host cell line CHOK1SV (utilizing the glutamine synthetase (GS) expression system) with GS vector (pEE12-GS) encoding the gene for IgG4 antibody (heavy chain and light chain) (Sellick et al., 2011). CHO-LB01 cells were maintained in CD OptiCHO™ medium supplemented with 25 µM methionine sulfoximine (MSX). CHO-S cells (host cell line) were maintained in CD CHO medium supplemented with 1x GlutaMAX™. CHO TRex cells (inducible erythropoietin producing cell line) were maintained in CD CHO supplemented with 0.2% [v/v] Zeocin, 1x [v/v] GlutaMAX™, 0.1% [w/v] Blasticidin and 0.1% [w/v] Tetracycline.

Cells were cultured in volumes of 20 mL or 50 mL medium in 125 mL and 250 mL Erlenmeyer flasks, respectively. Every 3-4 days the cells were sub-cultured into appropriate fresh medium with an initial density of $0.2x10^6$ cells/mL. All cells were maintained in suspension at 37°C, 5% CO_2 at 130 rpm orbital shaking (orbit diameter 19 mm).

For small-scale cell culture, cells were cultured in volume of 5 mL in 50 mL Mini Bioreactors (Corning Inc. Life Sciences, USA). The cells grow at 37°C, 5% CO_2 at 230 rpm orbital shaking (orbit diameter 12.5 mm).

2.2.2 Determination of cell number, cell viability and cell size

Cell growth was assessed at 24-h intervals by light microscopy using a Neubauer haemocytometer. The medium samples were mixed 1:1 with 0.5% (w/v) Trypan blue (in PBS). Cell size was measured by flow cytometry using a BD Accuri™ and Countess Automated Cell Counter.

2.2.3 Cryopreservation of cells

~$1.2x10^7$ CHO cells, in exponential growth phase, were centrifuged at 201 x *g* for 5 min at room temperature and the supernatant was removed. The cell pellet was resuspended in Cell Freezing Medium-DMSO (1.5 mL cell culture medium and 10% [v/v] DMSO) and were transfered into 1.8 mL cryovials and the vials were placed into a Nalgene® Mr Frosty freezing container. After incubation overnight at -80°C vials were transferred to liquid nitrogen for long-term storage.

2.2.4 Nutrient feeding strategies

Stock solutions of asparagine (75 mM), aspartate (37 mM), glutamate (20 mM), pyruvate (113 mM), β-hydroxybutyrate (HB) (0.5 M), glucose (2 M), leucine (0.08 M), isoleucine (0.08 M), tyrosine (0.02 M) and valine (0.08 M) were prepared in dd. H_2O. For tyrosine solution, the pH was adjusted to pH 10 to fully dissolve the stock solution. These stock solutions were sterilized by passage through a 0.02 µm filter before addition to cell cultures.

When added, asparagine, aspartate, glutamate, pyruvate and HB were supplemented into culture medium on day 4 of culture to give final concentrations of 1.5 mM asparagine, 1.5 mM aspartate, 1.36 mM glutamate, 2.3 mM pyruvate and 10 mM HB. Leucine, isoleucine, tyrosine and valine were supplemented into culture medium on day 5 to give final concentrations of 0.76 mM leucine, 0.76 mM isoleucine, 0.5 mM tyrosine and 0.76 mM valine. Glucose was supplemented into culture medium on day 6 to give final concentrations of 20 mM glucose. Unfed batch cultures (control) were performed in CD OptiCHO^{TM} medium supplemented with 25 µM MSX with no additional nutrients. Samples of culture medium were collected every 24-h and were stored at -80°C for subsequent analysis.

2.3 Metabolite analysis

2.3.1 Enzymatic assays

2.3.1.1 Glucose

Glucose concentration was measured by reading a 96 well plate at 505 nm detecting the quinone complex formed by the reaction catalyzed by glucose oxidase and horseradish peroxidase (Trinder 1969).

5 µL medium samples and D-glucose standards were added to 96 well plate, and after addition of 200 µL of glucose assay working reagent (2 U/mL glucose oxidase, 2 U/mL horseradish peroxidase, 0.4 mM 4-amino antipyrine, 0.4 mM phenol and 150 mM phosphate buffer pH 7.5) plates were incubated for 10 min at room temperature. The reading was performed using a microplate reader (Gen 5 software). The glucose concentration in the samples was determined from the linear portion of the standard curves (0-25 mM) in each assay using Microsoft Excel.

2.3.1.2 Lactate

Lactate concentration in the medium was determined by its conversion to pyruvate by lactate dehydrogenase (LDH) linked to the reduction of NAD^+ to NADH which absorbs light at 340 nm (Bergmeyer et al. 1983).

5 µL medium samples and L-lactate standards (0-25 mM) were added to 1.5 mL microcentrifuge tubes and 995 µL of assay buffer (2 mM NAD^+, 3.36 mM NaOH/10 mM glycine buffer pH 9.5 and 159 mM hydrazine monohydrate) was added to each tube. Absorbance was read at 340 nm and then 5.6 ml LDH (2 U/mL) was added to each sample. Following 60 min incubation at room temperature, a second reading was taken at 340 nm. The difference between second and first readings was used to determine lactate concentration by correlating to the standard curves in each assay using Microsoft Excel.

2.3.1.3 Alanine

Alanine concentration in the medium was determined by its conversion to pyruvate by alanine dehydrogenase (ADH) linked to the reduction of NAD^+ to NADH which absorbs light at 340 nM (Bergmeyer et al. 1983).

5 µL medium samples and L-alanine standards (0-25 mM) were added to 1.5 mL microcentrifuge tubes and 1 mL of alanine assay working reagent (40 mM Tris/1.4 mM EDTA buffer pH 9.0, 2.4 mM NAD^+, 1 U/mL ADH and 1 mM hydrazine) was added to each tube. Following 40 min incubation at room temperature, absorbance was read at 340 nm. The alanine concentration was determined by correlating to standard curves in each assay using Microsoft Excel.

2.3.1.4 Glycerol

Glycerol concentration in the medium was determined by its conversion to dihydroxyacetone phosphate (DHAP) by glycerokinase (GK) and glycerol-3-phosphate dehydrogenase (G3PDH) linked to the reduction of NAD^+ to NADH which absorbs light at 340 nM (Bergmeyer et al. 1983).

5 µL medium samples and glycerol standards (0-25 mM) were added to 1.5 mL microcentrifuge tubes and 500 µL glycerol assay working reagent (0.2 M glycine/ 2 mM $MgCl_2$ buffer pH 9.8, 2.4 mM NAD^+, 2.5 mM ATP, 0.5 U/mL GK, 1 U/mL G3PDH and 1 mM hydrazine) was added to each tube. Following 40 min incubation at room temperature, absorbance was read at 340 nm. The glycerol concentration was determined by correlating to standard curves in each assay using Microsoft Excel.

2.3.1.5 Ammonia

Ammonia concentration was determined spectrophotometrically using an adaption of the method of Fawcett and Scott (Fawcett and Scott 1960).

5 µL medium samples and ammonium chloride standards (0-50 mM) were added to 0.5 mL fresh phenol reagent (0.106 M phenol and 0.17 mM sodium nitroprusside) in

1.5 mL microcentrifuge tubes and then mixed with 0.5 mL fresh hypochlorite reagent (11 mM sodium hypochlorite and 0.125 M NaOH). The mixture was incubated at room temperature for 30 min in darkness before measuring the absorbance at 630 nm using a spectrophotometer.

2.3.2 Gas chromatography-mass spectrometry (GC-MS)

2.3.2.1 Sample preparation

For extracellular metabolites, 20 μL medium samples were mixed with 200 μL methanol and 5 μL myristic acid (3 mg/mL in 2:5:2 water/methanol/isopropanol) and then centrifuged at 12,000 x *g* for 2 min. The supernatants were removed to new 1.5 mL microcentrifuge tubes and lyophilised. The lyophilised samples were stored at -80°C until further analysis. After removal from storage, samples were briefly lyophilised (5 min) again to ensure removal of water and derivitised with 10 µL methoxyamine hydrochloride (MOX, 40 mg/mL in pyridine) for 90 min at 30°C at 190 rpm in an incubator. After that methoxyaminated samples were derivitised with 90 µL N-methyl-N-trimethylsilyltrifluoroacetamide (MSTFA) + 1% (2,2,2-trifluoro-N-methyl-N-(trimethylsilyl)-acetamide, chlorotrimethylsilane) TCMS at 37°C for 30 min. Derivitised samples were then centrifuged at 12,000 x *g* for 2 min and the supernatants were transferred to silanised glass vials immediately prior to analysis by GC-MS.

For intracellular metabolites, ~1 x 10^7 viable cells were collected from culture medium and processed according to Sellick et al. 2011. Cells were quenched in five volume of quenching solution (60% (v/v) methanol, 0.85% (w/v) ammonium bicarbonate, pH 7.4) at -40°C and metabolites were extracted using two 100% (v/v) methanol extractions followed by one water extraction. Five microlitres of myristic acid was added and samples were dried as described above for culture medium samples.

2.3.2.2 Sample injection

Samples were loaded onto a 7685B series Autosampler (Agilent Technologies) in random order to minimise bias and the sequence was programmed into the operating software running on the control PC (MSD Chemstation, Agilent Technologies). Samples were injected with a 7685B series Injector fitted with a 10 µL Agilent Gold Standard Syringe. One microlitre sample injections into the GC inlet were performed after the syringe was washed in methanol and pyridine (2 x 10 µL washes for each).

2.3.2.3 Gas chromatography

An Agilent 7890A Gas Chromatography setup was used fitted with a DB-5ms column (30 m, 0.25 mm, 0.25 µm), with 10 m DuraGuard column. The GC inlet contained a Split-mode glass liner containing inactivated glass wool. The GC-MS was retention time-locked using myristic acid. The GC settings used for a standard GC-MS run are described in Table 2.1.

Table 2.1 Gas Chromatography settings

GC settings	Value	Units
Carrier gas	Helium	
Inlet temperature	250	°C
Split ratio	01:10	
Oven temperature	60	°C
Temperature ramp 1	230 @ 20/min	°C
Temperature ramp 2	240	°C
Temperature ramp 3	270	°C

2.3.2.4 Mass spectrometry

An Agilent 5975C inert XL Quadrupole MSD Mass Spectrometer fitted with a triple-axis detector and using an inter electron impact (EI) source was used. Prior to use, the MS was tuned using the Autotune function with perfluorotributylamine as a calibration compound. The MS settings used for a standards GC-MS run are described in Table 2.2.

Table 2.2 Mass spectroscopy setting

MS setting	Value	Units
Operating mode	Scan	
Source temperature	230	°C
Quadrupole temperature	150	°C
Solvent delay	5.9	Min
Scan range	50 – 600	*m/z*
Scan type	High to Low	
Scan speed	5	Scan/s
Detector gain	5	
Threshold	50	Counts

2.3.2.5 Data analysis

Peak identification and spectral screening with the Fiehn GC/MS mass spectral library was performed. Data were expressed as normalised peak area, where the peak area of a quantifying fragment was normalised with the quantifying peak area of the myristic acid internal standard. The quantification of each metabolite was exported and plotted using Microsoft Excel. The analysis focused to metabolites related to glycolysis, TCA cycle and amino acids. In addition, other detected metabolites were also examined.

2.4 Analysis of protein expression

2.4.1 Enzyme-linked immunosorbent assay (ELISA)

ELISA was used to quantify secreted antibody IgG4 produced by the CHO-LB01 cell line. Maxisorp Nunc 96-well plates were coated overnight at 4°C with 100 ml Goat Anti-Human IgG Fcγ capture antibody diluted in PBS (1 µg/mL). The plates were washed three times with PBS-Tween (0.1% [v/v] Tween 20, 1x PBS) and blocked with 3% [w/v] milk in PBS-Tween for an hour at room temperature. IgG standards (62.5 µg/L to 0.48 µg/L) and the samples were appropriately diluted (1:128000) in sample buffer (1% [w/v] BSA in PBS-Tween) and incubated on plates for an hour at 37°C. The bound antibody was incubated for one hour at room temperature with Goat Anti-Human IgG F(ab')2-HRP-conjugated antibody diluted 1:15000 in the sample buffer and plates were washed three times with PBS-Tween. ELISA reaction was developed by addition of 100 µL tetramethylbenzidine (TMB) diluent chromogenic substrate (1 TMB tablets, 12 mL TMB diluent (50 mM dibasic sodium phosphate, 26.5 mM citric acid in dd. H_2O), 5 µL (v/v) 30% H_2O_2 immediately before use). The reaction was stopped after 5 min incubation by addition of 1 M hydrochloric acid and the absorbance was measured at 450 nm using a microplate reader (Gen 5 software). The antibody concentration in the samples was determined from the linear portion of the standard curves in each assay using Microsoft Excel.

Specific productivity (pg/cell/day) was determined using the following equation:

$$\frac{\left(\frac{P_1 - P_0}{\left\{\frac{X_1 + X_0}{2}\right\}}\right)}{T_1 - T_0}$$

Specific productivity (pg/cell/day) =

- P_0 = Productivity (mg/mL) at first point of analysis
- P_1 = Productivity (mg/mL) at second point of analysis
- X_0 = Cumulative cell number (x10^6 cells/mL) at first point of analysis
- X_1 = Cumulative cell number (x10^6 cells/mL) at second point of analysis
- T_0 = Day of first point of analysis
- T_1 = Day of second point of analysis

2.4.2 Protein extraction

~5x10^6 CHO cells from cultures were centrifuged for 2 min at 12,000 x *g* at room temperature. The supernatant was removed, the cell pellet was resuspended with 1 mL of PBS, and recentrifuged as before. The resultant supernatant was discarded and cells were re-suspended in 500 µL 2X sample buffer (20% [v/v] glycerol, 7 mM SDS, 6.2 M Trizma™, 0.01% [w/v] bromophenol blue, pH 6.8). The solution was sheared by 10 passages using a syringe fitted with a 21 gauge needle and was transferred to a fresh 1.5 mL microcentrifuge tube and stored at -80°C until further analysis.

2.4.3 SDS-PAGE

The Bio-Rad Mini-PROTEAN Tetra system was used for SDS PAGE. This system was used with a 12.5% (w/v) separating gel overlaid by a 12.5% (w/v) stacking gel. The separating gel for two gels was prepared by mixing 6.2 mL Protogel (30% [w/v] acrylamide), 3.75 mL separating buffer (1.5 M TrizmaTM, 14 mM SDS, pH 8.8), and

5.05 mL dd.H_2O. The stacking gel was prepared by mixing 1.6 mL Protogel, 2.5 mL stacking buffer (0.5 M TrizmaTM, 14 mM SDS, pH 6.8) and 6 mL dd.H_2O. Ammonium persulphate (final concentration 0.2 µg/mL) and 0.2% (v/v) TEMED was added to initiate polymerisation.

Extracted protein samples (Section 2.4.2) were mixed with 2-mercaptoethanol to a final concentration of 1.8% (v/v). The samples were heated at 100°C for 5 min, and cooled before loading into gels (60 µL sample was added to each lane) with a pre-stained broad range molecular weight markers. Electrophoresis was performed in SDS running buffer (10 mM TrizmaTM, 80 mM glycine, and 1.4 mM SDS) using 60 V until the tracking dye front reached the bottom of the stacking gel. Then the gel was run at 200 V until the dye front reached the bottom of the separating gel. The gel was used to identify proteins by Western blot (Section 2.4.4).

2.4.4 Western blot

Proteins that were separated by SDS-PAGE (Section 2.4.3) were transferred to nitrocellulose membranes by pre-soaking the gel, nitrocellulose membrane and filter paper in blotting buffer (25 mM TrizmaTM, 190 mM glycine, 20% [v/v] methanol, pH 7.4) for 5 min. After that a soaked filter paper, nitrocellulose membrane, the gel and the second piece of filter paper were placed (in that order) onto a Bio-Rad Trans-Blot SD Semi-Dry Transfer Cell. The transfer was performed for 40 min at 15 V.

When the transfer was finished, the nitrocellulose membrane was blocked to prevent non-specific binding by incubation in blocking buffer (3% [w/v] milk in PBS Tween (1% [v/v] Tween-20)) for 1 h with shaking at room temperature. After blocking, the blocking buffer was discarded and the membrane was incubated with primary antibody (which was diluted to the appropriate concentration, Table 2.3) in blocking buffer overnight at

4°C with shaking. Afterwards, the membrane was washed three times in PBS Tween for 5 min each wash. The secondary antibody was diluted to the appropriate concentration in blocking buffer (Table 2.3) and was incubated with the membrane for 1 h at room temperature with shaking. The membrane was then washed three times in PBS Tween for 5 min each wash and was rinsed with PBS to remove residual Tween-20. The membrane was scanned by Infrared Fluorescence (LI-COR system). The intensity of bands was determined by densitometric analysis using ImageStudioLite software.

Table 2.3 Antibodies used for Western blot.

The primary and secondary antibody combinations and dilutions used in Western blots are described.

Primary antibody	Dilution	Secondary antibody	Dilution
Cell Signaling rabbit anti-MDH II	1:1000	Licor IRDye® 800CW goat anti-rabbit	1:15000
SantaCruz rabbit anti-MDH II	1:1000	Licor IRDye® 800CW goat anti-rabbit	1:15000
Abnova mouse anti-MDH II	1:1000	Licor IRDye® 800CW goat anti-mouse	1:15000
SantaCruz mouse anti-AR	1:1000	Licor IRDye® 800CW goat anti-mouse	1:15000
SantaCruz mouse anti-ERK	1:1000	Licor IRDye® 800CW goat anti-mouse	1:15000

2.5 Determination of cellular phenotype

2.5.1 Oxygen consumption

Oxygen consumption rate was measured in 3 mL samples of cells (in culture medium) using a Clark-type oxygen cell calibrated between the maximum dissolved oxygen concentration in MilliQ water at 37°C (oxygen saturation) and the minimum dissolved oxygen concentration (set by the addition of sodium dithionite), respectively (Clark 1956). Oxygen consumption was measured for 10 min or until oxygen amount reached

zero. Data was collected using a SE120 BBC Chart Recorder (Goerz Metawatt) and transferred to an Excel file. Oxygen saturation (%) was converted into molarity (assuming a molecular oxygen solubility of 6.8 mg/L in pure water at 37°C and atmospheric pressure) and the rate of change was divided by the viable cell density to obtain the utilization rate of oxygen (moles per cell per min).

2.5.2 Mitochondrial membrane potential and cellular content of mitochondria and endoplasmic reticulum

Mitochondrial membrane potential, mitochondrial content and ER content were measured with Rhodamine123 (Rh123), MitoTracker® Green and ER-Tracker™ Green, respectively.

Rh123, MitoTracker® Green and ER-Tracker™ Green stock solutions were prepared in DMSO at concentrations of 1mM and were stored at -20°C. Working solutions of Rh123 (10 nM), MitoTracker® Green (10 nM) and ER-Tracker™ Green (250 nM) were prepared freshly in culture medium. Propidium iodide (PI, 1.5 mM in sterile water) (Life Technologies, UK) was used as a cell viability stain. The working solution of PI (1.5 mM) was prepared freshly in PBS.

$2x10^6$ cells were harvested on different days of culture, centrifuged for 5 min at 300 x *g*, and pellets were resuspended in working solutions of either Rh123, MitoTracker® Green or ER-Tracker™ Green and incubated for 15 min at 37°C before analysis. The cells were pelleted from suspension by centrifugation for 5 min at 300 x *g*, and the pellets were resuspended in working solution of PI and incubated for 2-3 min at room temperature prior to analysis by flow cytometry using a BD Accuri™ (BD Bioscience, UK).

2.6 Isolation, handling and analysis of RNA

2.6.1 RNA extraction

~$1x10^7$ cells were harvested at appropriate days of culture and, after centrifugation, pellets were re-suspended in 1 mL TRIzol® reagent and were stored at -80°C until purification. When required for analysis, the homogenized samples were incubated for 5 min at room temperature. 200 µL chloroform was added to each sample and tubes were shaken vigorously by hand for 15 s. After incubation for 3 min at room temperature, samples were centrifuged for 15 min at 12,000 x *g* at 4°C. The upper aqueous phase was transferred to a 1.5 mL microcentrifuge tube and RNA was precipitated by the addition of 500 µL isopropanol. The mixture was incubated for 10 min at room temperature and then centrifuged for 10 min at 12,000 x *g* at 4°C.

The supernatant was removed and the pellet was washed with 1 mL 75% (v/v) ethanol (in DEPC-treated dd.H2O) by vortex mixing. The samples were centrifuged for 5 min at 7,500 x *g* at 4°C and were air-dried for 5-10 min. After that, the pellets were resuspended in 30 µL of DEPC-treated dd.H_2O. This solution (containing RNA) was stored at -80°C until required for analysis.

2.6.2 Quantification of nucleic acid concentration

DNA and RNA concentration was determined using a NanoDrop® ND-1000 UV-Vis Spectrophotometer. The purity was assessed by using the A260nm/A280nm ratio where a ratio of 1.6-2.0 was considered pure.

2.6.3 DNase treatment of RNA

For further processing, 1 mg of each RNA sample (Section 2.6.1) was treated with 1 µL DNase I in 1x reaction buffer and the solution was made up to a final volume of 10 µL with DEPC-treated dd.H_2O. The mixtures were incubated for 30 min at 37°C, and then 5 µL 0.05 M EDTA was added to inactivate the DNase I. Samples were heated for 10 min at 75°C to denature the DNase I and unfold the RNA.

2.6.4 cDNA synthesis

cDNA was generated using a Tetro cDNA synthesis kit. Samples of quantified DNase-treated RNA-containing samples (up to 5 µg) (Section 2.6.3) were mixed with 1 µL oligo $(dT)_{18}$ primer, 1 µL 10 mM dNTP mix, 4 µL 5x RT buffer, 1 µL RNase inhibitor, 1 µL Tetro Reverse Transcriptase and DEPC-treated water to generate final volume 20 µL. The mixture was mixed gently by pipetting and was incubated for 30 min at 45°C. The reaction was terminated by incubation of the samples for 5 min at 85°C and reaction mixes were stored at -20°C until further analysis.

2.6.5 PCR

Primers were designed using Primer3 Input and NCBI/Primer-BLAST tool. All primers were purchased from Eurofins. A list of PCR primers used is shown in Table 2.4.

PCR reactions were prepared using BIOTAQ™ DNA Polymerase (Bioline, UK) according to the manufacturer's instruction. Reaction mixes were placed in TC-3000X Thermal Cycler with the following settings: 5 min at 95°C, followed by 30 cycles of denaturation for 30 s at 95°C, annealing for 30 s at X°C (where X is the Ta of the primer pair) and elongation for 30 s at 72°C. A final elongation step was performed for 10 min at 72°C. Once the PCR program had finished the samples were stored at 4°C until analysis by agarose gel electrophoresis.

Table 2.4 PCR and q-RT PCR Primers

Primer	Direction	Primer sequence 5'-3'	Tm (°C)	Ta (°C)
B2M	Sense	ATATGCCTGCAGAGTTACACA CACCACTC	66.7	60
	Antisense	GCCATTACTATTCCTTCCGTG TGCATAGA	65.3	60
PDHa1	Sense	AGGACGAAGAGGAGGTTGTG	59.4	60
	Antisense	GCAGCGCCATCACCATATAG	59.4	60
LDHa	Sense	ATACCGACAAGGAGCAGTGG	59.4	60
	Antisense	CCCAGGACACAAGGAACACT	59.4	60
CS	Sense	GATTGTGCCCAACATCCTCT	57.3	60
	Antisense	GGCCTTTCTAGTGGGAAACC	59.4	60
OGDH	Sense	AGAGCGGTTTCTGCAGATGT	57.3	60
	Antisense	GGGATTTCGGAGTGAAGACA	57.3	60
MDH2	Sense	CGAGACCAGAGCAAATGTGA	57.3	60
	Antisense	ACCAATGACAGGCACATTGA	55.3	60
GLUD1	Sense	GGTGAATCTGATGGGAGCAT	57.3	60
	Antisense	GACTTTGGGTGCATTGGACT	57.3	60
Slc25A11	Sense	TTCTGCTGAAAGCCCTGATT	55.3	58
	Antisense	CTCGAGCCATGGTAGGGAT	58.8	58
Slc25A12	Sense	GGCTATACAAGGGTGCCAAA	57.3	58
	Antisense	GACCCCGCTGTATGTTGTCT	59.4	58
MDHII primer set 1	Sense	ATGTTGTCCGCCCTCGC	57.6	60
	Antisense	ACCAATGACAGGCACATTGA	55.3	60
MDHII primer set 2	Sense	CTGGCTAACTAGAGAACCCA	57.3	60
	Antisense	CTGGCAACTAGAAGGCACAG	59.4	60
IgH	Sense	GGCTCTGCACAACCACTACA	59.4	58
	Antisense	TCAGGTTCAGGGGGAGGT	58.2	58

Tm = melting temperature
Ta = annealing temperature

2.6.6 Agarose gel electrophoresis

Agarose powder was dissolved in 1x TBE buffer (0.89 M Trizma™, 0.89 M orthoboric acid, and 10 mM EDTA) to give a final concentration of 1% (w/v) or 2% (w/v). This mixture was heated and then allowed to cool to ~55°C before SYBR Safe was added to the liquid agarose. The mixture was poured into agarose gel cassettes and left until it was set. Afterwards, 1x TBE buffer was added to cover the gel. PCR products (Section 2.6.5) were mixed with 5x sample loading buffer (supplied with HyperLadderTM) and 10 µL loaded into the wells in the gel, with a molecular weight marker (HyperLadder™ 25 bp, or HyperLadder™ 1 kb) included for comparison. Electrophoresis was performed for approximately 45 min at 100v until the dye front migrated sufficiently to visualise bands under UV illumination. Pictures were taken using a Bio Rad Gel Doc system.

In case of RNA samples, RNA samples were mixed with 2x RNA loading dye and were incubated at 65°C for 5 min to denature RNA before loading into wells.

2.6.7 Quantitative Real time (qRT) PCR

Primers were designed as described previously (Section 2.6.5). A list of qRT PCR primers used is shown in Table 2.4.

qRT-PCR was performed in triplicate with SensiMix™ SYBR No-Rox (Bioline, UK) according to the manufacturer's instruction using MJ white 96-well plate. The qRT-PCR reaction was performed using a Chromo 4 thermocycler with the following settings: 10 min at 95°C, followed by 35 cycles of denaturation for 10 s at 95°C, annealing for 10 s at X°C (where X is the Ta of the primer pair), elongation for 20 s at 72°C, denaturation for 1 s at 76°C. A final elongation step was performed for 10 min at 72°C and a melting curve was generated to check the quality of the amplified product.

Data from qRT-PCR products was quantified using Opticon Monitor analysis software according to the manufacturer's instructions. Standard curves were generated in each gene by dilution cDNA in 1:5, 1:10 and 1:100 and log [cDNA] was plotted against Ct value. Relative mRNA expression was calculated compared to the standard curve and this was normalised against the expression of β-2-Microglobulin (*B2m*) in each sample.

2.7 Isolation of genomic DNA

An adapted version of the protocol detailed by Blin & Stafford (1976) was used to extract genomic DNA from CHO cells.

~$2x10^7$ cells were harvested by centrifugation at 100 x *g* for 10 min at room temperature. The cell pellet was washed three times with 1XPBS with centrifugation between each wash as above. The final pellet was then resuspended in 100 µL of 1XPBS and 3 mL of EDTA-Sarcosine solution (0.1M EDTA, pH8.0, containing 0.5% [w/v] N-Lauroyl-Sarcosine) was added to the pellet in a dropwise fashion with continuous gentle mixing. After that 60 µL of Proteinase K (10 mg/mL) and 10 µL of RNase A (10 mg/mL) was added. The mixture was incubated at 55°C for 2 h and mixed by inversion every 15 min.

Afterwards, the mixture was mixed with an equal volume of phenol/chloroform/isoamyl alcohol (25:24:1) for 5 min and then centrifuged at 13,000 x *g* for 10 min at room temperature. The upper aqueous phase was removed into a fresh tube. This step was repeated three times as above. Four volumes of ddH_2O and 0.5 volumes of 3 M sodium acetate (pH 5.2) were added to the final aqueous phase. DNA was precipitated by addition of 3 volumes of 100% ethanol. Solutions were mixed by inversion and the mixture was centrifuged at 13,000 x *g* for 10 min. The supernatant was removed and discarded. The pellet was washed with 70% ethanol and re-centrifuged as above. The

final DNA pellet was air-dried for 5-10 min and resuspended in 200 µL of ddH_2O. DNA was quantified as described in Section 2.6.2.

2.8 EBPC inhibitor preparation

Stock solution of EBPC (5 mM) was prepared in dd. H_2O and sterilized by passage through a 0.02 µm filter before addition. EBPC was added into culture medium on day 4 to give final concentrations of 50 mM.

2.9 siRNA

2.9.1 siRNA design

The coding sequence of *Cricetulus griseus* aldo-keto reductase family 1, member B1 (aldose reductase (AR), Akr1b1) mRNA (NCBI accession XM_003503181.2) were used to design siRNA with Eurofins DNA siRNA design service. Control scrambled siRNA (scr) was designed using InvivoGen scrambled siRNA wizard. All siRNA were purchased from Eurofins (Table 2.5).

2.9.2 siRNA transfection

50 or 100 nM siRNA (in a volume of 5 µL) was mixed with 5 µL RNAiMAX and 500 µL CD OptiCHO^{TM} medium. The mixture was then incubated for 20 min at room temperature. Afterwards, the mixture was added dropwise to the cell culture at day 3. Cell samples at day 6 and 8 were collect to determine cell number and viability (Section 2.2.2), antibody production (Section 2.4.1) and AR protein expression by Western blot (Section 2.4.4).

Table 2.5 siRNA designed to target *Akr1b1*

siRNA name	Strand	Sequence (5'-3')
siAR_1	Sense	UUGCAUCCAAGUACAAUAA
	Antisense	UUAUUGUACUUGGAUGCAA
siAR_2	Sense	GAAUUGCUGAGAACCUGAA
	Antisense	UUCAGGUUCUCAGCAAUUC
siAR_3	Sense	CUCAGGAGAAGCUGAUUGA
	Antisense	UCAAUCAGCUUCUCCUGAG
AR_scr	Sense	GACAUUACGAACUCAAUUA
	Antisense	UAAUUGAGUUCGUAAUGUC

2.10 Generation and purification of plasmid vector in bacterial cells

2.10.1 Generation of competent bacterial cells

100 µL DH5α *E. coli* cells were cultured in 10 mL Luria Bertani (LB) broth medium (1% [w/v] tryptone, 0.5% [w/v] yeast extract and 0.5% [w/v] sodium chloride) overnight at 37°C in shaking incubator. 2 mL of the overnight culture were added to 40 mL LB broth and incubated at 37°C in shaking incubator until the culture was in the mid log growth phase (absorbance at 550 nm was approximately 0.3-0.6). Cells were harvested by centrifugation at 2,700 x *g* for 5 min at 4°C and cells were resuspended in 20 mL ice-cold sterile 50 mM calcium chloride and incubated on ice for 20 min. Cells were re-centrifuged as above and were resuspended in 2.5 mL of ice-cold sterile 50 mM calcium chloride containing 10% [v/v] glycerol. 200 µL Cells were aliquot into 0.5 mL tubes and were store at 80°C for 3-4 months.

2.10.2 Transformation of competent bacterial cells

10 ng plasmid DNA (Section 2.11.1) was added to 100 µL competent cells (Section 2.10.1) and incubated on ice for 30 min. After that the cells were heat-shocked at 42°C for 45 seconds and then placed on ice with addition of 1 mL LB broth immediately. The cells were incubated at 37°C for 1 h in shaking incubator and then 200 µL transformation mixture were spread onto LB agar plate containing the appropriate antibiotic and when appropriate for blue white screening, plates were pre-spread with 40 µL 100 mM IPTG and 40 µL 40 mg/mL X-GAL (dissolved in DMSO). The plates were incubated overnight at 37°C in incubator and colonies were then selected.

2.10.3 Purification of plasmid DNA

A single *E. coli* colony transformed with plasmid DNA (Section 2.10.2) was picked and cultured in 5 mL LB medium containing antibiotic (as appropriate) overnight at 37°C in shaking incubator. The cells were harvested and DNA was extracted using QIAprep Spin Miniprep kits according to the manufacturer's instructions.

2.11 Generation of stable CHO cells overexpressing MDH II

2.11.1 Vector construction

Cricetulus griseus Mdh2 nucleotide sequence (NCBI accession XM_007641683.1) was introduced into pcDNA3.1 vector (Figure 2.1) by GeneArt® Gene Synthesis to generate a *Mdh2* construction vector (Figure 2.2). The *Mdh2* construction vector was transformed into *E. coli* (Section 2.10.2) to amplify and maintain this plasmid vector and it was purified (Section 2.10.3) for transfection into CHO cells (Section 2.11.2).

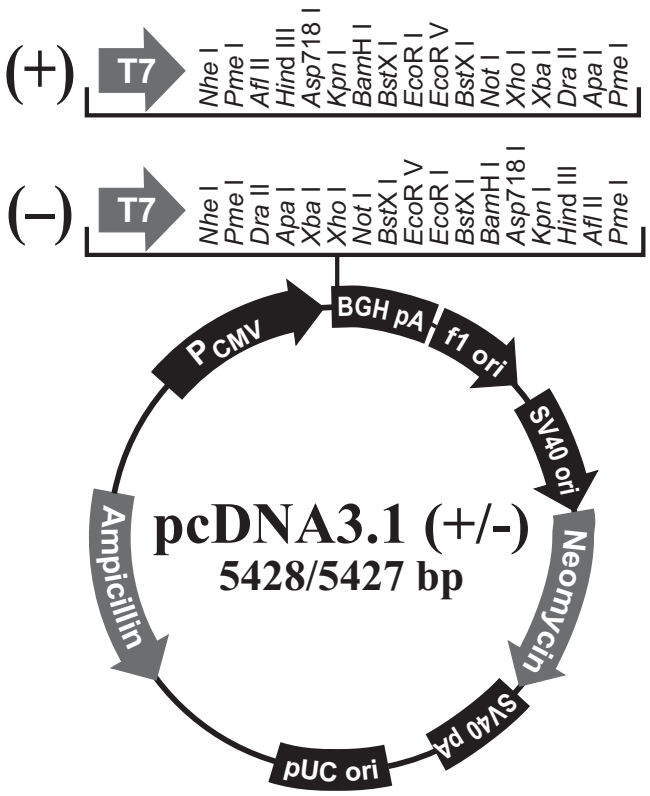

Figure 2.1 pcDNA3.1 vector

pcDNA3.1 vector contains a CMV promoter, T7 promoter, multiple cloning site, BGH reverse priming site, f1 origin, Neomycin/kanamycin resistance gene, pUC origin and ampicillin resistance gene.

(https://www.thermofisher.com/order/catalog/product/V79020).

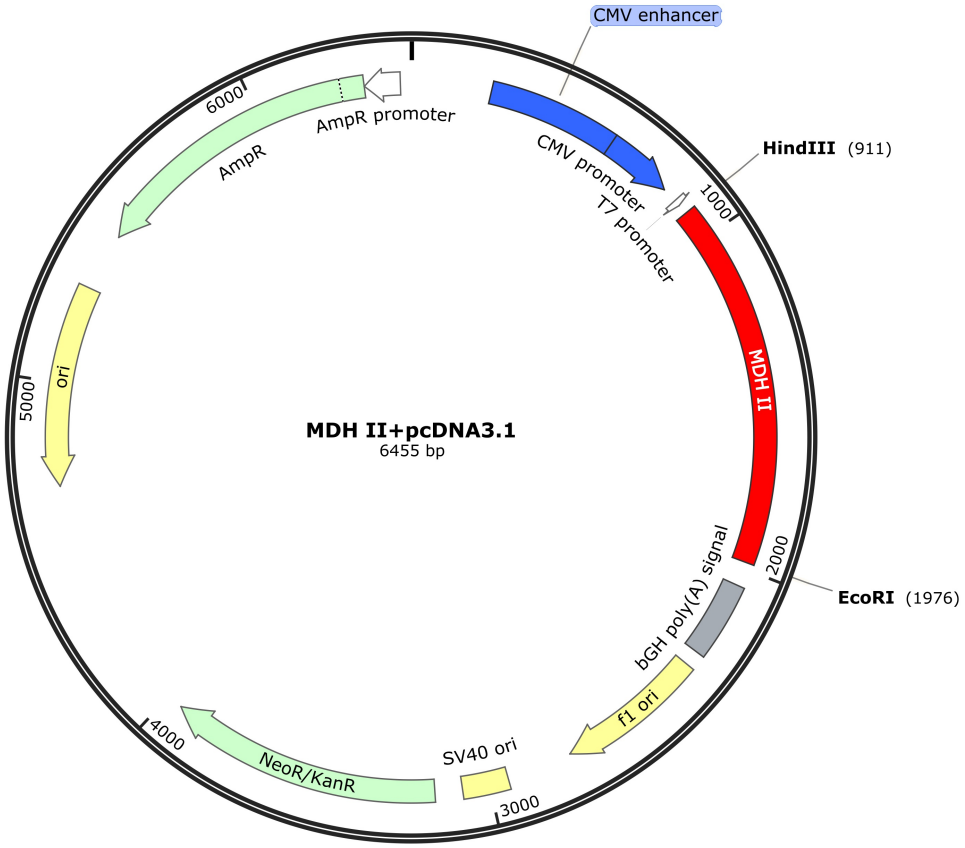

Figure 2.2 *Mdh2* construction vector

Mdh2 nucleotide sequence (red) was introduced into pcDNA3.1 vector by GeneArt® Gene Synthesis. Two restriction sizes (*Hind*III and *Eco*RI) were added into upstream and downstream of *Mdh2* sequence. This vector consisted of the components of pcDNA3.1 vector (Figure 2.1).

2.11.2 Transfection of CHO cells

CHO-LB01 cells were transfected with the *Mdh2* construction vector (Section 2.10.3). 1×10^7 cells were harvested by centrifugation at 100 x *g* for 10 min at room temperature. The supernatant was removed and the cell pellet was washed in 50 mL cold PBS and re-centrifuged as above. The final cell pellet was resuspended in 950 µL PBS. Two electroporation cuvettes were prepared, one containing 100 µL *Mdh2* construction vector and another one containing 100 µL sterile water as a control. A 950 µL cell-PBS suspension was added to each cuvette and the mixtures were incubated on ice for

5 min. Transfection was achieved by electroporation, using the BIORAD pulse controller/gene pulser. Two consecutive pulses (1500 volts, 3 µfd) were applied to each mixture. Afterwards, cuvettes containing cells were placed on ice for 5 min and then limiting dilution cloning was performed (Section 2.11.3).

2.11.3 Limiting dilution cloning

After transfection (Section 2.11.2), cells were diluted as below in non-selective medium (CD OptiCHO^{TM} medium):

(1) 1 mL of transfected cells plus 29 mL medium

(2) 10 mL of dilution (1) plus 30 mL medium

(3) 10 mL of dilution (2) plus 40 mL medium

For each dilution, 5x96 well plates were prepared by addition of 50 µL of each dilution per well. The plates were wrapped in foil to minimise evaporation of the medium and incubated at 37°C and 5% CO_2. Approximately 24 h later 150 µL fresh culture media plus 150 µg/mL geneticin was added to each well containing transfected cells to select positive clones. Plates were wrapped again in foil and incubated at 37°C and 5% CO_2 for about 14 days. The plates were then screened by light microscopy to identify wells with single colonies. Selected wells were fed by replacing the old medium with 200 µL fresh culture media containing 150 µg/mL geneticin. Cells were monitored for growth by light microscopy and transferred to 24-well plates when confluence was reached. Once in 24-well plates, cells were fed with culture media containing 150 µg/mL geneticin in a final volume of 1 mL and when confluence was reached the cells were transferred to 6-well plates. Cells were monitored by light microscopy until confluent and then transferred to 50 mL Mini Bioreactor (Section 2.2.1) to determine cell number and viability (Section 2.2.2), antibody production (Section 2.4.1), *Mdh2* gene expression (Section 2.6) and MDH II protein expression by Western blot (Section 2.4.4). Frozen stocks were created for all selected clones (Section 2.2.3).

2.12 RNA-Seq

RNA samples at day 4 were extracted (Section 2.6.1) and the quantity and purity were assessed using a NanoDrop® ND-1000 UV-Vis Spectrophotometer (Section 2.6.2) and agarose gel electrophoresis (Section 2.6.6). 0.01-4 μg of RNA samples were submitted to Genomic Technology Core Facility to perform sample preparation following TruSeq® Stranded mRNA Sample Preparation Guideline and sequencing using Illumina HiSeq2500 machine.

Afterwards, sequencing data underwent data preprocessing using *FASTQC* and *Trimmamotic* software, alignment using *STAR* software, counting using *HTSeq* software, normalization and identification of differential expression using *DESeq2.* These aspects were undertaken by the Bioinformatic Core Facility in the Faculty of Life Sciences.

The Ingenuity Pathway Analysis (IPA®) program was used to identify canonical pathways of differentially expressed genes.

2.13 Statistical analysis

Error bars represent the standard error of the mean (SEM) for three, five or six biological replicates, as specified for each experiment. SEM was applied due to use of separate biological replicate. Statistical significance was determined with independent samples t-test at $p < 0.05$ and $p < 0.1$.

CHAPTER 3

Effect of feeding nutrients on cell culture performances, metabolite profiles, gene expression and cellular phenotype of CHO cells

3.1 Introduction

As reported in Section 1.5, two main types of approach (optimization of the composition of culture medium and cell engineering) have been undertaken in order to increase the productivity of CHO cells. In medium optimization, several strategies have been conducted to improve culture longevity, including approaches to decrease the formation of metabolites that may negatively affect cell status and achievement of high titre (Section 1.5.1). The current study focused on approaches that might increase the flux in the TCA cycle due to the initial interpretation of earlier work on culture feeds in this laboratory (Sellick et al., 2011) and the positive correlation reported between antibody production and TCA cycle flux (Lee et al., 2015, Templeton et al., 2013) (Section 1.3.4). Therefore, we hypothesized that increased TCA cycle flux and related metabolism would enhance the growth and/or productivity of CHO cells (Section 1.6). Thus, the purpose of this chapter is to describe the effect of nutrient supplementations that may support TCA cycle flux on cell culture performance, metabolite profile and cellular phenotype of CHO-LB01 cells. The knowledge gained from the work described in this chapter is intended to clarify these relationships in CHO cells and define sites for potential engineering.

The nutrient supplementation regimes in this study were selected based on information provided from the previous work of Sellick et al. (2011) and Donamaria (2012). Sellick et al. (2011) reported that the combination of Glc, Py, Asp, Asn and Glu increased maximum viable cell density and antibody production (by 35% and 100%, respectively) compared with unfed cells. In addition, Donamaria (2012) found that antibody production was significantly greater (by 17%) than the control when HB was added. Asn and Asp, or Py and HB may support the TCA cycle at the point of oxaloacetate and acetyl-CoA, respectively, while Glu can support the TCA cycle via input at αKG. For this present study, these nutrients (Asn, Asp, Glu, Py and HB) were selected in order to identify which nutrient had an effect on cell growth, antibody production, metabolite profiles and cellular phenotype of CHO-LB01 cells by studying single nutrient and combined nutrient

feeding regimes to extend the knowledge for optimized feed composition (Chapter 4) and to narrow down the target genes for cell engineering (Chapter 5).

3.2 Effect of nutrient feeding on cell growth and antibody production

Based on the results of Sellick et al. (2011) and Donamaria (2012), five nutrients (1.5 mM Asn, 1.5 mM Asp, 1.36 mM Glu, 2.3 mM Py and 10 mM HB) were added as individual supplements to CHO-LB01 culture medium on day 4 of batch culture (Section 2.2.4) in a single experiment with three individual flasks for each condition to screen the response on cell growth and antibody production. Medium samples were collected every day to study cell growth (Section 2.2.2) and antibody production (Section 2.4.1).

In the absence of nutrient (control), cells exhibited growth with an exponential phase over the first 5 days of culture, a subsequent stationary phase until day 7 or 8 followed by decline phase, with no viable cells remaining after 10 or 12 days (Figure 3.1A). Cells reached maximum viable cell density at ~$7x10^6$ cells/mL at day 5, 6 or 7 (Figure 3.1A). The pattern of cell growth and maximum viable cell density of the control was similar to that previously reported by our laboratory (Sellick et al. 2011). In term of antibody production, the control produced a maximum yield of antibody about 0.4-0.6 g/L at day 10 (Figure 3.1B). This concentration was slightly greater than the concentration of IgG4 (0.4 g/L) that was produced from CHO-LB01 cells in the studies of Sellick et al. (2011). Addition of Asn significantly increased maximum viable cell density to $1x10^7$ cells/mL at day 7 and the cells died earlier (day 9) than observed in control conditions (where they died at day 10) (Figure 3.1A). This result is consistent with that of Sellick et al. (2011) who reported that CHO-LB01 cells died more quickly when fed with the combination of Asn, Asp, Glu and Py. Although, increased maximum viable cell number was observed,

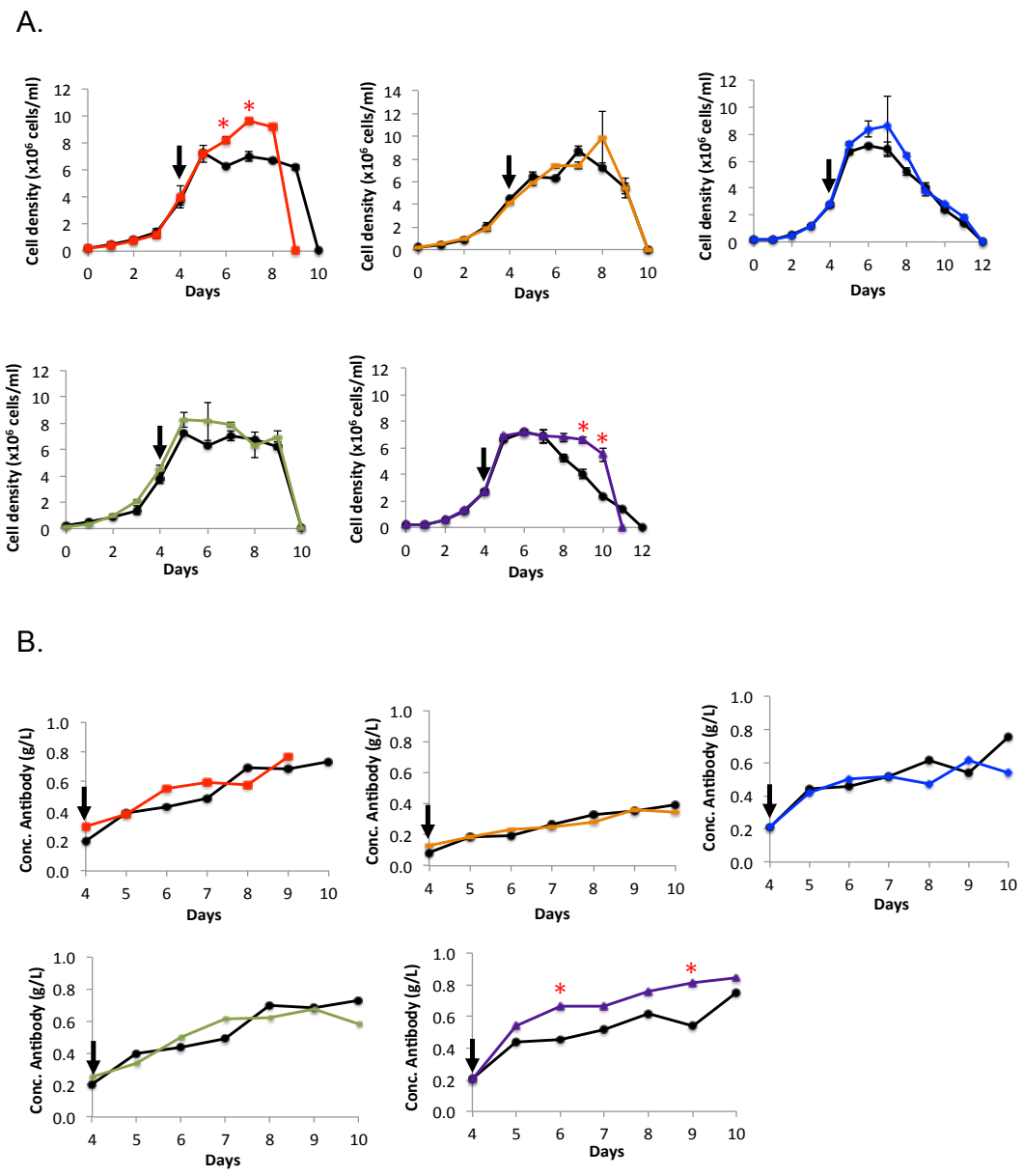

Figure 3.1 Screening cell growth and antibody production of LB01 cells in response to nutrient addition.

Viable cell density (A) and antibody production (B) were measured throughout batch culture. Culture was performed in CD OptiCHO™ medium as described in Section 2.2.1. All experiments were performed with a parallel unsupplemented control (black). Additions of nutrients were made individually at day 4 (shown by the arrow) of culture (Section 2.2.4) to give the defined final concentrations upon addition: Asn (1.5 mM, red), Asp (1.5 mM, orange), Glu (1.36 mM, blue), Py (2.3 mM, green) and HB (10 mM, purple). Medium samples were collected for cell counts (Section 2.2.2) and ELISA (Section 2.4.1). Values present the data from a single investigation with each nutrient. Each experiment consisted of 3 individual flasks to produce replicates and values presented are means ± SEM. * indicates significant difference from control at $p < 0.05$.

the maximum yield of antibody was not increased (0.6 g/L) (Figure 3.1B). In contrast, addition of HB did not increase maximum viable cell density (as observed in the presence of Asn) but the stationary phase was maintained for two additional days compared to the control (Figure 3.1A). In addition, the maximum yield of antibody was significantly increased to 0.8 g/L (Figure 3.1B). Supplementation with Asp, Glu or Py alone had no effect on cell growth or antibody production (Figure 3.1). Therefore, from these initial results, Asn and HB were used as main supplementary nutrients for further work.

In a detailed follow-up study, the impact of addition of Asn and HB on cell growth and antibody production was assessed individually and in combination. In the control (Figure 3.2A), the pattern of cell growth and maximum viable cell density of the control was similar to the previous results (Figure 3.1A). Again, addition of Asn significantly increased the maximum viable cell density to ~$9x10^6$ cells/mL at day 6 and the cells died earlier (Figure 3.2A) as observed in previous result of Asn feeding (Figure 3.1A). In keeping with the previous result (Figure 3.1A), supplementation with HB did not change the maximum viable cell density and the cells maintained a more prolonged higher viable cell density than the control for one day (Figure 3.2A). In combination, Asn and HB generated a significantly increased viable cell density (about $1x10^7$ cells/mL at day 6) with the early death (day 9), properties similar to those observed with feeding Asn alone (Figure 3.2A). In term of cumulative cell number, although addition of Asn altered a shift in the profile of cell growth, the cumulative cell number (about $4x10^7$ cells/mL attained by day 10) was very similar for all feeding regimes and the control (Figure 3.2B).

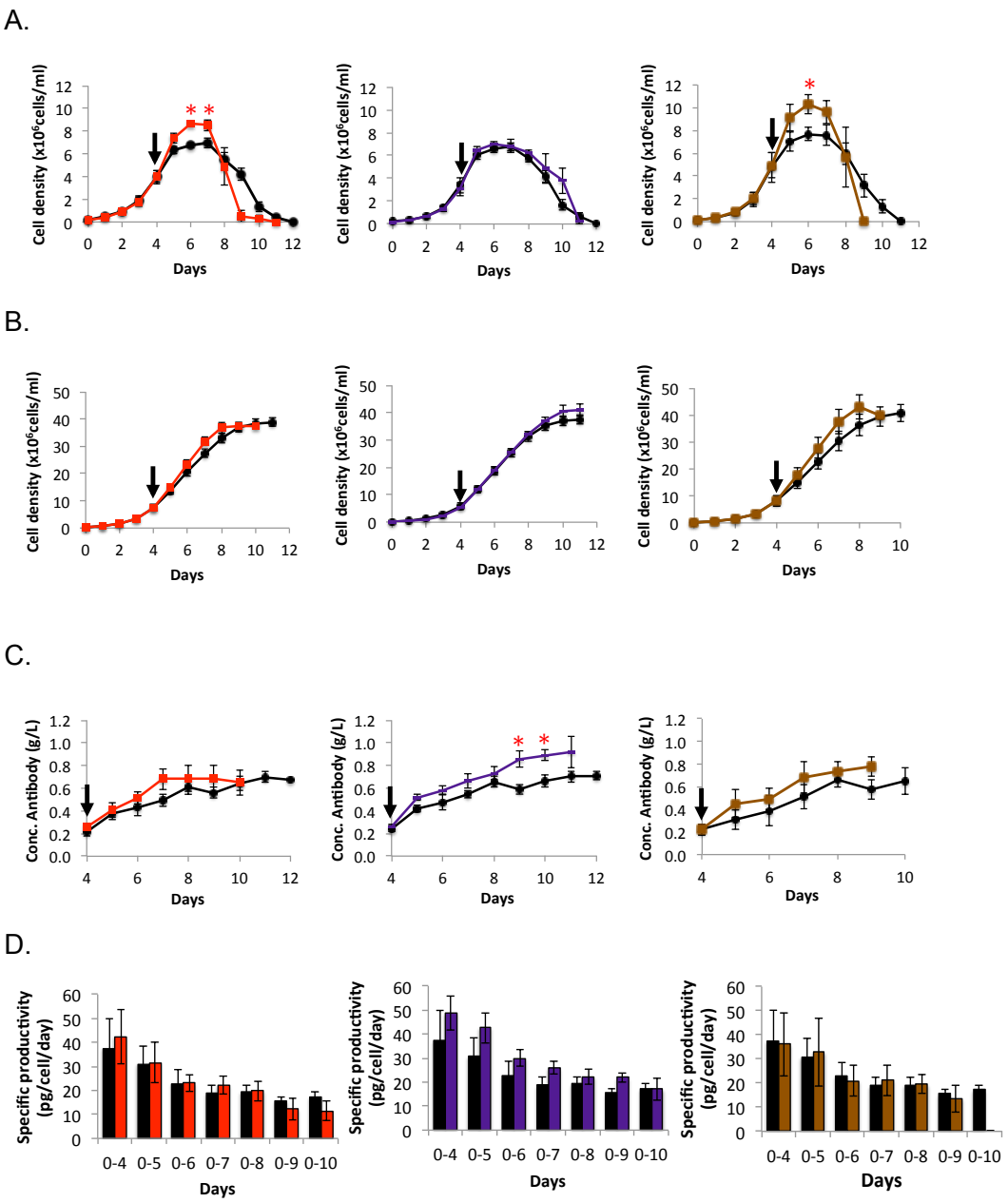

Figure 3.2 Cell growth and antibody production of LB01 cells in response to Asn and HB.

Viable cell density (A), cumulative cell number (B), antibody production (C) and specific productivity (D) were measured for LB01 cells throughout batch culture in CD OptiCHO™ (control, black symbols) or with supplemention at day 4 of culture (the arrow presents the time of addition) with Asn (1.5 mM, red) or HB (10 mM, purple) or both in combination (brown) (Section 2.2.4). Medium samples were collected for cell counts (Section 2.2.2) and ELISA (Section 2.4.1). Values presented are mean ± SEM for six replicates for Asn, five replicates for HB and three replicates for Asn plus HB, all shown against their respective controls. * indicates significant difference from control at $p < 0.05$.

Similar to the results in Figure 3.1B the maximum yield of antibody from control cultures was about 0.6 g/L at day 12 (Figure 3.2C). Addition of HB produced a significantly greater yield of antibody than the control by day 9 of culture (reaching 0.9 g/L) whereas feeding with Asn had no effect on antibody yield (Figure 3.2C). The combination of Asn and HB followed the same pattern of antibody production obtained by feeding Asn alone. Whilst there is no molecular interpretation for this effect, it can be surmised that the rapidity of cell death in the presence of Asn prevents the increased antibody yield associated with the prolonged survival in the presence of HB alone. Greatest specific productivity was found between days 0-4 of culture for all conditions (Figure 3.2D). Maximum specific productivities of about 40 pg/cell/day were observed for control, Asn-fed, and Asn plus HB-fed whilst feeding HB generated a maximum specific productivity slightly greater (50 pg/cell/day) than the control (Figure 3.2D).

In summary, the results indicate differential effects of Asn and HB on cell growth and antibody production while addition of Asp, Glu and Py did not affect cell growth and antibody production of CHO-LB01 cells. It is possible that transportation of Asp and Glu into the cell or mitochondria might be different from the transport of Asn and HB due to the net charge of them (Altamirano et al., 2001, Newsholme et al., 2003). Consequently, Asp and Glu may be transported into cell or mitochondria more limited than that of Asn and HB. An alternative explanation is that the concentration of Asp and Glu might affect the function of malate-aspartate shuttle lead to disturbing of redox balance. However, Zang et al. (2006) reported that cells cultured in glutamate-based culture increased recombinant protein production by 18% compared to that in glutamine-based culture but that the pattern of cell growth was similar. In case of Py, high concentration of Py might lead to increase lactate accumulation inside the cells which might be toxic to cells (Wilkens et al., 2011). However, metabolite profiles of cells fed these nutrients (Asp, Glu and Py) have not conducted in this study so it is impossible to give a clear explanation. Thus, investigation of metabolite profiles of cells fed Asp, Glu or Py would be required for better understanding in the future. In relation to the significantly increased antibody

yield observed in the presence of HB, this work represents the first study to examine the consequences of addition of HB. The addition of HB offers a simple effective strategy to increase recombinant protein production of CHO-LB01 cells.

Feeding Asn had a significant effect on cell growth and increased maximum cell density but led to an earlier cell death. Whilst the results reported here are internally consistent and robust there are conflicting reports on the effect of feeding Asn in CHO cell cultures. Kurano et al. (1990) found that a single feed of Asn caused enhanced maximum cell density of CHO cells (no detail of CHO cell type was given) cultured in standard MEM-a medium with serum. This result is consistent with the result of the current work but the cells did not show an earlier cell death. However, other authors have reported that Asn feeding had no effect on growth and recombinant protein production in CHO-GS (McCracken et al., 2014) and CHO-DHFR cells (Hansen and Emborg, 1994a, Hayter et al., 1991). The difference in the concentration of supplemented Asn, CHO-cell type, medium and cell culture conditions used might offer potential reasons to explain the differential effect of Asn on cell culture performance of CHO cells. In the case of combination feeds in which Asn was one of the components, three distinct types of response have been observed in terms of effects of feeding on cell growth and product yield. Reports have shown effects on growth only, effects on product yield only and effects on both. Firstly, Carinhas et al. (2013) found that addition of Asn in combination with Asp, Serine and Glc slightly increased maximum cell density and prolonged stationary phase of CHO cell clones (transfected CHOK1SV cells with IgG4) but product yield was not increased. Secondly, Xu et al. (2014) reported an improvement in cell viability and specific productivity of CHO-GS cells supplemented with Asn in combination with glutamine. Finally, positive effects on both growth and product yield have been observed in both GS and DHFR system in response to feeds that combined Asn with other components. Additions of Asn, Asp, Glu, Py and Glc in CHO-LB01 cells

culture lead to increased maximum viable cell density and increased product yield (Sellick et al., 2011). In CHO TF70R cells maximum cell density and product yield increased when Asn was combined with proline and serine (Altamirano et al., 2006b).

Since all of these reported experiments differed in many factors (cell type, medium, and cell culture condition), this might lead to distinct impact of addition Asn on CHO cells culture performance. We hypothesized that the differential effect of feeding Asn on CHO cells may be due to the difference in cell type and medium used. To test this, Asn and HB was used as a supplementation in the culture of two further CHO cells type (CHO-S and CHO-TRex cells) cultured in different medium (Section 2.2.1). CHO-S cells which are non-recombinant CHO cells were cultured in CD-OptiCHO plus glutamax and CHO-TRex cells which are CHO-K1 produced EPO in inducible system were cultured in CD-CHO plus glutamax plus 0.1% blasticidin plus 0.1% tetracycline. Under the experimental conditions used, the addition of Asn to CHO-S and CHO-TRex cells did not increase maximum cell density as had been observed with CHO-LB01 cells but CHO-S cells presented with Asn died more at an earlier stage (by one day) of batch culture than control CHO-S cells (Figure A2.1 and A3.1) as observed in CHO-LB01 cells fed Asn. In case of feeding HB, increased maximum viable cell density was observed in CHO-S at day 5 and after that viable cell density remained greater than the control until last day of culture while addition of HB had no effect on growth and antibody production of CHO-TRex cells (Figure A2.1 and A3.1). This result supported that the effect of nutrient feeding depends on many factors such as cell type and culture medium.

3.3 Extracellular and intracellular metabolite profiles of CHO-LB01 cells: Response to nutrient supplementation

Nutrient feeding experiments showed selective responses on cell growth and recombinant antibody yield to nutrient addition (Asn or HB). After the consequences of feeds for growth and recombinant protein production, the next steps were to analyze, by enzymatic assay and GC-MS, extra- and intra-cellular metabolite profiles associated with changes to growth and productivity. The analysis of this dataset will provide greater understanding of relationship between cell growth, feeds and recombinant protein production.

3.3.1 Extracellular metabolite profiles: Enzymatic analyses

Initial metabolite analyses from medium were performed on a selected group of metabolites (glucose, lactate, alanine, glycerol and ammonia) by enzymatic assays (Section 2.3.1).

In control cultures, the concentration of glucose gradually declined from about 20 mM at day 0 to less than 5 mM at day 6, a time when cells entered stationary growth phase and glucose was completely depleted at day 8 (Figure 3.3A). High glucose consumption has been observed during the growth phase of CHO cells (Neermann and Wagner, 1996, Wilkens et al., 2011). Feeding with Asn, HB, or the combination of both, had no effect on the overall profile of glucose metabolism but glucose was utilized slightly quicker and slower than the control in the presence of Asn and HB, respectively.

Figure 3.3 Extracellular metabolite profiles of LB01 cells in control and nutrient supplemented batch cultures.

Medium samples were collected from the cultures illustrated in Figure 3.2. Glucose (A), lactate (B), alanine (C), glycerol (D) and ammonia (E) in medium samples were determined by enzymatic assay (Section 2.3.1) for control (black symbols) and cultures supplemented with Asn (red), HB (purple) and a combination of Asn and HB (brown) at day 4 of culture (as indicated by the arrow). Values presented are mean ± SEM for six replicates for Asn, five replicates for HB and three replicates for Asn plus HB, all shown against their respective controls. * indicates significant difference from control at $p < 0.05$. The lines at the top of each graph are added to indicate stages of growth: exponential phase (dot-dash line), stationary phase (solid line) and decline phase (dashed line).

A.

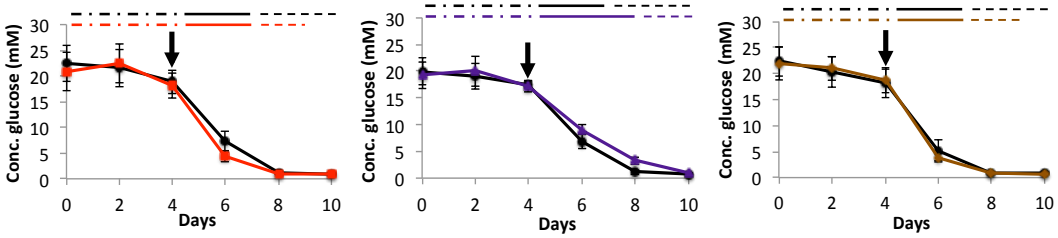
Conc. glucose (mM)
Days

B.

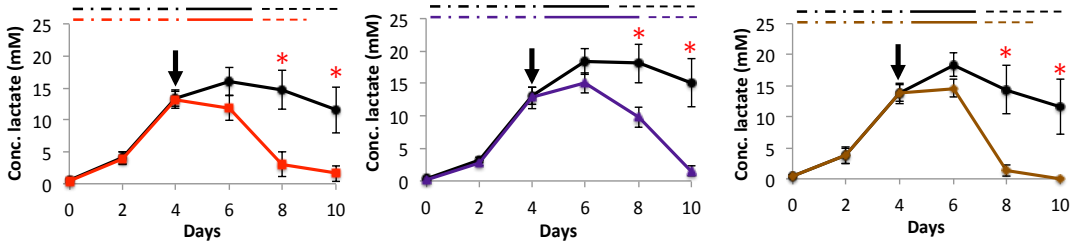
Conc. lactate (mM)
Days

C.

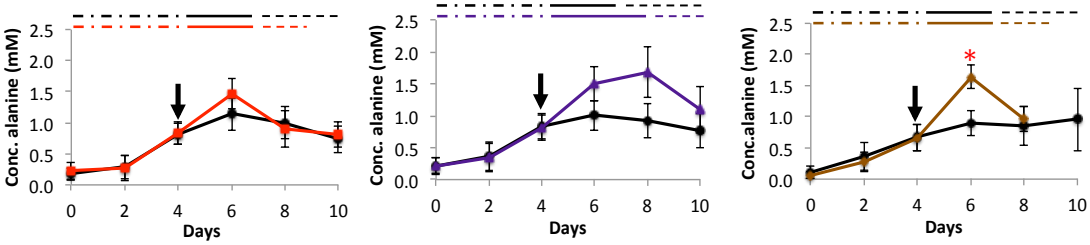
Conc. alanine (mM)
Conc.alanine (mM)
Days

D.

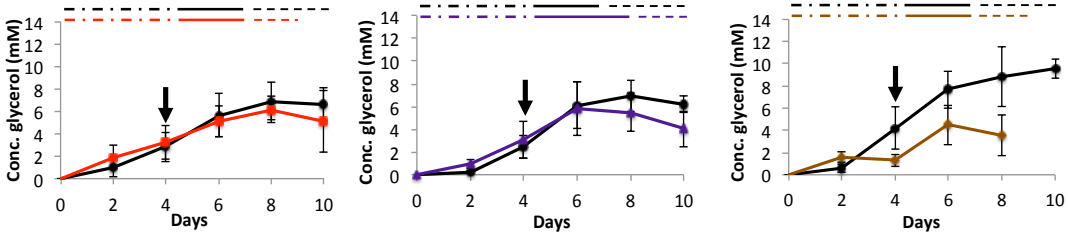
Conc. glycerol (mM)
Days

E.

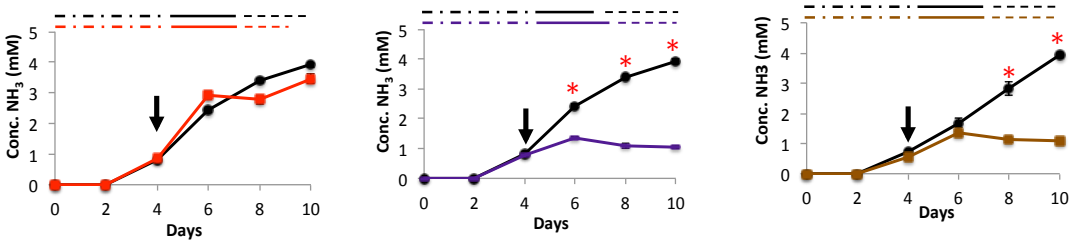
Conc. NH3 (mM)
Days

In contrast, the addition of Asn or HB or their addition in combination produced a significantly different profile of lactate metabolism compared to the control (Figure 3.3B). In the control condition, lactate was produced from day 1 to day 6 of culture (growth phase) reaching a maximum concentration about 18 mM at day 6. After that time cell cultures showed a slight consumption of lactate but the concentration of lactate remained relatively high (greater than 10 mM) until the last day of culture. In contrast, under all feeding regimes (where the feed was added at day 4 of culture), after the concentration of lactate reached the peak about 15 mM at day 4 or 6, the cells switched from lactate production to consumption (after day 4 for Asn-fed and after day 6 for HB-fed and Asn/HB-fed) and lactate was depleted by day 10 in all feeding conditions. Additionally, feeding Asn and Asn plus HB depleted lactate more rapidly than feeding HB. A similar metabolic switch (from lactate production to lactate use) has been reported to occur in CHO cells when glucose was depleted (Martinez et al., 2013, Wilkens et al., 2011) or entered late growth or stationary phases (Altamirano et al., 2006a, Wilkens et al., 2011, Carinhas et al., 2013, Dean and Reddy, 2013, Ma et al., 2009, Quek et al., 2010, Selvarasu et al., 2012, Sengupta et al., 2011) (Section 1.3.1). The shift from lactate production to consumption in this study is similar with the study of Sellick et al. (2011) and Sellick et al. (2015). Those authors found the consumption of lactate in CHO-LB01 cells (GS-system) supplemented with the combination of Asn, Asp, Glu and Py and supplementation with CHO CD EfficientFeeds^{TM} A or B. In addition, Xu et al. (2014) reported that a combined feed of glutamine and Asn prevented lactate generation by CHO-GS cells. Moreover, decreased lactate production was found in CHO-DG44 (DHFR system) cultures fed with αKG or citrate (Gilbert et al., 2013). In contrast, addition of the combination of proline, serine and Asn to cultures of CHO TF70R (DHFR system) cells did not generate a significant effect on lactate metabolism (Altamirano et al., 2006b).

In a manner similar to that seen for lactate profiling in control cultures, alanine accumulated from days 2 to day 6 of culture (growth phase), reaching about 1 mM, and after that time alanine was slightly consumed during stationary/decline phase (Figure 3.3C). A switch from alanine production to consumption has been observed in earlier study of CHO-GS and CHO-DHFR system (Carinhas et al., 2013, Gilbert et al., 2013, Li et al., 2012, Sellick et al., 2011). Feeding with Asn or HB resulted in the production of slightly greater amounts of alanine (1.5 -1.6 mM by days 6 to 8 of culture) and a significantly greater concentration of alanine was observed in the combination of Asn and HB (1.7 mM at day 6) (Figure 3.3C). After cells reached the peak of alanine, alanine was consumed in all feeding regimes as observed in the control. This result is similar to that seen by Sellick et al. (2011; 2015) who reported increased alanine production in the presence of a combination of Asn, Asp, Glu, Py and Glc or CHO CD EfficientFeeds^{TM} A or B in CHO-LB01 cells (GS system) culture, respectively. Li et al. (2012) also found a similar pattern of alanine metabolism in DUX-B11 cells (DHFR system) supplemented with Py.

Glycerol increased gradually during control cultures and reached a peak about 7-9 mM at day 8 and then remained constant for the remainder of culture (Figure 3.3D). This pattern is consistent with earlier studies in GS-CHO (Sellick et al., 2011, Carinhas et al., 2013). In the presence of Asn or HB, the pattern of glycerol metabolism was similar to the control but Asn/HB-fed produced slightly less glycerol than the control. In addition, concentration of glycerol was slightly decreased after day 6 in all feeding regimes (Figure 3.3D). This result correlates with the profile of glycerol metabolism reported by Sellick et al. (2011) who found the accumulation of glycerol during stationary phase of cell culture and also reported that feeding with Asp, Asn, Glu and Py resulted in the production of less glycerol.

Ammonia was produced after day 2 of culture and reached 4 mM by day 10 of control culture (Figure 3.3E), a result that was comparable with previous studies with CHO-GS system (Carinhas et al., 2013, Duarte et al., 2014, McCracken et al., 2014). Asn addition did not alter ammonia production. However, a positive correlation was observed between increased concentration of Asn feed and increased ammonia production and was observed in both CHO-DHFR (Hansen and Emborg, 1994a, Hayter et al., 1991) and CHO-GS cells (McCracken et al., 2014). Supplementation with HB or Asn plus HB significantly inhibited ammonia production (reaching only 1.5 mM). In addition to increased product yield, this is the first study reporting an effect of HB on ammonia production. Decreased ammonia accumulation has been reported in CHO-DG44 culture fed αKG or citrate but feeding αKG had a more pronounced effect than citrate (Gilbert et al., 2013). Li et al., (2012) also found that a lower concentration of ammonia was achieved when CHO DUX-B11 cell cultures were supplemented with lactate or pyruvate.

In summary, in control conditions, glucose consumption and lactate production were observed during the growth phase of CHO cells. The cells entered stationary phase when the concentration of glucose was low and lactate was slightly consumed when glucose was depleted and the cells entered late stationary phase. Similar to lactate, alanine accumulated during the growth phase of cell culture and was consumed in stationary/decline phases. The biphasic response may occur because, after the depletion of glucose, not enough pyruvate was produced to supply energy metabolism so lactate and alanine are used for pyruvate synthesis in order to maintain carbon precursor flow into the TCA cycle (Ahn and Antoniewicz, 2011, Wilkens et al., 2011, Li et al., 2012, Sengupta et al., 2011, Templeton et al., 2013). Accumulation of glycerol was found to occur during culture as observed by Sellick et al. (2011). In addition to generation of lactate from pyruvate, NAD^+ can be produced from the generation of glycerol (Lovatt et al., 2007, Wilkens et al., 2011) so it is possible that glycerol accumulation might maintain the redox state in the cytoplasm (Section 1.3.2.2). In yeast

cells under anaerobic or glucose-repressed growth conditions, glycerol has been hypothesized to be produced to help maintain a cytosolic redox state (Cronwright et al., 2002). Ammonia accumulated throughout cell culture especially in stationary/decline phase. This links to increased amino acid catabolism (Li et al., 2012). In the presence of nutrients, significant changes were detected in lactate and ammonia metabolism. In all supplemented cultures, cells switched to lactate consumption after day 4 or day 6 and lactate was depleted by the end of the culture period. The period of lactate use corresponded to the time in which cells were in stationary/decline phase of culture. It is possible that at this stage lactate was used for pyruvate synthesis in order to maintain carbon precursor flow into the TCA cycle (Wilkens et al., 2011, Li et al., 2012). In addition, ammonia production was inhibited in the present of HB. This might be one reason why feeding HB improved product yield because high ammonia accumulation had negative effects on cell growth and productivity of CHO cells (Altamirano et al., 2013, Hansen and Emborg, 1994b, Kurano et al., 1990, Xu et al., 2014, Yang and Butler, 2000).

Overall, it can be suggested that nutrient feeding affected metabolic alteration leading to changes in cell culture performance of cells fed Asn or HB. The obvious change of lactate metabolism in the presence of nutrients might link to change of other metabolites in metabolic pathway (such as metabolites in the TCA cycle) that might relate to differential effect of Asn or HB on cell growth and antibody production, respectively. Thus, more assessment of extra- and intra-cellular metabolite profiles by GC-MS will be conducted. This information would offer the potential for a more complete understanding of the overall relationship between cell culture performance and metabolite profiles especially in relation to metabolites of the TCA cycle, the functioning of which has been defined to be linked to increased recombinant protein production (Lee et al., 2014, Templeton et al., 2013) (Section 1.3.4). Better understanding of cellular metabolism will help to improve the efficiency of CHO-LB01 cells for antibody production by medium optimization and/or cell engineering.

3.3.2 Extracellular metabolite profiles: GC-MS analyses

Medium samples from control cells and cells fed with Asn and HB were collected for extracellular metabolite profiling (Section 2.3.2). Extracellular metabolite profiles for cultures (control at days 4, 5, 6 and 7; HB-fed at days 5, 6 and 7; Asn-fed at days 5 and 6) were mapped onto cellular metabolism (Figure 3.4) and individual metabolite charts were produced (Figures 3.5, 3.6 and 3.7).

As shown in Figure 3.4, glucose, pyruvate, and all detected amino acids (with the exception of glycine and alanine) were consumed during culture. Depletion of glucose (after day 5 in control conditions, earlier with Asn, later with HB) correlated with the entry of cells into stationary phase. This observation correlated with the result of the glucose profile detected by enzymatic assay (Section 3.2.1; Figures 3.4 and 3.5A). Pyruvate was almost depleted at day 4 in all conditions but pyruvate was above the background of the control at day 5 in the presence of Asn or HB when lactate consumption was observed (Figures 3.4 and 3.5A). Asn, Asp, Glu and serine were exhausted rapidly in all conditions (Figures 3.4 and 3.7A). Several groups have reported that this group of amino acids was consumed rapidly during CHO cell batch culture (Altamirano et al., 2006b, Hayter et al., 1991, Ma et al., 2009, Sellick et al., 2011, Carinhas et al., 2013, Dean and Reddy, 2013, Xing et al., 2011). Addition of Asn or HB increased the consumption of several amino acids (lysine, leucine, isoleucine, threonine, methionine, phenylalanine, valine, tyrosine and cysteine) above that of the control but feeding with Asn resulted in a more rapid consumption of these amino acids than was observed with HB addition. This observation correlated with higher maximum cell density and earlier cell death by three days in the presence of Asn and higher antibody production and earlier cell death by one day in the presence of HB (Figures 3.1A and 3.2A). For example, leucine was depleted in cell cultures supplemented with Asn at day 5, one day prior to depletion in the presence of HB (day 6) whilst the depletion of leucine was not observed in the control until day 7 (Figures 3.4 and 3.7A). Higher amino acid

consumption was reported to correlate with increased recombinant protein yield and increased viable cumulative cell numbers (Reinhart et al., 2015). Additionally, when fed with Asn or HB, cultures showed increased production of ketobutyrate (an intermediate of threonine catabolism that can enter the TCA cycle at the level of succinyl CoA) (Chen and Harcum, 2005, Sellick et al., 2015) at day 5 and the amount of ketobutyrate was decreased at day 6 (for Asn) or day 7 (for HB) (Figures 3.4 and 3.6). Succinyl CoA cannot be detected by GC-MS (it is not in the Fiehn GC/MS mass spectral library) but ketobutyrate accumulation may inform of TCA cycle flux under conditions of feeding. Glycine accumulated in culture medium throughout the culture period detected in the control (Figures 3.4 and 3.7A). This observation is consistent with previously studies in CHO-DHFR (Hayter et al., 1991), CHO-GS (Sellick et al., 2011) and mouse hybridoma cells (Duval et al., 1991). In the presence of either Asn or HB glycine accumulated to a lesser extent than the control (Figures 3.4 and 3.7A). The accumulation of glycine may be linked to a high rate of serine metabolism for biosynthesis of purine and pyrimidine and glycine was considered as amino acid for support cell growth (Duarte et al., 2014, Hayter et al., 1991, Narkewicz et al., 1996, Xing et al., 2011, Wang et al., 2013). No production of alanine was observed in the control after day 4 (Figures 3.4 and 3.7A). This result differs from the examination of alanine metabolism by enzymatic assay (Figure 3.3C).

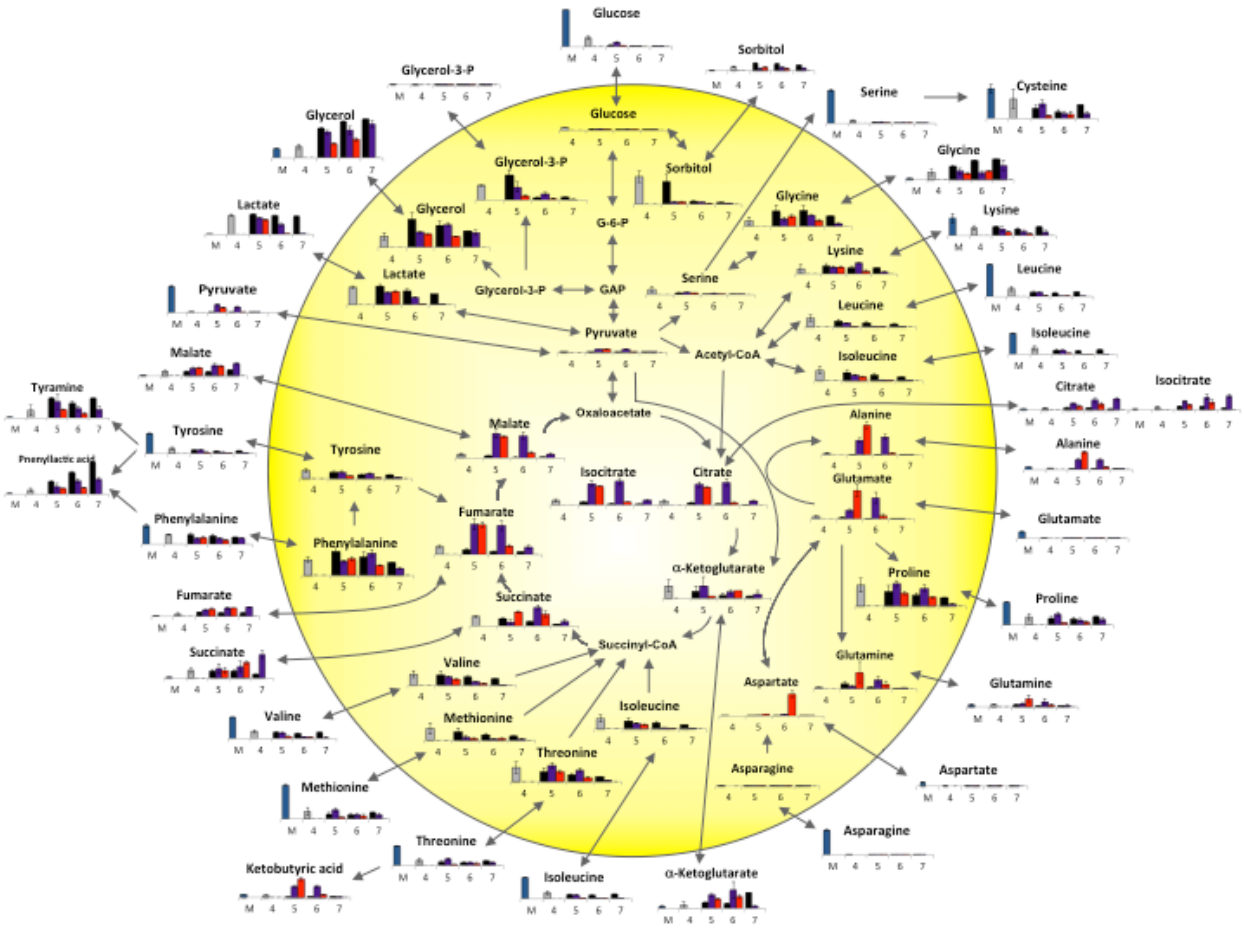

Figure 3.4 Profiles of extracellular and intracellular metabolites of LB01 during control and Asn and HB supplemented conditions.

LB01 cells were cultured in CD OptiCHO^{TM} (Section 2.2.1) in control and supplemented conditions (as described in Figure 3.2) and at appropriate times samples were harvested from medium (extracellular) and cells (intracellular) (Section 2.3.2.1). Metabolite assessment was performed as described in Section 2.3.2. The bar charts represent the quantities of each metabolite in CD OptiCHO^{TM} medium (blue), control culture at day 4 before feeding (gray), control at all subsequent days of culture (black), Asn-supplemented (red) and HB-supplelmented (purple) at day 5 (5), day 8 (8), day 9 (9) and day 10 (10). Values are arbitrary units normalized to an internal standard and represent the average of three replicates with ± SEM. For increase clarity, individually figures are shown in Figure 3.5, 3.6, 3.7 and 3.8. On those figures the unit of the scale are illustrated.

A.

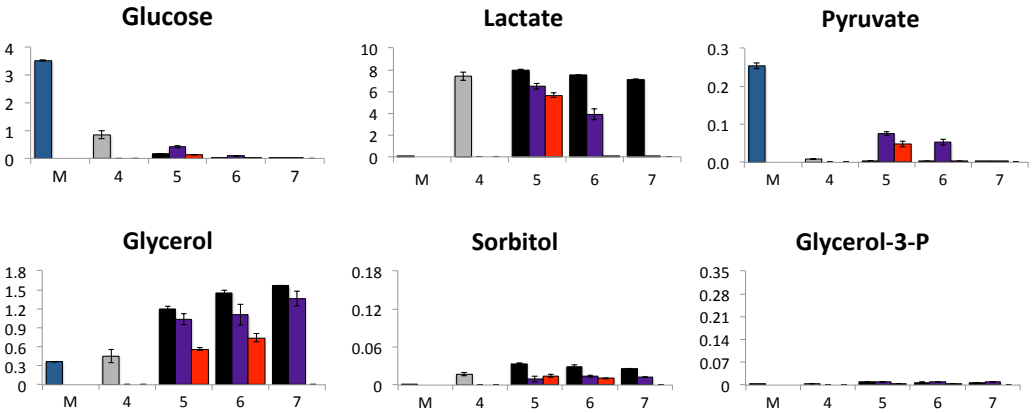

B.

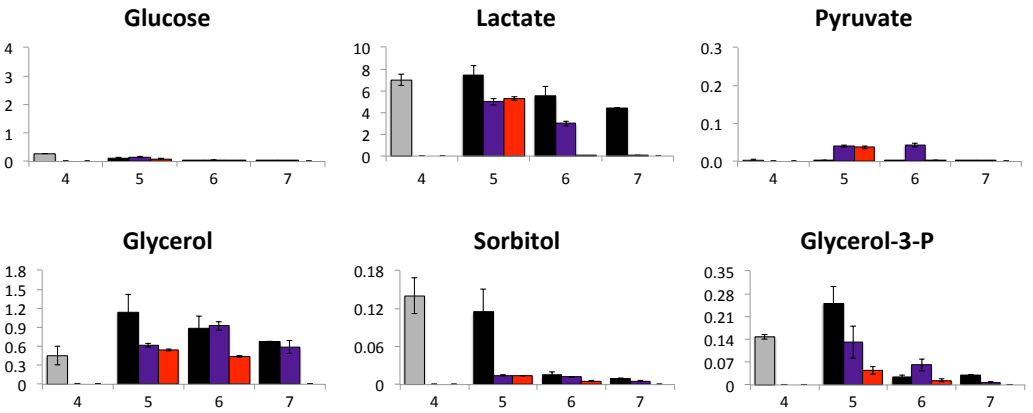

Figure 3.5 Extracellular and intracellular metabolite profiles of metabolites of interest related to glycolysis pathway of Asn and HB supplementation from Figure 3.4.

Medium and cell samples were collected for extracellular (A) and intracellular (B) metabolite profiles, respectively (Section 2.3.2.1). The bar charts represent the quantities of each metabolite in CD OptiCHO^{TM} medium (blue), control culture at day 4 before feeding (gray), control at all subsequent days of culture (black), Asn-supplemented (red) and HB-supplelmented (purple) at day 5 (5), day 8 (8), day 9 (9) and day 10 (10). Values (y-axis) are arbitrary units normalized to an internal standard and represent the average of three replicates with ± SEM.

A.

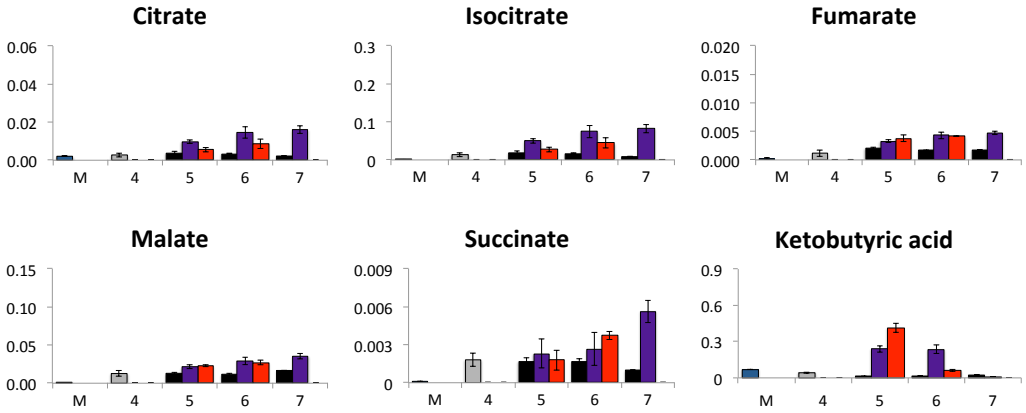

B.

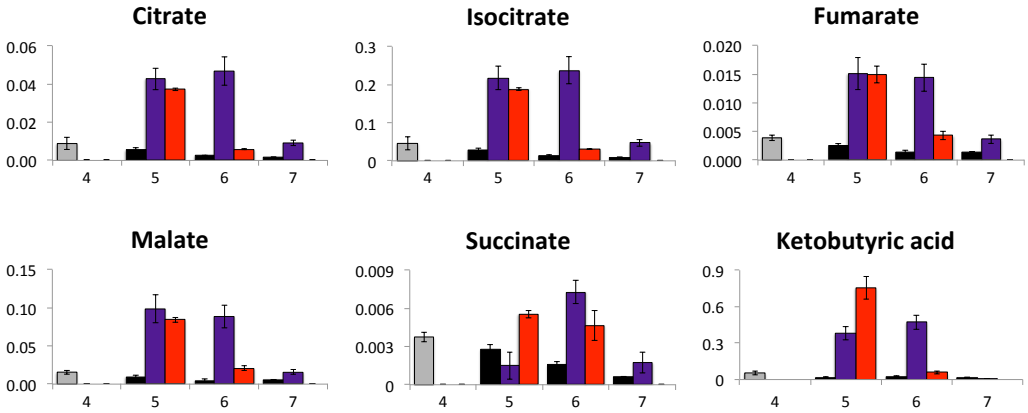

Figure 3.6 Extracellular and intracellular metabolite profiles of metabolites of interest related to TCA cycle pathway of Asn and HB supplementation from Figure 3.4.

Medium and cell samples were collected for extracellular (A) and intracellular (B) metabolite profiles, respectively (Section 2.3.2.1). The bar charts represent the quantities of each metabolite in CD OptiCHO^{TM} medium (blue), control culture at day 4 before feeding (gray), control at all subsequent days of culture (black), Asn-supplemented (red) and HB-supplelmented (purple) at day 5 (5), day 8 (8), day 9 (9) and day 10 (10). Values (y-axis) are arbitrary units normalized to an internal standard and represent the average of three replicates with ± SEM.

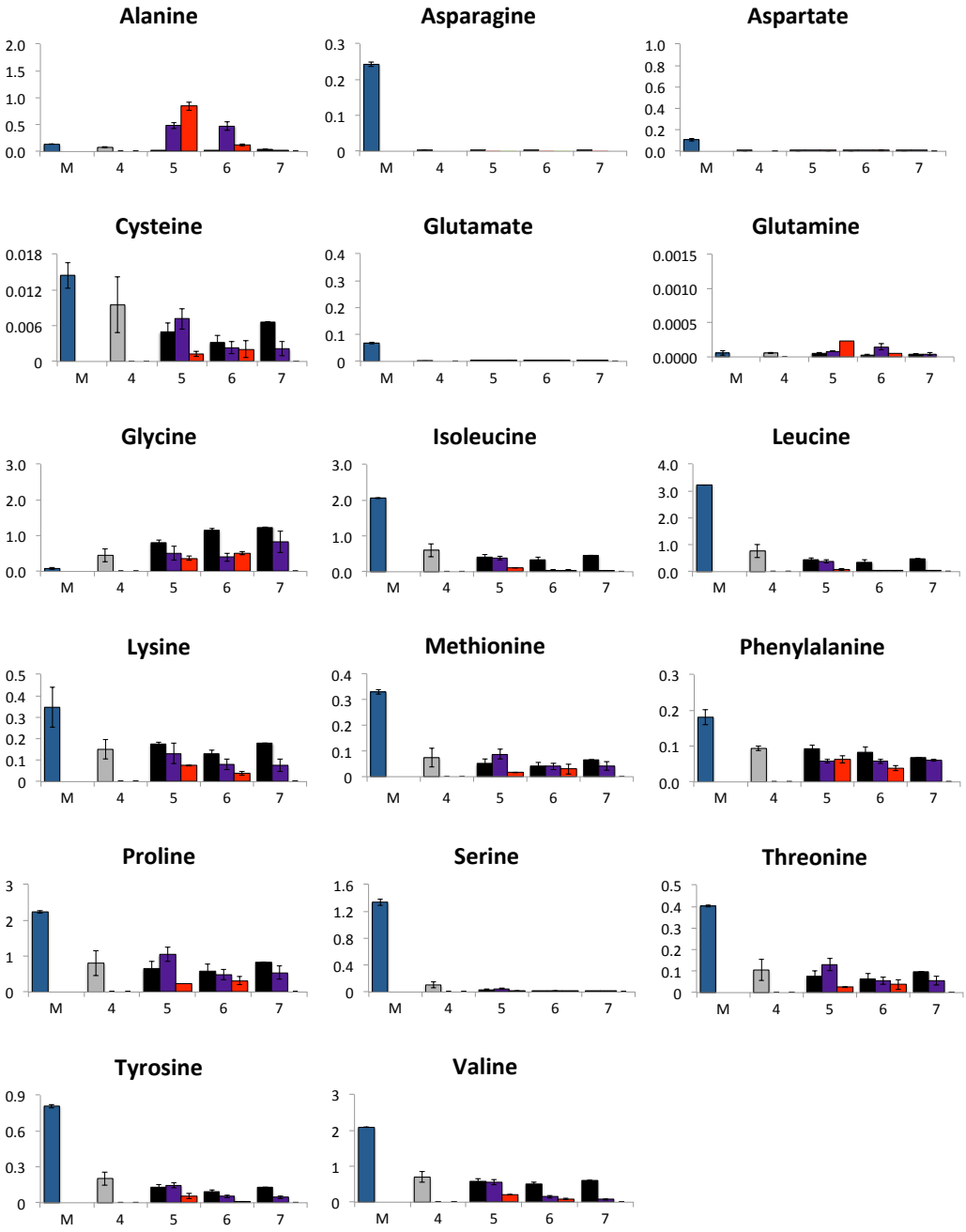

Figure 3.7 Extracellular metabolite profiles of amino acid of Asn and HB supplementation from Figure 3.4.

Medium samples were collected for extracellular metabolite profiles (Section 2.3.2.1). The bar charts represent the quantities of each metabolite in CD OptiCHO^{TM} medium (blue), control culture at day 4 before feeding (gray), control at all subsequent days of culture (black), Asn-supplemented (red) and HB-supplelmented (purple) at day 5 (5), day 8 (8), day 9 (9) and day 10 (10). Values (y-axis) are arbitrary units normalized to an internal standard and represent the average of three replicates with ± SEM.

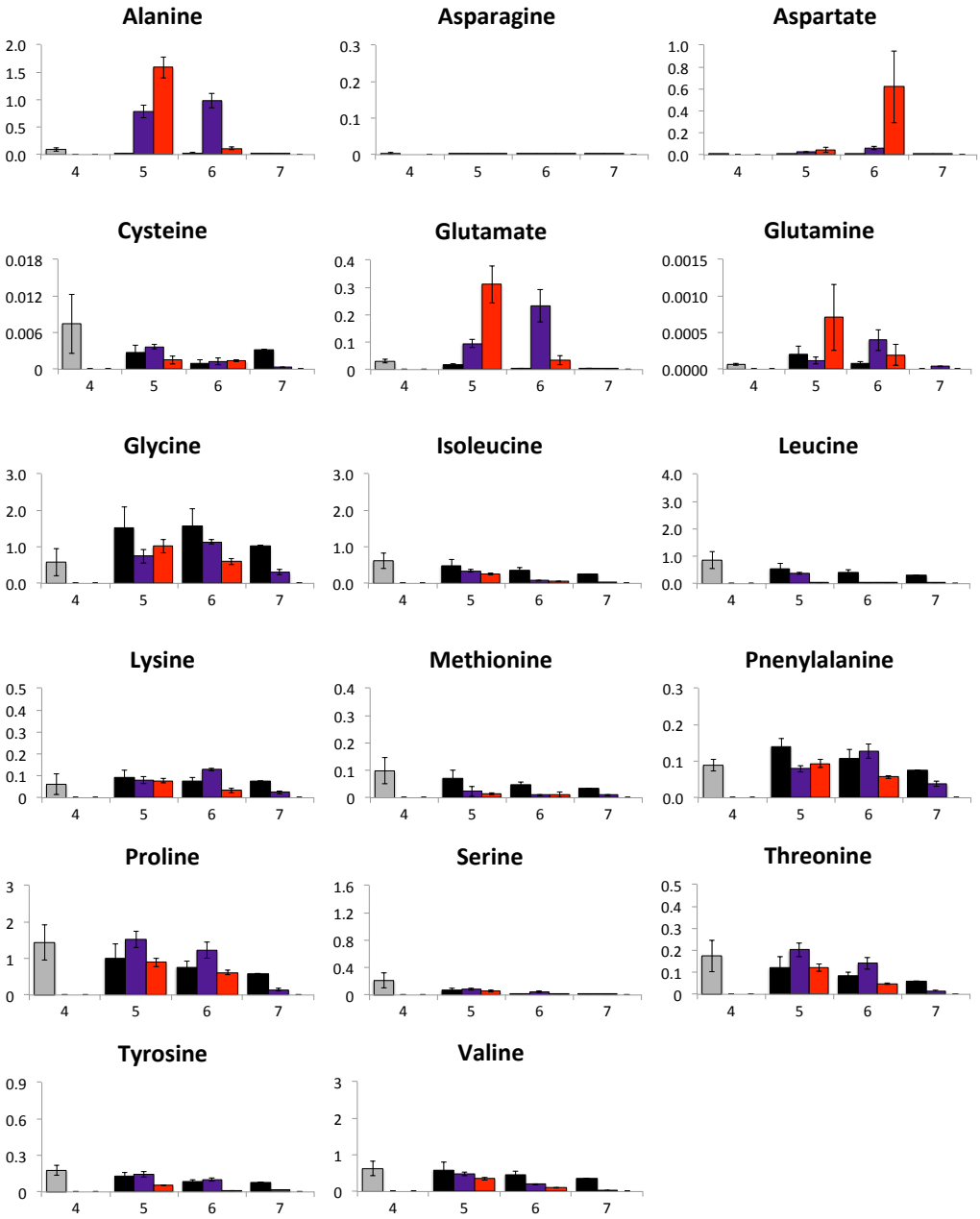

Figure 3.8 Intracellular metabolite profiles of amino acid of Asn and HB supplementation from Figure 3.4.

Cell samples were collected for intracellular metabolite profiles (Section 2.3.2.1). The bar charts represent the quantities of each metabolite in control culture at day 4 before feeding (gray), control at all subsequent days of culture (black), Asn-supplemented (red) and HB-supplelmented (purple) at day 5 (5), day 8 (8), day 9 (9) and day 10 (10). Values (y-axis) are arbitrary units normalized to an internal standard and represent the average of three replicates with ± SEM.

Alanine was produced during day 2 to day 6 and then was consumed until day 10 when assessed by enzymatic assay whereas the alanine profile generated by GC-MS analysis showed no alanine production after day 4. In this case, alanine might be produced before day 4 and was consumed after day 4 but the samples were not collected during day 2 to day 4 for GC-MS analyses. In cells supplemented with Asn or HB, there was high amount of alanine at day 5 and day 5 to 6, respectively and then utilization was observed at day 6 for Asn and day 7 for HB (Figures 3.4 and 3.7A). This observation corresponded with the alanine profile determined from enzymatic assay (Figure 3.3C). In addition, greater alanine production was also found in CHO-LB01 cells supplemented with the combination of Asn, Asp, Glu, Py and Glc (Sellick et al., 2011) and CHO DUX-B11 cells fed Py or lactate (Li et al., 2012). Moreover, the profile of alanine metabolism was similar to the profile of pyruvate in the presence of nutrient feeding. Greater alanine and pyruvate production were observed at day 5 and 6 in addition of Asn or HB compared to the control.

Several other metabolites accumulated in medium during culture and exhibited differential responses to Asn or HB feeding. In control conditions lactate was produced and the amount remained the same until the last day of sampling, whereas in the presence of Asn or HB cells switched from lactate production to consumption after day 4 and the cessation of culture under each feed condition correlated with the complete depletion of lactate (Figures 3.4 and 3.5A). This result correlated with the lactate changes detected by enzymatic assay (Section 3.2.1). Glycerol and sorbitol were produced during culture in control conditions and the presence of Asn or HB decreased production of both glycerol and sorbitol (Figures 3.4 and 3.5A). This result is consistent with CHO-LB01 cells supplementation with the combination of Asn, Asp, Glu, Py and Glc (Sellick et al., 2011) but contrasts with CHO-LB01 cells supplementation with EfficientFeeds A or B in which increased glycerol and sorbitol production were observed (Sellick et al., 2015). Metabolites involved in the TCA cycle (citrate, iso-citrate, succinate, fumarate and malate) were produced during control cultures (as reported by

Sellick et al. 2011) and their production was increased in the presence of Asn or HB (Figures 3.4 and 3.6A). This is consistent with the observation that feeding the combination of Asn, Asp, Glu, Py and Glc or CD CHO EfficientFeeds A and B increased TCA cycle intermediates in CHO-LB01 cells (Sellick et al., 2011 and Sellick et al., 2015).

In summary, under culture supplemented with Asn or HB, less lactate, glycerol and sorbitol were produced and this was accompanied by increased amounts of TCA cycle intermediates (citrate, isocitrate, fumarate and malate) and decreased amounts of amino acids (lysine, leucine, isoleucine, threonine, methionine, phenylalanine, valine, tyrosine and cysteine). This metabolic response to feeds (except for alteration of amino acids) correlates with the findings of Sellick et al. (2011) who reported that supplementation with the combination of Asn, Asp, Glu and Py or Asn, Asp, Glu, Py and Glc in CHO-LB01 cells decreased the amount of lactate, glycerol and sorbitol and also increased the amount of citrate. In addition, HB caused a similar impact of extracellular metabolite profiles as Asn and a significant enhancement of antibody yield was observed. Therefore, metabolite profiling was extended to intracellular metabolite profiles of control and nutrient-fed cells to give greater insight to the metabolic status of cells during nutrient feeding.

3.3.3 Intracellular metabolite profiles: GC-MS analyses

Intracellular metabolite profiles were also measured in cell samples collected in parallel to the medium samples (extracellular metabolite data described above). For intracellular samples quenching and extraction methods were conducted to diminish degradation of labile metabolites, metabolite turnover and contamination by extracellular metabolites (Section 2.3.2.1). Intracellular metabolite profiles for all conditions (control at days 4, 5, 6 and 7; HB-fed at days 5, 6 and 7; Asn-fed at days 5 and 6) were mapped onto cellular

metabolism (Figure 3.4) and individual metabolite charts are grouped and shown in Figures 3.5B, 3.6B and 3.8.

Glucose was hardly detected inside the cell in all conditions as expected (Figures 3.4 and 3.5B). This means there was low contamination (about 15% contamination) of the cellular metabolite extract with glucose from culture medium. Similar to the results of extracellular metabolite profiles, addition of Asn or HB increased the amount of intracellular pyruvate at day 5 and day 6 (Figures 3.4 and 3.5B). In the case of intracellular amino acids, for cells fed with Asn or HB the amount of almost all amino acids (except for alanine) were less than the control (Figures 3.4 and 3.8). This pattern is similar to that observed for extracellular amino acids. As for glycine, accumulation of glycine was observed between day 4 to day 6 and then the amount of glycine was decreased in the control (Figures 3.4 and 3.8). Lower amounts of glycine were found in the presence of Asn or HB as observed in the extracellular glycine profile. Addition of Asn or HB increased the amount of alanine at day 5 and 6 and then alanine was decreased (Figures 3.4 and 3.8) as observed in extracellular alanine. Two intracellular amino acids (aspartate and glutamate) were in greater amounts when Asn or HB were added (Figures 3.4 and 3.8). In the presence of Asn, the amount of intracellular glutamate and aspartate were greater at day 5 and day 6, respectively (Figures 3.4 and 3.8). Likewise, the amount of intracellular glutamate was greater at day 5 to day 6 in cells fed HB (Figure 3.4 and 3.8). This observation was not found in extracellular profiles of aspartate and glutamate in Asn-fed or HB-fed cells.

Intracellular lactate followed a similar trend to that observed for the extracellular profile in all conditions (Figures 3.4 and 3.5B). In control conditions, lactate was produced until day 5 and then was slightly consumed but remained high until the last day of assessment, whereas lactate was consumed after day 4 and was depleted at day 6 and day 7 in the presence of Asn or HB, respectively. Glycerol accumulated during culture in control conditions but the presence of Asn or HB decreased the amount of glycerol

(Figures 3.4 and 3.5B) as observed in extracellular metabolite profile. The profile of change for intracellular sorbitol in cells fed nutrients was similar to that in the medium (Figures 3.4 and 3.5B). The amount of sorbitol was high at day 4 and 5 then decreased in the control while, following the addition of Asn or HB, the amount of sorbitol was less than the control at day 5 onwards. The intracellular amount of TCA cycle intermediates (citrate, iso-citrate, fumarate and malate) in the presence of Asn or HB was clearly greater than the control (Figures 3.4 and 3.6B). In the control, the amount of TCA cycle intermediates slightly decreased throughout the detection period but cells fed Asn or HB had greater amount of metabolites in TCA cycle than the control at day 5 until the last day of assessment. This trend is similar to the extracellular metabolite profile of metabolites in the TCA cycle but the effect of Asn or HB toward intracellular TCA cycle intermediates was more pronounced than the changes noted for those extracellular metabolites. Glycerol-3-phosphate was detected inside the cells (Figures 3.4 and 3.5B). In the control, glycerol-3-phosphate was produced until day 5 and then it was consumed at day 6 while in the presence of Asn or HB the amount of glycerol-3-phosphate was less than the control at day 5 until the last day detected.

In summary, the results from intracellular metabolite profiling demonstrated the same trend with that of extracellular metabolites for all conditions. These results indicated the effect of Asn and HB toward alteration of extra- and intra-cellular metabolite profile related to cell culture performance. Although Asn and HB caused similar impact of metabolite profiles in term of lactate, glycerol, sorbitol, TCA cycle intermediates and amino acids profiles but only HB caused a significant enhancement of antibody yield. The potential explanations for this observation will be discussed in Section 3.6. According to the clear observation of decreased lactate accumulation and increased amounts of intermediates of the TCA cycle when cells were supplemented with Asn or HB, it was hypothesized that this behavior might link to the alteration of genes that form part of the malate-aspartate shuttle and/or the enzymes related to the TCA cycle. Thus, gene expression of enzymes linked to the TCA cycle and malate-aspartate shuttle were

investigated (to be described in the next section) in order to examine whether alteration of lactate and TCA cycle intermediates profiles related to gene expression.

3.4 Gene expression analysis for enzymes linked to the TCA cycle

Based on the result of metabolite profiles observed the alteration of lactate and TCA intermediates profiles in the presence of Asn or HB and the data of Zagari et al. (2013) who reported that the malate-aspartate shuttle was a key factor to promote a shift to lactate consumption in CHO-S cells (Section 1.3.2), assessment of gene expression level were conducted in this section. Analysis of expression of a series of genes involved in mitochondrial transporter activity (*Slc25a11* and *Slc25a12*) (Figure 1.6) and enzymes linked to the TCA cycle (*Ldha*, *Pdha1*, *Cs*, *Mdh2*, *Glud1* and *Ogdh*) (Figure 1.8) was investigated in cells under control conditions and in response to feeding with Asn (Section 2.6.5 and 2.6.7).

The results from PCR analyses showed that primers, designed against the appropriate mRNA for all genes tested, generated a product of the expected size although some gene products (*Slc25a11*, *Slc25a12* and *Ogdh)* had very low expression in both control and under conditions of Asn feeding (Figure 3.9). qPCR was undertaken to quantify potential differences in response to Asn addition (Figure 3.10). No difference was found in expression of all genes between Asn-fed cells and the control. It had been shown previously that increased expression of *Slc25a12* was observed under low lactate production conditions of non-recombinant CHO-S cells cultured in CD CHO medium (Zagari et al., 2013). This did not appear to be in the case for *Slc25a12* in this study. This inconsistency may be due to the differences of cell culture medium and CHO cells used. In this study, CHO-LB01 cells produced IgG4 and were cultured in CD OptiCHO^{TM} medium and the shift of lactate profile might result from the effect of Asn feeding which caused increased the flow of TCA cycle as observed from increased production of TCA

cycle intermediates (Section 3.3.2). As a result, lactate was used to provide input flow to the TCA cycle. In the case of the other gene products examined, there had been no prior literature reports related to lactate metabolism and the TCA cycle.

In addition to investigation the effect of nutrient feeding on gene expression profile, the effect of supplementation with nutrients towards oxygen consumption rate, mitochondrial membrane potential, cell size and mitochondrial and ER content will be studied next.

3.5 Profiling the effect of nutrient feeding on cellular phenotype

Since addition of Asn or HB increased the amount of TCA cycle metabolites (in cells and in medium), it was hypothesized that addition of these nutrients enhanced oxidative metabolism, a response that might be detected by measurement of oxygen consumption. Additionally, as lactate, sorbitol and glycerol amounts were decreased in the presence of Asn or HB, a differential recycling of NADH might lead to an altered $NADH/NAD^+$ ratio, a feature that, again, could influence mitochondrial activity. Zagari et al. (2013) reported a correlation between high lactate production and decreased mitochondrial membrane potential and oxygen consumption in CHO cell cultures and it was hypothesized that feeding Asn or HB might affect mitochondrial membrane potential of CHO cells. Moreover, increased maximum cell density and product yield were observed in the presence of Asn or HB, respectively. Consequently, cell size and the quantity of mitochondria and ER might be expected to positively correlate with more productive CHO cells. Kim et al. (2001) and Lloyd et al. (2000) found that larger cells were more productive than smaller cells. In addition, more productive cells might be expected to increase mitochondrial and ER content in order to provide sufficient energy and protein processing to support the potential for an increased load of recombinant protein production and supply the necessary protein synthesis, folding and processing apparatus (O'Callaghan et al., 2015).

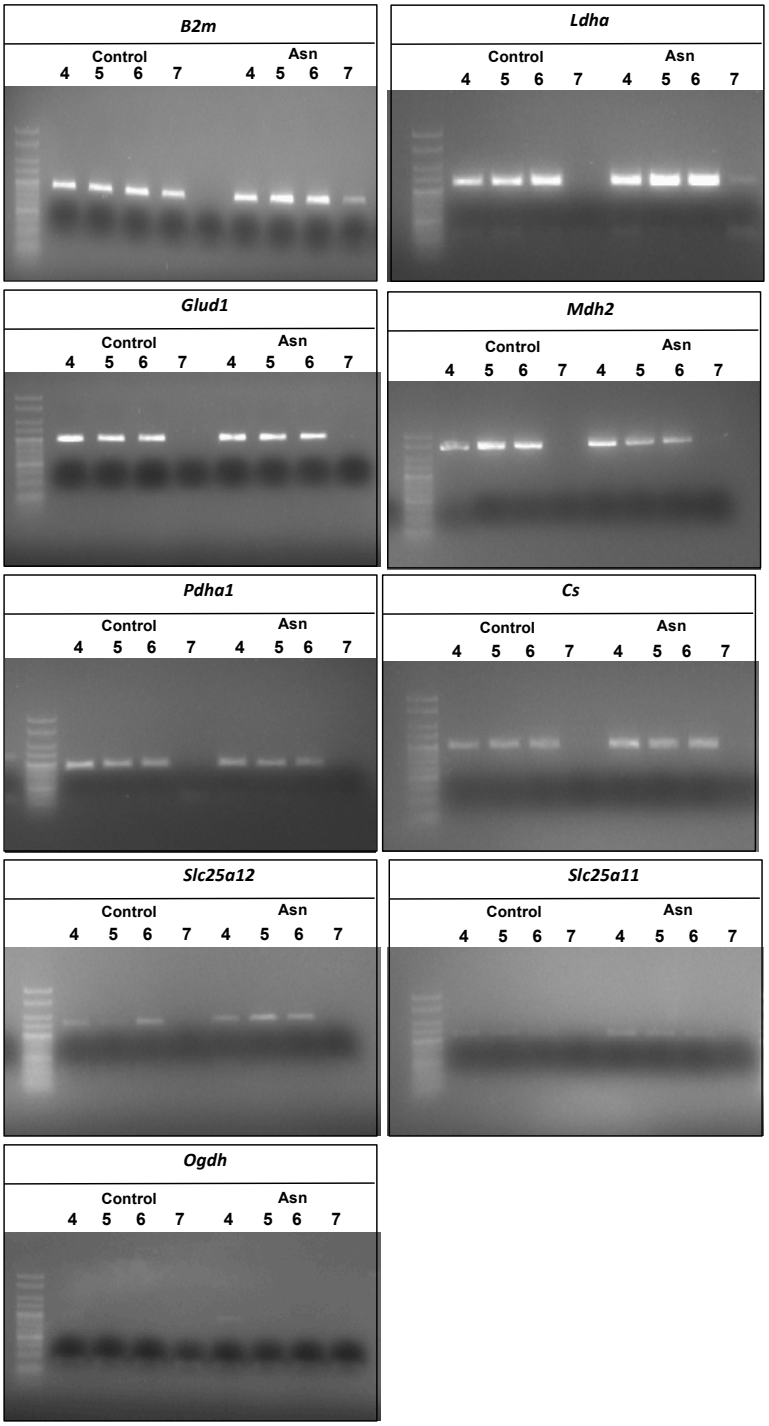

Figure 3.9 Assessment of expression of mRNA for enzymes linked to the TCA cycle by PCR.

Cell samples from the control (black) and Asn-fed (red) at day 4, 5, 6 and 7 were harvested for RNA extraction (Section 2.6.1) and cDNA synthesis (Section 2.6.4). cDNA samples were examined by PCR (Section 2.6.5). The PCR products and HyperLadder™ 25bp were separated by 1% (w/v) gel electrophoresis and image was taken by UV transillumination (Section 2.6.6). The PCR product size was around 182 bp (*B2m*), 226 bp (*Ldha*), 198 bp (*Glud1*), 424 bp (*Mdh2*), 180 bp (*Pdha1*), 201 (Cs), 245 bp (*Slc25a12*), 216 bp (*Slc25a11*) and 200 bp (*Ogdh*).

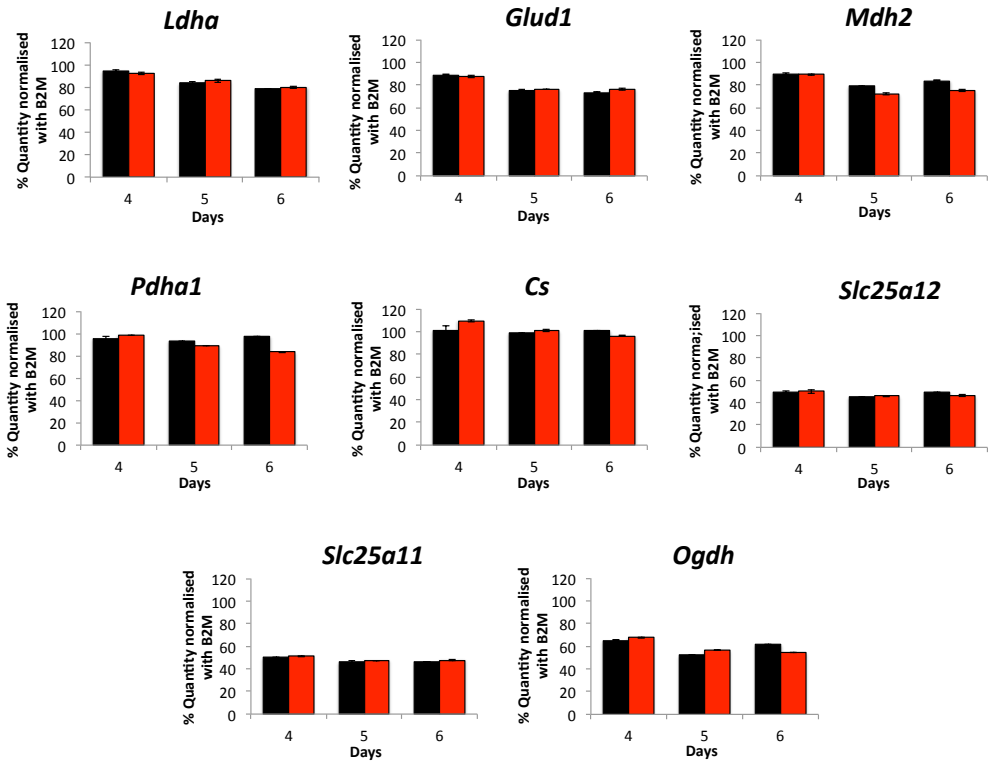

Figure 3.10 Assessment of expression of mRNA for enzymes linked to the TCA cycle by qPCR.

cDNA samples from the control (black) and Asn-fed (red) at day 4, 5, 6 and 7 were synthesized as describe in Figure 3.9 and were examined by qPCR (Section 2.6.7). The values from qPCR were normalised to *B2m* expression. Values presented are mean ± SEM for three replicates.

Therefore, in light of this background oxygen consumption (Section 3.5.1), mitochondrial membrane potential (Section 3.5.2), cell size (Section 3.5.3) and the amount of mitochondria and ER (Section 3.5.4) were investigated in control cells and those supplemented with Asn or HB throughout culture.

3.5.1 Oxygen consumption rate

It was hypothesized that increased TCA cycle function might enhance oxidative phosphorylation or increase oxygen consumption rate. Cells were harvested from the cultures of control, Asn-feeding and HB-feeding from day 4 of culture onwards (i.e. the time following feed addition) and an oxygen electrode was used directly to measure oxygen consumption of cells in their pre-existing medium conditions (Section 2.5.1). Control cells exhibited a decrease in the rate of oxygen consumption per cell with the progression of culture (Figure 3.11A). Cells fed with Asn generated greater oxygen consumption per cell than the control at day 5 (but not significantly so) and this effect was significantly greater of control at day 6. Likewise, addition of HB produced greater oxygen consumption per cell than the control at all time points and this increase was significantly greater than that of the control at days 6 and 7.

Cells fed with Asn or HB maintained higher oxygen consumption rates than the control at all time points examined although oxygen consumption rates declined when as cells of any treatment entered decline phase. A decreased oxygen consumption rate has been noted previously as CHO cells entered decline phase (Deshpande and Heinzle, 2004, Zagari et al., 2013). It can be suggested that increased production of intermediates in the TCA cycle in the presence of Asn or HB might correlate with enhanced activity of the TCA cycle leading to enhanced oxidative metabolism and increased oxygen consumption rate. Such findings and interpretations are consistent with other another publication that reported that cells that produced large amounts of lactate had low oxygen consumption rates (Zagari et al., 2013).

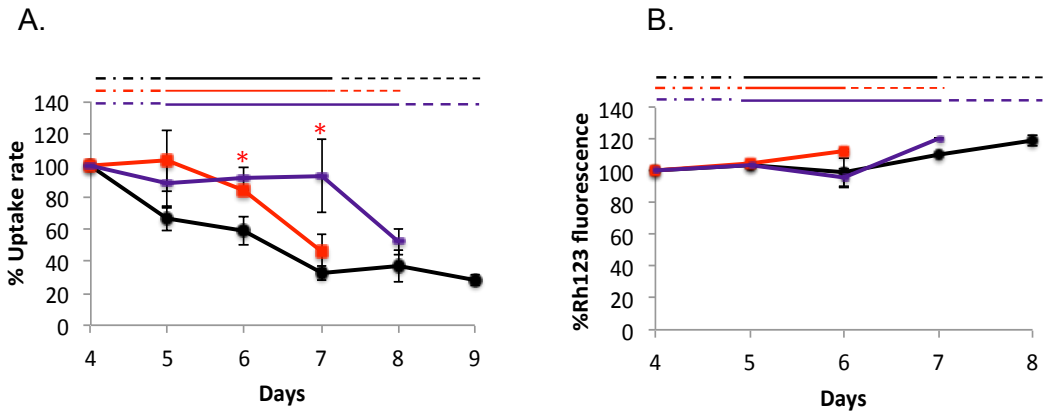

Figure 3.11 Oxygen consumption and mitochondrial membrane potential of LB01 cells during control and feed supplemented cultures.

The oxygen consumption rate (A) and mitochondrial membrane potential (B) were measured at different day of culture. LB01 cells were culture as describe in Figure 3.2. Cell samples from the control (black), Asn-fed (red), HB-fed (purple) at day 4, 5, 6, 7, 8 and 9 were harvested for the study of oxygen consumption (Section 2.5.1) and mitochondrial membrane potential (Section 2.5.2). Data are shown in % of day 4. Values presented are mean ± SEM for three replicates. * indicate significant difference from control at $p < 0.05$. The lines at the top of each graph are added to indicate stages of growth: exponential phase (dot-dash line), stationary phase (solid line) and decline phase (dashed line).

3.5.2 Mitochondrial membrane potential

As the mitochondrial membrane potential was shown to correlate to lactate profile and mitochondrial function in term of oxygen consumption (Zagari et al., 2013, Zagari et al., 2013), Rhodamine123 (a dye that monitors mitochondrial membrane potential) (Shapiro, 2000, Solaini et al., 2007, Hinterkoerner et al., 2007) was used as a probe of mitochondrial membrane potential and fluorescent signal of Rhodamine123 which was proportional with mitochondrial membrane potential or electrophoretic accumulation in mitochondria was measured by flow cytometry with cells under control conditions or after feeding with Asn or HB (Section 2.5).

The fluorescence intensity of the control remained the same from day 4 onwards and the intensity was slightly increased at the end of culture period (Figure 3.11B). Cells in the presence of either Asn or HB exhibited the same pattern of fluorescence intensity as the control (Figure 3.11B). Hence the addition of Asn or HB did not affect mitochondrial membrane potential although the profile of lactate metabolism was changed by addition of Asn or HB. However, there was disagreement in the relationship between lactate profile and mitochondrial membrane potential in CHO cells. Zagari et al. (2013) showed that high lactate production cells had low mitochondrial membrane potential monitored by tetramethylrhodamine ethyl ester (TMRE) dye. In contrast, Gilbert et al. (2013) and Hinterkoerner et al. (2007) reported that high lactate production cells associated with increased mitochondrial membrane potential using Rhodamine123. However, the inconsistency of the result of mitochondrial membrane potential may be due to the different type and concentration of fluorescent dye used in the experiment.

3.5.3 Cell size

As the relationship between cell size and recombinant protein production was mentioned before (Kim et al., 2001, Lloyd et al., 2000), cell samples were harvested throughout the culture period and flow cytometry was used to compare relative cell size between the control and those fed with nutrients (Section 2.2.2). An automated cell counter was also used to measured diameter of the control cells. Flow cytometry indicated that control cells had a relatively constant size from day 0 to day 6 of culture with a subsequent slight decrease observed as cells entered and progressed through decline phase (Figure 3.12A). This profile is consistent with the engagement with apoptotic cell death in CHO cell decline phase (Bortner and Cidlowski, 2002). The diameter of the cells was about 13.5 mm at day 0 to day 6 and it was slightly decreased to 12 mm at day 9. The diameter of CHO-LB01 cells in this study is similar to that reported for CHO G6-1 cells

where the diameter of the cells decreased from 15 mm at day 1 to 14 mm at day 9 (Han et al., 2006). The addition of either Asn or HB was associated a change to cell size with both generating cells of a greater size than the control after day 5 while the size of cells feed with HB was significantly greater (about 40%) than the control at day 7 and 8. The enlarged cell phenotype was maintained until cells entered their appropriate decline phase (Figure 3.12A).

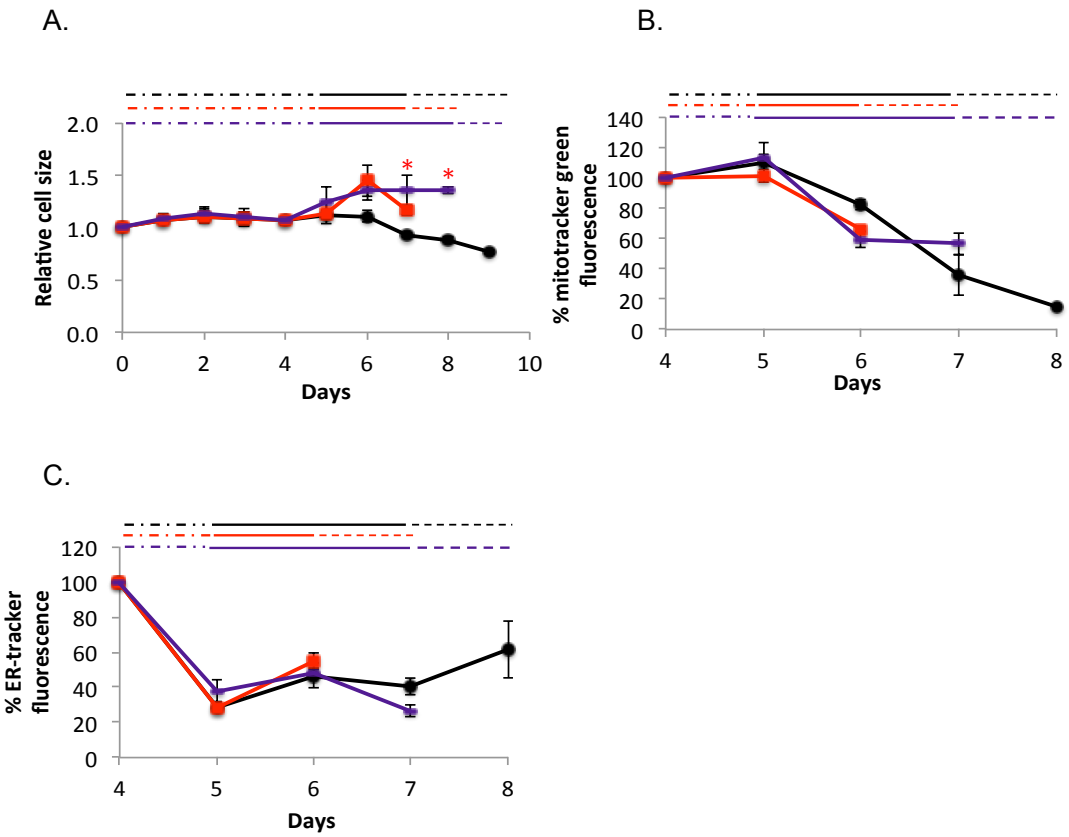

Figure 3.12 Cell size and cell mitochondrial and ER content of LB01 during control and feed supplemented cultures.

Cell size (A) mitochondrial content (B) and ER content (C) were measured at different day of culture. LB01 cells were culture as describe in Figure 3.2. Cell samples from the control (black), Asn-fed (red), HB-fed (purple) at day 4, 5, 6, 7, 8 and 9 were harvested for the study of cell size (Section 2.2.2), mitochondrial and ER content (Section 2.5.2). Data are shown in % of day 4. Values presented are mean ± SEM for three replicates. * indicate significant difference from control at $p < 0.05$. The lines at the top of each graph are added to indicate stages of growth: exponential phase (dot-dash line), stationary phase (solid line) and decline phase (dashed line).

It can be suggested that cells under conditions associated with greater product yield (cells fed HB) might have bigger cell size. Kim et al. (2001) and Lloyd et al. (2000) found that big cells were more productive than small cells. In addition, changing of cell size might associate with a linked activity of the mammalian target of rapamycin complex 1 (mTORC1) pathway because many key cellular functions of the cells including cell size are regulated by mTORC1 (Laplante and Sabatini, 2012, Meyuhas and Dreazen, 2009). Dadehbeigi and Dickson (2015) found that feeding Glc, Asp, Asn, Glu and Py of CHO-LB01 cells increased growth and product yield and also increased the phosphorylation downstream target of mTORC1 (S6 kinase 1 (S6K1) and eukaryotic initiation factor 4E binding protein 1 (4E-BP1)). However, molecular level of mTORC1 pathway was not investigated in that study. Moreover, overexpression of S6K1 resulted in increased cell size in Human U2O2 osteosarcoma cell (Fingar et al., 2002). Thus, it can be hypothesized that alteration of cell size and cell culture performance in response to nutrient feeding might involve the mTORC1 pathway. This hypothesis could be investigated further by examination of the effect of nutrient feeding at the molecular level of mTORC1 pathway by immunoblotting to assess the phosphorylation degree of downstream target of mTORC1 (Chapter 7).

3.5.4 Mitochondrial and ER content

Highly productive cells have been associated with increased mitochondrial and ER content (O'Callaghan et al., 2015). Therefore investigation of mitochondrial and ER content in the control and nutrient-fed cells was achieved by live cell staining using Mito-Tracker® and ER-Tracker (Section 2.5.2), respectively. Flow cytometry of the control using Mito-Tracker® showed that the fluorescence intensity was steady from day 4 to day 5 and then gradually declined throughout the culture (Figure 3.12B). Likewise, cells supplemented with Asn or HB generated the same pattern of fluorescence intensity as the control (Figure 3.12B). In the case of ER content, there was a dramatic drop in the

fluorescence intensity of ER-Tracker at day 5 in the control. Afterward, the fluorescence intensity fluctuated between 20 and 50% for the remaining of the culture (Figure 3.12C). Similarly, cells in the presence of Asn or HB exhibited the same pattern of fluorescence intensity as the control (Figure 3.12C). These results suggest that addition of Asn or HB had no effect on mitochondrial and ER content although increased maximum cell density and product yield was observed in the presence of Asn or HB, respectively. However, Callaghan et al. (2015) reported no linear correlation between mitochondrial content and high productivity clones of CHOK1SV cells transiently transfected with IgG4 constructs. In contrast, the relationship between high producing clones and greater ER content was observed in the same study.

In summary, these data indicate that addition of Asn or HB generated increased oxidative metabolism in the CHO cells, read out in terms of oxygen consumption and generated bigger cell size but had no effect on mitochondrial membrane potential and mitochondrial/ER content.

3.6 Discussion

This chapter focused on approaches that might increase the flux in the TCA cycle because the relationship between increased TCA cycle and increase product yield was reported earlier (Lee et al., 2015, Sellick et al., 2011, Templeton et al., 2013). Therefore, it was hypothesized that increased TCA cycle flux and related metabolism would enhance the growth and/or productivity of CHO cells. Asn, Asp, Glu, Py and HB were selected to be nutrient feeding base on initial interpretations of earlier work on culture feeds in this laboratory (Donamaria 2012, Sellick et al., 2011) in order to identify which nutrient had an effect on cell growth, antibody production, metabolite profile and cellular phenotype of CHO-LB01 cells.

The results described in this chapter demonstrate the effects of Asn and HB supplementation on cell culture performance, metabolite profiles and cellular phenotype (summarized in Figure 3.13 and 3.14) while addition of Asp, Glu and Py did not affect cell growth and antibody production of CHO-LB01 cells. Feeding Asn had a significant effect on cell growth by increased maximum cell density and early cell death while supplementation with HB significantly increased product yield. Although both had differential effect on cell culture performance, the extra- and intra-cellular metabolite profiles were similar.

Analysis of data from extra- and intra-cellular metabolite profiles showed that Asn and HB addition decreased the amount lactate, glycerol, sorbitol and amino acids. Moreover, there was very clear enhancement of metabolites in TCA cycle. It can be suggested that Asn and HB might increase the flow of the TCA cycle at the point of oxaloacetate, an intermediate associated with a bottleneck limited by MDH II activity (Chong et al., 2010), and acetyl-CoA, respectively. As a result less glucose would be converted to sorbitol and glycerol and lactate was used in order to increase the flow of carbon intermediates into the TCA cycle and maintain energy generation by TCA cycle. In addition, decreased amounts of amino acids reflected that amino acids were consumed quicker in order to replenish the flow of the TCA cycle. A correlation between enhanced TCA cycle flux and productivity has been reported (Templeton et al., 2013, Lee et al., 2014). It is possible that increased TCA metabolites may be a result of more active TCA cycle flux. Thus high TCA cycle flux would require increased replenishment from carbon sources or amino acids. When the cells produce high amounts of ATP, high titer would be achieved since formation of peptide bonds and maintain high viability is an ATP-dependent process (Dean and Reddy 2013). Therefore, it can be suggested that increased production of metabolites in the TCA cycle should increase the flow of TCA cycle and result in enhance energy and recombinant protein production. This suggestion was supported by the result of oxygen consumption rate in Section 3.5.1 which illustrated that the oxygen consumption rate was greater in the presence of Asn or HB.

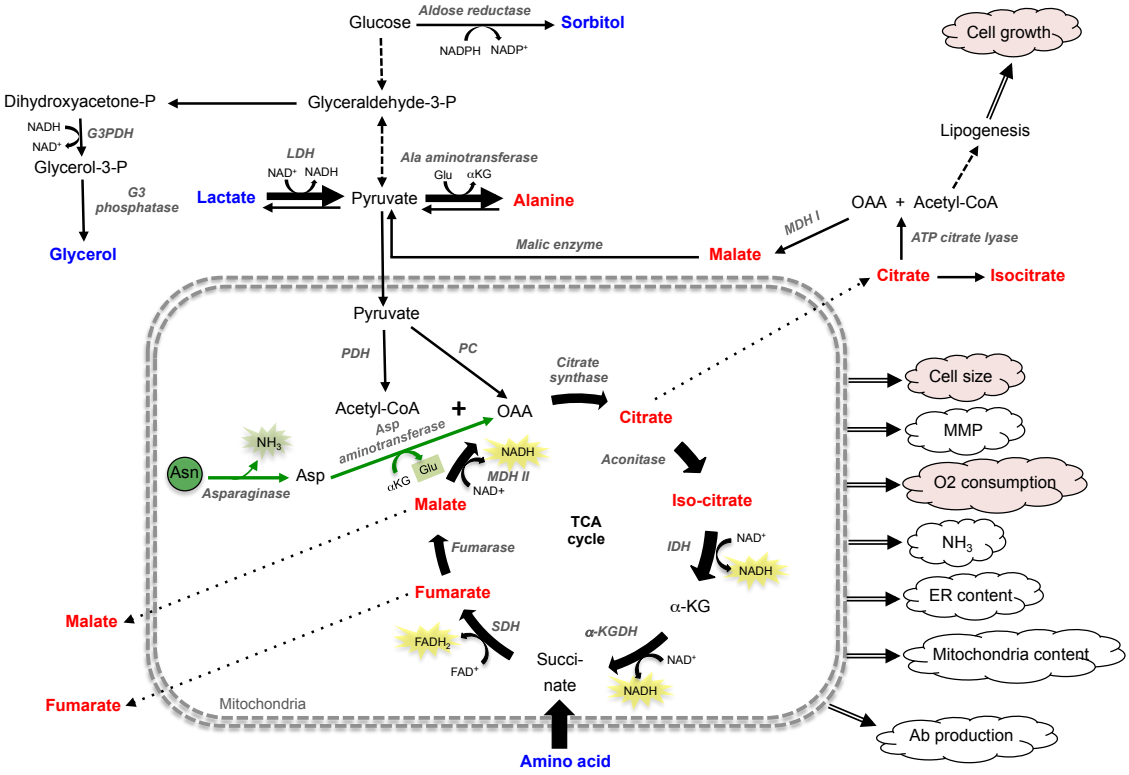

Figure 3.13 Summary of the effect of feeding Asn on cell growth, Ab production, metabolite profiles and cellular phenotypes.

Asn gets into the TCA cycle via OAA. First step, Asn is conversed to Asp by asparaginase producing ammonia (NH_3). Next, OAA is generated from Asp by transamination of αKG to Glu by aspartate aminotransferase. Supplementation with Asn increased cell growth, cell size and oxygen consumption. In term of metabolite profiles, lactate, glycerol and sorbitol production were decreased, whereas metabolites in TCA cycle (citrate, isocitrate, fumarate and malate) were increased. Additionally, amino acid consumption was increased. The red characters indicate increased production or decreased consumption. The blue characters indicate decreased production or increased consumption. The red and white clouds indicate increased and no effect, respectively. Single reactions indicate with solid black lines and multiple steps by dash lines. Dot lines indicate transport across mitochondrial membrane. (Asn = asparagine, Asp = aspartate, αKG = α-ketoglutarate, Glu = glutamate, OAA = oxaloacetate, G3PDH = glyceroldehyde-3-phosphate dehydrogenase, G3 phosphatase = glycerol 3 phosphatase, LDH = lactate dehydrogenase, PDH = pyruvate dehydrogenase, PC = pyruvate carboxylase, IDH = isocitrate dehydrogenase, αKG = α-ketoglutarate dehydrogenase, SDH = succinate dehydrogenase, MDH II = malate dehydrogenase II).

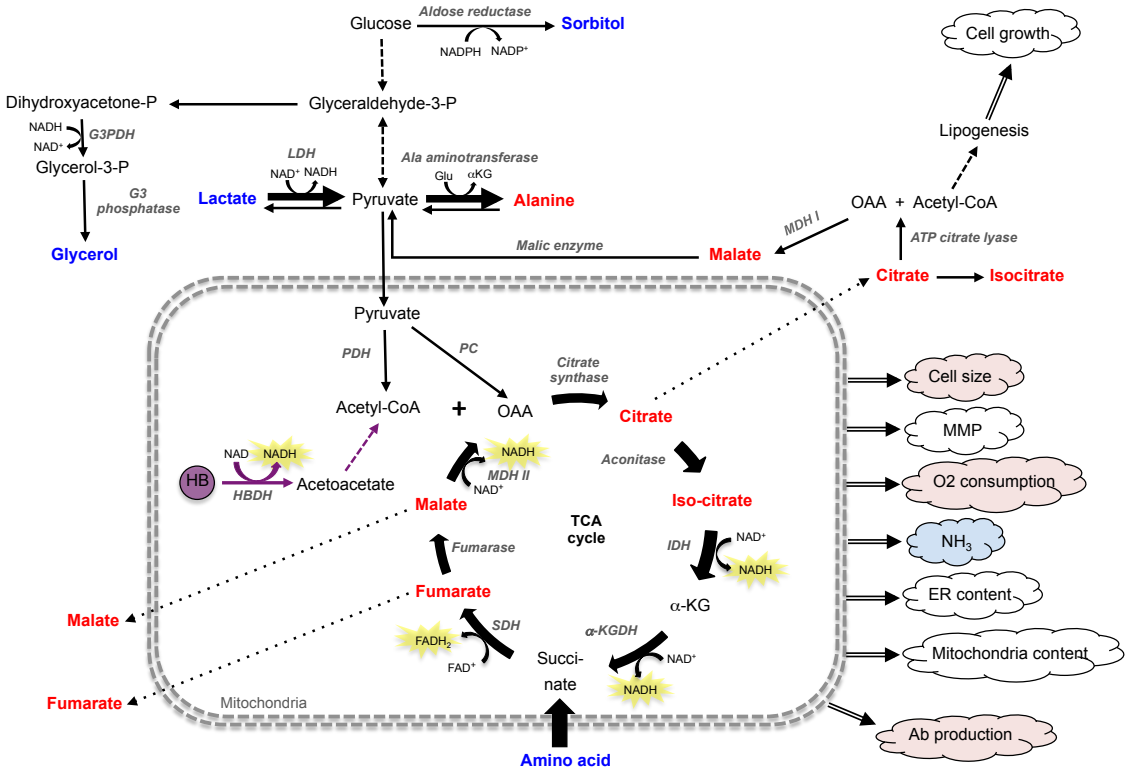

Figure 3.14 Summary of the effect of feeding HB on cell growth, Ab production, metabolite profiles and cellular phenotypes.

HB gets into the TCA cycle via acetyl-CoA. NADH is generated in mitochondria from the conversion of HB to acetoacetate by HBDH. Supplementation with HB increased Ab production, cell size and oxygen consumption and also decreased ammonia accumulation. In term of metabolite profiles, lactate, glycerol and sorbitol production were decreased, whereas metabolites in TCA cycle (citrate, isocitrate, fumarate and malate) were increased. Additionally, amino acid consumption was increased. The red characters indicate increased production or decreased consumption. The blue characters indicate decreased production or increased consumption. The red, blue and white clouds indicate increased, decreased and no effect, respectively. Single reactions indicate with solid black lines and multiple steps by dash lines. Dot lines indicate transport across mitochondrial membrane. (HB = β-hydroxybutyrate, OAA = oxaloacetate, αKG = α-ketoglutarate, HBDH = hydroxybutyrate dehydrogenase, G3PDH = glyceroldehyde-3-phosphate dehydrogenase, G3 phosphatase = glycerol 3 phosphatase, LDH = lactate dehydrogenase, PDH = pyruvate dehydrogenase, PC = pyruvate carboxylase, IDH = isocitrate dehydrogenase, aKG = α-ketoglutarate dehydrogenase, SDH = succinate dehydrogenase, MDH II = malate dehydrogenase II).

Although both nutrients increased the amount of metabolite in the TCA cycle but only HB increased antibody yield. Two possibilities may explain this observation.

Firstly, from the conversion of HB to acetoacetate, NADH was also produced in mitochondria (Figure 3.14), which helps the cell generate energy. As a result, antibody production was increased.

Secondly, in the presence of HB, ammonia production was decreased (around three-fold from the control) (Section 3.3.1). Several papers have reported that the accumulation of ammonia can inhibit growth, impair productivity and impacts on protein glycosylation (Chen et al., 2001, Xu et al., 2014). In CHO-GS system, ammonia is normally generated from the deamination (Duarte et al., 2014) of glutamate and asparagine (Schneider et al., 1996, Chen and Harcum, 2005) in the concentration around 2-4 mM (Carinhas et al., 2013, McCracken et al., 2014). Alanine is hypothesized to be secreted into the media as a mechanism to decrease ammonia toxicity by redirecting the amine group from glutamate to pyruvate to produce alanine, instead of free ammonia (Chen and Harcum, 2005, Carinhas et al., 2013, Butler and Jenkins, 1989). From the extracellular metabolite profile of cells fed HB, high alanine production was detected. Thus, it can be suggested that alanine was produced for ammonia detoxification. In case of Asn addition, alanine was also produced higher than control, similar with HB, but decreased ammonia production did not observe. It is possible that ammonia was produced from the conversion of Asn to Asp. Therefore, the concentration of ammonia was still high although alanine was produced to decrease ammonia accumulation in case of supplementation with Asn.

Thus, it can be concluded that in addition to increased the metabolite in the TCA cycle, generation of NADH in mitochondria and the inhibition of ammonia production may be another important reason to explain why feeding HB significantly increased antibody production. Moreover, in starvation, HB can replace glucose as the energy source for

brain metabolism (Owen et al., 1967). However, in order to confirm such an explanation, MFA and determination of mitochondrial NADH would be required (Chapter 7).

In case of Asn-fed cells, although similar metabolite profiles were observed to that found with HB feeding, addition of Asn increased maximum cell density and showed earlier cell death but did not increase antibody production. There are three possible reasons to explain this observation.

Firstly, it is possible that Asn itself might have a positive effect on cell growth and feeding Asn can generate glutamate which might be important for cell growth by transamination of Asp to oxaloacetate in mitochondria (Figure 3.13). This is in agreement with Kurano et al. (1990) who reported that Asn can support the growth of CHO cell as a stable substitute for glutamine and Duarte et al. (2014) who found growth arrest in the medium in which Asn was absent. Dean and Reddy (2013) also suggested that consumption of Asn to replenish the TCA cycle is linked to cell growth. However, from the result of glutamate profiling, both cells fed Asn and cells fed HB increased the amount of glutamate inside the cells (Figure 3.8). It is possible that glutamate was generated in different compartments inside the cells. In case of feeding Asn, glutamate might be generated inside mitochondria (Figure 3.13) resulting in enhanced cell growth because glutamate can produce αKG and other amino acid to supply the TCA cycle. Therefore, in order to test this assumption, measurement the concentration of glutamate inside mitochondria of cells fed Asn compared to cells fed HB would be required in the future (Chapter 7). However, as shown in Section 3.2, feeding Glu did not affect cell growth and antibody production of CHO-LB01 cells. It is possible due to the difficulty of Glu to transport into the cell or mitochondria because of the net charge (Altamirano et al., 2001, Newsholme et al., 2003).

Secondly, It can be suggested that by producing more citrate this would increase more citrate export into the cytoplasm for lipid formation, which is an essential feature for cell proliferation (Coleman and Lavietes, 1981). Addition of HB did not generate an effect on cell growth although it led to increased citrate formation, as observed for feeding Asn. This might be because, in addition to increased citrate formation, feeding Asn would also produce glutamate in mitochondria, which might be important for cell growth as mentioned before. In addition, it can be concluded that citrate efflux for lipid formation might not be the main factor related to cellular proliferation.

Finally, more rapid glucose consumption and lower amount of amino acids compared to the control and feeding HB were observed in cells fed Asn. These are probably also the reason why cells fed Asn grew and died quicker than the control and HB-fed cells. As a result, the cells cannot produce antibody as much as in the presence of HB although cells fed Asn had higher cell number than the addition of HB. It might be because high growth rate is usually accompanied by low productive cell because cell resources are allocated for cell proliferation rather than protein production (Altamirano et al., 2001, Chusainow et al., 2009, Edros et al., 2014, Fussenegger et al., 1997, Jiang et al., 2006, Mastrangelo and Betenbaugh, 1998, Wilkens and Gerdtzen, 2015). Therefore, supplementation with glucose and some potential limiting amino acids in Asn-fed cells in order to maintain cell growth will be examined in Chapter 4.

Although there were changes to lactate profile, increased TCA cycle intermediates and enhanced oxygen consumption rate for cells fed with Asn or HB, no changes were observed in the expression of a group of enzymes involved in the TCA cycle and malate/aspartate shuttle and mitochondrial membrane potential were not found in this study. It can be suggested that changing of metabolite profiles in addition of Asn or HB did not change gene expression level of gene detected and mitochondrial membrane potential of CHO-LB01 cells. Additionally, feeding Asn or HB did not have an effect on mitochondrial and ER content but cell size was larger than the control. Alteration of cell

size in response to nutrient feeding might involve in mTOR pathway as discussed in Section 3.5.

Overall, the effect of nutrient addition on cell growth, antibody production, metabolite profiles and cellular function were investigated in CHO-LB01 cell. Thus, the first objective was achieved (Section 1.6). From the overall result in this chapter, three main points are raised. Firstly, Asn is the key amino acid that support cell growth of CHO-LB01 cells. Secondly, to our knowledge, this work represents the first study to examine addition of HB as a feed and this has been shown to offer a simple effective strategy to increase recombinant protein production and overcome ammonia accumulation of CHO-LB01 cells. Finally, this result confirms the association between increased recombinant protein production and increased TCA cycle flux. In addition, increased TCA cycle flux also found to support cell growth. It should be noted that differential effect of Asn and HB on cell culture performance may be dependent on additional factors which were not examined in the present study such as NAD^+/NADH ratio, $NADP^+$/NADPH ratio and other metabolites. Thus, It would be interesting to assess these parameters in future study. However, based on the positive effect of feeding Asn or HB on cell culture performance observed in this chapter, further improvement of product yield and/or cell growth of CHO-LB01 cells by modification of nutrient feeding in order to extend stationary phase or prolong cell survival will be investigated in the next chapter.

CHAPTER 4

Increased productivity of CHO cells by modification of feeding nutrients

4.1 Introduction

It has been shown that enhancement of cell growth and antibody titre of CHO-LB01 cell could be achieved by a simple strategy of specific medium supplementation with Asn or HB (Chapter 3). Chapter 4 focused on extension of the period of productivity (stationary phase) of Asn-fed and HB-fed cells in order to obtain greater yield. There is a widely-accepted view that glucose is a critical nutrient to support the growth and recombinant protein production of CHO cells (Ahn and Antoniewicz, 2013, Behjousiar et al., 2012, Duarte et al., 2014, Sellick et al., 2015). Sellick et al. (2011) reported that CHO-LB01 cells exhibited a prolonged stationary phase and that entry into decline phase could be delayed when glucose was added in the culture medium. Additionally, as observed from glucose profiles associated with cell growth in Chapter 3 (Figure 3.3A), depletion of glucose occurred at times associated with the entry of cells into decline phase. Therefore, addition of glucose into Asn-fed and HB-fed cells, prior to glucose depletion, offers a potential strategy to extend cell culture period. However, several papers report that high glucose concentrations can have inhibitory effects on CHO cell growth (Kurano et al., 1990, Liu et al., 2015, Mulukutla et al., 2010).

As described for glucose, depletion of specific amino acids was also associated with the entry of cells into decline phase and a feeding regime with supplementation with these amino acids presented an alternative, and/or complementary, approach to enhance production. Several amino acid supplementations have been used in CHO cell culture. A combination of serine, cysteine and tyrosine improved antibody titre and cell viability for CHO DUX-XB11 cells cultured in CHO-S-SFMII medium (Kishishita et al., 2015). Under supplementation conditions, clear differences were seen for metabolite profiles with a switch from lactate production to consumption. An addition of a mixture of eight amino acids (cysteine, isoleucine, leucine, tyrosine, valine, asparagine, aspartate, glutamate), improved titre for $DHFR^-$ CHO cells cultured in DMEM/F-12 medium supplemented with

5% serum (Crowell et al., 2007). Yu et al. (2011) demonstrated that increased concentrations of nutrient components (amino acids, vitamin and trace elements) resulted in increased culture longevity and product titre of CHO DUX-XB11. They also found that translation limitation resulting from tyrosine depletion might be the bottleneck for production. Chemically-synthesized dipeptides have been used to increase the delivery of poorly soluble amino acids such as tyrosine. Kang et al. (2012) found that culture viability and product yield were improved when tyrosine-histidine or tyrosine-lysine were added to CHO cells. Additionally, the results from Chapter 3 (Figures 3.3A and 3.7) showed the relationship between low amounts of amino acids and earlier cell death in the presence of Asn. Thus, based on this background, it was hypothesized that addition of glucose and/or amino acids to cells fed Asn or HB would further extend stationary phase and increase antibody titre. Therefore, the work described in this chapter examines nutrient means to extend culture duration in order to increase product yield of CHO-LB01 cells, building from approaches and results described in Chapter 3.

In this chapter, glucose (Section 4.2 and 4.3) and specific amino acids (Section 4.4) were added to cultures supplemented with Asn or HB. In parallel to measurement of growth and antibody production, metabolite profiles were measured to examine possible relationships between specific metabolic changes and cell growth and recombinant protein production.

4.2 Effect of a combination of Asn and Glc on cell culture performance and metabolite profiling

Based on the results in Chapter 3, feeding Asn increased maximum cell density. Glucose was added on day 6 of culture (when glucose was greater than 5 mM, Figure 3.3A) to increase glucose concentration by a further 20 mM (the approximate initial concentration of glucose in CD OptiCHO^{TM} medium obtained by glucose assay in Section 3.3.1, Figure 3.3A). Therefore, the experimental protocol for cell culture places cells under one of four conditions: unfed (control), fed with asparagine alone at day 4 (Asn), fed with glucose alone at day 6 (Glc) and fed with asparagine at day 4 plus fed with glucose at day 6 (Asn+Glc). Medium samples were collected every day to determine cell growth (Section 2.2.2), antibody amount (Section 2.4.1), ammonia concentration (Section 2.3.1.5) and extra- and intra-cellular metabolite profiles (Section 2.3.2).

4.2.1 Cell growth and antibody production

In control conditions, cells reached a maximum viable cell density at ~1x10^7 cells/mL at day 6 and died at day 12 (Figure 4.1A). The pattern of cell growth of the control was similar to previous results in this thesis (Figure 3.1A and 3.2A) but maximum viable cell density in this set of experiments was greater than observed in previous sets of experiments (7x10^6 cells/mL) (Section 3.2). Addition of Asn significantly increased the maximum viable cell density to ~1.2 x 10^7 cells/mL at day 5 and the cells died earlier (day 8) than the control (day 12) (Figure 4.1A) as observed in previous results for Asn feeding (Figure 3.1A and 3.2A). However, cells fed Asn in this set of experiments reached higher maximum viable cell density and died earlier than observed in previous results where cells reached maximum cell densities of ~1x10^7 cells/mL and died at day 9 (Figure 3.1A and 3.2A). Surprisingly, cells supplemented with glucose alone reached

maximum viable cell density at ~1.2x10^7 cells/mL at day 7 after glucose addition at day 6 (Figure 4.1A). Afterwards, viable cell density slightly decreased at day 8 and then cells died at day 9 which was earlier than observed for the control (by three days). This is in contrast with the results obtained by Sellick et al. 2011 where glucose addition to CHO-LB01 cells at day 4 of bacth culture had no effect on maximum viable cell density but prolonged the stationary phase by one day. The addition of Asn+Glc, generated culture conditions in which cells reached a maximum viable cell density of ~1.3x10^7 cells/mL at day 5 (Figure 4.1A), comparable to that with addition of Asn alone. Under these conditions, viable cell density slightly decreased to ~1x10^7 cells/mL at day 6 and then remained constant (until day 8) after glucose was added at day 6. Thereafter, viable cell density was decreased to ~8x10^6 cells/mL at day 9 which was significantly greater than the control. This density remained relatively constant until day 13 after which time cells entered decline phase and died by day 15, three days after the control. This pattern of cell growth is similar to the effect of supplementation with CHO CD EfficientFeed™ A and B on CHO-LB01 cells (Sellick et al., 2015).

In terms of cumulative cell number, all conditions, except for addition of Asn+Glc, generated similar cumulative cell numbers (~5.5 x10^7 cells/mL for the control and Glc-fed cells and 4.5 x10^7 for Asn-fed cells) (Figure 4.1B) This was almost two-fold greater than that observed in previous results (Figure 3.2B) due to a generally greater viable cell density obtained with cells in this series of experiments. In the presence of Asn+Glc, cumulative cell number was twice that observed under any other conditions (Figure 4.1B).

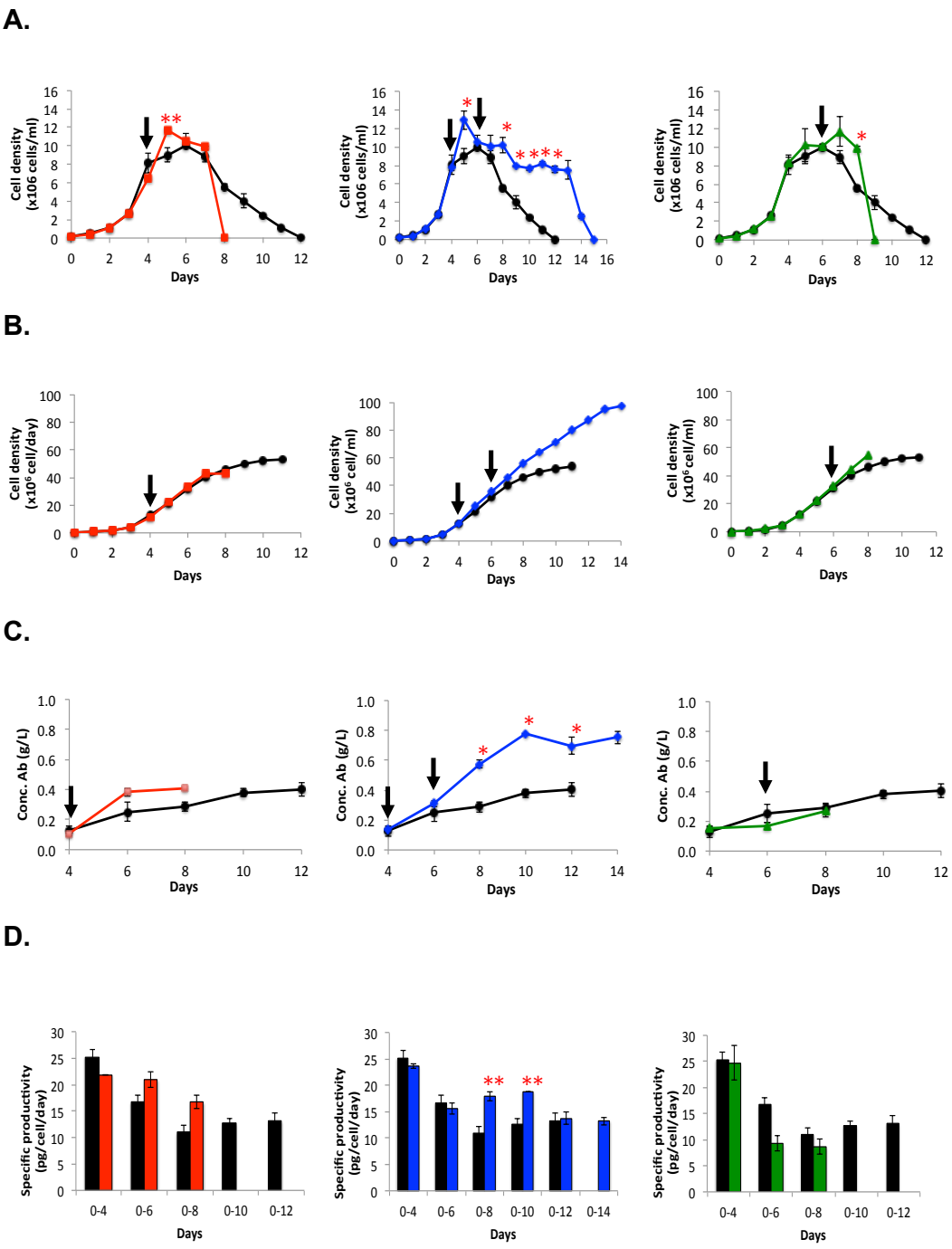

Figure 4.1 Cell growth and antibody production of LB01 cells in response to Asn, Asn+Glc and Glc.

Viable cell density (A), cumulative cell number (B), antibody production (C) and specific productivity (D) were measured for LB01 cells throughout batch culture in CD OptiCHO™ (control, black symbols) or with supplemention at day 4 (for Asn) or day 6 (for Glc) of culture (the arrow presents the time of addition) with Asn (1.5 mM, red), Glc (20 mM, green) or Asn+Glc (blue) (Section 2.2.4). Medium samples were collected for cell counts (Section 2.2.2) and ELISA (Section 2.4.1). Values presented are mean ± SEM for three replicates for all conditions, all shown against their respective controls. * and ** indicates significant difference from control at $p < 0.05$ and 0.1, respectively.

The control produced maximum antibody yield about 0.4 g/L at day 12, (Figure 4.1C), a value that was less than previous results (0.6 g/L, Section 3.2). In the presence of Asn the same concentration of antibody (0.4 g/L) was obtained by day 6 and this remained constant until the last day of culture (day 8) (Figure 4.1C). Again this concentration was less than the concentration of antibody (0.6 g/L) detected in the presence of Asn from previous results (Figure 3.1B and 3.2C). Cells supplemented with glucose produced slightly less antibody (0.3 g/L) than the control at day 8 before the cells died at day 9 (Figure 4.1C). This is consistent with the previous observation that feeding glucose alone did not enhance antibody production (Sellick et al., 2011). In the case of feeding Asn+Glc, the concentration of antibody was significantly greater than the control from day 8 of culture onwards (after glucose was supplemented in the cell culture at day 6) (Figure 4.1C). The maximum concentration of antibody was twice (0.8 g/L) that of the control. The prolonged stationary phase of culture observed in the presence of Asn+Glc was a major factor for the enhanced antibody yield. Greatest specific productivity was found between days 0-4 (for the control, feeding glucose and feeding Asn+Glc) or day 0-6 for (feeding Asn) (Figure 4.1D). Maximum specific productivities of about 25 pg/cell/day were observed for all conditions. In the present of Asn and Asn+Glc specific productivity was slightly higher than the control at day 0-6 and day 0-8 for cells fed Asn and day 0-8 and day 0-10 for cells fed Asn+Glc. Specific productivity was less than that observed in previous results (40 pg/cell/day) because in this study cells generated almost two-fold higher cumulative cell number and lower antibody production than previously (Figure 3.2D).

In summary, the results from these experiments confirm the impact of Asn on cell growth by increased maximum cell density and earlier death although there was a slight shift of cell growth patterns, with cells fed Asn in this experiment reaching higher maximum cell density and entering decline phase earlier than previously. The possible explanation for this alteration will be discussed in Section 4.5. Contrary to expectations, addition of glucose alone caused earlier (by 3 days) entry into cell death. Although glucose is a

necessary carbon source to maintain cell growth and viability, with high amounts of glucose, toxic metabolites (such as lactate) can be generated from glucose metabolism. This might lead to inhibitory effects on CHO cell growth (Kurano et al., 1990, Liu et al., 2015). Liu et al. 2015 observed decreased viable cell density and increased cell death with addition of increased amounts of glucose from 27 mM to 80 mM to CHO-DG44 cultures. An especially interesting finding from the present study was that cells exhibited a prolonged stationary phase (by 5 days) and achieved greater cumulative cell number in the presence of Asn+Glc. As a result total antibody titre was significantly improved. Despite the fact that feeding glucose alone had a negative effect on cell growth, the combination of Asn and glucose had an additive effect on both cumulative cell number and antibody production. Based on this result two hypotheses were raised. Firstly, Asn+Glc-fed cells could generate similar extra- and intra-cellular metabolite profiles to cells fed Asn or HB. Secondly, application of metabolite profiles could give a molecular understanding of the differential effects of combinations of glucose and asparagine. Therefore, further investigation of metabolite profiles were undertaken in order to understand the relationship of cell culture performance and metabolite profiles.

4.2.2 Extracellular and intracellular metabolite profiling

In order to test the hypothesis developed above and to seek an explanation why cells fed Asn+Glc had improved cell culture performance, metabolite profiling of cells was performed by GC-MS. The analysis of this dataset will provide greater understanding of the relationship between metabolic status (as generated by selective feed regimes) and recombinant protein production.

4.2.2.1 Extracellular metabolite profiles: GC-MS analyses

Medium samples from control cells and cells fed Asn, Glc and Asn+Glc were collected for extracellular metabolite profiling (Section 2.3.2). Extracellular metabolite profiles for medium and cultures (control at days 4, 6, 8, 10 and 12; Asn-fed at days 6 and 8; glucose-fed at days 6 and 8; Asn+Glc-fed at day 6, 8, 10 and 12) were mapped onto cellular metabolism (Figure 4.2) and individual metabolite charts were grouped (Figure 4.3A, 4.4A and 4.5).

As shown in Figure 4.2, glucose, pyruvate, and all detected amino acids (with the exception of glycine and alanine) were consumed during culture. Depletion of glucose after day 4 in control conditions correlated with the entry of cells into stationary phase (Figure 4.2 and 4.3A). This observation correlated with the result of glucose profiling in Section 3.2.2. In response to feeding glucose at day 6, the amount of glucose was increased after day 6 and then glucose was depleted by day 8 (Figure 4.3A). Pyruvate was depleted at day 4 in all conditions (Figure 4.2 and 4.3A). Asn, Asp, Glu and serine were exhausted rapidly in all conditions (Figure 4.2 and 4.5) as observed in Section 3.2.2. Addition of Asn decreased the amount of most amino acids, including lysine, leucine, isoleucine, threonine, methionine, phenylalanine, valine, tyrosine and cysteine to a greater extent than observed for the control. These results correspond with the results in Section 3.2.2. Cells fed glucose generated greater amounts of amino acids than the control after the addition of glucose to cell cultures (day 8) but this behavior was not observed in the Asn+Glc condition (Figure 4.2 and 4.5). In combination, cells fed Asn+Glc generated decreased amounts of amino acids (Figure 4.2 and 4.5), properties similar to those observed with feeding Asn alone. Moreover, some amino acids (leucine, isoleucine, tyrosine, valine) exhibited a greater extent of depletion at day 8 in the presence of Asn+Glc. Additionally, when fed with Asn or Asn+Glc cultures showed increased production of ketobutyric acid. This might reflect increased production

of succinyl CoA as mentioned in Section 3.3.2. Some amino acids were produced during culture. Glycine accumulated in the culture medium throughout the culture period under all conditions (Figure 4.2 and 4.5). In the presence of Asn, glycine accumulated to a lesser extent than the control at day 6 (Figures 4.2 and 4.5). Alanine was produced in cultures until day 4 and then it was consumed in the control and cells fed glucose (Figure 4.2 and 4.5). In contrast, there was high alanine production in cells supplemented with Asn or Asn+Glc at day 6 and then utilization was observed (Figure 4.2 and 4.5). This pattern corresponds with the alanine profile of Asn-fed cells (Section 3.2.2).

Other metabolites accumulated in culture medium, and supplementation with Asn or Asn+Glc showed differential effects on these metabolites. In the control, lactate was produced and the amount remained the same until the last day of culture (as described in Section 3.2.2). Cells fed Glc alone generated a similar lactate profile to the control but the amount of lactate was slightly increased at day 8 after the addition of glucose to culture medium at day 6. In contrast, in the presence of Asn cells switched from lactate production to consumption after day 4 and cells entered decline phase when lactate was depleted (Figure 4.2 and 4.3A). This result correlated with the result of lactate changes described in Section 3.2.2. In cells fed Asn+Glc, the lactate profile was similar to cells fed Asn alone (Figure 4.2 and 4.3A). Lactate was consumed after day 4 and was depleted at day 10 although glucose was added into culture medium at day 6. Additionally, a relationship was observed between lactate and alanine profiles. High alanine production at day 6 was detected when lactate shifted from production to consumption in the presence of Asn. Glycerol and sorbitol were produced during culture in control and cells fed glucose alone but addition of glucose alone generated higher amount of glycerol and sorbitol than the control at day 8 (Figure 4.2 and 4.3A). By contrast, feeding Asn or Asn+Glc decreased the production of both metabolites (Figure 4.2 and 4.3A). This observation is consistent with the results observed for cells fed Asn

(Section 3.2.2). Metabolites of the TCA cycle (citrate, iso-citrate, succinate, fumarate and malate) were produced in all conditions but their production was increased in the presence of Asn (as observed in Section 3.2.2) and the effect was more pronounced in cells fed Asn+Glc where the amounts of these metabolites remained high until the last day of sampling (Figure 4.2 and 4.4A). The TCA cycle metabolite profile of cell fed glucose alone was similar to the control. In contrast with extracellular metabolite profiles in Section 3.2.2 (where glycerol-3-phosphate was not detected in the medium), small amounts of extracellular glycerol-3-phosphate were detected in all conditions in this experiment (Figure 4.2 and 4.3A).

In summary, the overall extracellular metabolite profiles of the control and cells fed Asn in this experiment are consistent with the results of the control and Asn feeding described in the previous chapter (Section 3.3.2). This verified the effect of feeding Asn on extracellular metabolite profiles of CHO-LB01 cells. Additionally, Asn+Glc-fed cells generated similar extracellular metabolite profiles to Asn-fed cells as hypothesized in Section 4.2.1 and feeding regimes that contained Asn (feeding Asn alone and feeding Asn+Glc) showed less accumulation of lactate, glycerol and sorbitol and greater amount of TCA cycle intermediates and lower amounts of amino acids. However, the effect of Asn+Glc towards extracellular metabolite profiles was more pronounced than feeding Asn because the cells had a longer survival period. It can be suggested that addition of glucose in cells fed Asn resulted in increased carbon atom flux to support high activity of the TCA cycle as can be seen from the greater amounts of metabolites in TCA cycle (citrate, fumarate and malate) and decreased amount of amino acids (as a result of replenishment of the metabolites in TCA cycle). Maintenance of high TCA cycle activity might lead to prolonged cell survival and increased antibody yield.

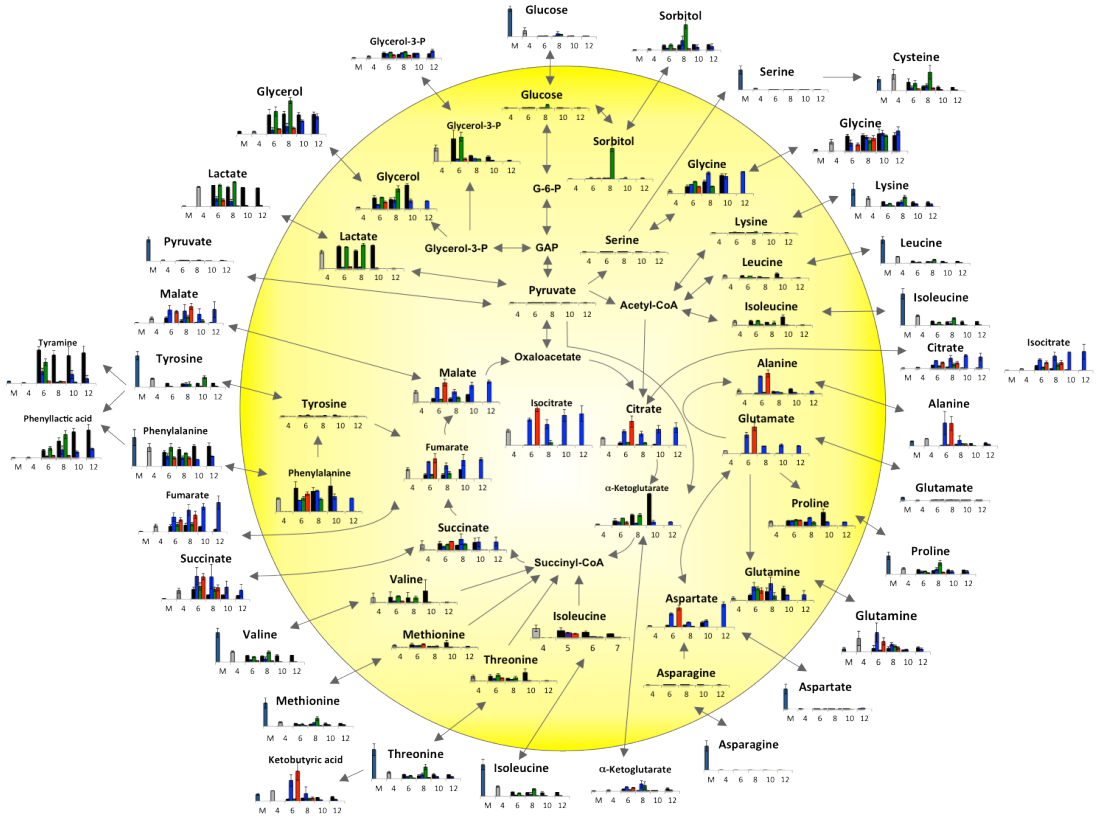

Figure 4.2 Profiles of extracellular and intracellular metabolites of LB01 during control and Asn, Glc and Asn+Glc supplemented conditions.

LB01 cells were cultured in CD OptiCHO^{TM} (Section 2.2.1) in control and supplemented conditions (as described in Figure 4.1) and at appropriate times samples were harvested from medium (extracellular) and cells (intracellular) (Section 2.3.2.1). Metabolite assessment was performed as described in Section 2.3.2. The bar charts represent the quantities of each metabolite in CD OptiCHO^{TM} medium (blue), control culture at day 4 before feeding (gray), control at all subsequent days of culture (black), Asn-supplemented (red), Glc-supplelmented (green) and Asn+Glc-supplement (blue) at day 6 (6), day 8 (8), day 10 (10) and day 12 (12). Values are arbitrary units normalized to an internal standard and represent the average of three replicates with ± SEM. For increase clarity, individually figures are shown in Figure 4.3, 4.4, 4.5 and 4.6. On those figures the unit of the scale are illustrated.

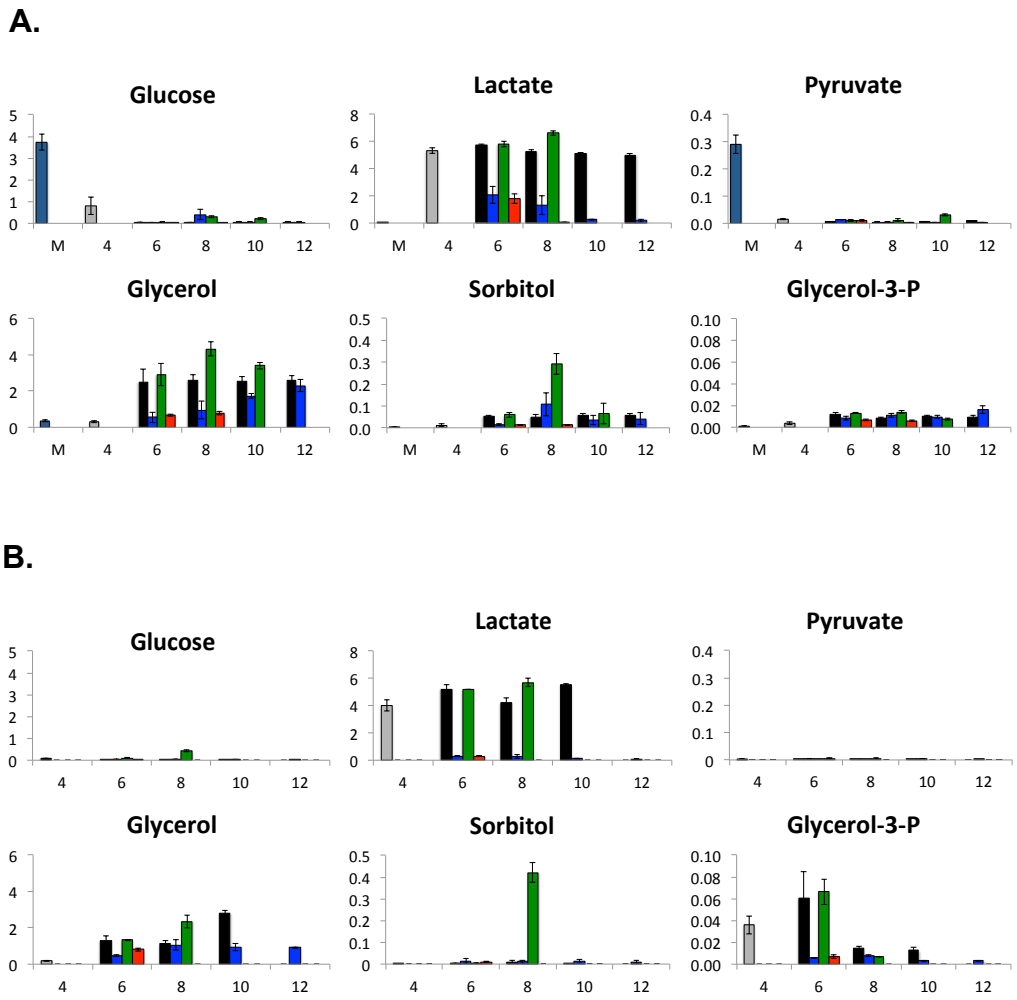

Figure 4.3 Extracellular and intracellular metabolite profiles of metabolites of interest related to glycolysis pathway of Asn, Glc and Asn+Glc supplementation from Figure 4.2.

Medium and cell samples were collected for extracellular (A) and intracellular (B) metabolite profiles, respectively (Section 2.3.2). The bar charts represent the quantities of each metabolite in CD OptiCHO^{TM} medium (blue), control culture at day 4 before feeding (gray), control at all subsequent days of culture (black), Asn-supplemented (red), Glc-supplemented (green) and Asn+Glc-supplement (blue) at day 6 (6), day 8 (8), day 10 (10) and day 12 (12). Values (y-axis) are arbitrary units normalized to an internal standard and represent the average of three replicates with ± SEM.

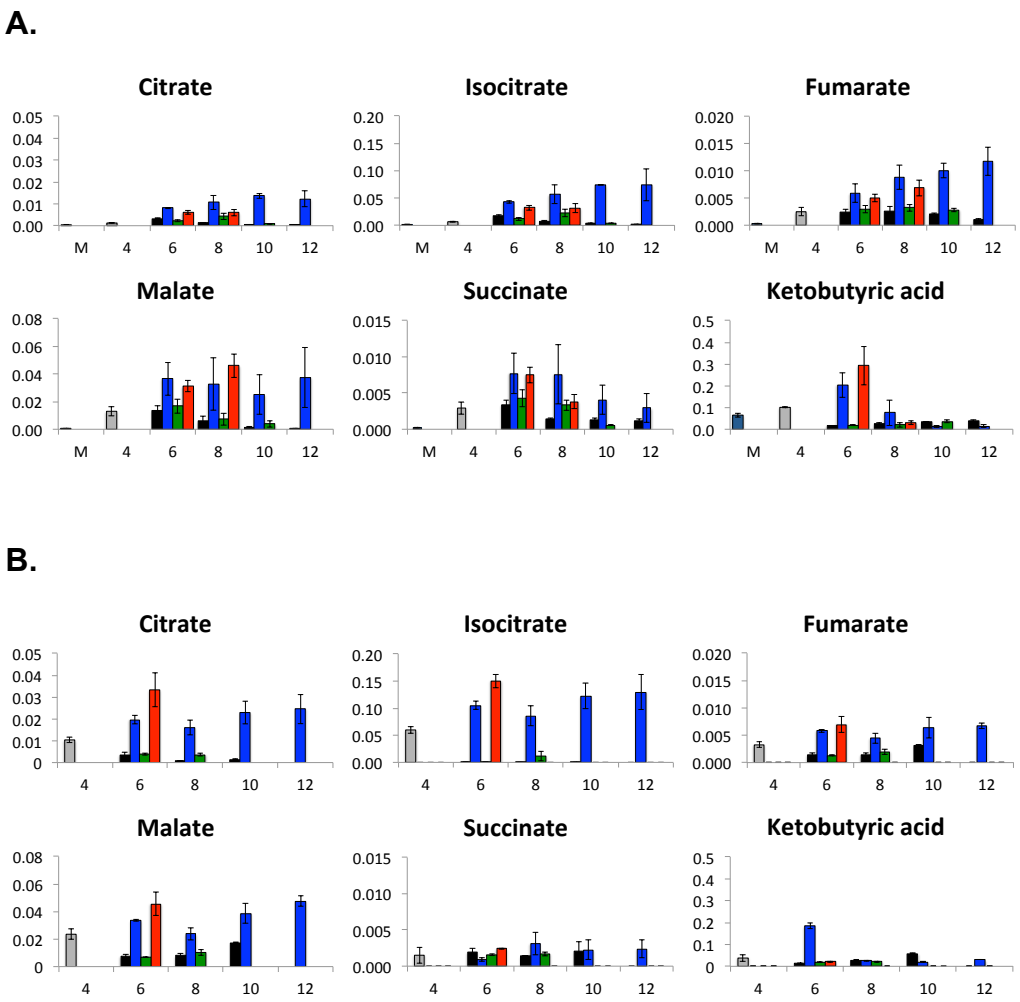

Figure 4.4 Extracellular and intracellular metabolite profiles of metabolites of interest related to TCA cycle pathway of Asn, Glc and Asn+Glc supplementation from Figure 4.2.

Medium and cell samples were collected for extracellular (A) and intracellular (B) metabolite profiles, respectively (Section 2.3.2). The bar charts represent the quantities of each metabolite in CD OptiCHO^{TM} medium (blue), control culture at day 4 before feeding (gray), control at all subsequent days of culture (black), Asn-supplemented (red), Glc-supplemented (green) and Asn+Glc-supplement (blue) at day 6 (6), day 8 (8), day 10 (10) and day 12 (12). Values (y-axis) are arbitrary units normalized to an internal standard and represent the average of three replicates with ± SEM.

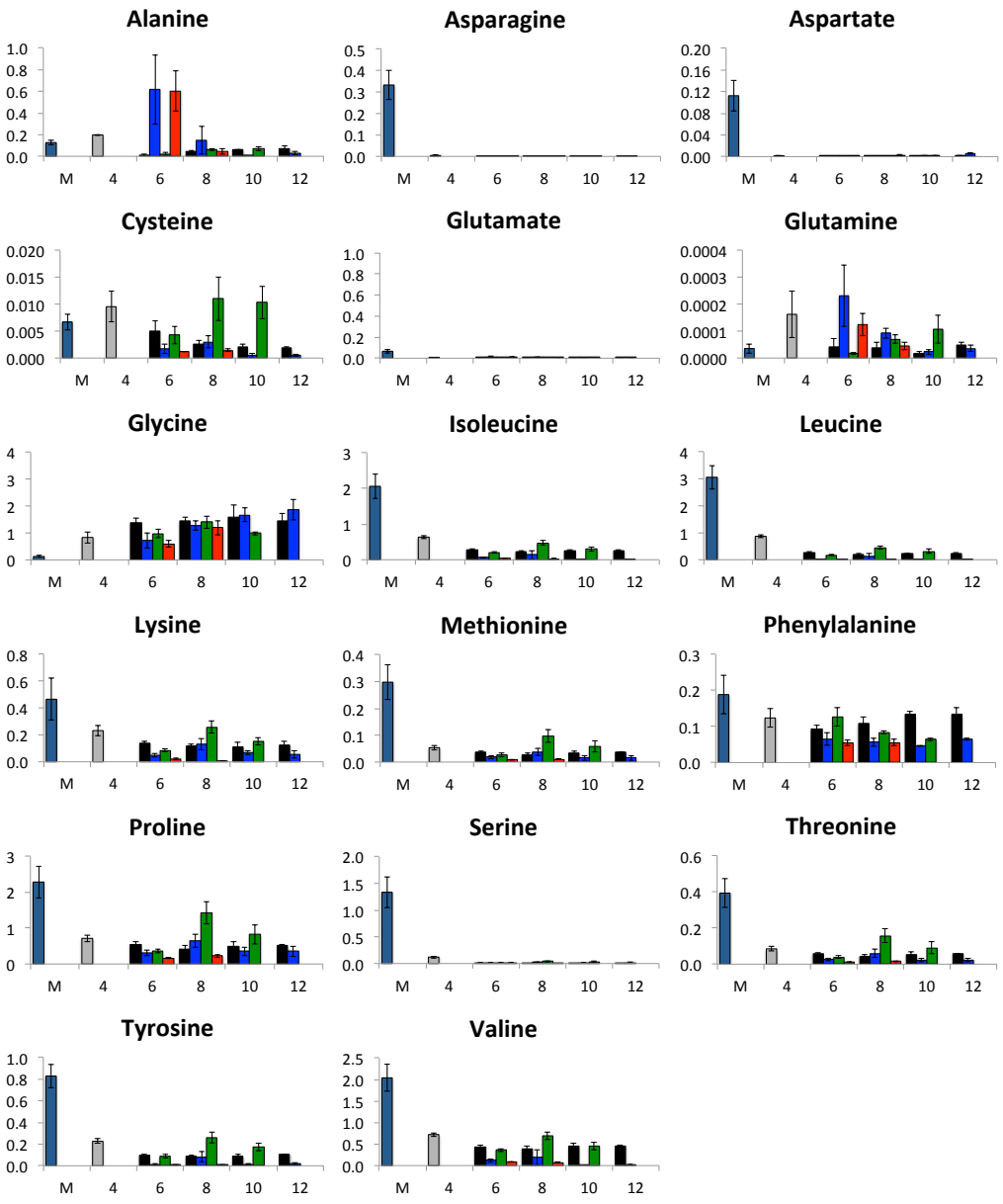

Figure 4.5 Extracellular metabolite profiles of amino acid of Asn, Glc and Asn+Glc supplementation from Figure 4.2.

Medium samples were collected for extracellular metabolite profiles (Section 2.3.2). The bar charts represent the quantities of each metabolite in CD OptiCHO medium (blue), control culture at day 4 before feeding (gray), control at all subsequent days of culture (black), Asn-supplemented (red), Glc-supplemented (green) and Asn+Glc-supplement (blue) at day 6 (6), day 8 (8), day 10 (10) and day 12 (12). Values (y-axis) are arbitrary units normalized to an internal standard and represent the average of three replicates with ± SEM.

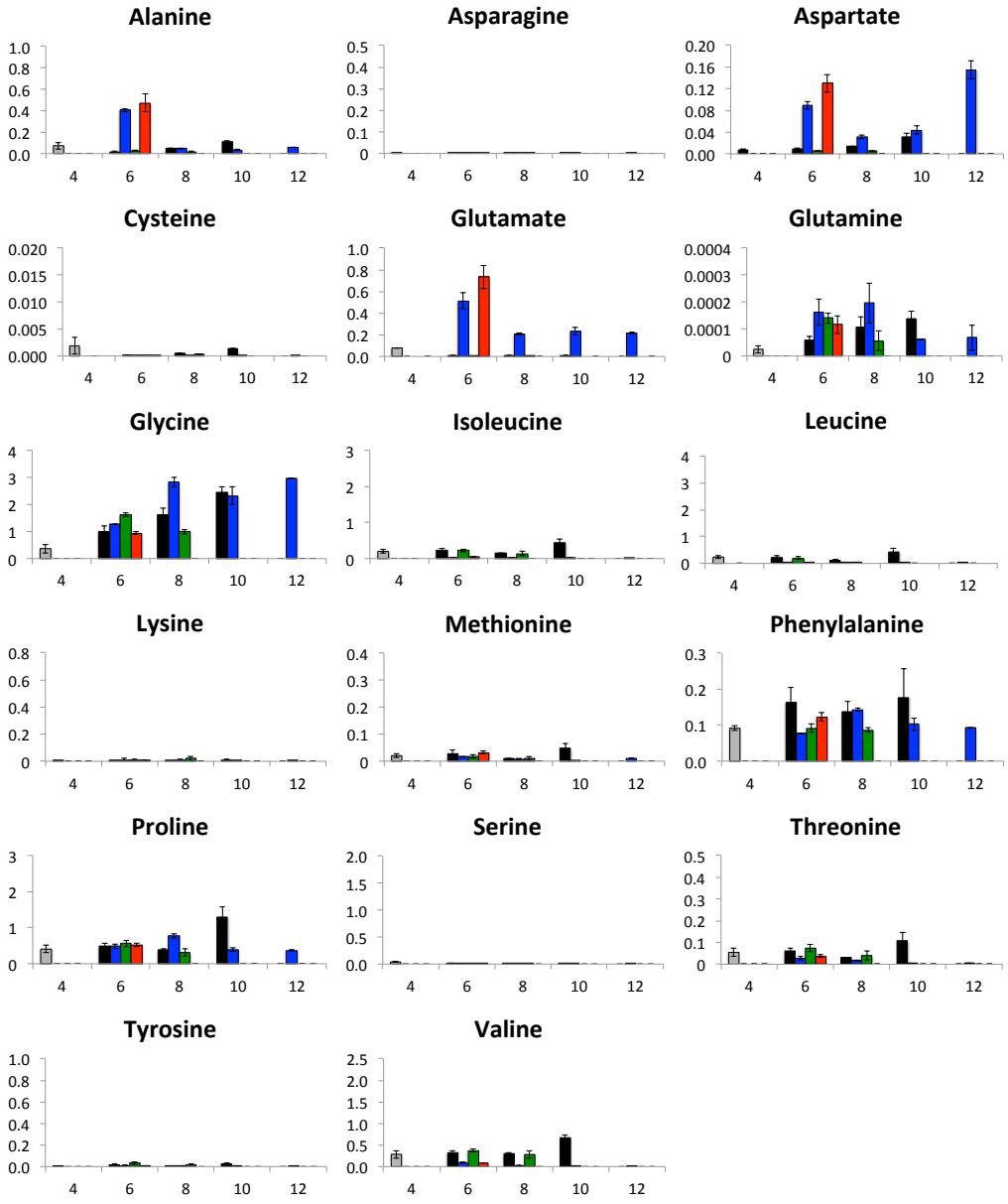

Figure 4.6 Intracellular metabolite profiles of amino acid of Asn, Glc and Asn+Glc supplementation from Figure 4.2.

Cell samples were collected for intracellular metabolite profiles (Section 2.3.2). The bar charts represent the quantities of each metabolite in control culture at day 4 before feeding (gray), control at all subsequent days of culture (black), Asn-supplemented (red), Glc-supplemented (green) and Asn+Glc-supplement (blue) at day 6 (6), day 8 (8), day 10 (10) and day 12 (12). Values (y-axis) are arbitrary units normalized to an internal standard and represent the average of three replicates with ± SEM.

In contrast, addition of glucose alone did not have an effect on the metabolites in TCA cycle and amino acids. The results were similar to the results obtained for the control but higher accumulation of lactate, glycerol and sorbitol was observed in the presence of glucose alone as hypothesized in Section 4.2.1. High sorbitol production was observed in CHO-LB01 cells after feeding glucose alone at day 6 but alteration of lactate and glycerol profile were not observed in this condition (Sellick et al., 2011). From the present results, it is possible that more carbon atoms directed from added glucose could generate high accumulation of metabolite in glycolysis in term of lactate. To overcome the potential toxicity of lactate to cells, glycerol and sorbitol were produced as alternative redox sinks and accumulated in greater amount than lactate in order to avoid toxicity from lactate accumulation. Consequently, high accumulation of glycerol and sorbitol might lead to unbalanced redox state, with a consequence of early death for Glc-fed cells. However, no clear evidence has been reported about the direct toxicity of glycerol and sorbitol in CHO cells. It is possible that high accumulation of glycerol and sorbitol might be a reflection of toxicity but it might not be the causative factors for early cell death (Neuhofer and Beck, 2005, Luo et al., 2012). Another potential explanation for this observation is that increased production of sorbitol arising from excessive amounts of glucose in culture medium may lead to decreased amounts of NADPH because aldose reductase converts glucose into sorbitol via use of NADPH. Since NADPH is essential for generation of intracellular antioxidants, the depletion of NADPH may impair intracellular antioxidant defense and lead to early cell death (Tang et al., 2012). The effect of nutrient feeding on cell culture performance and metabolite profiles will be discussed in Section 4.5.

In the next section, intracellular metabolite profiles of control cells and those fed nutrients will be investigated in order to study the relationship between extra- and intra-cellular metabolites.

4.2.2.2 Intracellular metabolite profiles: GC-MS analyses

To examine the effect of nutrient feeding on metabolite profiles inside the cells, intracellular metabolite profiles were measured by collection of cell samples in parallel to medium samples (extracellular metabolite). For intracellular samples, quenching and extraction methods were conducted to diminish degradation of labile metabolites, metabolite turnover and contamination of extracellular metabolites (Section 2.3.2). Intracellular metabolite profiles for the control, Asn-fed, Glc-fed and Asn+Glc-fed were mapped onto cellular metabolism (Figure 4.2) and individual metabolite charts are grouped (Figure 4.3B, 4.4B and 4.6).

Intracellular glucose was barely detected in all conditions except for feeding glucose alone where glucose was detected in low amounts inside cells at day 8 (2 days after addition of glucose) (Figure 4.2 and 4.3B). As for intracellular amino acids, almost all amino acids (except for glycine and alanine) were decreased in the presence of Asn or Asn+Glc (Figure 4.2 and 4.6) as observed in extracellular amino acids profile (Section 4.2.2.1). Asn, serine, lysine and tyrosine were exhausted rapidly in all conditions (Figure 4.2 and 4.6). Asp and Glu were depleted quickly in the control and cells fed glucose alone whereas in the presence of Asn or Asn+Glc the quantity of these amino acids was greater than the control at day 6 for Asn-fed cells and day 6, 8 and 12 for Asn+Glc-fed cells. This pattern is similar to the observation of cells supplemented with Asn (Section 3.3.3). Glycine accumulated inside the cells in all conditions (Figure 4.2 and 4.6) as observed for the extracellular glycine profile. Greater amounts of glycine were observed at day 8 in the presence of Asn+Glc. Addition of Asn increased the production of alanine at day 6 in both Asn-fed cells and Asn+Glc-fed cells and then alanine was consumed (Figure 4.2 and 4.6), a pattern observed for extracellular alanine (Section 4.2.2.1).

In the case of metabolites that were increased inside the cells, intracellular lactate followed a similar trend to the extracellular profile in all conditions (Figure 4.2 and 4.3B).

Lactate was produced and the amount of lactate remained steady until the last day of sampling for the control and after feeding with glucose alone. In contrast, lactate was used after day 4 and was depleted at day 6 in the presence of Asn in cells-fed Asn and cells-fed Asn+Glc as observed in cells supplemented with Asn in previous results (Section 3.3.3). Glycerol accumulated during culture inside the cells in control and cells fed Glc but in the presence of Glc greater amounts of glycerol were observed at day 8. The amount of glycerol was less in Asn-supplemented and Asn+Glc-supplemented conditions (Figure 4.2 and 4.3B) as observed in extracellular metabolite profile (Section 4.2.2.1). Sorbitol was hardly detected inside the cell in the control, cells fed Asn and cells fed Asn+Glc whereas high amounts of sorbitol were observed at day 8 in cells supplemented with glucose alone (Figure 4.2 and 4.3B) as observed in extracellular metabolite profiles. The trend for intracellular TCA cycle intermediates (citrate, iso-citrate, fumarate and malate) was similar to that seen for extracellular profiles of these intermediates (Section 4.2.2.1). In the presence of Asn or Asn+Glc intracellular TCA cycle metabolites were more abundant than the amounts observed for control and glucose-fed cells (Figure 4.2 and 4.4B). High amounts of these metabolites were observed until the last day of analysis and the effect of Asn and Asn+Glc toward intracellular TCA cycle intermediates was more pronounced than that observed for extracellular profiles. Glycerol-3-phosphate was produced initially and then was consumed after day 6 in the control and cells fed glucose alone while in the presence of Asn or Asn+Glc glycerol-3-phosphate was produced less than the control as observed in Section 3.3.3. This differs from the finding for the extracellular profile for glycerol-3-phosphate where no difference was observed for the profile of glycerol-3-phosphate between each condition.

Overall, the results from these analyses demonstrate that the general pattern of intracellular metabolite profiles was comparable with that of extracellular profiles in all conditions. Additionally, aspartate, glutamate and glycerol-3-phosphate showed greater amounts inside cells, a feature that is consistent with previous results (Section 3.3.3).

Ammonia (which cannot be detected by GC-MS) is one of the potentially toxic byproducts of metabolism. Therefore, the accumulation of ammonia in the medium of cells supplemented with nutrients was examined by colorimetric assay (Section 4.2.2.3).

4.2.2.3 Extracellular ammonia profile

To investigate the effect of nutrient feeding on ammonia production, medium samples from Asn-fed cells, Glc-fed cells, Asn+Glc-fed cells and the control were collected after day 4 onwards for ammonia assessment (Section 2.3.1.5).

Ammonia in control cultures gradually increased after day 4 and reached about 3 mM at day 10 and after that ammonia concentration slightly decreased (Figure 4.7A). This result was consistent with previous assessments (Section 3.3.1). Asn addition produced a maximum ammonia concentration about 2 mM at day 8 (Figure 4.7A). This was slightly less than observed in a previous experiment (3.5 mM) under the same conditions (Section 3.3.1). Glucose-fed cells generated a pattern of ammonia production that was similar to the control (2 mM at day 8). Interestingly, addition of Asn+Glc produced maximum concentrations of ammonia less than the control. Cells fed Asn+Glc showed a similar pattern of ammonia production to cells fed Asn between day 4 to day 6 but after day 6 (the time that glucose was added into the cell culture) the concentration of ammonia remained constant at 1 mM and reached 2 mM at day 12.

All in all, the combination of Asn and Glc on CHO-LB01 cells showed great promise as an effective feed regime, generating an increase in antibody titre along with increased amounts of TCA cycle intermediates and decreased lactate and ammonia production. In the next section the effect of a combination of HB and Glc on CHO-LB01 cells toward cell culture performance and metabolite profiles will be examined.

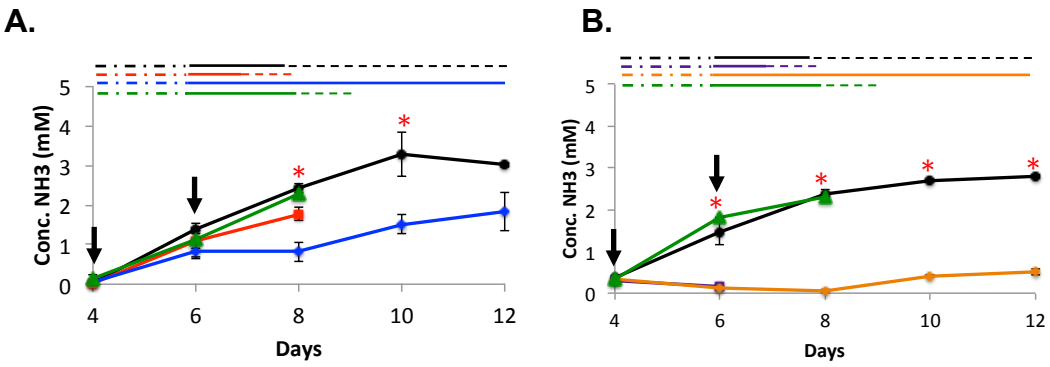

Figure 4.7 Extracellular ammonium profiles of LB01 cells in control and nutrient supplemented batch cultures.

Medium samples were collected from the cultures of Asn+Glc experiment (A) and HB+Glc experiment (B). Ammonia in medium samples were determined by enzymatic assay (Section 2.3.1.5) for control (black symbols) and cultures supplemented with Asn (red), HB (purple), Glc (green), Asn+Glc (blue) and HB+Glc (orange) at day 4 (for Asn and HB) and day 6 (for Glc) of culture (as indicated by the arrow). Values presented are mean ± SEM for three replicates for all conditions, all shown against their respective controls. * indicates significant difference from control at $p < 0.05$. The lines at the top of each graph are added to indicate stages of growth: exponential phase (dot-dash line), stationary phase (solid line) and decline phase (dashed line).

4.3 Effect of a combination of HB and Glc on cell culture performance and metabolite profiling

Since significant improved antibody yield was observed for CHO-LB01 cells as a result of medium supplementation with HB (Chapter 3), we hypothesized that addition of glucose in cells fed HB might help the cells to extend stationary phase to increase production period lead to enhance antibody titre. Therefore, informed by the studies with Asn, glucose was added to the CHO-LB01 cultures at day 6 at the final concentration of 20 mM as described in Section 4.2. In this study there were four conditions: unfed (control), feeding HB alone at day 4 (HB), feeding glucose alone at day 6 (Glc) and feeding HB at day 4 plus feeding glucose at day 6 (HB+Glc). Medium samples were collected every day to study cell growth (Section 2.2.2), antibody production

(Section 2.4.1), ammonia profile (Section 2.3.1.5) and extra- and intra-cellular metabolite profiles by GC-MS (Section 2.3.2).

4.3.1 Cell growth and antibody production

The pattern of growth for the control and addition of glucose alone was similar to that of previous results (Section 4.2.1). Cells fed HB alone reached maximum viable cell density at ~$1.4x10^7$ cells/mL at day 7, which was higher than the control, and then the cells entered a rapid decline phase at day 8, four days earlier than the control (Figure 4.8A). As observed in cells fed Asn in this chapter (Section 4.2.1), HB-fed cells in this experiment reached higher maximum viable cell density and died earlier than had been observed in previous chapter in which cells reached a maximum cell density of ~$7x10^6$ cells/mL and died at day 11 (Figure 3.1A and 3.2A). Interestingly, in the case of HB+Glc, after cells reached maximum viable cell density at ~$1.2x10^7$ cells/mL at day 4, viable cell density slightly decreased to $1x10^7$ cells/mL at day 5 and then it remained constant until day 6 (Figure 4.8A). Afterwards, viable cell density slightly increased to ~$1.2x10^7$ cells/mL at day 7 after glucose was added (at day 6) and then viable cell density was decreased to ~$8x10^6$ cells/mL at day 8 and it remained the same until day 11 which was significantly greater than viable cell density in the control. After that time, cells entered decline phase and died at day 13, one day later than observed for the control. This pattern was similar to the effect of feeding Asn+Glc (Section 4.2.1) but addition of HB+Glc generated a lower maximum cell density and cells died earlier than observed with Asn+Glc by two days.

In term of cumulative cell number, all conditions (except for HB+Glc) had similar cumulative cell number (about $6x10^7$ cells/mL) (Figure 4.8B) which was similar to the value reported in an earlier section in this chapter (Section 4.2.1) but higher than the

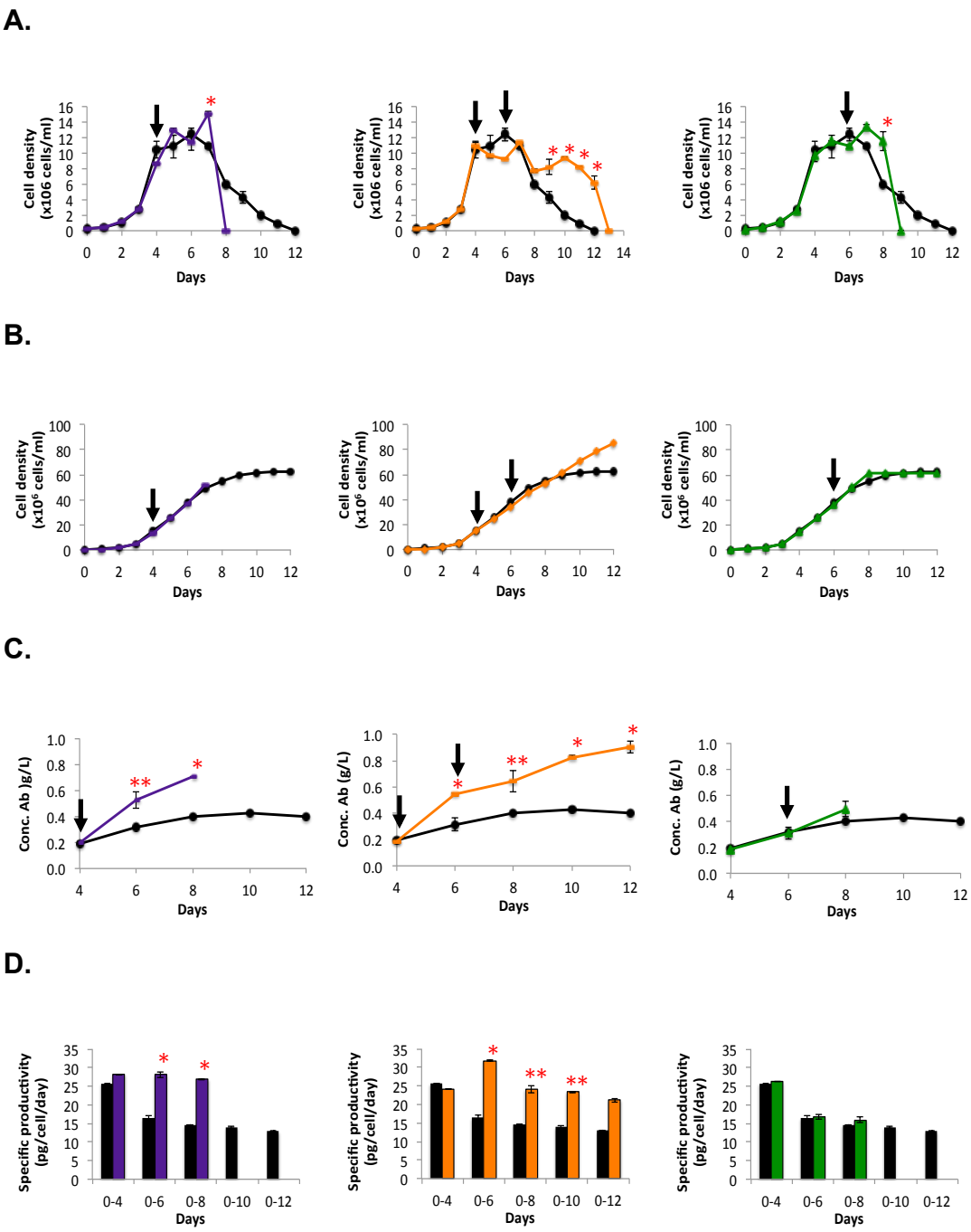

Figure 4.8 Cell growth and antibody production of LB01 cells in response to HB, HB+Glc and Glc.

Viable cell density (A), cumulative cell number (B), antibody production (C) and specific productivity (D) were measured for LB01 cells throughout batch culture in CD OptiCHO (control, black symbols) or with supplemention at day 4 (for HB) or day 6 (for Glc) of culture (the arrow presents the time of addition) with HB (10 mM, purple), Glc (20 mM, green) or HB+Glc (orange) (Section 2.2.4). Medium samples were collected for cell counts (Section 2.2.2) and ELISA (Section 2.4.1). Values presented are mean ± SEM for three replicates for all conditions, all shown against their respective controls. * and ** indicates significant difference from control at $p < 0.05$ and 0.1, respectively.

cumulative cell number reported in the previous Chapter (4 x 10^7 cells/mL) (Section 3.2.1). In the case of feeding HB+Glc, cumulative cell number was about 8x10^7 cells/mL which was higher than the control due to prolongment of the cell culture period (Figure 4.7B).

As for antibody production, the control produced a maximum yield of antibody about 0.4 g/L at day 12 (Figure 4.8C) which was similar to the control in previous section (Section 4.2.1) but lower than the previous result of the control in previous chapter (0.6 g/L) (Section 3.2.). Addition of HB alone generated a significantly greater concentration of antibody (0.7 g/L at day 8) than the control (Figure 4.8C) as observed in previous chapter. However, the amount of antibody produced by HB-fed cells was less than previous results of feeding HB (0.9 g/L) in the previous chapter (Section 3.2.). Cells supplemented with glucose alone produced the same concentration of antibody (0.4 g/L) as the control at day 8 (Figure 4.8C). This is consistent with the result of feeding glucose in the previous section (Section 4.2.1). In case of feeding HB+Glc, the concentration of antibody was significantly greater than the control at day 6 onward (Figure 4.8C). The maximum concentration of antibody was double (0.85 g/L) that of the control. The prolonged stationary phase of culture observed in the presence of HB+Glc and the effect of HB itself are a major aspect for the enhanced antibody yield. Greatest specific productivity was found between days 0-4 (for the control, feeding HB alone and feeding Glc alone) or day 0-6 for (feeding HB+Glc) (Figure 4.8D). Maximum specific productivities of about 25 pg/cell/day were observed for all conditions. Specific productivity in these experiments was less than that observed in the previous chapter (40 pg/cell/day) (Section 3.2.1). In the present of HB and HB+Glc specific productivity was significantly higher than the control at day 0-6 and day 0-8 for cells fed HB and day 0-6, 0-8 and day 0-10 for cells fed HB+Glc.

In summary, these experiments confirmed the impact of HB on antibody production by increased maximum concentration of antibody although there was also a shift of cell

growth patterns which cells fed HB in this experiment reached higher maximum cell density and died earlier than previously (Section 3.2). The possible explanation for this behavior will be discussed in Section 4.5. As hypothesis, cells can prolong stationary phase for 4 days and achieved higher cumulative cell number in the presence of HB+Glc. As a result total antibody titre was significantly improved. This effect is similar with the effect of Asn+Glc (Section 4.2.1). Despite the fact that feeding glucose alone caused earlier cell death, the combination of HB+Glc led to enhanced cumulative cell number and antibody production. Based on this result, we hypothezied that feeding HB+Glc could generate similar extra- and intra-cellular metabolite profiles to cells fed Asn+Glc. Therefore, further investigation of metabolite profiles related to the effect of nutrient feeding were undertaken in order to understand the relationship between metabolite profiles and cell culture performance.

4.3.2 Extracellular and intracellular metabolites profiling

In order to test the hypothesis that the addition of HB+Glc might generate similar metabolite profiles to cells fed Asn+Glc, extra- and intra-cellular metabolite profiles by GC-MS were conducted. The analysis of this dataset will confirm and provide greater understanding of relationship between cells, feeds and recombinant protein production.

4.3.2.1 Extracellular metabolite profiles: GC-MS analyses

Medium samples of control cells and cells fed HB, Glc and HB+Glc were collected for extracellular metabolite profiling (Section 2.3.2). Extracellular metabolite profiles for medium and cultures (control at days 4, 6, 8, 10 and 12; HB-fed at days 6 and 8; Glc-fed at days 6 and 8; HB+Glc-fed at day 6, 8, 10 and 12) were mapped onto cellular metabolism (Figure 4.9) and individual metabolite charts were grouped and shown in Figure 4.10A, 4.11A and 4.12.

As shown in Figure 4.9, glucose, pyruvate, and all detected amino acids (with the exception of glycine and alanine) were consumed during culture. Depletion of glucose after day 4 in control conditions correlated with the entry of cells into stationary phase. (Figure 4.9 and 4.10A) This observation correlated with the result of the glucose profile already described in Section 4.2.2.1. With addition of glucose at day 6 in cells fed Glc alone or HB+Glc, the amount of glucose was increased after day 6 and then glucose was depleted after day 8 (for Glc) or day 10 (for HB+Glc). The glucose profile of feeding Glc is consistent with the results described in a previous section (Section 4.2.2.1). Also, the glucose profile of cells supplemented with HB+Glc was similar to that of cells fed Asn+Glc (Section 4.2.2.1) but glucose was consumed more slowly in the presence of HB (Section 3.3.1). Pyruvate was almost depleted at day 4 in all conditions but pyruvate was above the background of the control at day 6 in the presence of HB in cells fed HB alone or HB+Glc (Figures 4.9 and 4.10A). Similar to the results described in Section 4.2.2.1, Asn, Asp, Glu, Gln and serine were exhausted rapidly in all conditions (Figures 4.8 and 4.11A). Addition of HB decreased the amount of several amino acids (lysine, leucine, isoleucine, threonine, methionine, valine and tyrosine) (Figures 4.9 and 4.12). This observation correlated with the results observed with HB feeding in previous chapter (Section 3.3.2). Supplementation with glucose alone had a similar amino acid profile to the control at day 6 and then the amount of amino acids was greater than the control (day 8) after glucose was added into cell culture medium (Figure 4.9 and 4.12). Addition of HB+Glc generated decreased amounts of amino acids (Figure 4.9 and 4.12) as observed with feeding HB alone. Moreover some amino acids (leucine, isoleucine, tyrosine, valine) were depleted at day 8 in cells fed HB+Glc. Additionally, cultures supplemented with HB (both with and without Glc) showed increased amounts of ketobutyrate at day 6 (Figure 4.9 and 4.11A). This result was noted as a response to feeding HB in described in Chapter 3 (Section 3.3.2) which might reflect the amount of succinyl Co-A. Glycine accumulated in culture medium throughout culture for control and Glc fed conditions (Figures 4.9 and 4.12). In the presence of HB glycine accumulated to a lesser extent than the control at day 6 and 8 (Figures 4.9 and 4.12). Alanine was

produced in the culture until day 4 and then it was consumed in the control and cells fed glucose (Figures 4.9 and 4.12) as observed previously (Section 4.2.2.1). In cells supplemented with HB and HB+Glc, there was greater production of alanine at day 6 and then utilization was observed (Figures 4.9 and 4.12). This observation corresponds with the alanine profile of cells fed Asn and Asn+Glc in Section 4.2.2.1.

Several other metabolites accumulated in medium during culture and exhibited differential responses to HB or HB+Glc feeding. In control and feeding Glc conditions lactate was produced until day 6 and the amount was slightly decreased until the last day of sampling for the control while in the presence of Glc the amount of lactate was slightly increased at day 8 after glucose was added into culture medium at day 6 as observed in previous section (Section 4.2.2.1) (Figures 4.9 and 4.10A). In the presence of HB, cells switched from lactate production to consumption after day 4 (Figures 4.9 and 4.10A). This result is similar to the lactate changes detected in Chapter 3 (Section 3.2.2). Similar to feeding HB alone, lactate was consumed after day 4 and was almost depleted by day 8 in the presence of HB+Glc (Figure 4.9 and 4.10A). This profile is similar to the lactate profile observed in response to addition of Asn+Glc (Section 4.2.2.1). Glycerol and sorbitol were produced during culture in control conditions and when cultures were supplemented with Glc alone but addition of Glc alone generated greater amounts of glycerol and sorbitol than observed for the control at day 8 (Figure 4.8 and 4.9A) as observed in previous section (Section 4.2.2.1). In contrast, the presence of HB or HB+Glc decreased production of both metabolites (Figures 4.9 and 4.10A). This observation is consistent with the result of cells fed Asn and Asn+Glc in a previous section (Section 4.2.2.1). Metabolites involved in the TCA cycle (citrate, isocitrate, succinate, fumarate and malate) were produced during control cultures and their production was increased in the presence of HB (as observed in Section 3.2.2). The increased production was more pronounced in cells fed HB+Glc and under those conditions the amount of these metabolites remained high until the last day of sampling (Figures 4.9 and 4.11A). Similar to observations for extracellular metabolite profiles in

previous section (Section 4.2.2.1), low amounts of glycerol-3-phosphate were detected in the medium in all conditions (Figure 4.9 and 4.10A).

In summary, the overall extracellular metabolite profiles of cells fed HB in this experiment are consistent with the result of feeding HB described in Chapter 3 (Section 3.3.2). This verified the effect of feeding HB on extracellular metabolite profiles of CHO-LB01 cells. Accumulation of glycerol and sorbitol was observed after addition of glucose alone as determined in Section 4.2.2.1. The combination of HB+Glc generated extracellular metabolite profiles that were similar to those observed with addition of Asn+Glc as hypothesized in Section 4.3.1. Feeding HB+Glc showed less accumulation of lactate, glycerol and sorbitol and greater amounts of TCA cycle intermediates and, in addition, the amounts of several amino acids were decreased by addition of HB+Glc (as determined in the presence of Asn+Glc). It can be suggested that addition of glucose in cells fed HB resulted in increased amount of metabolites in TCA cycle (citrate, fumarate and malate), leading to prolonged cell survival and enhanced antibody yield. The effect of nutrient feeding on cell culture performance and metabolite profiles will be discussed in Section 4.5. The next section examines the parallel assessment of intracellular metabolite profiles to study the relationship between extra- and intra-cellular metabolites in response to nutrient feeding.

4.3.2.2 Intracellular metabolite profiles: GC-MS analyses

Intracellular metabolite profiles were measured in cell samples (Section 2.3.2) collected from the same experiments used for assessment of medium samples (extracellular metabolite data described above). Intracellular metabolite profiles for the control, HB-fed, Glc-fed and HB+Glc-fed were mapped onto cellular metabolism (Figure 4.9) and individual metabolite charts were grouped and are shown in Figures 4.10B, 4.11B and 4.13.

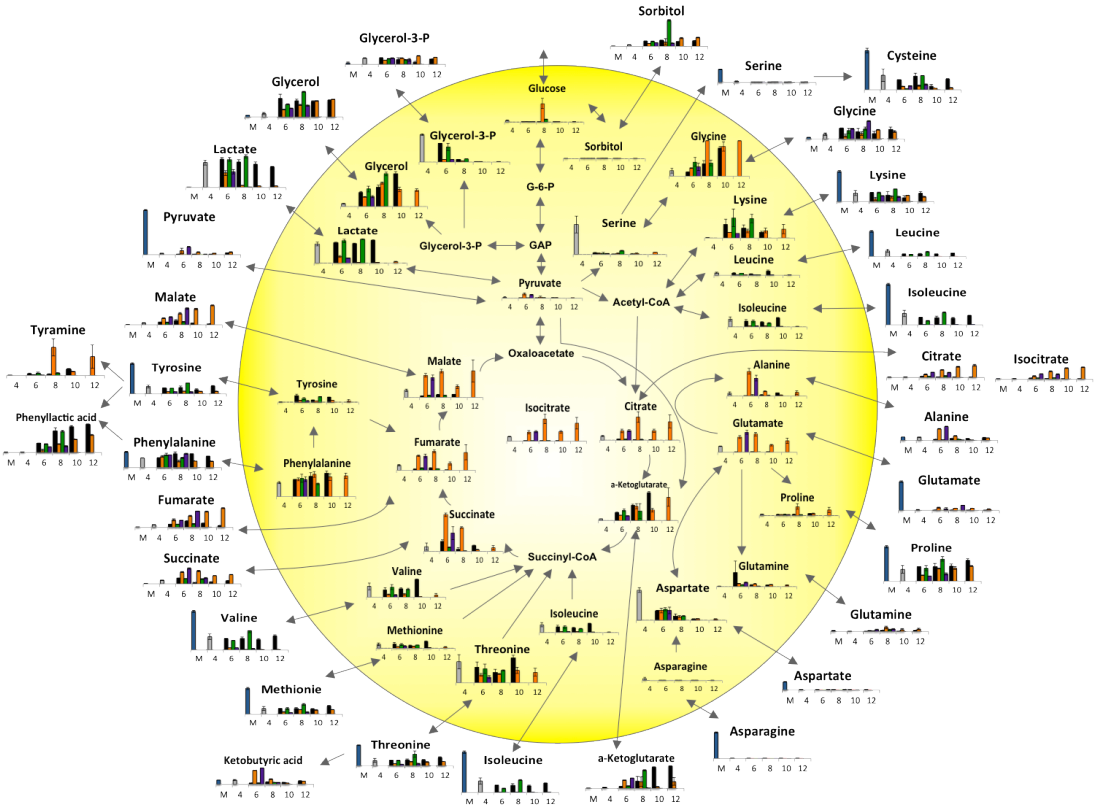

Figure 4.9 Profiles of extracellular and intracellular metabolites of LB01 during control and HB, Glc and HB+Glc supplemented conditions.

LB01 cells were cultured in CD OptiCHO^{TM} (Section 2.2.1) in control and supplemented conditions (as described in Figure 4.7) and at appropriate times samples were harvested from medium (extracellular) and cells (intracellular) (Section 2.3.2.1). Metabolite assessment was performed as described in Section 2.3.2.1. The bar charts represent the quantities of each metabolite in CD OptiCHO medium (blue), control culture at day 4 before feeding (gray), control at all subsequent days of culture (black), HB-supplemented (purple), Glc-supplelmented (green) and HB+Glc-supplement (orange) at day 6 (6), day 8 (8), day 10 (10) and day 12 (12). Values are arbitrary units normalized to an internal standard and represent the average of three replicates with ± SEM. For increase clarity, individually figures are shown in Figure 4.10, 4.11, 4.12 and 4.13. On those figures the unit of the scale are illustrated.

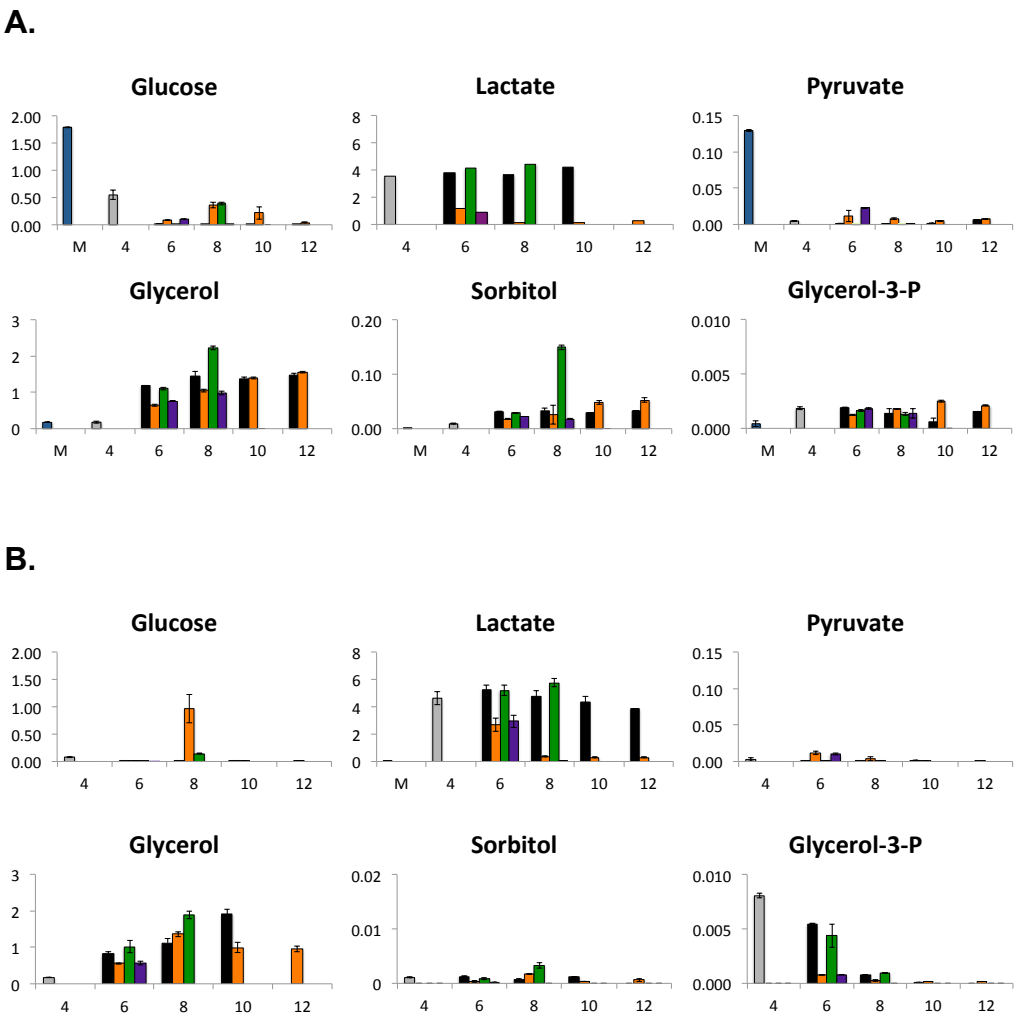

Figure 4.10 Extracellular and intracellular metabolite profiles of metabolites of interest related to glycolysis pathway of HB, Glc and HB+Glc supplementation from Figure 4.9.

Medium and cell samples were collected for extracellular (A) and intracellular (B) (Section 2.3.2) metabolite profiles, respectively. The bar charts represent the quantities of each metabolite in CD OptiCHO^{TM} medium (blue), control culture at day 4 before feeding (gray), control at all subsequent days of culture (black), HB-supplemented (purple), Glc-supplemented (green) and HB+Glc-supplement (orange) at day 6 (6), day 8 (8), day 10 (10) and day 12 (12). Values (y-axis) are arbitrary units normalized to an internal standard and represent the average of three replicates with ± SEM.

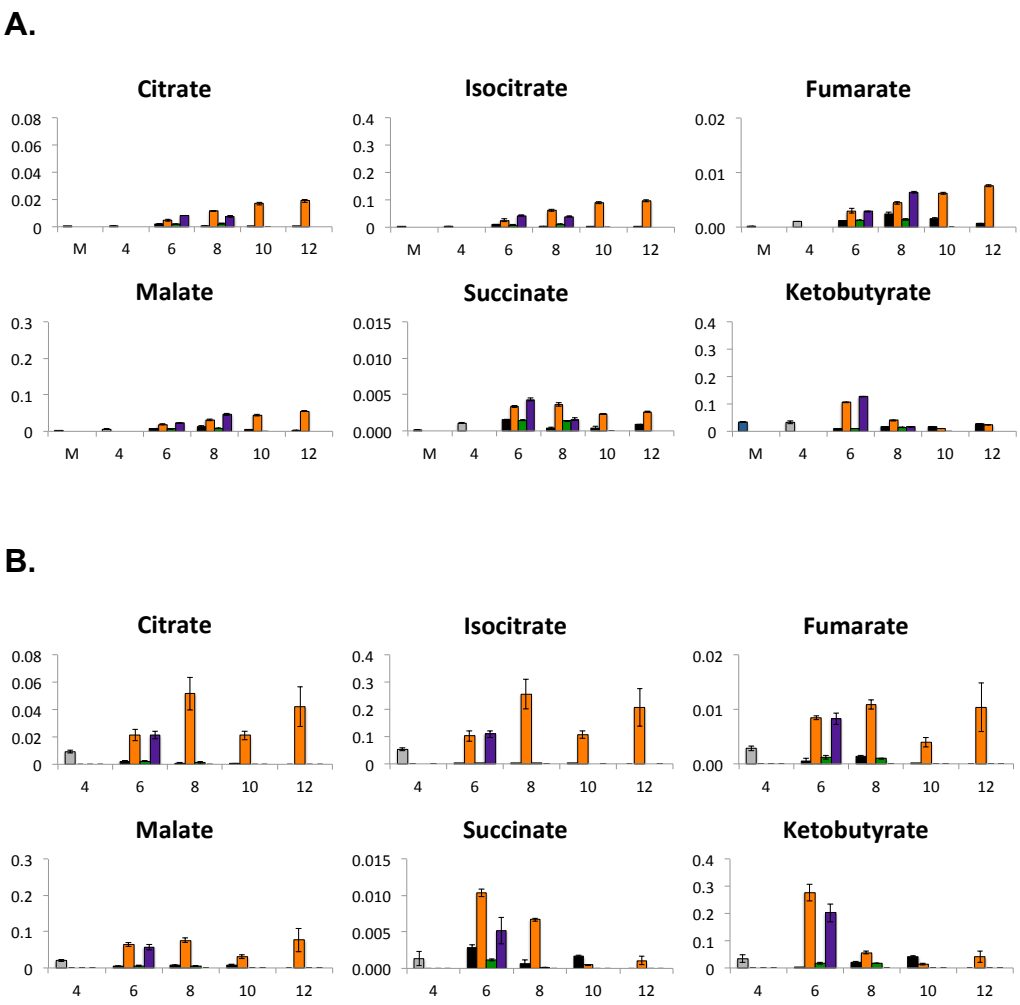

Figure 4.11 Extracellular and intracellular metabolite profiles of metabolites of interest related to TCA cycle pathway of HB, Glc and HB+Glc supplementation from Figure 4.9.

Medium and cell samples were collected for extracellular (A) and intracellular (B) (Section 2.3.2) metabolite profiles, respectively. The bar charts represent the quantities of each metabolite in CD OptiCHO^{TM} medium (blue), control culture at day 4 before feeding (gray), control at all subsequent days of culture (black), HB-supplemented (purple), Glc-supplemented (green) and HB+Glc-supplement (orange) at day 6 (6), day 8 (8), day 10 (10) and day 12 (12). Values (y-axis) are arbitrary units normalized to an internal standard and represent the average of three replicates with ± SEM.

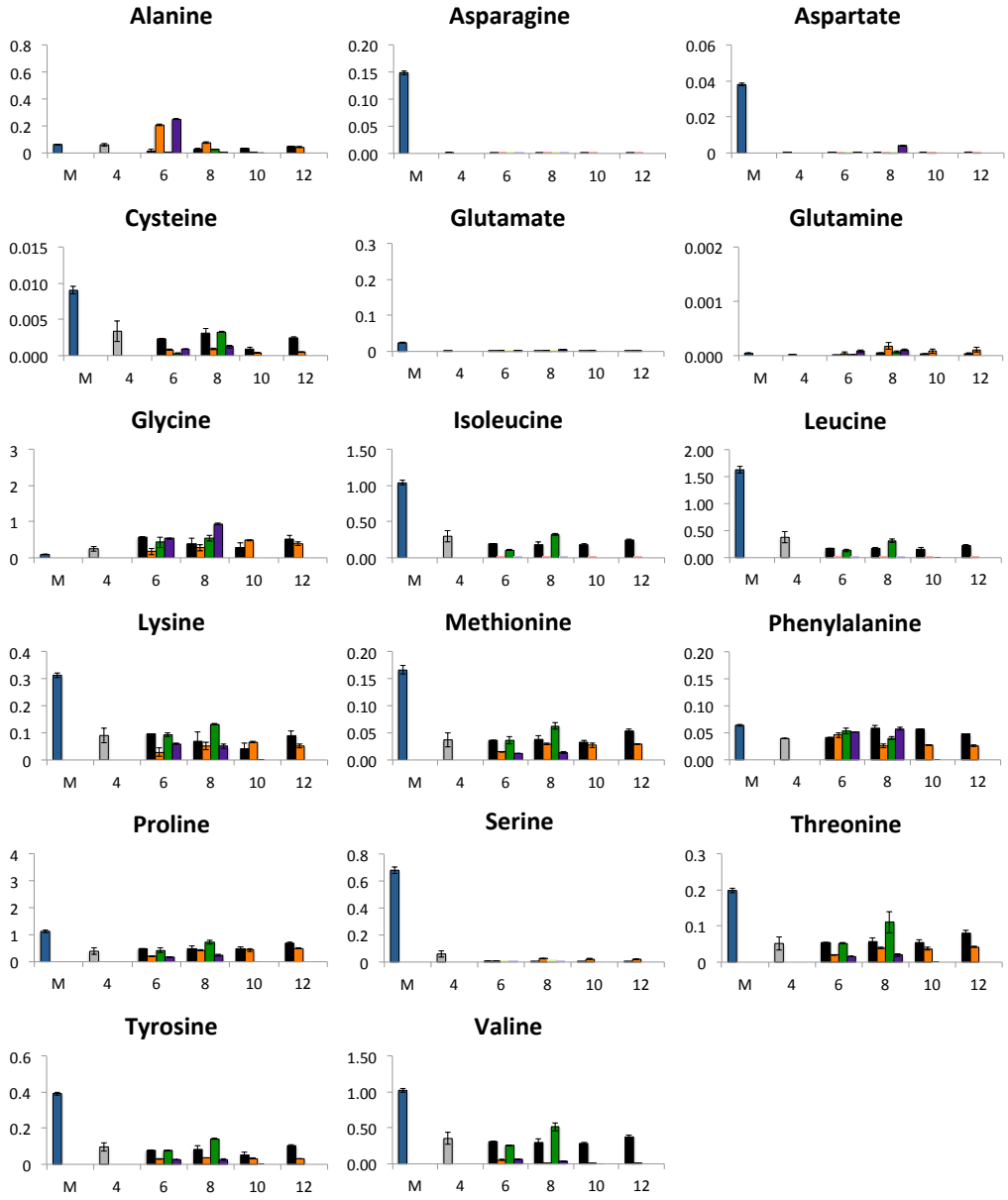

Figure 4.12 Extracellular metabolite profiles of amino acids of HB, Glc and HB+Glc supplementation from Figure 4.9.

Medium samples were collected for extracellular metabolite profiles (Section 2.3.2). The bar charts represent the quantities of each metabolite in CD OptiCHO^{TM} medium (blue), control culture at day 4 before feeding (gray), control at all subsequent days of culture (black), HB-suppemented (purple), Glc-supplelmented (green) and HB+Glc-supplement (orange) at day 6 (6), day 8 (8), day 10 (10) and day 12 (12). Values (y-axis) are arbitrary units normalized to an internal standard and represent the average of three replicates with ± SEM.

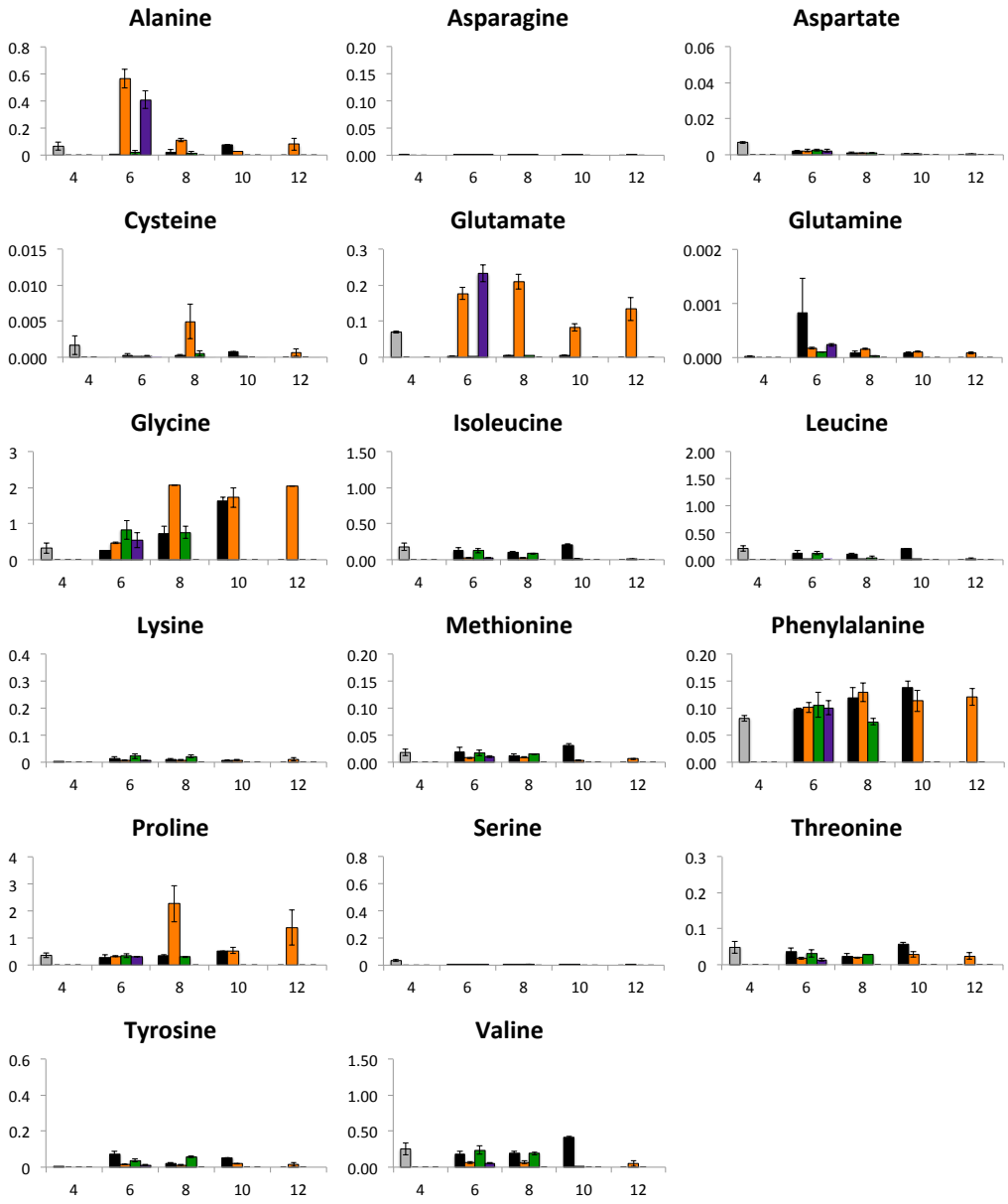

Figure 4.13 Intracellular metabolite profiles of amino acids of HB, Glc and HB+Glc supplementation from Figure 4.9.

Cell samples were collected for intracellularmetabolite profiles (Section 2.3.2). The bar charts represent the quantities of each metabolite in control culture at day 4 before feeding (gray), control at all subsequent days of culture (black), HB-supplemented (purple), Glc-supplemented (green) and HB+Glc-supplement (orange) at day 6 (6), day 8 (8), day 10 (10) and day 12 (12). Values (y-axis) are arbitrary units normalized to an internal standard and represent the average of three replicates with ± SEM.

Glucose was hardly detected inside the cell in all conditions (Figures 4.9 and 4.10B) as observed before. Small amounts of intracellular glucose were detected at day 8 in the presence of glucose since glucose was supplemented into the culture at day 6. Similar to the result of addition of glucose alone, cells fed HB+Glc generated high amounts of glucose inside the cells at day 8 and then it was depleted. This result corresponds to previous result of HB (Section 3.3.1 and 3.3.2) which showed that HB-fed cells consumed glucose slightly slower than the control. Intracellular pyruvate was not detected in all conditions except under feeding HB and HB+Glc conditions when pyruvate was be detected at day 6 (Figure 4.9 and 4.10B). In the case of intracellular amino acids, the amounts of almost all amino acids (except for glycine and alanine) in HB-fed and HB+Glc-fed cells were less than the control (Figures 4.9 and 4.13). This pattern is similar to that observed for extracellular amino acids. Asparagine and serine were exhausted rapidly in all conditions (Figure 4.9 and 4.13). Glutamate was depleted quickly in the control and for cells fed Glc alone whereas in the presence of HB or HB+Glc the amount of glutamate was greater than the control at day 6 for HB-fed cells and day 6, 8 and 12 for HB+Glc-fed cells. This pattern is similar to that observed for intracellular glutamate profile of cells supplemented with HB or Asn+Glc in Section 3.3.3 and Section 4.2.2.2, respectively. However, this observation was not found for the extracellular profiles of glutamate in HB-fed or HB+Glc-fed cells. Glycine accumulated inside the cells in all conditions (Figure 4.9 and 4.13) as observed for the extracellular glycine profile. Addition of HB or HB+Glc increased the amount of alanine at day 6 and then alanine decreased (Figures 4.9 and 4.13) as observed in extracellular alanine.

Intracellular lactate followed a similar trend to that observed for the extracellular profile in all conditions (Figures 4.9 and 4.10B). In control and feeding Glc alone, lactate was produced and the amount of lactate remained steady until the last day of assessment, whereas lactate was consumed after day 4 and was depleted at day 8 in the presence of HB or HB+Glc. Glycerol accumulated during culture in control and cells fed Glc condition

but the amount of glycerol in cells fed Glc was greater than the control at day 8 (Figures 4.9 and 4.10B) as observed in extracellular metabolite profiles. In the presence of HB or HB+Glc the amount of glycerol was decreased (Figures 4.9 and 4.10B) as observed in extracellular metabolite profile. The profile of change for intracellular sorbitol in cells fed nutrients was similar to that in the medium (Figures 4.9 and 4.10B). Sorbitol was hardly detected inside the cell in all conditions except for in the presence of Glc alone when a high amount of sorbitol was observed at day 8 (Figure 4.9 and 4.10B). This reflects the observations for extracellular and intracellular sorbitol profile of Glc-fed cells in previous section (Section 4.2.2.2). The intracellular amount of TCA cycle intermediates (citrate, isocitrate, succinate, fumarate and malate) in the presence of HB or HB+Glc was greater than the control and Glc-fed cells (Figures 4.9 and 4.11B). In the control and addition of Glc alone, the amount of TCA cycle intermediates slightly decreased throughout the detection period but cells fed HB or HB+Glc had greater amounts of metabolites in TCA cycle than the control at day 6 until the last day of assessment. This trend is similar to extracellular metabolite profiles of metabolites in the TCA cycle but the effect of HB or HB+Glc toward intracellular TCA cycle intermediates was more pronounced than the changes noted for those extracellular metabolite profiles. This result is also consistent with the profile of intracellular TCA cycle intermediates for cells fed HB (described in the previous Chapter, Section 3.3.3). Glycerol-3-phosphate was detected inside the cells (Figures 4.9 and 4.10B). In the control and feeding glucose alone, glycerol-3-phosphate was produced until day 6 and then it was consumed while in the presence of HB or HB+Glc the amount of glycerol-3-phosphate was less than the control at day 6 until the last day assessed.

In summary, the results from intracellular metabolite profiles demonstrated the same trend to that of extracellular metabolites for all conditions. Additionally, HB+Glc-fed cells generated similar intracellular metabolite profiles to that observed with addition of Asn+Glc (as hypothesized in Section 4.3.1). In the presence of Glc alone, high amounts

of glycerol and sorbitol were observed inside the cells as observed in previous section (Section 4.2.2.2). This might lead to earlier cell death in cells fed glucose. Ammonia (which cannot be detected by GC-MS) is a potential toxic byproduct of metabolism. The profile of ammonia in the medium of cells supplemented with nutrients is examined in next section.

4.3.2.3 Extracellular ammonia profile

To investigate the effect of nutrient feeding on ammonia production, medium samples from HB-fed cells, Glc-fed cells, HB+Glc-fed cells and the control were collected after day 4 onward for ammonia assay (Section 2.3.1.5).

Similar to the result in Section 4.2.2.3, ammonia production of the control gradually increased after day 4 and reached about 3 mM at day 12 (Figure 4.7B). The ammonia concentration of the control is consistent with data from a previous chapter (Section 3.3.1). HB addition significantly decreased ammonia production (<1 mM) as observed in a previous Chapter (Section 3.3.1). Glc-fed cells generated a similar pattern of ammonia production to the control. Ammonia concentration of feeding Glc reached about 2 mM at day 8 which was comparable with that of the control at day 8. Unsurprisingly, addition of HB+Glc followed similar trend of ammonia production to feeding HB alone. Cells fed HB+Glc exhibited a maximum concentration of ammonia (<1 mM) significantly less than that the control. In addition, the inhibitory effect of feeding HB+Glc on ammonia production was more pronounced than that of feeding Asn+Glc (Section 4.2.2.3).

After the effects of addition of glucose in cells fed Asn (Section 4.2) or HB (Section 4.3) were investigated and the result showed great promise to increase antibody titre. Based on results described in a previous chapter (Section 3.3.2), four amino acids (leucine, isoleucine, tyrosine and valine) were almost depleted after day 4 (for Asn-fed cells) or day 5 (for HB-feds cells) while the amount of those amino acids were still appreciable in

the control (Figure 3.7). Therefore, supplementation with the combination of leucine, isoleucine, tyrosine and valine in Asn-fed and HB-fed cells was hypothesized to prolong cell growth lead to increase antibody yield.

4.4 Effect of supplementation of amino acids with Asn- and HB-fed cells

In order to examine whether addition of some amino acids (that were almost depleted in cells fed Asn or HB) could improve cell growth and antibody yield, four amino acids (leucine, isoleucine, tyrosine and valine) were selected as supplementary nutrients in cells fed Asn or HB. These amino acids were added as a combination to CHO-LB01 culture medium supplemented with Asn or HB at day 5 before they reached low concentrations. Upon re-addition components were added to generate additional concentrations of 0.1 g/L each for leucine, isoleucine and tyrosine and 0.09 g/L for valine (Section 2.2.4). The concentrations of these amino acids were defined based on their concentration in DMEM medium. In this study there were six conditions: unfed (control), feeding four amino acids alone at day 5 (A.A.), feeding Asn alone at day 4 (Asn), feeding Asn at day 4 plus feeding four amino acids at day 5 (Asn+A.A.), feeding HB alone at day 4 (HB) and feeding HB at day 4 plus feeding four amino acids at day 5 (HB+A.A.). Medium samples were collected every day to study cell growth (Section 2.2.2), antibody production (Section 2.4.1) and extracellular metabolite profiles by GC-MS (Section 2.3.2).

4.4.1 Cell growth and antibody production

In control conditions, cells reached maximum viable cell density at ~1.2x10^7 cells/mL at day 5 and cells died at day 12 (Figure 4.14A). The pattern of cell growth of the control was similar to that previous result (Figure 4.1A and 4.8A). In the case of feeding Asn alone, maximum viable cell density was ~1.5 x 10^7 cells/mL at day 5 which was greater than the control and the cells died earlier (day 7) than the control (day 11) (Figure 4.14A) as observed in previous results of Asn feeding (Figure 4.1A). Cells fed HB alone reached maximum viable cell densities of 1.2 x10^7 cells/mL at day 6 and then the cells died at day 8 which was earlier than the control by three days (Figure 4.14A) as observed in Figure 4.8A. In case of addition of four amino acids (leucine, isoleucine, tyrosine and valine), surprisingly, no difference was found for the pattern of cell growth between cells fed with amino acids (A.A, Asn+A.A. and HB+A.A.) and without amino acids (control, Asn, HB) (Figure 4.14A). For example, cells fed Asn+A.A. or HB+A.A. showed similar pattern of growth to that seen with addition of Asn or HB alone. These results indicated that supplementation with the selected amino acids did not have any effect on cell growth in all conditions studied.

As for antibody production, similar to the reports in a previous a section, the control produced a maximum yield of antibody about 0.35 g/L at day 10 (Figure 4.14B). Cells supplemented with Asn produced a similar concentration of antibody (0.3 g/L) to the control at day 6 (Figure 4.14B). This is consistent with the result observed for feeding Asn in a previous section (Section 4.2.1). Addition of HB alone generated a significantly greater concentration of antibody (0.5 g/L at day 7) than the control (Figure 4.14B) as observed in previous Chapter. In the case of addition of four amino acids (leucine, isoleucine, tyrosine and valine), similar to cell growth, cells fed with four amino acids (A.A., Asn+A.A. and HB+A.A.) generated the same antibody production pattern of the respective culture without amino acids in all conditions (control, Asn, HB) (Figure 4.14B).

These results suggest that addition of selected amino acids did not affect antibody yield in all condition studied.

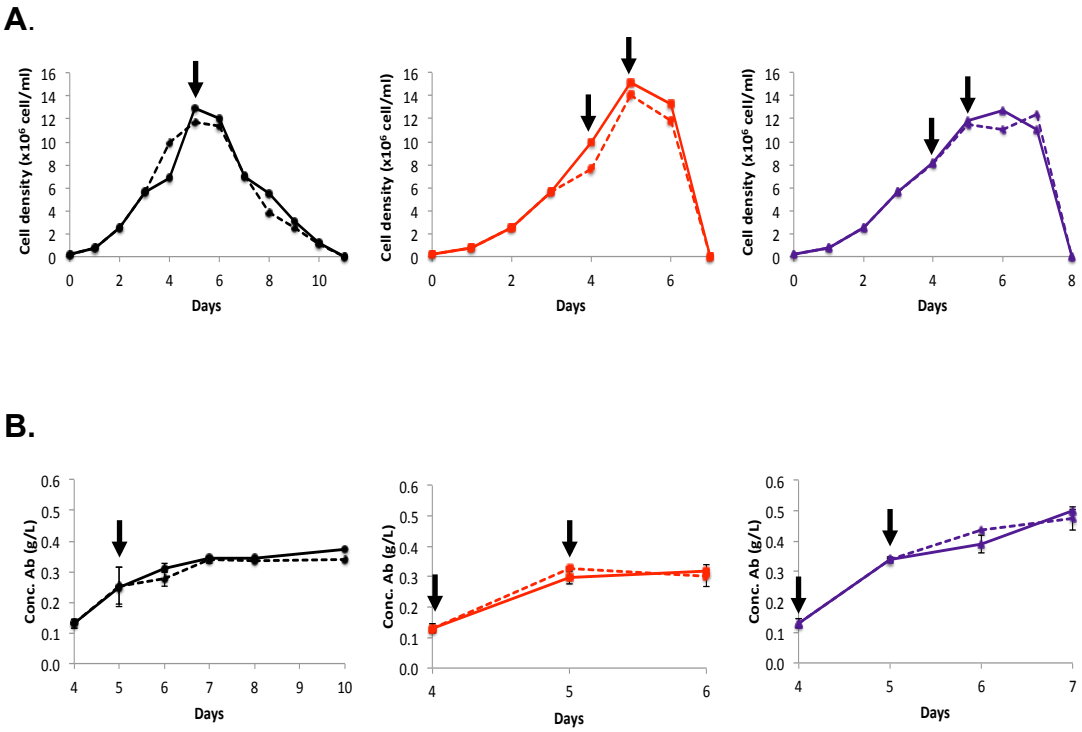

Figure 4.14 Cell growth and antibody production of Asn- or HB-fed cells in response to cells supplementation with and without selected four amino acids.
Viable cell density (A) and antibody production (B) were measured for the control (black), Asn-fed cells (red) and HB-fed cells (purple) as described in Figure 4.1 and 4.7 with (dash line) and without (solid line) supplementation of the combination of leucine (0.1 g/L), isoleucine (0.1 g/L), tyrosine (0.1 g/L) and valine (0.09 g/L) at day 5 of culture (Section 2.2.4). Medium samples were collected for cell counts (Section 2.2.2) and ELISA (Section 2.4.1). Values presented are mean ± SEM for three replicates for all conditions. The arrow presents the time of nutrients addition.

In summary, the results of these experiments indicated that supplementation with selected four amino acids in Asn- or HB-fed cells did not help the cells to prolong cell growth and increase antibody yield. It might be because these nutrients are not growth-limiting nutrients or there might be another nutrients (such as vitamins) which are also vital for cell survival. Thus, the hypothesis that was raised in Section 4.3.2.3 that supplementation with the combination of leucine, isoleucine, tyrosine and valine in cells fed Asn or HB could extent cell growth is incorrect. Therefore, in order to examine the impact of added four amino acids towards metabolism, extracellular metabolite profiles were undertaken by GC-MS in Section 4.4.2.

4.4.2 Extracellular metabolite profiling: GC-MS

Extracellular metabolite profiles by GC-MS of the control, A.A., Asn, Asn+A.A., HB and HB+A.A. conditions were conducted in this experiment The information from these results will provide clearer understanding of the effect of selected amino acids addition with Asn- or HB-fed cells toward metabolite profiles. Medium samples from control cells, cells fed Asn and cells fed HB with and without four amino acids addition (leucine, isoleucine, tyrosine and valine) were collected at day 5, 6 and 7 for extracellular metabolite profiling (Section 2.3.2).

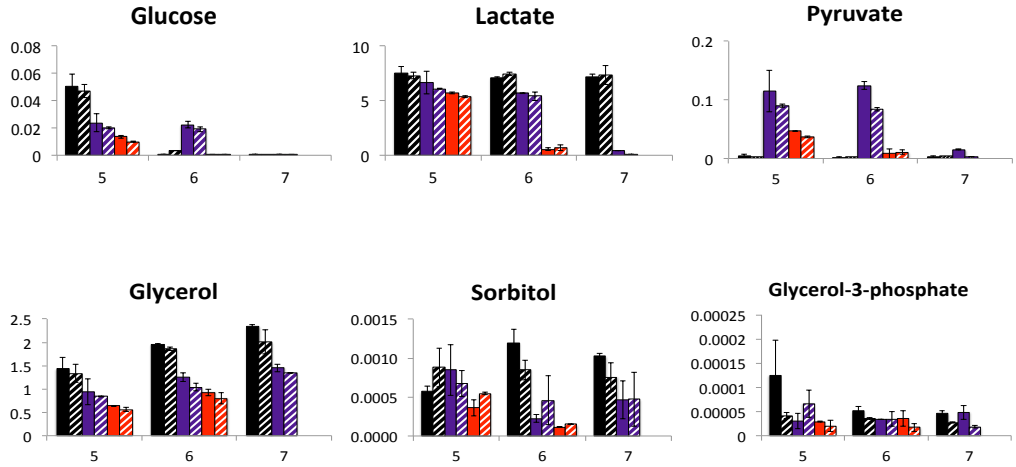

Figure 4.15 Extracellular metabolite profiles of metabolites related to glycolysis pathway of the control, HB-fed and Asn-fed in condition of with and without the combination of leucine, isoleucine, tyrosine and valine feeding.

Medium samples were collected for extracellular metabolite profile (Section 2.3.2). The bar charts represent the quantities of each metabolite of the control (black), HB-supplemented (purple) and Asn-supplemented (red) at day 4 (4), day 5 (5) and day 6 (6) in condition of with (stripe bars) and without (solid bars) the combination of four amino acids addition. Values (y-axis) are arbitrary units normalized to an internal standard and represent the average of three replicates with ± SEM.

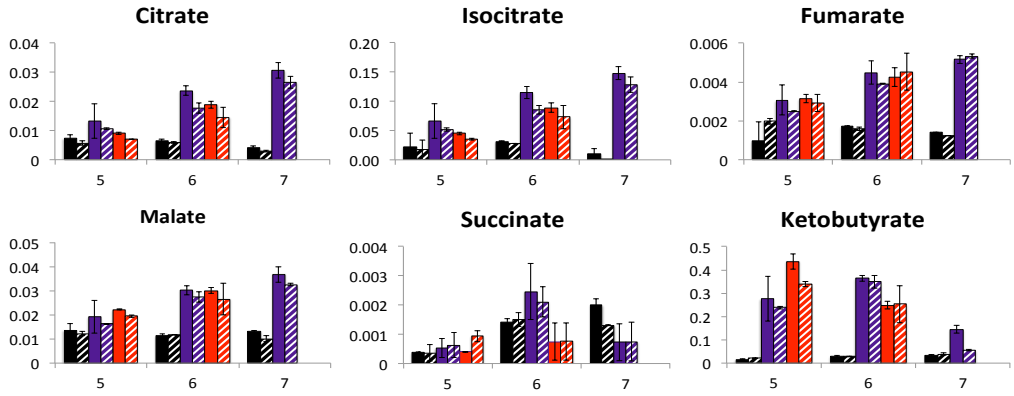

Figure 4.16 Extracellular metabolite profiles of metabolites related to the TCA cycle of the control, HB-fed and Asn-fed in condition of with and without the combination of leucine, isoleucine, tyrosine and valine feeding.

Medium samples were collected for extracellular metabolite profile (Section 2.3.2). The bar charts represent the quantities of each metabolite of the control (black), HB-supplemented (purple) and Asn-supplemented (red) at day 4 (4), day 5 (5) and day 6 (6) in condition of with (stripe bars) and without (solid bars) the combination of four amino acids addition. Values (y-axis) are arbitrary units normalized to an internal standard and represent the average of three replicates with ± SEM.

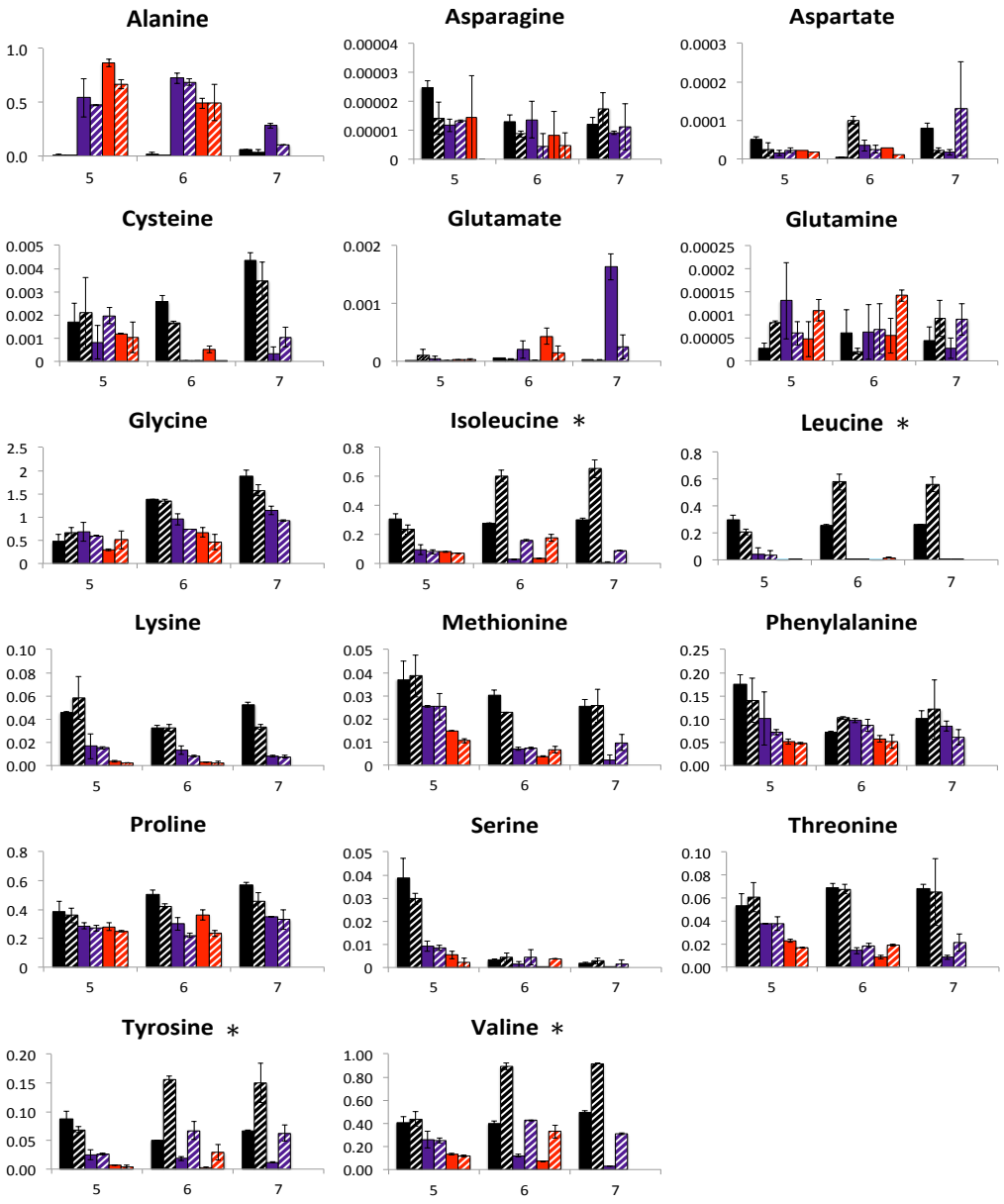

Figure 4.17 Extracellular metabolite profiles of amino acids of the control, HB-fed and Asn-fed in condition of with and without the combination of leucine, isoleucine, tyrosine and valine feeding.

Medium samples were collected for extracellular metabolite profile (Section 2.3.2). The bar charts represent the quantities of each metabolite of the control (black), HB-supplemented (purple) and Asn-supplemented (red) at day 4 (4), day 5 (5) and day 6 (6) in condition of with (stripe bars) and without (solid bars) the combination of four amino acids addition. Amino acids that were included in the feeds are indicated (*). Values (y-axis) are arbitrary units normalized to an internal standard and represent the average of three replicates with ± SEM.

Comparing between feeding A.A. conditions (A.A., Asn+A.A. or HB+A.A.) and without feeding A.A. conditions (control, Asn or HB), there was no difference in all metabolites except for the profile of added four amino acids (Figure 4.15-4.17). In the presence of Asn (Asn or Asn+A.A.) or HB (HB or HB+A.A.), the cells showed decreased lactate, glycerol and sorbitol production (Figure 4.15), increased amounts of metabolites in the TCA cycle (Figure 4.16) and decreased amount of amino acids (Figure 4.17) as observed previously as the effect of Asn or HB. In case of the profiles of supplemented four amino acids, increased amount of leucine, isoleucine, tyrosine and valine were found at day 6 after they were added into culture medium at day 5 in A.A., Asn+A.A. or HB+A.A. condition. In the control, the amounts of leucine, isoleucine, tyrosine and valine were constant throughout the detection period (as observed previously) while the amount of these amino acids at day 6 were clearly greater than that of day 5 and remained constant at day 7 in A.A. condition (Figure 4.17). Addition of Asn or HB alone exhibited similar profiles of four selected amino acids. The amounts of isoleucine, tyrosine and valine were decreased at day 5 (Figure 4.17). This result is consistent with previous results. In case of Asn+A.A. or HB+A.A., the amount of all added amino acids except for leucine were obviously increased at day 6 in both condition but their amount was less than in A.A. condition. Afterward, their amounts were slightly decreased at day 7 in HB+A.A. condition (Figure 4.17). For leucine, although leucine was added into the culture of cells fed Asn or HB at day 5, this amino acid was almost depleted at day 6 in both conditions.

In summary, addition of the combination of isoleucine, leucine, tyrosine and valine with the control, Asn- or HB-fed cells did not alter overall metabolite profiles. In case of feeding four selected amino acids alone in the control, in A.A. condition, the cells might not need added amino acids since the amount of these amino acids did not reach low amount in this condition. As a result the amount of added amino acids were not decreased. In Asn+A.A. or HB+A.A., added amino acids were slightly consumed to

support high amino acids consumption in cells fed Asn or HB. However, these amino acids were not depleted except for leucine. Although four selected amino acids were consumed in Asn+A.A. or HB+A.A. condition but no improvement of cell growth and antibody production were observed in Section 4.4.1. This finding suggest that the cells might utilize added amino acids but addition only these amino acids might not have an enough effect to prolong cell growth and enhance antibody production. As mentioned previously, there might be other nutrients (such as vitamin and glucose) that are also necessary to sustain cell growth or antibody production. In addition, leucine might be a key amino acid since leucine was the only one added amino acid that was depleted in cells fed Asn+A.A. and HB+A.A.. Therefore, increased the concentration of leucine addition might be required in the future for Asn- or HB-fed cells in order to maintain cell survival.

4.5 Discussion

The aim of this chapter is to extend culture duration of Asn- or HB-fed cells which had a potential to increase cell growth or antibody titre as shown in Chapter 3 in order to achieve greater titre of CHO-LB01 cells. Therefore, it was hypothesized that addition of glucose or amino acids in cells fed Asn or HB could increase antibody titre by extend stationary phase. Many previous results showed that supplementation with glucose or several amino acids delayed the start of the decline phase (Crowell et al., 2007, Kang et al., 2012, Kishishita et al., 2015, Sellick et al., 2011, Yu et al., 2011). Thus, addition of glucose or amino acids (leucine, isoleucine, tyrosine and valine) in cells fed Asn or HB were the focus in this chapter.

Alteration of cell culture performance of CHO-LB01 cells was observed in this chapter. Cells generated greater viable cell number, earlier death and produced less antibody than previous chapter. It is probably due to genetic changing during subculture

(O'Callaghan et al., 2015) and changing of cell culture factor such as medium lot and MSX stock. However, in the presence of Asn or HB, cells still showed greater maximum viable cell density and antibody titre than the control, respectively.

The results in this chapter reveal that feeding glucose alone caused early cell death and had no effect on antibody production. Based on the analysis of data from extra- and intra-cellular metabolite profiles, it is possible that high accumulation of glycerol and sorbitol in cells fed glucose alone caused earlier cell death especially intracellular sorbitol which was very high amount at day 8 before the cells died at day 9 (Figure 4.18C). Although no direct toxicity of high glycerol and sorbitol accumulation were reported in CHO cells but decreased amounts of NADPH from sorbitol generation associated with alteration of intracellular antioxidant might be one potential explanation for this observation (Tang et al., 2012). In addition, high accumulation of glycerol and sorbitol which were produced as alternative redox sinks might lead to unbalanced redox state. This result is contrast with Sellick et al. (2011) who found that addition of glucose alone had no effect on antibody production but delayed the entry of decline phase of CHO-LB01 cells. This conflict may be due to the difference of addition day and concentration of glucose used. Sellick et al. (2011) added 1.1 mM glucose into cell culture medium at day 4 while 20 mM glucose was supplemented into cell culture medium at day 6 in our experiment. In addition, Sellick et al. (2011) found that only sorbitol was accumulated in cells fed glucose alone but its amount was not much different compared to unfed cells as our result which sorbitol was accumulated about three fold greater than the control.

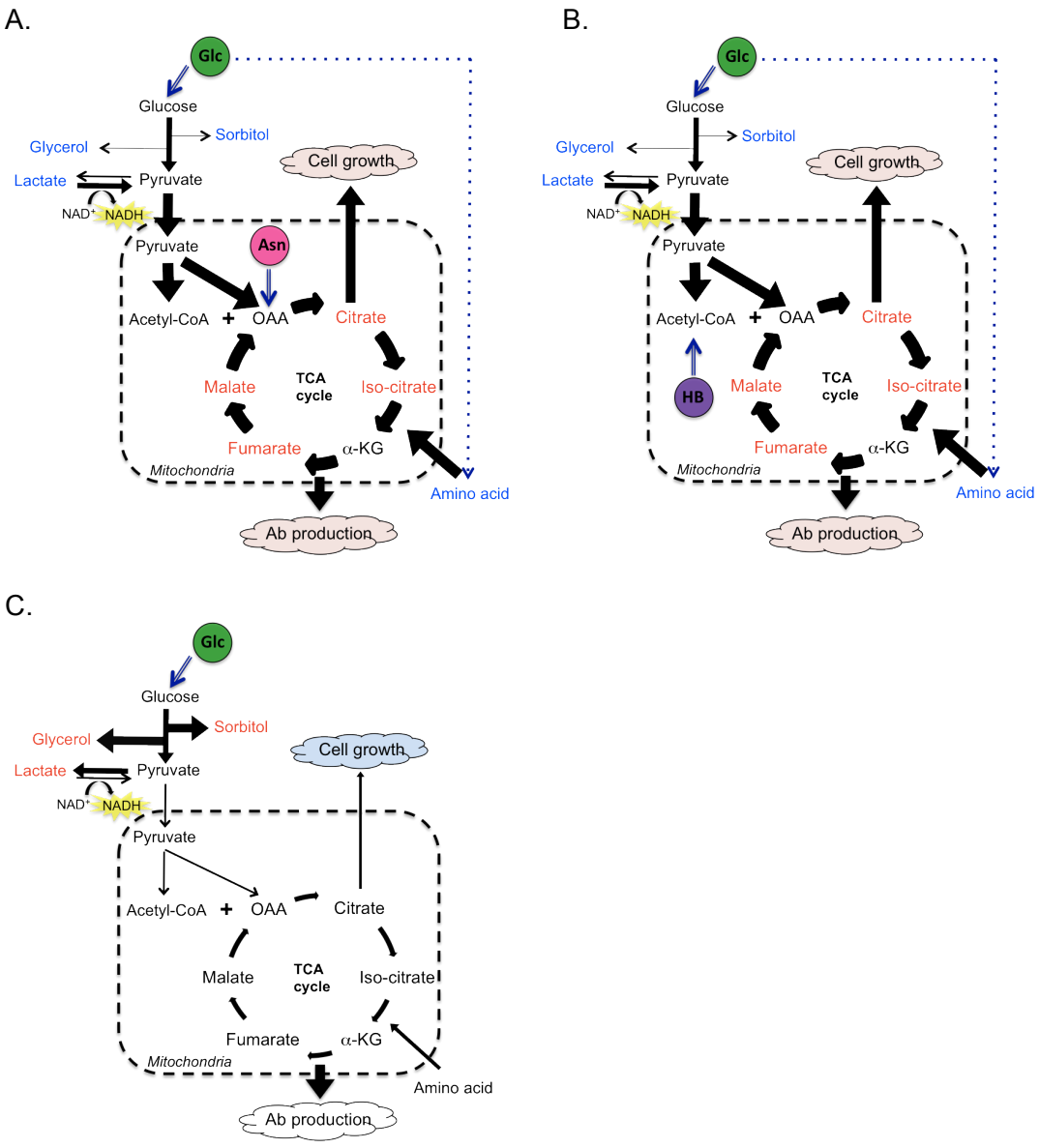

Figure 4.18 Summary of the effect of nutrients supplementation on cell growth, antibody production and metabolite profiles.

Supplementation with Asn+Glc (A) or HB+Glc (B) showed increased amount of TCA cycle metabolites and decreased amount of lactate, glycerol, sorbitol and amino acids. As a result, the cells can prolong stationary phase lead to increase antibody yield. In case of addition of glucose alone (C), the cells died early probably due to high lactate, glycerol and sorbitol accumulation. In addition, there was no effect toward metabolites in TCA cycle and amino acids. The red characters indicate increased production or decreased consumption. The blue characters indicate decreased production or increased consumption. The red, blue and white clouds indicate increased, decreased and no effect, respectively.

Interestingly, when glucose was fed along with Asn or HB, cells exhibited a prolonged stationary phase of three to four days, which in turn led to enhanced antibody yield (by two fold). Once glucose was supplemented into the Asn or HB fed cells while cells required more nutrients to support increased TCA cycle flux, glucose can provide replenishment balance to the effects of Asn or HB. Consequently, high amounts of citrate, fumarate and malate were observed until last day of culture. As a result, the cells can survive longer and increased antibody yield because of prolonged survival. However, some amino acids were depleted although glucose was supplemented into culture medium. This might be the reason why cells fed Asn+Glc or HB+Glc maintained stationary phase but cannot continue growing. In order to clarify the impact of glucose addition with Asn or HB, metabolic flux analysis are necessary to investigate how the compliment of glucose and Asn or HB can support cell growth in the future (Chapter 7).

In addition to glucose, four amino acids (leucine, isoleucine, tyrosine, valine) were selected as supplementary base on extra- and intra-cellular metabolite profiles analysis of cells fed Asn or HB in Chapter 3 in order to prolong production phase of Asn- or HB-fed cells. Contrary to expectations, addition of selected four amino acids with Asn or HB did not have any effect on cell growth, antibody production and overall extracellular metabolite profiles. The extracellular metabolite profiles of these four amino acids demonstrated that these amino acids did not reach low amounts in the control. Thus, the cells do not need more amounts of these amino acids. Isoleucine, tyrosine and valine were slightly consumed in Asn+A.A. and HB+A.A. and the amounts of them were still greater than that of feeding Asn or HB alone. Although these amino acids were slightly consumed but improvement of cell growth and antibody production were not found. Thus, It can be suggested that isoleucine, tyrosine and valine were not growth-limiting nutrients. As for leucine, the amount of leucine was hardly detected in Asn+A.A. and HB+A.A.. This indicates that added leucine is utilized by the cells. Therefore, increased concentration of leucine addition in cells fed Asn or HB might be required in the future.

From these result, it seems possible that in addition to the combination of these amino acids with Asn or HB other nutrients such as glucose or vitamin might be need to extend stationary phase of the cells. However, many researches were successful to improve antibody yield by supplementation of amino acids as mentioned in Section 4.1 (Crowell et al., 2007, Kang et al., 2012, Kishishita et al., 2015, Yu et al., 2011).

Overall, enhanced cell growth and recombinant protein production by modification of nutrient supplementation was obtained in this chapter. Thus, the second objective was achieved (Section 1.6). From the overall result in this chapter, it can be concluded that addition of glucose with Asn or HB exhibited additive effect to maintain high amount of TCA cycle intermediates. As a result cells can prolong stationary phase and maintain high titer for 3-4 days. Although the result of modification of nutrient supplementation showed the great promise to enhance antibody yield but this approach is not the only one strategy to improve productivity of CHO-LB01 cells. In addition, the result analysis from Chapters 3 and 4 provide useful information that increased TCA cycle intermediates and decreased lactate, glycerol and sorbitol production could enhance the growth/or productivity of CHO-LB01 cells. Therefore, based on this finding, identification of target genes and improvement of product yield and/or cell growth of CHO-LB01 cells by cell engineering will be investigated in the next chapter.

CHAPTER 5

Examining the possibility to improve productivity of CHO cells by cell engineering

5.1 Introduction

In addition to optimization of the composition of culture medium, cell engineering is a major approach that has been used to improve the efficiency of CHO cells. In this thesis, modification of feeding nutrients was reported in Chapters 3 and 4. This chapter focused on the use of genetic engineering to modify the metabolism of CHO-LB01 cells in order to enhance antibody titre based on understanding of the relationship between antibody production and metabolite profiles reported in Chapters 3 and 4. Improving cell metabolism has been a common objective for researchers for many years. Several target genes have been engineered for two main purposes: inhibition of the accumulation of toxic metabolic by-products such as lactate and improvement of the efficiency of central carbon metabolism to generate cell lines with improved metabolic characteristics, cell growth and productivity (Section 1.5.2 and Figure 1.8). Decreased accumulation of lactate has been obtained by down-regulation of enzymes such as LDH-A (Jeong et al., 2001, Kim and Lee, 2007a, Zhou et al., 2011) and PDHK (Zhou et al., 2011). Additionally, cell engineering has been used to improve central carbon metabolism. PC (Bollati Fogolin et al., 2004, Kim and Lee, 2007b, Wilkens and Gerdtzen, 2015) and MDH II (Chong et al., 2010, Wilkens and Gerdtzen, 2015) in CHO cells have been overexpressed in CHO cells. These interventions have improved cell viability and product yield of CHO cells. However, variable outcome have been found in different CHO cells types and culture medium (detail in Section 1.5.2.1).

As mentioned above, it can be seen that many target genes in metabolic pathways have been engineered to improve bioprocess performance of CHO cells. Therefore, cell engineering approaches (overexpressing or knocking down of genes involved in the central carbon metabolism) was seen as an potential route to improve cell metabolism for enhancement of cell growth and/or antibody production. Thus, the aim of this chapter is to improve productivity of CHO-LB01 cells by cell engineering.

Target genes for cell engineering were selected (Section 5.2) based on previous result (Chapters 3 and 4) and cell engineering approach (knockdown, Section 5.3 and overexpression, Section 5.4) was undertaken in CHO-LB01 cells. Afterwards, the behavior of engineered cells was characterised in terms of cell culture performance and metabolite profiles.

5.2 Selection of target genes

As seen in Chapters 3 and 4, the metabolites in the TCA cycle were increased when the cells produced higher maximum cell density or antibody yield in case of feeding Asn, HB, Asn+Glc and HB+Glc. In addition, a decreased production of sorbitol was observed under all conditions of feeding. Therefore, increased flux in the TCA cycle and/or increased flow of carbon atoms from glycolysis to TCA cycle was hypothesized to underpin the enhanced antibody yield in CHO-LB01 cells. In this study, aldose reductase (*Akr1b1*) and malate dehydrogenase 2 (*Mdh2*) were selected as targets for cell engineering (Figure 5.1). The reason to choose these enzymes is explained below.

Akr1b1 encodes an aldose reductase (AR) enzyme. This enzyme catalyzes the conversion of glucose to sorbitol using NADPH. The enzyme comprises 316 amino acids (35.8 kDa). From previous results (Chapters 3 and 4), a correlation between decreased sorbitol production and enhanced product yield was observed in cell fed nutrients. Therefore, it was hypothesized that inhibition of the activity of AR or suppression *Akr1b1* expression would be associated with an increased flux of carbon atoms from glycolysis to TCA cycle lead to improved cell growth and/or product yield. However, no evidence has been reported about the function of AR in CHO cells and there is no prior information related to metabolism and productivity of CHO cells.

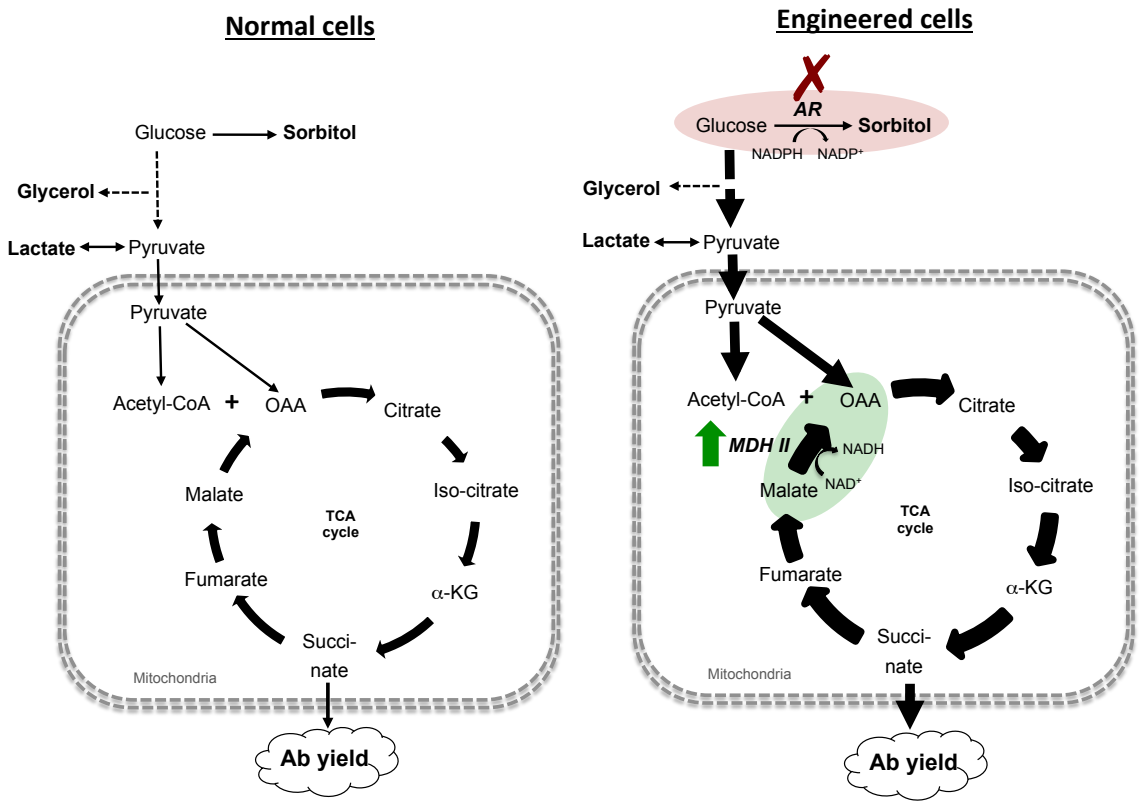

Figure 5.1 Target genes for cell engineering.

Increase the flow of carbon atoms from glucose by decrease sorbitol production by inhibit AR activity (red circle) and increased the flow of TCA cycle by overexpression of MDH II (green circle) was hypothesized to improve antibody yield of CHO-LB01 cells. The thickness of the lines indicates increased the flow of the pathways.

Mdh2 encodes malate dehydrogenase 2 (MDH II) which converts malate to oxaloacetate by oxidization of NAD^+ to NADH in mitochondria as part of the TCA cycle (Figure 1.8). The enzyme comprises 352 amino acids (35.5 kDa). Among the extra- and intra-cellular TCA metabolites identified in Chapters 3 and 4, malate accumulation was one of the most abundant metabolite in the presence of Asn, HB, Asn+Glc and HB+Glc. In addition, it has been reported that MDH II might be the enzymatic bottleneck of the TCA cycle (Chong et al., 2010, Wilkens and Gerdtzen, 2015). Moreover, Nissom et al. (2006) undertook transcriptome profiling of CHO-cell (by microarray) and found that transcripts for MDH II were increased in high producer cells. Thus, overexpression of MDH II could increase the efficiency of the TCA cycle hence support increased product yield. Engineering strategies targeting MDH II have shown promising results in previous

studies. Overexpression of MDH II in mAb-secreting CHO cells has been demonstrated to increase intracellular ATP and NADH, improve in integral viable cell number and antibody titre (Chong et al., 2010). Recently, overexpression of MDH II in IgG-producing CHO DP12 cells was reported to decrease cellular productivity recently (Wilkens and Gerdtzen, 2015). These conflicting outcomes arose from the use of different CHO cell types and culture conditions and the basic rationale for examination of the effects of MDH II remains valid.

Overall, inhibition of sorbitol production and/or overexpression of *Mdh2* could potentially lead to an enhance efficiency of CHO-LB01 cells. In addition, transcripts level of *Mdh2* of CHO-LB01 cells will be shown in the next chapter (Section 6.3.1).

5.3 Inhibition of sorbitol production by chemical reagent and siRNA approaches

Inhibition of sorbitol production was hypothesized to be associated with increased flow of carbon atom directly from glucose to the TCA cycle as mentioned in Section 5.2. In this study, two approaches were used to achieve this objective. Firstly, a chemical reagent, 2,5-dihydro-4-hydroxy-5-oxo-1-(phenylmethyl)-1H-pyrrole-3-carboxylic acid ethyl ester (EBPC) was used to inhibit the activity of AR (Section 5.3.1). Secondly, siRNA was designed against *Akr1b1* to examine the consequences of the addition (Section 5.3.2).

5.3.1 Chemical reagent approach

Several chemical reagents have been using to inhibit the activity of AR including Sorbinil, Epalrestat and EBPC (Zhu, 2013). For the current study EBPC was selected as an AR inhibitor.

5.3.1.1 Concentration-dependency and timing of addition of EBPC on cell growth and viability

First of all, the effects of EBPC on cell growth and viability was examined at various concentrations (0-200 μM) with addition of EBPC at day 4 of batch culture (Section 2.8). In the presence of 200 and 100 μM EBPC, with cells at maximum viable cell density at day 4, cells died at day 5 and 6, respectively, times earlier than the control by 5 and 4 days, respectively (Figure 5.2). With the addition of 50 mM EBPC, cultures showed a pattern of growth that was similar to the control during the first five days of the culture. Afterwards, viable cell density was significantly lower than the control at day 7 and it remained low until the end of culture. Given the rapid toxicity observed with EBPC above 100 μM, EBPC was used at a concentration of 50 μM in further analysis because this concentration exhibited minimum negative effect on cell growth.

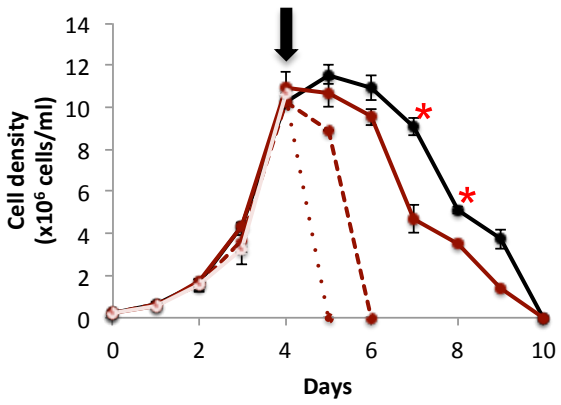

Figure 5.2 Effects of various concentrations of EBPC on cell growth of CHO-LB01 cell.

Culture was performed in CD OptiCHO™ medium as described in Section 2.2.1. Addition of EBPC inhibitor was made at day 4 (shown by the arrow) of culture (Section 2.8) to give the final concentrations at 50 μM (red solid line), 100 μM (red dashed line) and 200 μM (red dotted line). The experiment was performed with a parallel unsupplemented control (black line). Medium samples were collected for cell counts (Section 2.2.2). Values presented are mean ± SEM for three replicates. * indicates significant difference from control at $p < 0.05$.

Next, the timing of addition of EBPC was investigated (50 μM EBPC added at day 0, 2 or 4 of batch culture). As shown in Figure 5.3, when EBPC was added at day 0, cell growth was negligible. Low viable cell density (less than ~1x10^6 cells/mL) was detected throughout the detection period. When EBPC was added on day 2 a similar response was seen to the addition of EBPC on day 4 but the latter generated slightly higher maximum viable cell density (~1x10^7 cells/mL) at day 5 than the former and the cells died earlier (day 9) than the control (day 11) in both conditions. However, addition of EBPC on either day 2 or day 4 showed lower viable cell density than the control after day 3 and day 5, respectively. Therefore addition of 50 μM EBPC on day 4 was used for further analysis since it showed minimum negative effect on cell growth.

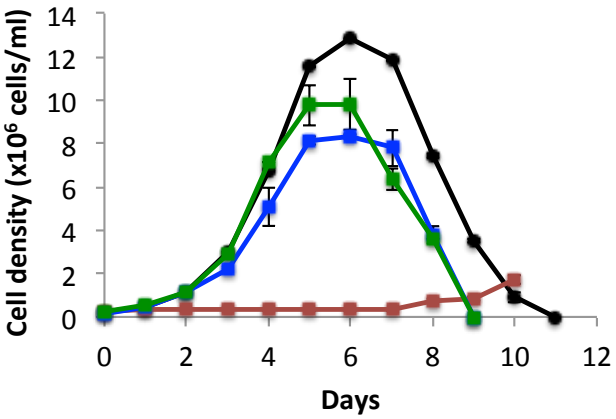

Figure 5.3 Effects of timing addition of EBPC on cell growth of CHO-LB01 cell. Culture was performed in CD OptiCHO™ medium as described in Section 2.2.1. 50 μM EBPC inhibitor was added into the culture at day 0 (red), 2 (blue), and 4 (green) (Section 2.8). The experiment was performed with a parallel unsupplemented control (black). Medium samples were collected for cell counts (Section 2.2.2). Values presented are mean ± SEM for three replicates.

5.3.1.2 Metabolic characterization of the effect of EBPC on CHO-LB01 cells

The consequence of addition 50 μM EBPC at day 4 of CHO-LB01 cell batch culture was examined in relation to cell growth, antibody production and extracellular metabolite profiles, in particular for confirmation of effects on sorbitol production.

First of all, extracellular metabolite profiles by GC-MS was conducted to examine whether EPBC generated any effect on sorbitol and another metabolites. As shown in Figure 5.4, In the presence of EBPC, sorbitol production was decreased by 50% at days 5 and day 7. This suggested that EBPC inhibited the activity of AR. At the same time, EBPC addition resulted in glucose and lactate profiles that were similar to those observed for control conditions. The production and use of other metabolites showed contrasting effects in response to addition of EBPC. Glycerol production was decreased by about 50% in the presence of EBPC (day 5 to day 9). In contrast, significantly increased amounts of pyruvate and alanine were detected (day 5 to day 9 for pyruvate and day 7 to day 9 for alanine). EBPC addition had no effect on the amount of TCA metabolites observed in culture medium. This result indicates that decreased sorbitol production resulted from addition of EBPC. It is not because of fewer cell number since increased amounts of pyruvate and alanine were observed in the presence of EBPC.

As for cell culture performance, at the time of EBPC addition, viable cell density was ~1x10^7 cells/mL (Figure 5.5A). In agreement with data presented in Section 5.3.1.1, the addition of EBPC decreased viable cell density throughout the duration of culture and produced a significant decrease in antibody production (Figure 5.5B). Maximum concentration of antibody in the presence of EBPC was about 0.2 g/L (control at 0.3 g/L). Specific productivity profile was similar between cells treated EBPC and the control throughout cell culture period (Figure 5.4C).

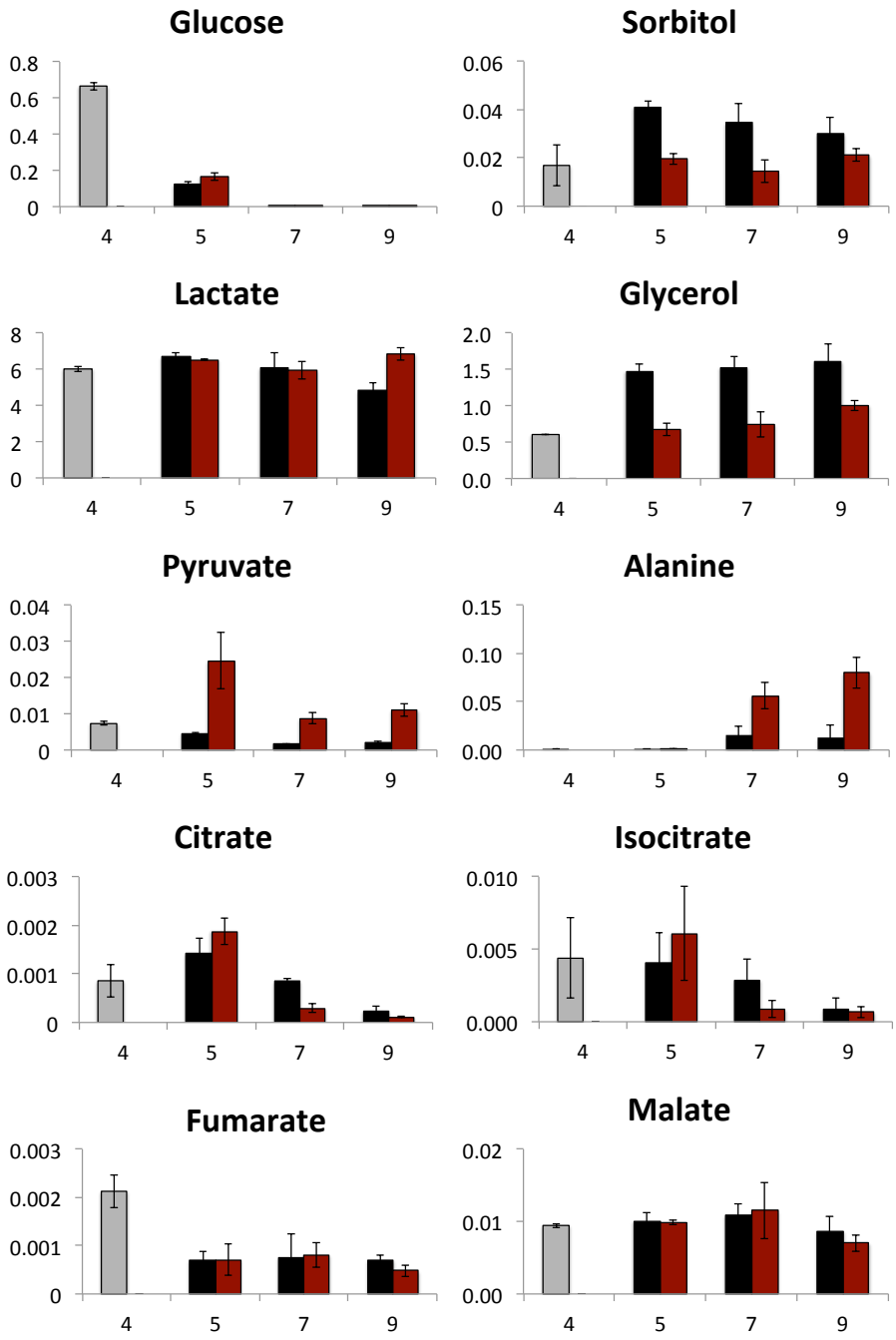

Figure 5.4 Effects of EBPC inhibitor addition on extracellular metabolite profiles. Medium samples were collected for extracellular metabolite profile (Section 2.3.2). The bar charts represent the quantities of each metabolite in CD OptiCHO™ medium comparing between unsupplemented control at day 4 before EBPC inhibitor addition (gray), unsupplemented control at all subsequent days of culture (black) and EBPC inhibitor addition (red) at day 5 (5), day 7 (7) and day 9 (9). Values are arbitrary units normalized to an internal standard and represent the average of three replicates with ± SEM.

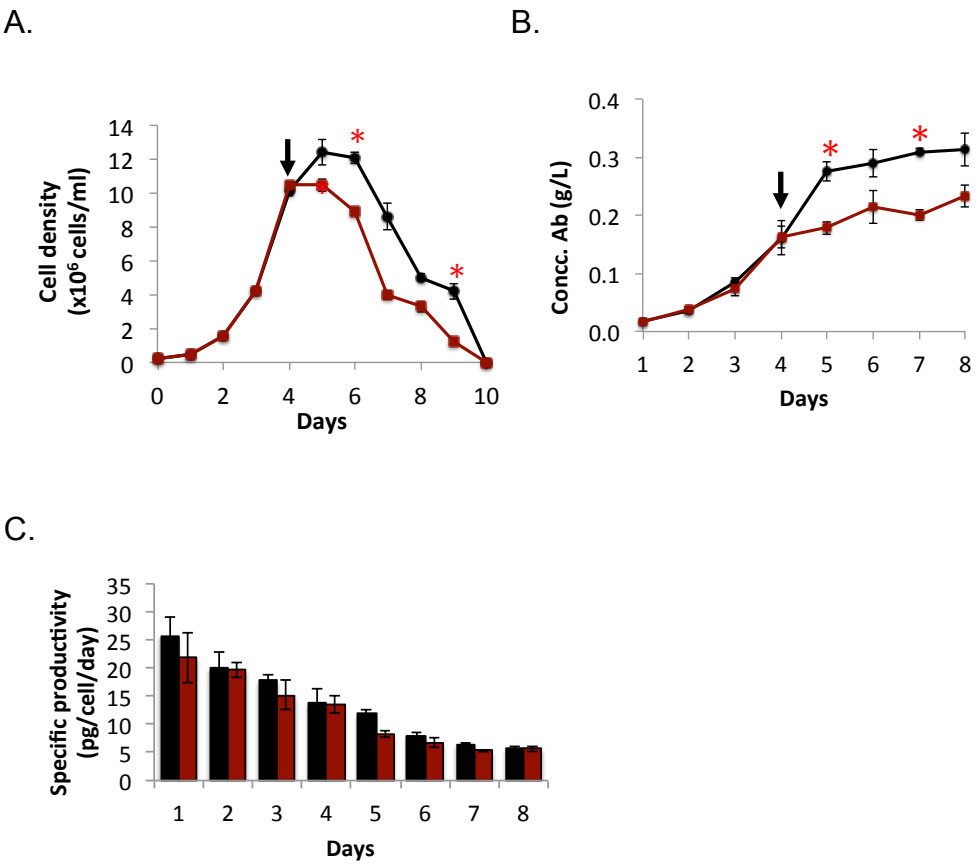

Figure 5.5 Cell growth and antibody production of CHO-LB01 cells in response to EBPC inhibitor addition.

Viable cell density (A), antibody production (B) and specific productivity (D) were measured for LB01 cells throughout batch culture in CD OptiCHO^{TM} medium (control, black) or with 50 μM EBPC inhibitor addition at day 4 (red) (the arrow presents the time of addition). Medium samples were collected for cell counts (Section 2.2.2) and ELISA (Section 2.4.1). Values presented are mean ± SEM for three replicates. * indicates significant difference from control at $p < 0.05$.

Overall, it can be concluded that EBPC can inhibit sorbitol production without the positive effect on cell growth and/or antibody production. Inhibition of sorbitol production by EBPC also decreased glycerol production, increased alanine and pyruvate production but had no effect on lactate and metabolites in TCA cycle. Although using EBPC was successful to inhibit sorbitol production but this approach also had an effect on glycerol production. It is probably due to EBPC might also inhibit the function of glycerol-3-phosphate dehydrogenase which is an enzyme that catalyzes the conversion of dihydroxyacetone phosphate to glycerol-3-phosphate. Therefore, in order to get the specific target to AR, suppression the expression of *Akr1b1* was conducted by siRNA technique.

5.3.2 siRNA approach

An siRNA approach was designed to knockdown the expression of *Akr1b1* which is the gene encoded AR. Three siRNAs targeting *Akr1b1* (siAR1, siAR2 and siAR3) were designed by Eurofin DNA siRNA design service (Section 2.9.1). Control scrambled siRNA (Scr) was designed using Invivo scrambled siRNA wizard. Figure 5.6 shows the location of the three siRNAs against the sequence of *Akr1b1*.

Three strategies of siRNA usage were trialed including a combination of three siRNAs at a combined concentration of 50 nM, individual siRNAs each at 50 nM and individual siRNAs each at 100 nM. siRNAs was transfected into CHO-LB01 cells at day 3 in all strategies (Section 2.9.2) and the expression of AR was examined at day 6 and 8 by Western blot. The Western blot results of three strategies are shown in Figure 5.7, 5.8 and 5.9, respectively. Unfortunately, the protein expression of AR was not decreased by any strategy. No difference of the intensity of AR signal was observed between the control, Scr and siRNA at day 6 and day 8. It can be concluded that the siRNA approaches as used here did not decrease AR expression.

TTCCTTTCTGCAGGCCGTTGGGGCTATTTAAGGGGGGCGCCGGAGCCGGAGCCGCACAGTTGCCGGTCCT
GGTGCGCAGCGTGCAGCCGTCATGGTCAGCCACCTGCAGCTCAACAACGGCGCCAAGATGCCCATCCTGG
GCCTGGGCACCTGGAAGTCCCCTCCCGGCCAGGTGACTGAGGCCGTGAAGGCTGCCATTGACATTGGGTA
CCGCCACATTGACTGTGCCCAGGTGTACCAGAATGAGAAGGAGGTGGGAATGGCCCTCCAGGAGAAGCTC
AAGGAGCAGGTGGTGAAACGCCAAGACCTCTTCATCGTCAGCAAGCTGTGGTGCACGTTTCACGACAAGA
GCATGGTGAAAGGAGCTTGCCAGAAGACGCTCAGTGACCTGCAGCTGGACTACCTGGACCTCTACCTTAT
TCACTGGCCAACAGGTTTCAAGCCCGGGCCTGATTACTTCCCACTGGACGAATCAGGAAATGTGATTCCC
AGTGAGACTGATTTTGTGGACACTTGGACGGCCATGGAACAGCTGGTGGATGAAGGTTTGGTGAAATCCA
TTGGTGTCTCCAACTTCAACCCTCTTCAGATTGAGAGAATCTTAAACAAACCCGGCTTAAAATATAAGCC
TGCGGTTAATCAGATTGAATGCCACCCGTACCTAACTCAGGAGAAGCTGATTGAGTACTGCCAATCCAAA
GGCATCGTGGTGACCGCGTACAGTCCCCTTGGCTCTCCTGACAGGCCCTGGGCCAAGCCTGAAGACCCTT
CTCTCTTGGAGGATCCCAGGATTAAGGCAATTGCATCCAAGTACAATAAAACAACAGCTCAGGTGCTGAT
CCGGTTCCCCATACAAAGGAACTTGGTGGTGATCCCCAAGTCCGTGACACCAGCAAGAATTGCTGAGAAC
CTGAAGGTCTTTGACTTCGAGCTGAGCAAGGAGGATGTGACCACTCTACTCAGCTACAACAGGAACTGGA
GGGTGTGTGCCTTGATGAGCTGTGCTAAACACAAGGATTACCCCTTCCACGCAGAAGTCTGAAGCTTCGG
ATGCCTGCTCTCTCCCACGAGACTTGCACCTGCTCTTCCTGTTTCATCTGTCCTTGTGGGTGTAGTGTAG
ACTGTGTCCCTCTGCACTGTGTGGAACCTGGAAGATCAGACAACGAGGGTCTGTTAGTTTGATGTAGTCT
CCAGAGAGCATTATCAGTAGCTGAGTGATTTTCTTCAGCCTTTCTTGATCTTTCTTCTTACCCACCTGGA
AAATGTTTAACACAAGTACCCTTTCCAACCAAAGAGAAGCAAGATTTATAGTCCAAGTAGTGCCACTAAC
AGTTAAGTTTTGAGTGCTCAGAGCTGTAGTCTTTGGGTCAGTCTTCTCTTTGCTTCAAATAAAAACTGCT
TTTGTGAA

Figure 5.6 Location of three siRNAs against aldose reductase (*Akr1b1*).

siRNA was designed to target *Cricetulus griseus Akr1b1* mRNA (accession XM_003503181.2). Green and red highlight are start and stop codon, respectively. Three siRNAs : siAR1 (underline), siAR2 (double underline) and siAR3 (dashed underline) were designed by Eurofin DNA siRNA design service (Section 2.9.1).

A.

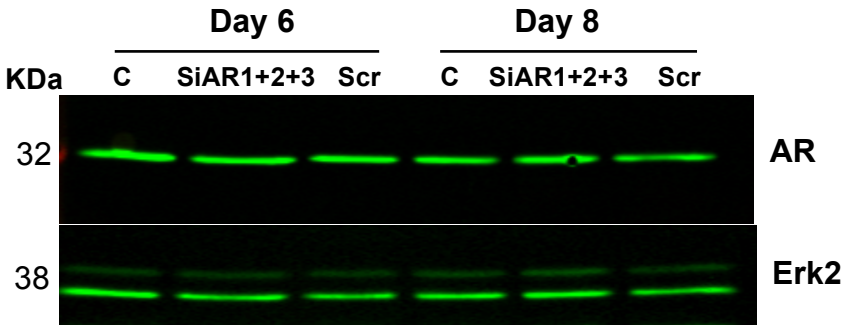

B.

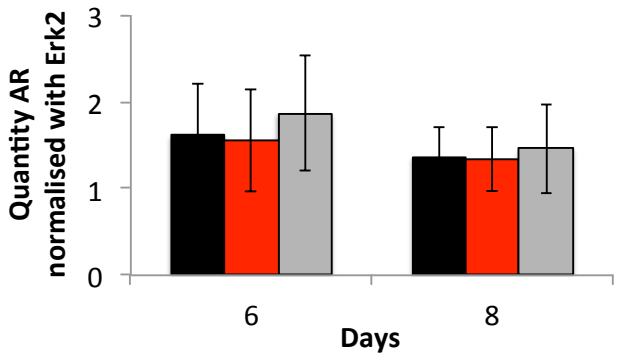

Figure 5.7 Western blot Analysis of AR protein expression after siRNA treatment strategy 1.

CHO-LB01 cells were transfected with a combination of siAR1, siAR2 and siAR3 at 50 nM (siAR1+2+3) or scrambled siRNA (Scr) at day 3 (Section 2.9.2). Protein samples from total cellular extraction (Section 2.4.2) at day 6 and 8 were determined by Western blot using AR (top) and Erk2 (bottom) primary antibody (Section 2.4.4) (A) and the quantity of AR expression was normalized with Erk2 (B). The bar charts represent the quantities of AR protein expression of the control (black), three siRNAs transfection (red) and scrambled siRNA transfection (grey). Values presented are mean ± SEM for three replicates.

A.

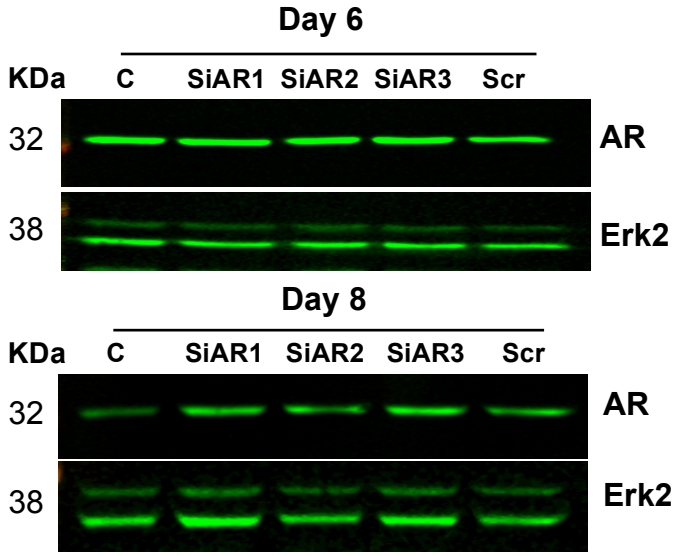

B.

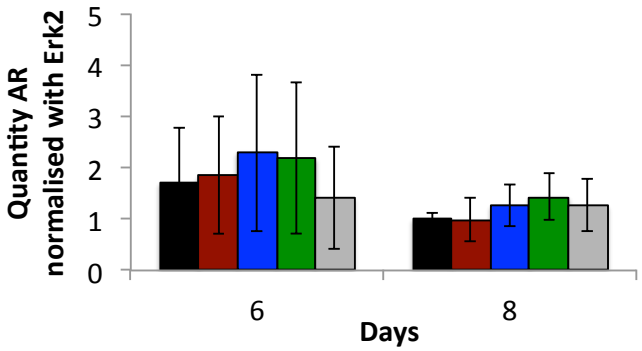

Figure 5.8 Western blot Analysis of AR protein expression after siRNA treatment strategy 2.

CHO-LB01 cells were transfected with an individual of siAR1, siAR2 and siAR3 at 50 nM or scrambled siRNA (Scr) at day 3 (Section 2.9.2). Protein samples from total cellular extraction (Section 2.4.2) at day 6 and 8 were determined by Western blot using AR (top) and Erk2 (bottom) primary antibody (Section 2.4.4) (A) and the quantity of AR expression was normalized with Erk2 (B). The bar charts represent the quantities of AR protein expression of the control (black), siAR1 transfection (red), siAR2 transfection (blue), siAR3 transfection (green) and scrambled siRNA transfection (grey). Values presented are mean ± SEM for three replicates.

A.

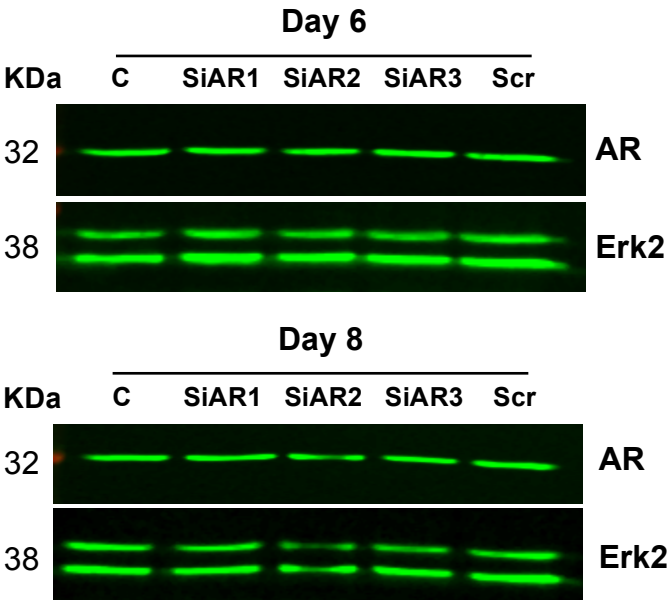

B.

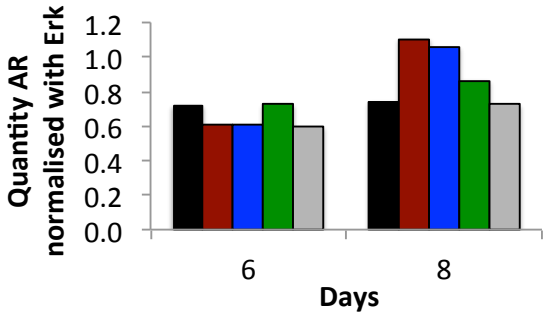

Figure 5.9 Western blot Analysis of AR protein expression after siRNA treatment strategy 3.

CHO-LB01 cells were transfected with an individual of siAR1, siAR2 and siAR3 at 100 nM or scrambled siRNA (Scr) at day 3 (Section 2.9.2). Protein samples from total cellular extraction (Section 2.4.2) at day 6 and 8 were determined by Western blot using AR (top) and Erk2 (bottom) primary antibody (Section 2.4.4) (A) and the quantity of AR expression was normalized with Erk2 (B). The bar charts represent the quantities of AR protein expression of the control (black), siAR1 transfection (red), siAR2 transfection (blue), siAR3 transfection (green) and scrambled siRNA transfection (grey).

In summary, two approaches (EBPC and siRNA) were used to examine the potential to decrease sorbitol production (via AR modulation), and hence to define the significance of metabolic redirection to CHO cell growth and productivity but only EBPC decreased sorbitol production. However, under these conditions there was no increase in antibody production. In addition, whilst increased amounts of TCA cycle intermediates were found in response to feeding regimes that were associated with increased CHO cell growth and productivity (Chapters 3 and 4), decreased sorbitol production in response to EBPC was not associated with changes to TCA cycle intermediates but high amount of pyruvate and alanine were accumulated instead. Based on these results, it can be concluded that the hypothesis that was raised in Section 5.2 was wrong. There are two possible explanations for this result. Firstly, high toxicity of EBPC might cause cell stress lead to alteration of cell growth and cell metabolism. Thus, investigation of cell stress could be performed in the future in order to confirm whether these behaviors result from toxicity of EBPC. Secondly, decreased sorbitol production resulted in more carbon atoms directly flow to the glycolysis pathway and accumulated in form of glycolysis metabolites as seen from high amount of alanine and pyruvate in the presence of EBPC. Thus it was hypothesized that combination effect of inhibit sorbitol production (to increase the flow of carbon atom from glucose) and overexpression of MDH II (to increase the flow of TCA cycle) might improve antibody yield of CHO-LB01 cells. The generation of stable CHO-LB01 cells overexpressing *Mdh2* is described in the next section.

5.4 Generation of stable CHO-LB01 cells overexpressing *Mdh2* (CHO-MDH II cells)

In addition to *Akr1b1*, *Mdh2* was a selected target gene. Overexpression of *Mdh2* was hypothesized to increase the flow of the TCA cycle lead to improve antibody yield as mentioned in Section 5.2. In this study, stable CHO-LB01 cells overexpressing *Mdh2* were generated and are referred as CHO-MDH II cells.

5.4.1 Generation of *Mdh2* construction vector and stable cell line expressing MDH II

The *Mdh2* nucleotide sequence (*Cricetulus griseus Mdh2*, accession XM_007641683.1) used in this study is shown in Figure 5.10. *Mdh2* sequences was introduced into pcDNA3.1 vector by GeneArt® Gene Synthesis (Figure 2.2) as described in Material and Methods (Section 2.11.1). The construct (MDH II + pcDNA3.1) was verified by double digestion of restriction enzymes (Figure A4.1) and sequencing (Figure A5.1).

CHO-MDH II cells were obtained by transfection of CHO-LB01 cells with MDH II + pcDNA3.1 vector, followed by limiting dilution cloning and antibiotic selection (geneticin) (Section 2.11.3). A total of 50 single-cell clones were isolated. These were subsequently scaled up to 24-well and six-well plates. Only 20 of those single-cell clones proliferated well and these were successfully expanded to 5 mL culture in minibioreactor (Section 2.2.1: small-scale cell culture). Cell growth and antibody production of 20 single-cell clones was characterized (Section 5.4.1.1). Subsequently, they were screened for MDH II expression by Western blot (Section 5.4.1.2) and PCR (Section 5.4.1.3).

```
   1 atgttgtccgccctcgcccgaccggccggcgccgctctccgccgc
     M  L  S  A  L  A  R  P  A  G  A  A  L  R  R
  46 agcttcagcacttcggcccagaacaatgctaaagtagccgtgctc
     S  F  S  T  S  A  Q  N  N  A  K  V  A  V  L
  91 ggagcatctgggggcattgggcagccccttccctcctcctgaag
     G  A  S  G  G  I  G  Q  P  L  S  L  L  L  K
 136 aacagccccctagtgagccgcctgaccctctacgatattgctcat
     N  S  P  L  V  S  R  L  T  L  Y  D  I  A  H
 181 acacctggtgtggcggcggatctgagtcacatcgagaccagagca
     T  P  G  V  A  A  D  L  S  H  I  E  T  R  A
 226 aatgtgaaaggctacctcggacctgagcagctgccagactgcctg
     N  V  K  G  Y  L  G  P  E  Q  L  P  D  C  L
 271 aaaggttgtgatgtggtggtgatcccagctggagtgcccaggaag
     K  G  C  D  V  V  V  I  P  A  G  V  P  R  K
 316 ccaggaatgacacgagatagaaacatagaaacaggctcttttaca
     P  G  M  T  R  D  R  N  I  E  T  G  S  F  T
 361 aagtacagatcacatggcatggccatcttgccttgcagatggctc
     K  Y  R  S  H  G  M  A  I  L  P  C  R  W  L
 406 acagttattgacagggcctgttgctggtctccaccctcagctgac
     T  V  I  D  R  A  C  C  W  S  P  P  S  A  D
 451 atctgtctcatggttttcccagttaactccaccatccccatcaca
     I  C  L  M  V  F  P  V  N  S  T  I  P  I  T
 496 gctgaagtttttaagaagcatggagtgtacaaccccaacaagatc
     A  E  V  F  K  K  H  G  V  Y  N  P  N  K  I
 541 ttcggtgtgacaacccttgacatcgtcagagcgaacacattcgtg
     F  G  V  T  T  L  D  I  V  R  A  N  T  F  V
 586 gcagagctgaagggtttggatccctctcgagtcaatgtgcctgtc
     A  E  L  K  G  L  D  P  S  R  V  N  V  P  V
 631 attggtggccacgctgggaagaccatcatcccattgatctctcag
     I  G  G  H  A  G  K  T  I  I  P  L  I  S  Q
 676 tgtacccccaaggttgactttccccaagaccagctgaccgcactc
     C  T  P  K  V  D  F  P  Q  D  Q  L  T  A  L
 721 accgggagaatccaggaggctggcacggaagtcgtgaaggccaag
     T  G  R  I  Q  E  A  G  T  E  V  V  K  A  K
 766 gctggagcaggttctgccactctgtccatggcttacgctggagcc
     A  G  A  G  S  A  T  L  S  M  A  Y  A  G  A
 811 cgttttgtcttctcccttgtggacgccatgaatgggaaggaaggt
     R  F  V  F  S  L  V  D  A  M  N  G  K  E  G
 856 gtcgttgagtgttcttttgttcagtccaaagagacagagtgcact
     V  V  E  C  S  F  V  Q  S  K  E  T  E  C  T
 901 tacttctccacacccttgctgttggggaaaaaaggcctggagaag
     Y  F  S  T  P  L  L  L  G  K  K  G  L  E  K
 946 aacctgggcattggcaaaatcactccttttgaggagaagatgatt
     N  L  G  I  G  K  I  T  P  F  E  E  K  M  I
 991 gccgaggccatccctgagctaaaagcctccatcaagaaaggcgag
     A  E  A  I  P  E  L  K  A  S  I  K  K  G  E
1036 gactttgtcaagaacatgaagtga 1059
     D  F  V  K  N  M  K  *
```

Figure 5.10 Malate dehydrogenase 2 (*Mdh2*) nucleotide and amino acid sequence for *Mdh2* construction vector.

Mdh2 nucleotide sequence for Mdh2 construction vector comprised of signaling sequencing (underline) to transport the protein to mitochondria and coding sequencing of *Cricetulus griseus Mdh2* (accession XM_007641683.1).

5.4.1.1 Cell culture performance of single-cell clones

The initial study of 20 single-cell clones was performed by comparing cell growth and antibody production in culture against parental cells (control). The growth of 20 single-cell clones varied (Figure 5.11). Some (clones 2, 5, 9, 10 and 12) had a growth pattern similar to that of the control. These cells reached a maximum cell density of about 1-1.2 x10^7 cells/mL at day 6 and died at day 12. A second group (clones 1, 4, 6, 8, 11, 15, 16, 20, 22, 23, 24, 25, 26, 27 and 28) died 2 or 4 days earlier than the control and/or had less viable cell density throughout the culture period.

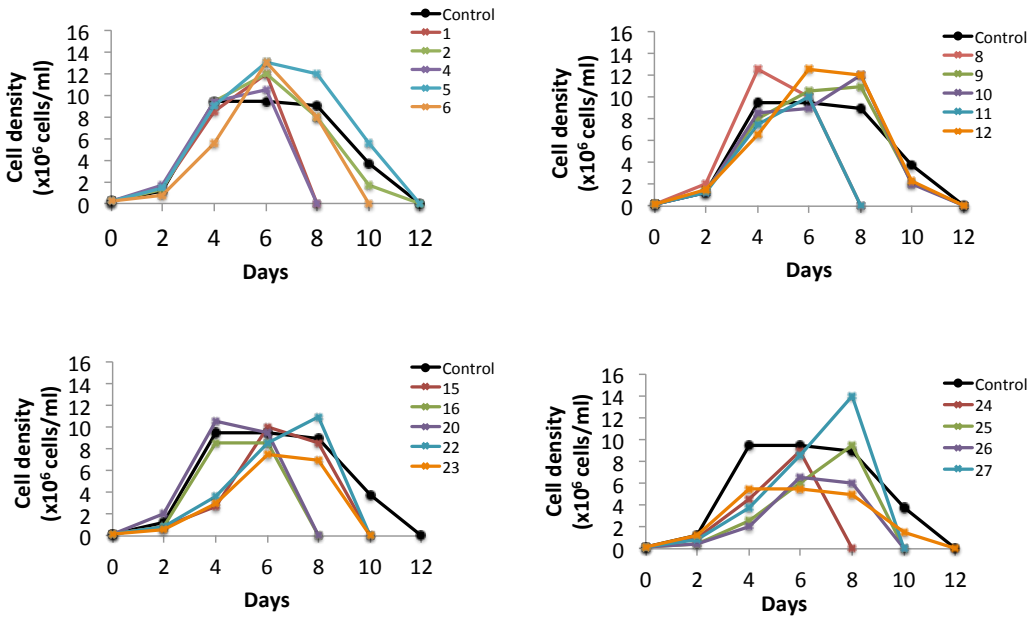

Figure 5.11 Cell growth of CHO-MDH II 20 clones.
Generation of stable cell line overexpressing MDH II was performed by transfection with *Mdh2* construction vector (Figure 2.2) into CHO-LB01 cells followed by limiting dilution and antibiotic selection (Section 2.11.3). Twenty of single-cell clones can be successfully expanded to 5 mL culture in minibioreactor (Section 2.2.1: small-scale cell culture). Medium samples were collected for cell counts (Section 2.2.2).

The panel of 20 single-cell clones exhibited a variable antibody production pattern (Figure 5.12). Clones 1, 2, 4, 5, 6, 8, 11, 15, 16, 20, 23, 24 generated amounts of antibody similar to that of the control with a maximum yield of 0.4 g/L, a value consistent with previous results (Chapter 4). A second group (clones 9, 10, 12, 25, 26, 27 and 28) produced a lower maximum yield of antibody (0.3 g/L). Clone 22 produced a higher yield of antibody than the control (between days 4 to 10). In order to select CHO-MDH II cells, investigation of MDH II protein expression of 20 single-cell clones was carried out by Western blot in the next section.

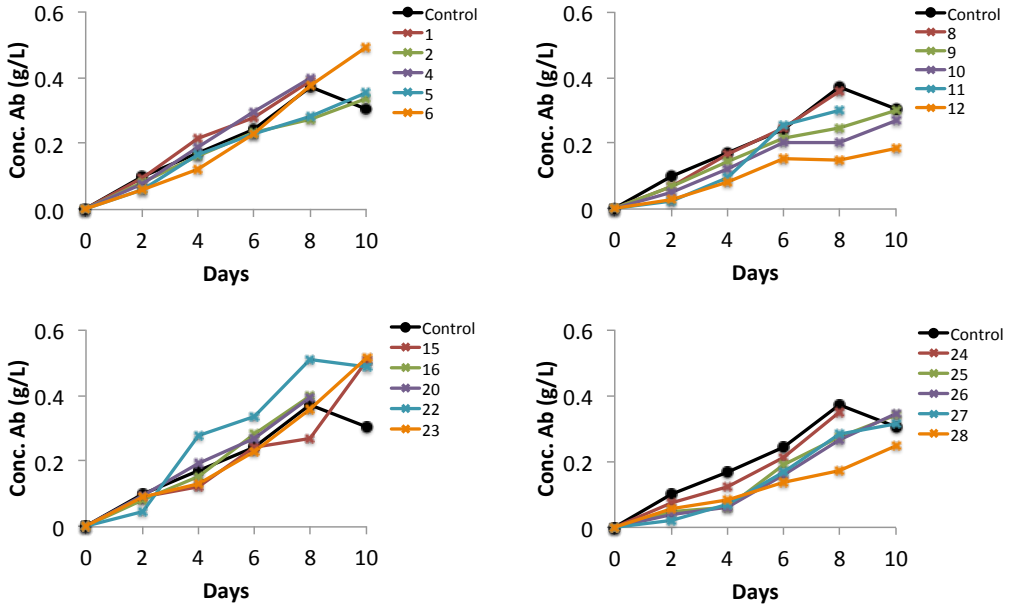

Figure 5.12 Antibody production of CHO-MDH II 20 clones.

CHO-MDH II cells were generated and cultured as described in Figure 5.11. Twenty of single-cell clones can be successfully expanded to 5 mL culture in minibioreactor (Section 2.2.1: small-scale cell culture). Medium samples were collected for ELISA (Section 2.4.1).

5.4.1.2 Detection of MDH II protein expression of 20 single-cell clones by Western blot

The 20 clones were assessed for MDH II protein by Western blot (Section 2.4.4). MDH II antibodies from three companies (Cell Signalling, SantaCruz and Abnova) were tested with control cell extracts. All three antibodies produced poor MDH II signal (Figure 5.13) with a faint band (at the correct molecular weight, 35 kDa) for the antibody from Cell Signaling (Figure 5.13A) and no signal with the antibody from SantaCruz (Figure 5.13B). With the antibody from Abnova (which Chong et al. (2010) used for detection of MDH II protein), two bands (25 and 45 kDa) were detected, neither the expected size of MDH II protein (Figure 5.13C). We decided to detect the MDH II band from 20 single-cell clones by using MDH II antibody from Cell Signaling and Abnova.

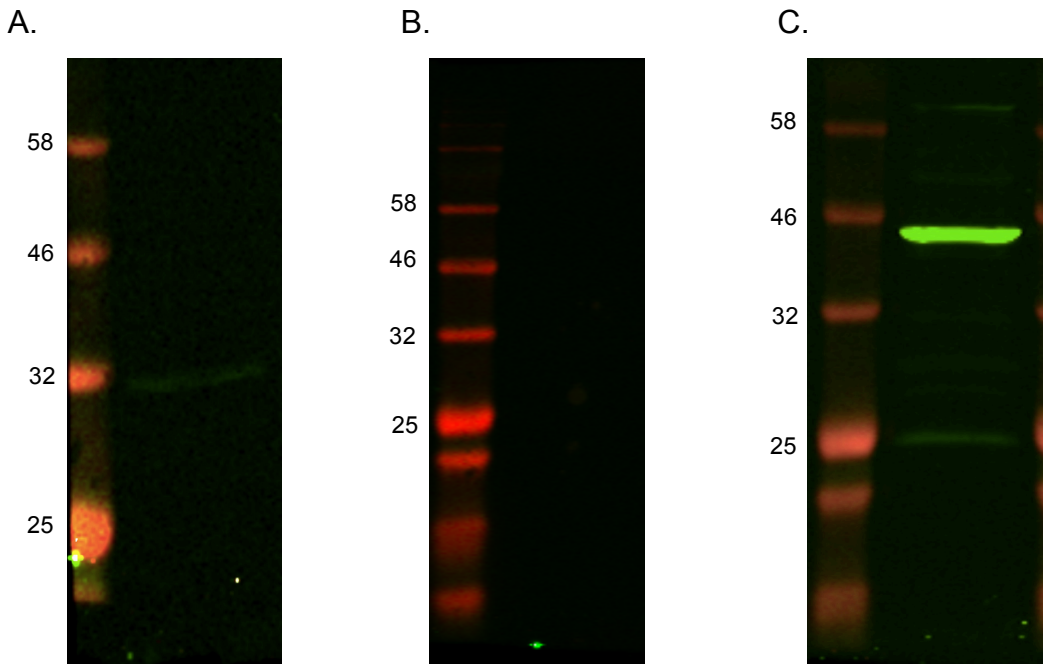

Figure 5.13 Western blot Analysis of test MDH II primary antibody from three companies.
Protein samples from total cellular extraction (Section 2.4.2) of CHO-LB01 cells cultured in CD OptiCHO medium at day 4 were determined by Western blot (Section 2.4.4) using MDH II primary antibody from three companies: Cell Signalling (A), SantaCruz (B) and Abnova (C).

The results of screening of MDH II protein expression of 20 individual clones by Western blot using MDH II antibody from Cell Signaling is shown in Figure 5.14. MDH II bands can be detected from every clone at correct molecular weight. However, the band intensity among samples cannot be clearly distinguished because of poor signal. Thus, positive clones cannot be detected by this approach.

MDH II antibody from Abnova was also used to detect MDH II expression (Figure 5.15). Every clone had almost the same intensity of top band (45 kDa) while the density of lower band (25 kDa) varied among 20 clones. No lower band was observed for clones 15, 23, 27 and 28. Although some difference of band intensity was found in this study, this cannot be used as a criteria for selection of positive clones because of the lack of certainty in specificity of the species detected by the antibody. Therefore, detection at gene expression level was examined in order to screen for recombinant MDH II expression.

A.

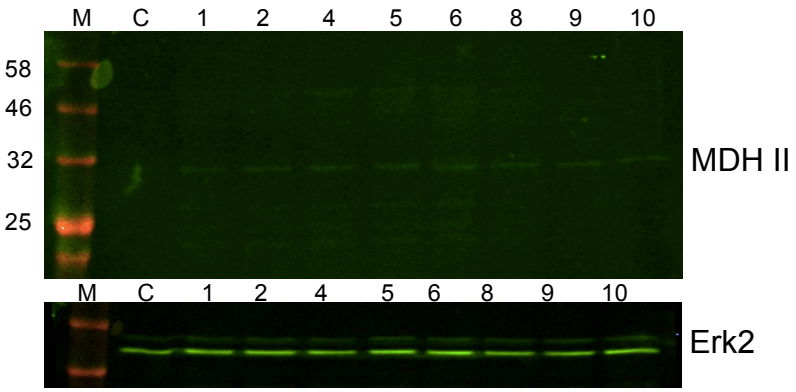

B.

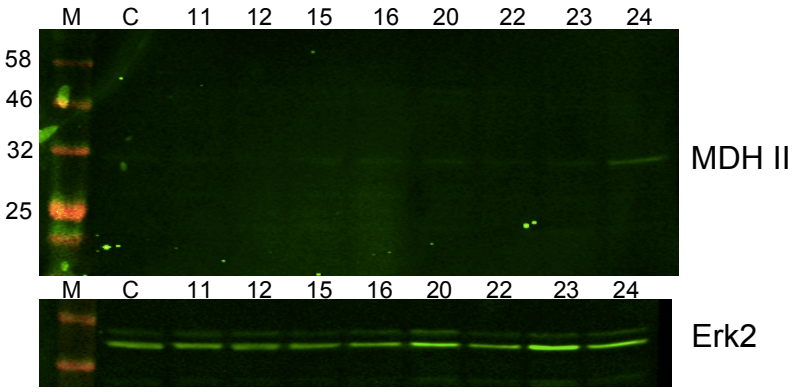

C.

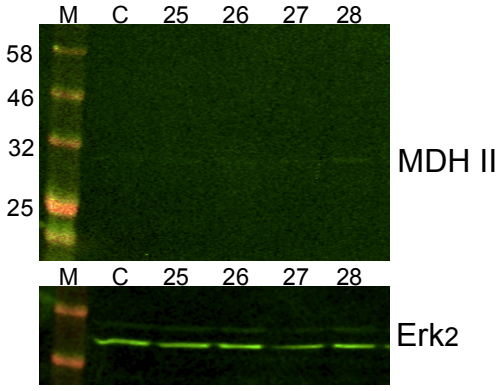

Figure 5.14 Western blot Analysis of MDH II protein expression of CHO-MDH II 20 clones by Cell Signaling antibody.

Protein samples of the control and CHO-MDH II 20 clones at day 5 were extracted as described in Figure 5.13. MDH II protein expression was determined by Western blot using MDH II primary antibody from Cell signaling (top) and compared with the expression of Erk2 protein (bottom) (Section 2.4.4). Shown are Western blot analysis of the control, clone 1, 2, 4, 5, 6, 8, 9 and 10 (A), the control, clone 11, 12, 15, 16, 20, 22, 23 and 24 (B), the control, clone 25, 26, 27 and 28 (C) (M = protein marker).

A.

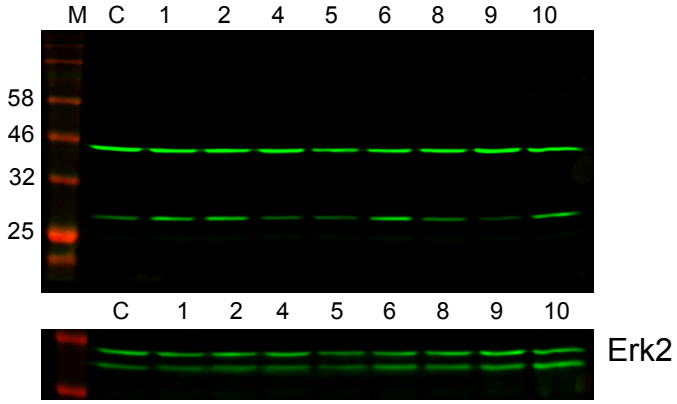

B.

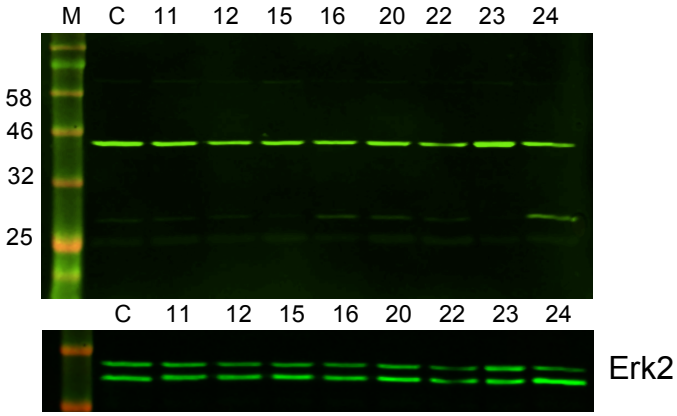

C.

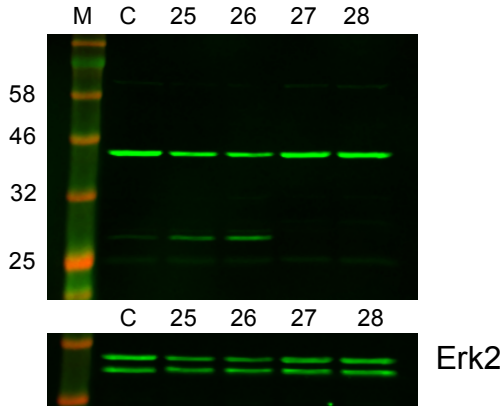

Figure 5.15 Western blot Analysis of MDH II protein expression of CHO-MDH II 20 clones by Abnova antibody.

Protein samples of the control and CHO-MDH II 20 clones at day 5 were extracted as described in Figure 5.13. MDH II protein expression was determined by Western blot using MDH II primary antibody from Abnova (top) and compared with the expression of Erk2 protein (bottom) (Section 2.4.4). Shown are Western blot analysis of the control, clone 1, 2, 4, 5, 6, 8, 9 and 10 (A), the control, clone 11, 12, 15, 16, 20, 22, 23 and 24 (B), the control, clone 25, 26, 27 and 28 (C) (M = protein marker).

5.4.1.3 Detection of *Mdh2* gene expression of 20 single-cell clones by PCR

The expression of the recombinant *Mdh2* gene in clones was examined at the nucleotide level by PCR of cDNA. Total RNA was extracted and cDNA was synthesized as described in Section 2.6.1 and 2.6.4. Subsequently, the amount of *Mdh2* gene expression was assessed by PCR of cDNA with MDH II primer set 1 (Section 2.6.5). As shown in Figure 5.16, the observed band of the control corresponded to the size of MDH II primer (636 bp) as expected. For 20 single-cell clones, all displayed a band at the same size with the control. For some clones (clones 1, 2, 8, 9, 11, 22, 27 and 28) this band intensity was greater than the control. Since *Mdh2* is an endogenous gene in CHO-LB01 cells, PCR analysis demonstrated the expression of *Mdh2* in both the control and 20 single-cells clones but differences of intensity of the band among samples was not obvious. Therefore, in this current study, detection in genomic DNA (gDNA) was required to confirm the insertion of exogenous *Mdh2* gene into CHO-LB01 genome using PCR primers that cover upstream and downstream of exogenous *Mdh2* gene (MDH II primer set 2).

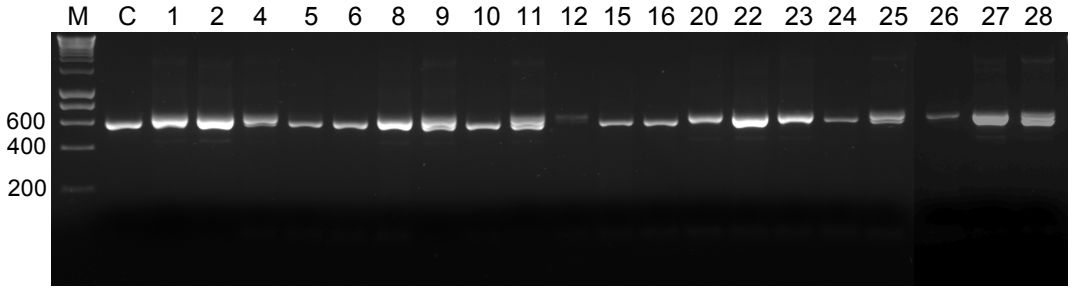

Figure 5.16 Detection of *Mdh2* expression of CHO-MDH II 20 clones by PCR.
cDNA was generated from total RNA extraction of the control and CHO-MDH II 20 clones (Section 2.6.1 and 2.6.4). PCR was performed to amplify *Mdh2* gene using primer set 1 (Section 2.6.5). The PCR products and HyperLadder™ 1kb (M) were separated by 1% (w/v) gel electrophoresis and image was taken by UV transillumination (Section 2.6.6). The PCR product size was around 636 bp.

gDNA of clones and the control cell line was extracted and was purified by phenol extraction (Section 2.7). Amplification of gDNA with MDH II primer set 2 (Section 2.6.5) and for the control, no band was observed as expected (Figure 5.18) (as MDH II-pcDNA 3.1 vector was not transfected in this cells). Twelve clones (clones 1, 2, 4, 8, 9, 11, 20, 22, 23, 24, 25 and 27) exhibited a band (1251 bp) that corresponded to the inserted recombinant sequences (Figure 5.17), results that reflect the successful transfection of MDH II-pcDNA 3.1 vector into CHO-LB01 cells. No band was observed in eight clones (clones 5, 6,10, 12, 15, 16, 26 and 28), consequently considered as negative clone. Thus, three clones that showed a band and three clones that showed no band from this result were randomly selected to serve as positive clones (clones 1, 2 and 22) and negative clones (clones 10, 15 and 16), respectively, and these six clones were selected and used for further analysis.

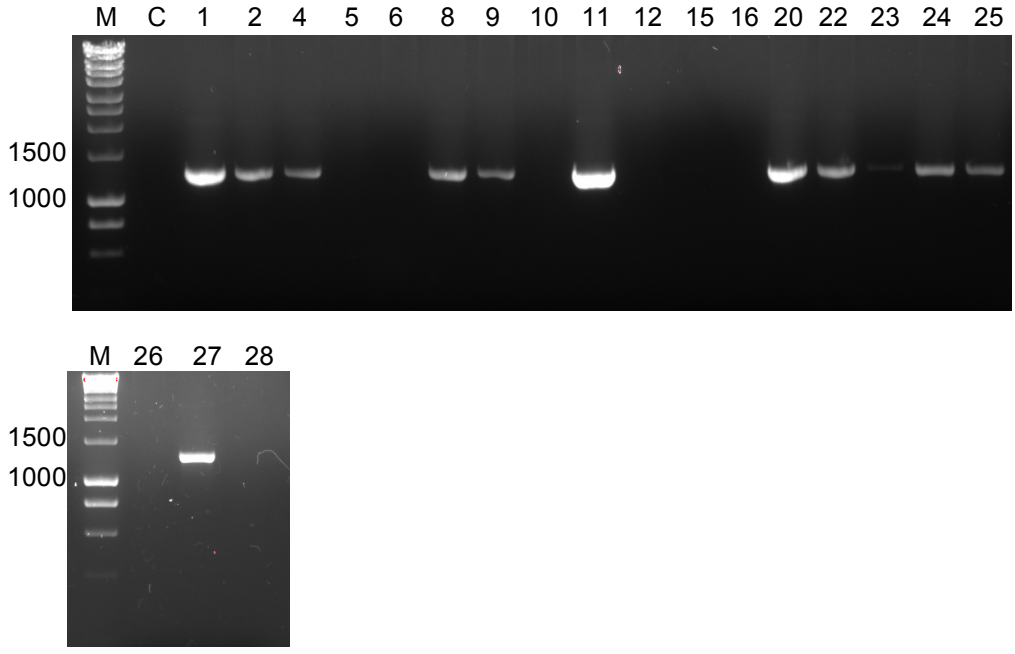

Figure 5.17 Detection of the insertion of *Mdh2* construction vector into gDNA of CHO-MDH II 20 clones by PCR.

gDNA of the control and CHO-MDH II 20 clones were extracted and purified by phenol extraction (Section 2.7). PCR was performed to amplify *Mdh2* gene using primer set 2 (Section 2.6.5). The PCR products and HyperLadder™ 1kb (M) were separated by 1% (w/v) gel electrophoresis and image was taken by UV transillumination (Section 2.6.6). The PCR product size was around 1251 bp.

In summary, CHO-MDH II clones were successfully established in this study and three positive (clones 1, 2 and 22) and three negative (clones 10, 15 and 16) clones were selected based on the insertion of exogenous *Mdh2* into gDNA of CHO-LB01 cells. However, it cannot be proven that MDH II was overexpressed in CHO-LB01 cells since overexpression of MDH II protein cannot be detected by Western blot because of poor quality of all available commercial MDH II antibodies. In spite of this, six clones were selected for use for further analysis in terms of cell culture performance and metabolite profiles.

5.4.2 Further characterization of CHO-MDH II clones

MDH II expression and cell culture performance and metabolite profiles were determined for control, positive (clones 1, 2 and 22) and negative clones (clones 10, 15 and 16). Since detection of MDH II protein expression by Western blot cannot be used as criteria to reassure overexpression of MDH II protein because of poor quality of MDH II antibody, six clones were confirmed for their exogenous *Mdh2* insertion into gDNA by PCR.

5.4.2.1 Integration of exogenous *Mdh2* gene into gDNA of six clones

To confirm the insertion of exogenous *Mdh2* gene in gDNA of six clones, PCR analysis with MDH II primer set 2 was conducted again. In addition, PCR analysis of gDNA with B2M primer (Section 2.6.5) was conducted as a positive control.

As shown in Figure 5.18A, no band for exogenous *Mdh2* was found in the control and the “negative” clones (clones 10, 15 and 16). All “positive” clones (clones 1, 2 and 22), displayed a clear band at correct size for *Mdh2* (1251 bp) as expected reflecting that exogenous *Mdh2* was inserted into gDNA of CHO-LB01 cells. PCR analysis with B2M

primer showed that both positive and negative clones including the control exhibited the band of *B2m* at correct size (1696 bp) (Figure 5.18B). This result confirmed that clone 1, 2 and 22 had integrated the exogenous gene.

A.

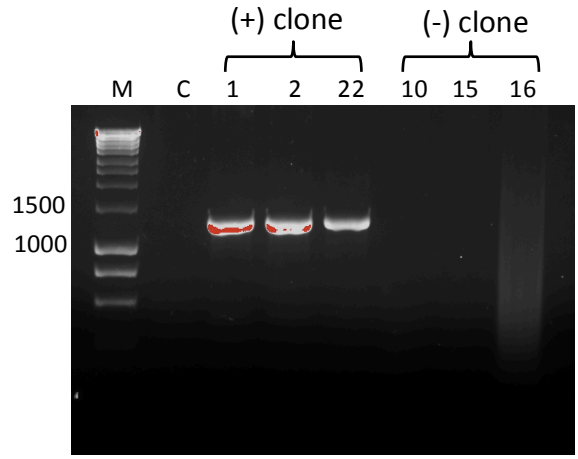

B.

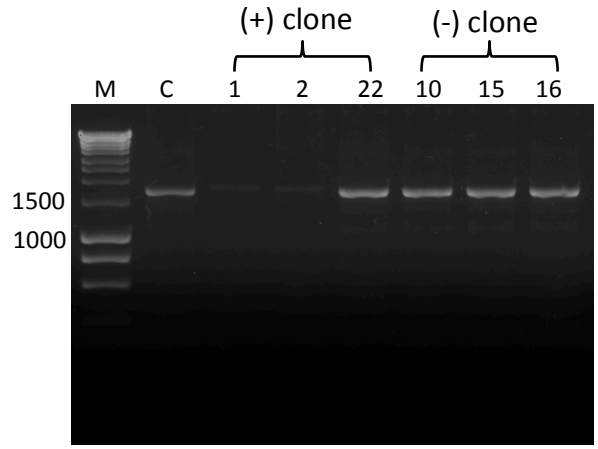

Figure 5.18 Detection of the insertion of *Mdh2* construction vector into gDNA of selected six CHO-MDH II clones by PCR.

gDNA was prepared as described in Figure 5.17. PCR was performed to amplify *Mdh2* (A) and *B2m (B)* gene using MDH II primer set 2 and B2M primer, respectively (Section 2.6.5). The PCR products and HyperLadder™ 1kb (M) were separated by 1% (w/v) gel electrophoresis and image was taken by UV transillumination (Section 2.6.6). The PCR product size of *Mdh2* and *B2m* were around 1251 and 1697 bp, respectively.

5.4.2.2 Cell culture performance

After three positive clones were confirmed to contain exogenous *Mdh2* gene, more detailed analyses were made of cell growth and antibody production for “positive” and “negative” clones and for the control.

In the control (Figure 5.19A), the pattern of cell growth and maximum viable cell density of the control was similar to that observed in previous results (Chapters 3 and 4). Cells exhibited growth with an exponential phase over the first 4 days of culture, reached maximum viable cell density about $1.2x10^7$ cells/mL at day 4 and died at day 12. The growth patterns of both positive and negative clones were different from the control (Figure 5.19A). All clones (positive or negative) reached lower viable cell density than the control during the first five days of culture and the maximum viable cell density (at day 6) was less than the control. After that point, some clones (clones 1 and 2) attained higher viable cell densities than the control until the last day of culture (day 12). Other clones (clones 22, 10, 15 and 16) had the same viable cell density as the control. This was consistent with the recent observation that MDH II overexpression in CHO DP12 cells led to decreased cell density (Wilkens and Gerdtzen, 2015). However, this is in contrast with the result obtained by Chong et al. (2010), who found improvement of viable cell number of CHO cells overexpressing MDH II.

A.

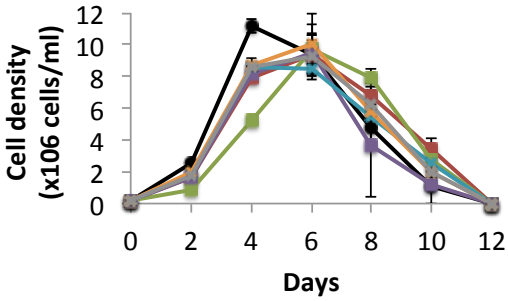

B.

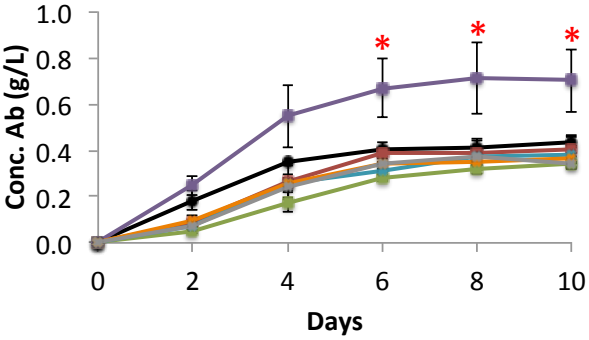

C.

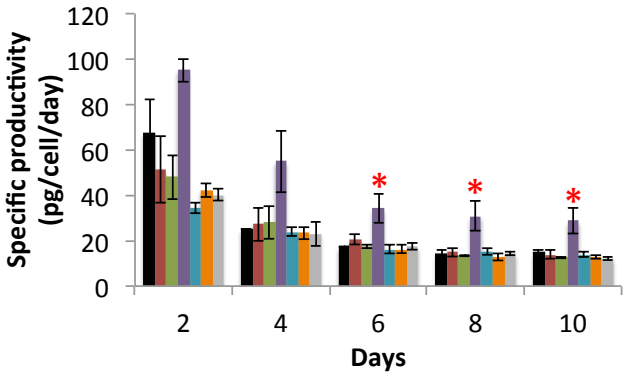

Figure 5.19 Cell growth and antibody production of six selected CHO-MDH II clones.

Viable cell density (A) antibody production (B) and specific productivity (C) were measured for the control (black), three positive CHO-MDH II clones: clone 1 (red), clone 2 (green) and clone 22 (purple) and three negative CHO-MDH II clones: clone 10 (blue), clone 15 (orange) and clone 16 (grey). Medium samples were collected for cell counts (Section 2.2.2) and ELISA (Section 2.4.1). Values presented are mean ± SEM for three replicates. * indicates significant difference from control at $p < 0.05$.

As for antibody production, similar to previous result (Chapters 3 and 4), the maximum yield of antibody from control cultures was about 0.4 g/L at day 10 (Figure 5.20B and 5.19C). All clones except for clone 22 had similar antibody production and specific productivity pattern to the control and attained the same maximum yield of antibody as the control. Over the first five days of culture less antibody accumulated than the control because of lower viable cell density (Figure 5.19B). Interestingly, clone 22 produced a significant greater yield of antibody (reaching 0.7 g/L) and specific productivity than the control during day 6 to day 10 (Figure 5.19B and 5.19C). Wilkens and Gerdtzen (2015) found significantly decreased antibody yield associated with MDH II overexpression in CHO DP12 cells. In contrast, Chong et al. (2010) reported that antibody yield of CHO cells overexpressing MDH II was increased by only 1.2 fold compared to parental cell lines.

Overall, from these results, it can be concluded that positive CHO-MDH II clones did not improved cell growth or antibody yield. The greater antibody yield of clone 22 was probably due to a result of clonal variation since other “positive” clones did not show the same behavior. However, it is noted that although insertion of exogenous *Mdh2* was detected in gDNA of positive CHO-MDH II clones, overexpression of MDH II cannot be detected at protein level. Thus, it remains difficult to conclude any effect of CHO-MDH II clones.

5.4.2.3 Metabolite profiles

To assess if transfection with MDH II changed cell metabolism, ammonia assay (Section 2.3.1.5), lactate assay (Section 2.3.1.2) and extracellular metabolite profiles by GC-MS (Section 2.3.2) were conducted for the six selected clones and the control.

The profile of ammonia production by all clones was similar to that of the control (Figure 5.20A). Ammonia was produced after day 1 of culture and reached about 3 mM by day 10. This result is consistent with previous results (Chapters 3 and 4).

Interestingly, the profile of lactate metabolism of clone 22 (which produced the greatest amount of antibody) was different form that of the control and other clones (Figure 5.20B). In the control, lactate was produced from day 1 to day 4 of culture reaching a maximum concentration about 25 mM at day 4. After that time cell cultures showed a slight consumption of lactate but the concentration of lactate remained relatively high (greater than 20 mM) until the last day of culture, as observed before (Chapters 3 and 4). All clones, except for clone 22, exhibited a lactate profile similar to that of the control but the maximum concentration of lactate was slightly lower than the control because of lower cell density. For example, clones 10, 15 and 16 produced maximum concentration of lactate about 20 mM. This type of profile contrasts to that of clone 22 where, after the lactate reached about 20 mM at day 4 of culture, the cells switched from lactate production to consumption and lactate was depleted by day 8. This pattern of lactate metabolism is consistent with the lactate profile observed for cells fed Asn, HB, Asn+Glc and HB+Glc (Chapters 3 and 4). Therefore, a more extensive extracellular metabolite profiling was performed for clone 22 (in parallel with clone 16 and the control).

A.

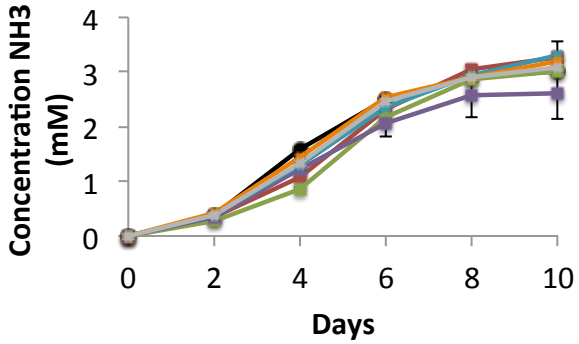

B.

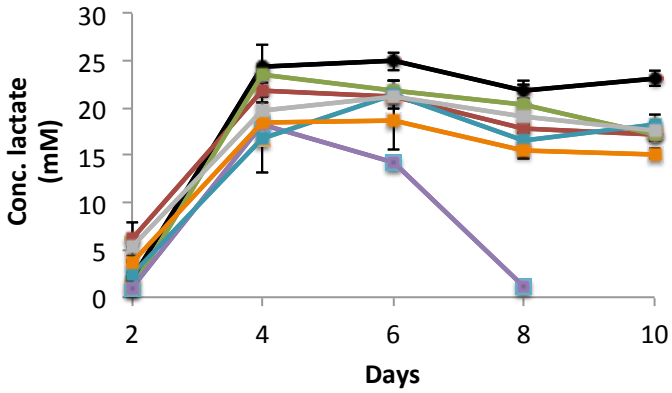

Figure 5.20 Extracellular ammonia and lactate profile of selected six CHO-MDH II clones.

Medium samples were collected from the cultures of the control and selected six CHO-MDH II clones. Ammonia (A) and lactate (B) in medium samples were determined by enzymatic assay (Section 2.3.1.5 and 2.3.1.2) throughout the culture. Values presented are mean ± SEM for three replicates.

The results of extracellular metabolite profiling by GC-MS of clones 16 and 22 are shown in Figure 5.21. In control, the amount of glucose gradually declined after day 2 and glucose was depleted after day 4. The overall profile of glucose metabolism of clones 16 and 22 was similar to the control but glucose was utilized more slowly than the control during day 2 to day 4, perhaps reflecting the lower viable cell density as observed in Section 5.4.2.2. Pyruvate was almost depleted at day 4 in the control but

the amount of pyruvate was greater than the control at day 5 in clone 16 and day 5 to day 6 in clone 22 and after that time pyruvate was exhausted. This difference in pyruvate metabolism may be associated with the slower rates of glucose consumption of clones 16 and 22. Alanine was produced during day 2 to day 4 and then was consumed until day 10 in all conditions but clones 16 and 22 generated higher amounts of alanine that the control at day 4 for clone 16 and day 4 to day 6 for clone 22. In agreement with enzymatic studies (Figure 5.19B), clone 22 exhibited use of lactate after day 4 while this behavior was not observed in clone 16 and the control. Glycerol and sorbitol were produced during culture in all conditions but clone 22 decreased the production of glycerol and sorbitol as observed in cells fed Asn, HB, Asn+Glc and HB+Glc (Chapters 3 and 4). Metabolites involved in the TCA cycle (citrate, iso-citrate, fumarate and malate) were produced during cultures in all conditions but their production was greater in clone 22. This observation corresponded with the TCA metabolite profiles determined from cells fed Asn, HB, Asn+Glc and HB+Glc (Chapters 3 and 4). In case of amino acids, asparagine, aspartate, glutamate and serine were exhausted rapidly in all cases. Clones 16 and 22 had greater amounts of almost all amino acids than the control at day 2 and day 4 corresponding to lower viable cell density of clones 16 and 22 than the control. After that stage of culture, the amount of amino acids of clone 16 was similar to the control throughout the assessment period. In contrast, clone 22 had lower amount of several amino acids (lysine, leucine, isoleucine, threonine, methionine, valine and tyrosine) than clone 16 and the control after day 6. This observation is consistent with amino acids profiles of cells fed Asn, HB, Asn+Glc and HB+Glc (Chapters 3 and 4).

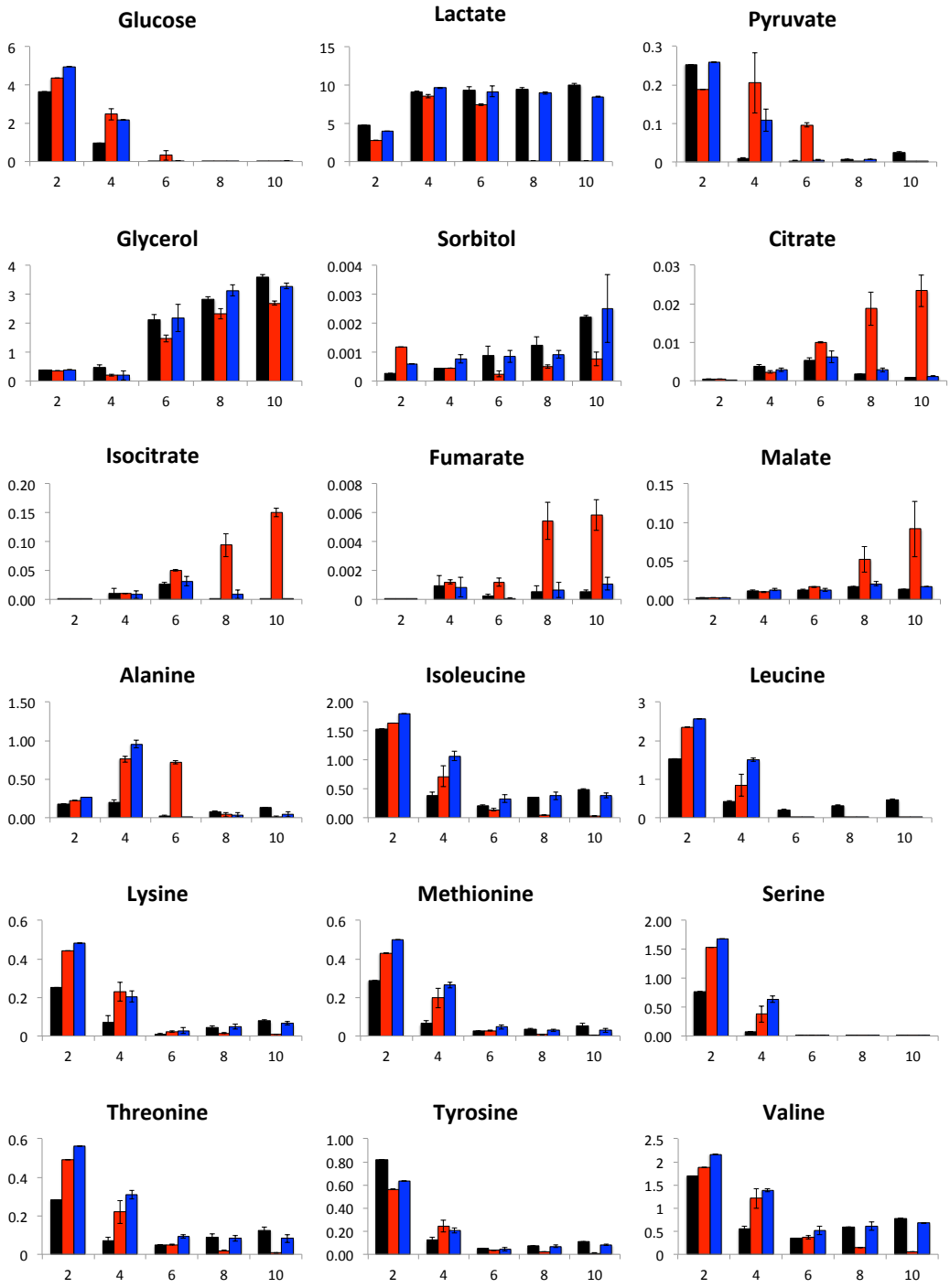

Figure 5.21 Extracellular metabolite profile of CHO-MDH II clones 22 and 16.
Medium samples were collected for extracellular metabolite profile (Section 2.3.2). The bar charts represent the quantities of each metabolite in CD OptiCHO medium comparing between the control (black), CHO-MDH II clone 22 (red) and clone 16 (blue) at day 2 (2), day 4 (4), day 6 (6), day 8 (8) and day 10 (10). Values are arbitrary units normalized to an internal standard and represent the average of three replicates with ± SEM.

Based on the result of metabolite profiles of six clones, it can be concluded that clone 22 exhibited a distinct metabolite profile to the control and another clones. Clone 22 showed less lactate, glycerol and sorbitol production, greater production of TCA metabolites and lower amounts of amino acids. This behavior is similar with the metabolite profiles of when cells were fed with Asn, HB, Asn+Glc and HB+Glc (Chapters 3 and 4). However, this effect could not be the effect of MDH II overexpression since this behavior was not found in other positive clones (clones 1 and 2).

Overall, it can be concluded that CHO-MDH II cells did not exhibit improved cell growth and antibody yield. This result is consistent with Wilkens and Gerdtzen (2015) who found decreased cell growth and protein production as a result of MDH II overexpression. In addition, introduction of MDH II into cells did not produce profound effects on metabolism. Clone 22 showed increased antibody yield, distinctive lactate metabolism and increased production of TCA cycle metabolites but this is thought to be a consequence of clonal variation rather than cell engineering. It is intriguing that clone 22, which produced greater antibody yield than control, exhibited metabolite profiles that were similar to those of cells fed Asn, HB, Asn+Glc and HB+Glc, conditions that also enable greater cell biomass or antibody yield. Thus, this result reinforces that increased TCA cycle flux and biphasic production and use of lactate presents a marker of highly productive CHO-LB01 cells. However, since overexpression of MDH II protein cannot be confirmed by Western blot, it cannot be assured that MDH II protein was overexpressed in positive CHO-MDH II cells although the insertion of exogenous *Mdh2* into gDNA was detected. The detail will be discussed in Section 5.6. Since sorbitol production was successfully decreased by EBPC inhibitor in Section 5.3 and it was hypothesized that the combination effect of decreased sorbitol production (increased more carbon atom to supply the TCA cycle) with overexpression of MDH II (increased the flow of the TCA cycle) could enhance cell growth and/or antibody yield, the combination effect on sorbitol production in CHO-MDH II cells will be investigated in next section.

5.5 The combination of CHO-MDH II clones with decreased sorbitol production

Decreased sorbitol production was obtained by use of EBPC inhibitor in Section 5.3 and CHO-MDH II clones were generated in Section 5.4. Thus, in this experiment, both positive (clones 1, 2 and 22) and negative clones (clones 10, 15 and 16) of CHO-MDH II cells and the parental cells (control) were treated with 50 μM EBPC inhibitor at day 4 and medium samples were collected in order to study cell growth (Section 5.5.1), antibody production (Section 5.5.1) and extracellular metabolite profiles by GC-MS (Section 5.5.2).

5.5.1 Cell culture performance

Without addition of EBPC inhibitor, all clones and the control reached maximum viable density about 1.2 $x10^7$-1.5 $x10^7$ cells/mL and cells died at day 10 or day 11 (Figure 5.22; solid line). These growth patterns are similar to previous results (Section 5.4). With addition of EBPC, viable cell density of all clones and the control was decreased as observed in Section 5.3 (Figure 5.22; dotted line). In this situation, some clones (clones 1, 2, 15 and 16) died earlier than the absence of EBPC.

In the absence of EBPC, the maximum antibody concentration of all clones except for clone 22 was about 0.35-0.4 g/L a value similar to the control (Figure 5.23). Clone 22 generated higher maximum antibody concentration (0.6 g/L) than other clones and the control as observed in Section 5.4.2.2. This behavior was the effect of clonal variation as mentioned in Section 5.4. In the presence of EBPC, the concentration of antibody for all clones and for the control was decreased (less than 0.35 g/L) and this was associated with a lower viable cell density. This response is similar to the result in Section 5.3.

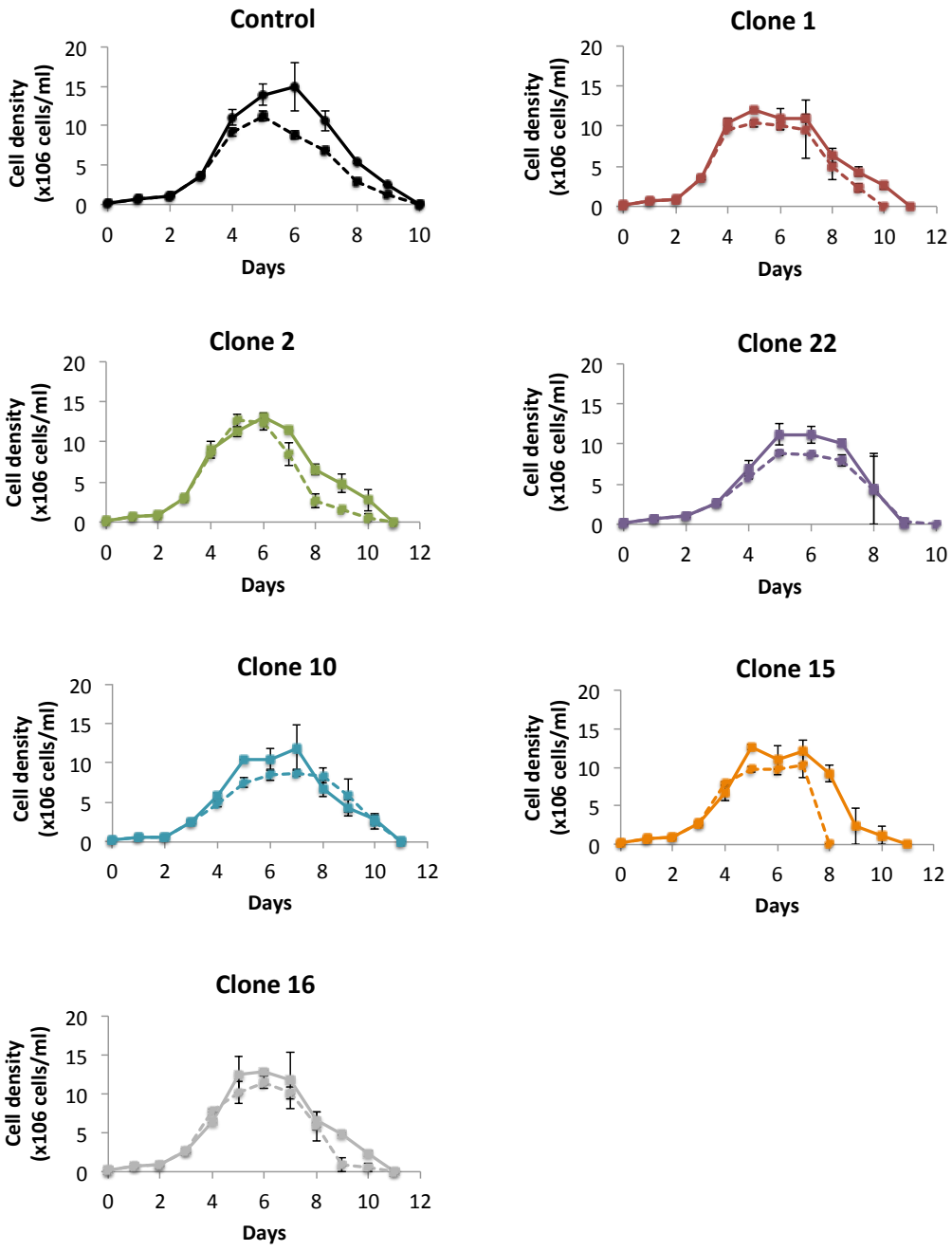

Figure 5.22 Cell growth of six selected CHO-MDH II clones addition with EBPC inhibitor.

CHO-MDH II clones were cultured in 5 mL CD OptiCHO medium in spintube and EBPC inhibitor was added into the culture at day 4 (Section 2.8). Medium samples were collected for cell counts (Section 2.2.2). Viable cell density was measured comparing between addition of EBPC inhibitor (dash line) and without addition of EBPC inhibitor (solid line) for the control (black), three positive CHO-MDH II clones: clone 1 (red), clone 2 (green) and clone 22 (purple) and three negative CHO-MDH II clones: clone 10 (blue), clone 15 (orange) and clone 16 (grey). Values presented are mean ± SEM for three replicates.

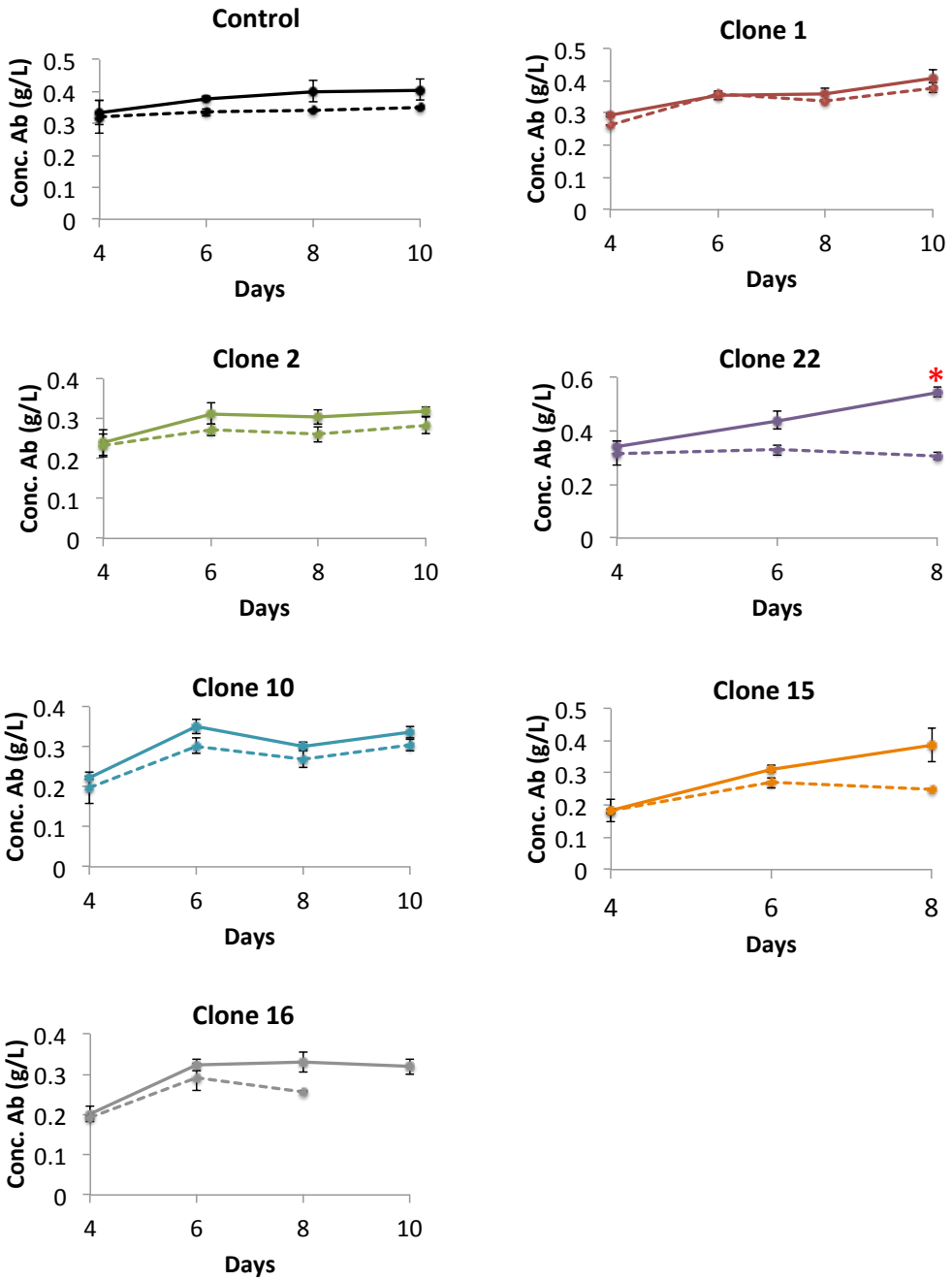

Figure 5.23 Antibody production of six selected CHO-MDH II clones addition with EBPC inhibitor.

CHO-MDH II clones were cultured as described in Figure 5.23. Medium samples were collected for ELISA (Section 2.4.1). Antibody concentration was measured comparing between addition of EBPC inhibitor (dash line) and without addition of EBPC inhibitor (solid line) for the control (black), three positive CHO-MDH II clones: clone 1 (red), clone 2 (green) and clone 22 (purple) and three negative CHO-MDH II clones: clone 10 (blue), clone 15 (orange) and clone 16 (grey). Values presented are mean ± SEM for three replicates. * indicates significant difference from control at $p < 0.05$.

In summary, it can be concluded that no improvement of cell growth and antibody yield was observed in all CHO-MDH II clones treated with EBPC. This is contrary to the hypothesis that was mentioned in Section 5.4.2.3. Next, extracellular metabolite profiling were investigated in order to confirm whether sorbitol production was decreased in the presence of EBPC and investigate the alteration of another metabolites.

5.5.2 Extracellular metabolite profiles by GC-MS

Extracellular metabolite profiling (by GC-MS, Section 2.3.2) was conducted for all six clones and the control at day 6, enabling a comparison between cells in the presence and absence of EBPC.

As shown in Figure 5.24, decreased sorbitol production was observed in all clones and the control when EBPC was added in the culture. This result re-affirmed the effect of EBPC on sorbitol production. In addition, all clones and the control treated EBPC showed decreased glycerol production. This result confirmed the side effect of EBPC addition toward glycerol production as observed in Section 5.3.1.2. No alteration of lactate profile was found in response to EBPC addition in all clones and the control. Increased amounts of pyruvate and alanine were detected in response to EBPC addition for all clones and the control (a response observed previously, Section 5.3.1.2). For metabolites of the TCA cycle, no difference was observed as a result of addition of EBPC to all clones and the control.

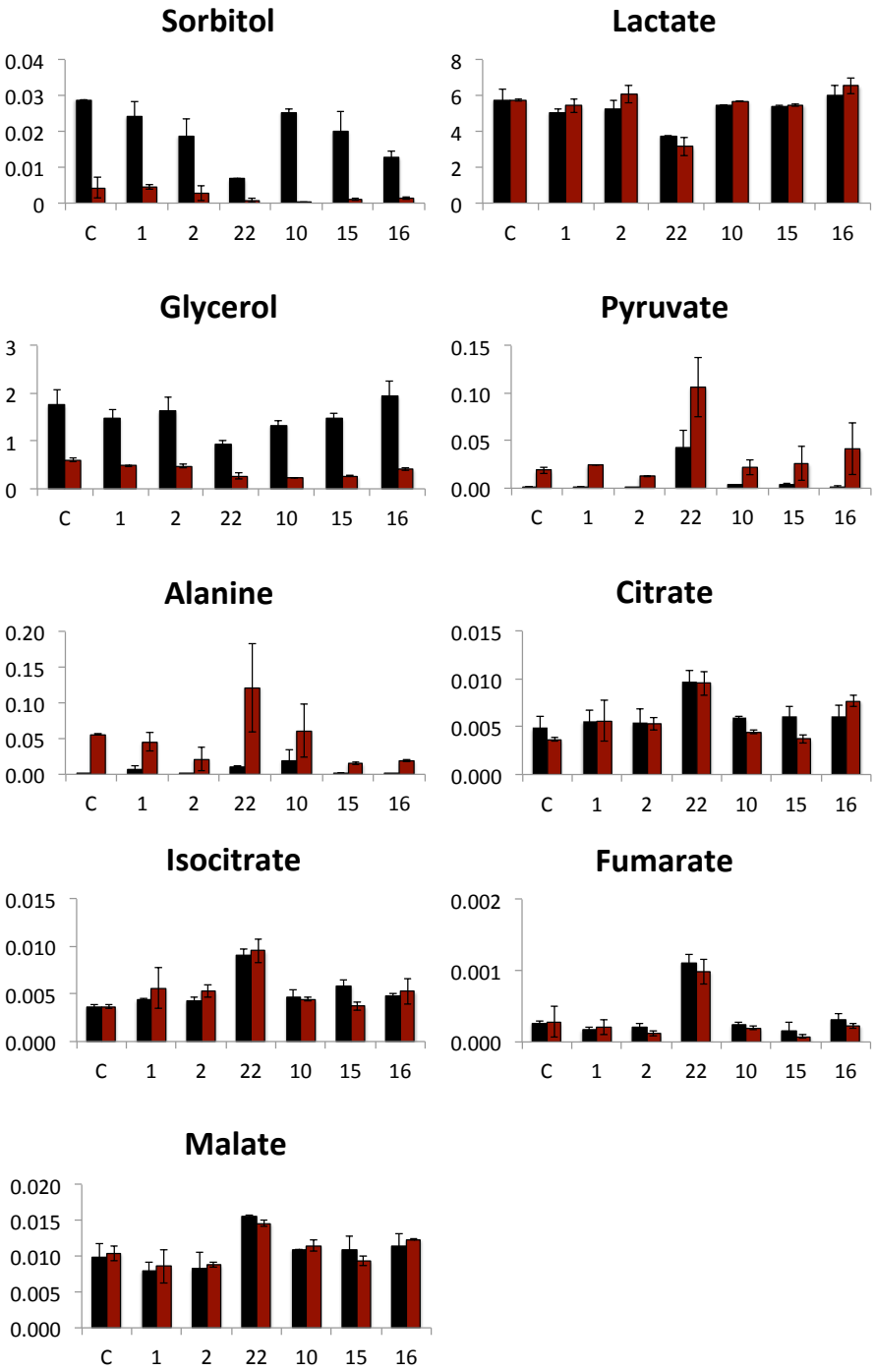

Figure 5.24 Extracellular metabolite profile of six selected CHO-MDH II clones addition with EBPC inhibitor.

CHO-MDH II clones were cultured as described in Figure 5.23. Medium samples at day 6 were collected for extracellular metabolite profile (Section 2.3.2). The bar charts represent the quantities of each metabolite in CD OptiCHO medium comparing between addition of EBPC inhibitor (red bar) and without addition of EBPC inhibitor (black bar) for the control (C), three positive CHO-MDH II clones: clone 1, 2 and 22 and three negative CHO-MDH II clones: clone 10, 15 and 16 at day 6. Values are arbitrary units normalized to an internal standard and represent the average of three replicates with ± SEM.

Overall, it can be concluded that all CHO-MDH II clones treated with EBPC generated similar cell culture performance and metabolite profiles with the control treated with EBPC. We expected that clone 22 which showed distinct metabolite profiles and high productivity could further enhance antibody yield resulted from increased the flow of TCA cycle in the presence of EBPC. However, greater amount of TCA cycle intermediate and antibody yield were not found when EBPC inhibitor was added into the culture of clone 22 but higher amount of pyruvate and alanine were detected instead. Based on this result, it is possible that PDH or PC which are the enzymes connected between glycolysis and the TCA cycle pathway might be rate limiting step enzymes. In addition, high toxicity of EBPC might be an important reason for this event as mentioned in Section 5.3.2.

5.6 Discussion

Based on the result from Chapters 3 and 4, it has been shown that greater antibody titre of CHO-LB01 cells can be achieved by nutrient supplementation. In addition, the relationship between increased the flow of TCA cycle, decreased the production of lactate, glycerol and sorbitol and enhanced antibody production was observed in cells fed HB, Asn+Glc and HB+Glc. Therefore, this chapter aimed to improve productivity of CHO-LB01 cells by cell engineering. Increased the flow of carbon atoms from glucose by decreased sorbitol production and increased the flow of TCA cycle by overexpression of MDH II was hypothezised to enhance antibody yield. There were two published data on overexpression of MDH II in CHO cells which showed conflict result. Chong et al. (2010) reported that MDH II overexpressing in CHO mAb cells increased integral viable cell number and antibody titre. On the contrary, decreased productivity of CHO DP12 cells was observed from overexpression of MDH II (Wilkens and Gerdtzen, 2015). To date, in case of AR, there has been no detail investigation of this enzyme in CHO cells.

In order to decrease sorbitol production, two approaches were undertaken: chemical reagent (EBPC inhibitor) and siRNA approach. The result showed that only EBPC inhibitor can decrease sorbitol production by inhibition the activity of AR. siRNA approach was not successful to knockdown *Akr1b1*. Perez and Ferraris (1995) reported that the half-life of AR is about six days. It can be suggested that although siRNA approach can be used to suppress the expression of *Akr1b1* but AR enzyme has long lifetime. The cells might still have enough AR to convert glucose to sorbitol resulted in no decreased sorbitol production. Although addition of EBPC can decrease sorbitol production, cell growth and antibody yield did not improve. Once sorbitol was decreased, greater amount of TCA cycle intermediates were not observed but greater accumulation of pyruvate and alanine were found. This occurrence may be due to two reasons. Firstly, high toxicity of EBPC leads to disturbance of cell growth and cell metabolism. Secondly, decreased sorbitol production resulted in more carbon atoms directly flow to the glycolysis pathway and accumulated in form of alanine and pyruvate. Thus, we hypothesized that combination effect of decreased sorbitol production by EBPC inhibitor and increased the flow of TCA cycle by overexpression of MDH II could enhance cell growth and/or antibody yield.

The result of generation of CHO-MDH II cells showed that MDHII-pcDNA3.1 vector was successfully transfected into gDNA of CHO-LB01 cells as seen the insertion of exogeneous *Mdh2* into gDNA detected by PCR. However, it cannot be said that MDH II was overexpressed in this study since overexpression of MDH II cannot be confirmed by Western blot because of poor quality of available commercial MDH II antibody. Thus, positive clones were selected based on the insertion of exogenous *Mdh2* into gDNA. Positive CHO-MDH II clones except for clone 22 exhibited no enhancement of cell growth and antibody production and no alteration of metabolite profiles. Thus, the result can be concluded into three possibilities. Firstly, MDH II protein might not be overexpressed in positive CHO-MDH II cells led to no improvement of cell growth and

antibody production or alteration of metabolite profiles. Since the effect of an inserted gene is dependent on the surrounding DNA, this gives unpredictable results (Wurm, 2004). In this case, it is possible that *Mdh2* gene might be integrated into inactive heterochromatin resulted in little or no transgene expression (Wurm, 2004) (59). Furthermore, the expression also depends on the number of transgene integrations into gDNA (gene copy number) (He et al., 2012, Kim et al., 2012) (327, 54). Secondly, exogenous *Mdh2* might be expressed but the expression was low. Repeating with increased concentration of antibiotic might improve the expression of exogenous *Mdh2* (Wurm, 2004). Finally, MDH II protein might be overexpressed but it had no effect on cell culture performance and metabolite profiles. In this case, target only one gene in metabolic pathway might not have enough effect to improve the efficiency of CHO cells for recombinant protein production. A dramatic increased in productivity may require engineering of multiple genes or pathways which coordinated interaction and all of them have to be expressed and active in a balanced way. Therefore, based on this result it cannot be summarized whether the hypothesis that was raised in Section 5.2 which is overexpression of MDH II could increase the flow of the TCA cycle lead to improve antibody production and/or cell growth of CHO-LB01 cells is true or not. In order to prove this hypothesis, it is necessary to assure that MDH II protein was overexpressed or not by Western blot. Basically, Histidine Tag antibody (His-tag) is one of the powerful antibody to detect protein target but MDH II is the enzyme located in mitochondria. Addition of His-tag to *Mdh2* might interfere the transportation to mitochondria. Thus, made to order (custom made) MDH II antibody and generation of Mdh2 construct with Histidine Tag might be tried for further study. However, expression of *Mdh2* transcript of CHO-MDH II clones and the control will be shown in next chapter (Section 6.3.1).

In case of clone 22, it was only one positive clone which showed decreased lactate, glycerol and sorbitol production and increased the production of TCA cycle metabolites led to enhance antibody yield as observed in cells fed HB, Asn+Glc and HB+Glc. This

behavior is thought to be the consequence of clonal variation rather than cell engineering. However, when EBPC was added into the culture of CHO-MDH II clones including clone 22 showed no improvement of cell growth and antibody yield were observed. In addition, metabolite profiles of CHO-MDH II treated with EBPC generated the same pattern with the control treated with EBPC. It can be concluded that neither parental cells nor CHO-MDH II clones improved productivity in the presence of EBPC.

Overall, although we cannot achieve greater product yield from inhibit sorbitol production or transfection of exogenous *Mdh2* but we unexpectedly found that among selected three positive CHO-MDH II clones only clone 22 improved antibody production and generated similar metabolite profiles with cells fed Asn, HB, Asn+Glc or HB+Glc. This finding strongly supports that increased TCA cycle flux and biphasic production and use of lactate presents a marker of highly productive CHO-LB01 cells. It is interesting to investigate the transcriptome of clone 22 compared to clone 16 (negative CHO-MDH II cell which showed different antibody yield and metabolite profiles with clone 22) in order to examine the correlation between productivity, metabolome and transcriptome. Therefore, RNA sequencing (RNA-seq) will be performed in next chapter.

CHAPTER 6

Transcriptomic profiling of high and low producing CHO-MDH II clones

6.1 Introduction

Among selected positive CHO-MDH II clones generated in the work described in Chapter 5, clone 16 exhibited metabolite profiles and antibody productivity similar to the parental cells (the control). Clone 22 was distinctly different from clone 16 and the parental cell line with enhanced antibody productivity and a change in metabolism. This was considered to be a consequence of clonal variation, rather than a result of MDH II engineering but the distinction offered the possibility via transcriptomic profiling (of clone 22, clone 16 and the control) to examine the potential correlation betweens transcriptome, metabolome and productivity of CHO cells. Several publications have reported relationships between CHO cell productivity and gene expression profiles (Section 1.4.1). Genes related to generation of energy (Clarke et al., 2011, Kang et al., 2014, Mulukutla et al., 2012, Vishwanathan et al., 2015), cell cycle (Charaniya et al., 2009), protein translation and processing (Doolan et al., 2008, Harreither et al., 2015, Nissom et al., 2006), vesicle trafficking (Clarke et al., 2011, Harreither et al., 2015) and cytoskeletal elements (Charaniya et al., 2009, Seth et al., 2007) have been identified by different groups to contribute to increased productivity of CHO cells. However, to date, little is known of correlations between transcriptome and metabolome in relation to productivity (Korke et al., 2004, Ley et al., 2015, Mulukutla et al., 2012). The cell lines generate in the current study offer the opportunity to investigate the metabolic phenotype and productivity variation between different CHO cell lines, using RNA-Seq to complement metabolite profiling data.

In this chapter, mRNA amounts for IgG heavy chain (*IgH*) gene was assessed by qPCR between clone 16, clone 22 and the control (Section 6.2). In addition, RNA-Seq was performed in order to determine the profile of expressed genes in the CHO cells used and to provide comparison between CHO-MDH II clones *vs.* the control (Section 6.3) and clone 22 *vs.* clone 16 (Section 6.4) associated with difference in metabolic profiles

and productivity. Specifically, analyses were focused on comparison of clone 22 *vs*. clone 16.

6.2 Quantification of mRNA of *IgH*

Since clone 22 produced greater antibody titre than clone 16 and the control (Chapter 5), it was hypothesized that differential expression of *IgH* gene might be the reason for this observation. *IgH* mRNA abundance was identified as an important factor in determining specific antibody production. Several studies have demonstrated a good correlation between specific antibody production and mRNA level, particularly *IgH* rather than IgG light chain (*IgL*) (O'Callaghan et al., 2010, Prashad and Mehra, 2015, Vishwanathan et al., 2015). Therefore, quantification of mRNA of *IgH* gene was performed by qPCR. RNA samples at day 4 from clone 16, clone 22 and the control were extracted (Section 2.6.1) and converted to cDNA (Section 2.6.4). Afterward, cDNA was used as a template for qPCR with IgH primers (Section 2.6.7).

Figure 6.1 illustrates the abundance of *IgH* cDNA normalized to a house keeping gene (*B2m*) for clone 16, clone 22 and the control. The mRNA quantitation for *IgH* was not significantly different between clone 16, clone 22 and the control, cell lines that had different antibody titre. This result is consistent with many papers that reported a lack of correlation between transgene transcript amount and product titre (Fann et al., 2000, Kang et al., 2014, Ley et al., 2015, Vishwanathan et al., 2015, Yu et al., 2011).

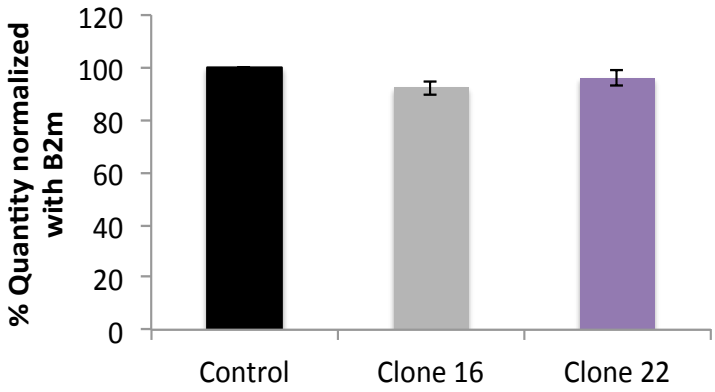

Figure 6.1 Quantity of *IgH* gene.

Cell samples from the control (black), clone 16 (grey) and clone 22 (purple) at day 4 were harvested for RNA extraction (Section 2.6.1) and cDNA synthesis (Section 2.6.4). cDNA samples were examined by qPCR (Section 2.6.7). Values from qPCR were normalised to *B2m* expression. Values presented are mean ± SEM for three biological replicates.

Overall, it can be suggested that amount of *IgH* mRNA would not be the bottleneck to increase antibody production. There are two main possible reasons to explain the different antibody yield between clone 16 and clone 22: difference in transcriptional level (Charaniya et al., 2009, Clarke et al., 2011, Doolan et al., 2008, Harreither et al., 2015, Vishwanathan et al., 2015) and difference in post-transcriptional level (translation and post-translational processes) (Kang et al., 2014, Mohan and Lee, 2010, Peng et al., 2011). Therefore, transcriptomics profiling of clone 16, clone 22 and the control will be examined in Section 6.3.

6.3 Transcriptomic analysis of differences between CHO-MDH II clones and the parental cells

To investigate transcriptome-phenotype relationships, RNA-Seq was performed on RNA isolated from two CHO-MDH II clones (clones 16 and 22) and the control, cell lines that differ in antibody titre and metabolic profiles. The global gene expression profiles might reveal the signature for high producing cells associated with metabolic or productivity differences. An overview of the RNA-Seq analysis workflow is shown in Figure 6.2. RNA samples at day 4 from clone 16, clone 22 and the control were selected for this analysis because it was the day prior metabolic shift of clone 22. RNA samples were extracted (Section 2.6.1) in duplicate and RNA-seq (Section 2.12) was performed in the Genomic Technology Core Facility (University of Manchester). The Bioinformatic Core Facility (University of Manchester) performed data preprocessing (quality assessment and trimming), alignment and differential expression analysis (normalization and identification of differential expression).

The first stage of data preprocessing was examination of raw data for quality control (QC) using the *FASTQC* program. In the second stage, adaptor sequences were removed and low quality reads were trimmed using the *Trimmomatic* program. Next, the remaining RNA-Seq reads were aligned to genomic reference sequences (CHO genome release in 2014, NCBI Accession: GCF_000419365.1) using the *STAR* program, followed by a counting step with the *HTSeq* program to determine the number of reads mapping to the reference sequence of each gene in order to produce a gene count. Afterwards, the *DESeq2* program was used to perform differential expression analysis from raw count of genes. The analysis is initiated by normalization of gene count and subsequently analyzed by *DESeq2* to estimate the log2 fold change for each gene. The p-value and false discovery rate (FDR) which defines as the percentage of genes that are identified as differentially expressed by chance were also provided. Finally, a total of 26,577 genes were obtained from RNA-Seq data analysis. Afterwards, all 26,577 genes

from annotation were submitted for Ingenuity Pathway Analysis (IPA®) program to identify canonical pathways containing these genes (Section 6.3.2).

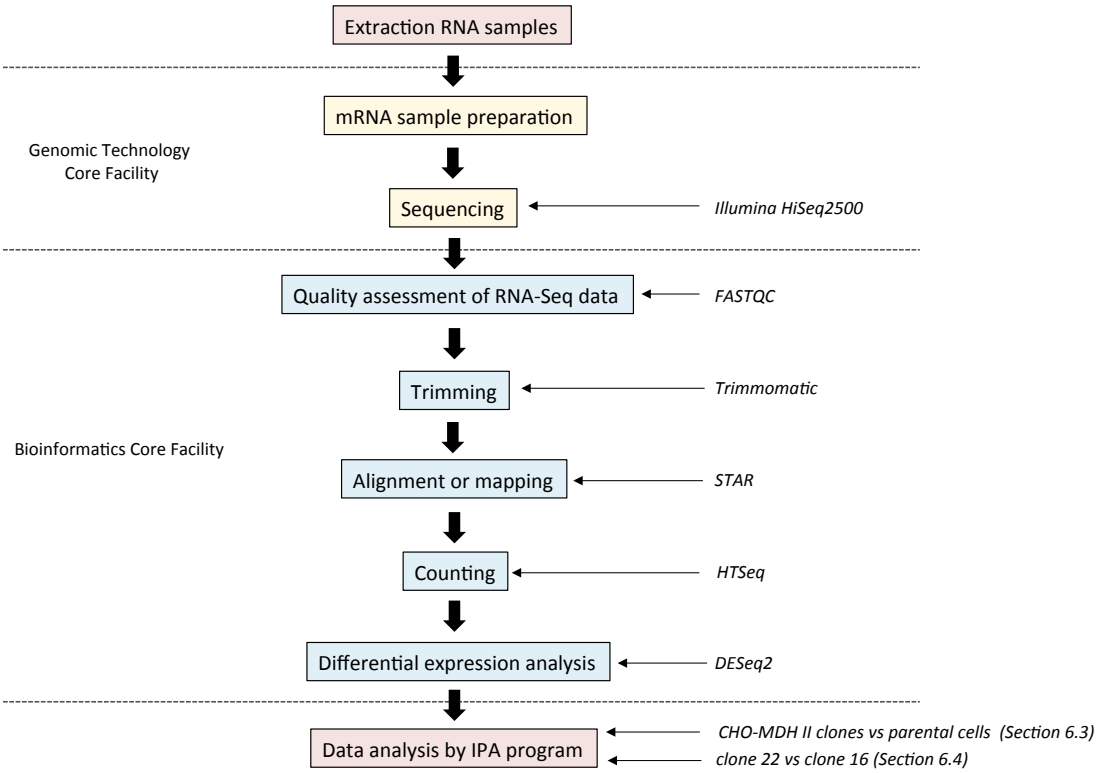

Figure 6.2 Overview of differential expression analysis stages for RNA- Seq data. The RNA-Seq approach is described in four main stages: RNA sample preparation, mRNA sample preparation and sequencing, bioinformatics analysis and data analysis by IPA® program. Italicised text highlights machine or software used in the approach.

6.3.1 Transcript level for *Mdh2* in comparison of CHO-MDH II clones and the control

CHO-MDH II clones 16 and 22 were generated by transfection of CHO-LB01 cells with MDH II construct (MDH II + pcDNA3.1) as described in a previous chapter (Section 5.4.1). Based on gene expression data from RNA-Seq, it can be seen that the abundance of *Mdh2* transcript of clones 16 and 22 was greater than the control 0.33 and 0.77 log2-fold change above the basal line of zero, respectively. This result

corresponded with the greater intensity of the *Mdh2* band detected by PCR for clone 22 (Figure 5.16). It can be suggested that the greater abundance of *Mdh2* transcript of clone 22 was the consequence of the expression of exogenous *Mdh2* or enhanced expression of endogenous *Mdh2*. However, the slightly increased expression of *Mdh2* detected in clone 16 is more likely to be a result of enhanced expression of endogenous *Mdh2* because there was no insertion of exogenous *Mdh2* into gDNA detected in clone 16 (Figure 5.18) or there was no difference in the expression of endogenous *Mdh2* between clone 16 and the control because the abundance of *Mdh2* transcript of clone 16 were not much difference from the control.

Overall, greater amount of *Mdh2* transcript of clone 22 was found in this study. However, this result cannot confirm whether MDH II was overexpressed in clone 22 as long as overexpression of MDH II protein cannot be detected.

6.3.2 A series of genes expressed in clone 16 and clone 22 exhibit a common differential pattern of expression compared to control

All 26,577 genes from annotation were submitted to IPA®. Of the 26,577 genes, only 14,714 genes mapped to the IPA® program. The remaining sequences were unidentified, untranslated regions, or had no known homology. Thus, 14,714 genes with known homology were mapped to pathways. In this analysis, genes with fold-change ≥ 1 (p-value <0.05 and FDR ≤0.05) were taken into consideration. A total of 561 and 536 genes were identified as differentially expressed genes between clone 16 *vs.* the control and clone 22 *vs*. the control, respectively. Among these genes, we found that 385 genes exhibited a common differential expression for clone 16 and clone 22 while 176 and 151 genes exhibited a unique differential expression for clone 16 and clone 22 compared to the control, respectively (Section 6.3.3).

Canonical pathways for these 385 common genes were identified by IPA®. The genes were categorized to be part of several pathways (data not shown). All canonical pathways were ranked in order of p-value indicating a significant association between a set of genes and that particular pathway. Therefore, the top 10 canonical pathways with the lowest p-value (as determined by IPA®) were examined and the list of the genes belong to 10 canonical pathway are shown in Table 6.1.

Analysis of mRNA abundances revealed a general up-regulation of genes involved in cholesterol biosynthesis, down-regulation of genes related to tRNA charging, UPR responses, serine and glycine biosynthesis, methylglyoxal degradation and isoleucine degradation and a mixture of induction and repression of genes related to cell cycle regulation, retinoate biosynthesis, phosphodiesterases and phospholipases in clones 16 and 22 comparing to the control (Table 6.1).

6.3.2.1 Cholesterol biosynthesis

IPA® identified the cholesterol biosynthesis pathway as the most significantly affected in clones 16 and 22 compared to the control. Many genes involved in the cholesterol biosynthesis pathway are differentially expressed between CHO-MDH II clones and the control. All of these are up-regulated in the range of 2.31-1.02 log2-fold change in clones 16 and 22 (Table 6.1). Cholesterol plays an essential role in cell membrane synthesis, cell growth and differentiation (Seth et al., 2005). The cholesterol content and the rate of cholesterol biosynthesis are elevated in proliferating cells (Rao, 1995).

Table 6.1 List of top ten canonical pathways of gene commonly expressed by both clones 16 and 22 compared to the control

Gene Symbol	Entrez Gene Name	Log2 fold change	
		clone 16 *vs*. control	clone 22 *vs*. control
1. Cholesterol biosynthesis			
Idi1	isopentenyl-diphosphate delta isomerase 1	2.31	2.22
Hmgcs1	3-hydroxy-3-methylglutaryl-CoA synthase 1	2.22	2.09
Acat2	acetyl-CoA acetyltransferase 2	2.09	1.97
Dhcr24	24-dehydrocholesterol reductase	1.98	1.94
Lss	lanosterol synthase	1.53	1.32
Mvd	mevalonate diphosphate decarboxylase	1.34	1.22
Msmo1	methylsterol monooxygenase 1	1.32	1.15
Nsdhl	NAD(P) dependent steroid dehydrogenase-like	1.26	1.12
Sc5d	sterol-C5-desaturase	1.16	1.08
Hmgcr	3-hydroxy-3-methylglutaryl-CoA reductase	1.12	1.10
Fdft1	farnesyl-diphosphate farnesyltransferase 1	1.10	1.07
Hsd17b7	hydroxysteroid (17-beta) dehydrogenase 7	1.09	1.05
Ebp	emopamil binding protein (sterol isomerase)	1.02	1.02
2. tRNA charging			
Sars2	seryl-tRNA synthetase 2, mitochondrial	1.35	1.20
Yars	tyrosyl-tRNA synthetase	-1.84	-1.87
Sars	seryl-tRNA synthetase	-1.60	-1.57
Nars	asparaginyl-tRNA synthetase	-1.51	-1.51
Aars	alanyl-tRNA synthetase	-1.43	-1.43
Iars	isoleucyl-tRNA synthetase	-1.32	-1.40
Mars	methionyl-tRNA synthetase	-1.21	-1.23
Tars	threonyl-tRNA synthetase	-1.21	-1.14
Gars	glycyl-tRNA synthetase	-1.11	-1.13
Lars	leucyl-tRNA synthetase	-1.10	-1.19
Cars	cysteinyl-tRNA synthetase	-1.01	-1.07
3. UPR response			
Ddit3	DNA damage inducible transcript 3	-3.31	-3.31
Cebpg	CCAAT/enhancer binding protein gamma	-1.75	-1.75
Atf4	activating transcription factor 4	-1.59	-1.62
Ern1	endoplasmic reticulum to nucleus signaling 1	-1.34	-1.40
Atf6	activating transcription factor 6	-1.16	-1.23

Table 6.1 (Cont.) List of top ten canonical pathways of gene commonly expressed by both clones 16 and 22 compared to the control

Gene Symbol	Entrez Gene Name	Log2 fold change	
		clone 16 *vs*. control	clone 22 *vs*. control
4. Serine and glycine biosynthesis			
Psat1	phosphoserine aminotransferase 1	-1.21	-1.32
Psph	phosphoserine phosphatase	-1.17	-1.13
Phgdh	phosphoglycerate dehydrogenase	-1.01	-1.01
5. Cell cycle regulation			
Ccne2	cyclin E2	1.78	1.71
Pcna	proliferating cell nuclear antigen	1.28	1.23
Ccne1	cyclin E1	1.16	1.04
Ccnd2	cyclin D2	-1.42	-1.23
6. Retinoate biosynthesis			
Adh7	alcohol dehydrogenase 7	1.66	2.17
Dhrs9	dehydrogenase/reductase (SDR family) member 9	-1.76	-1.75
7. Phosphodiesterases			
Pde2a	phosphodiesterase 2A	1.73	1.69
Pde9a	phosphodiesterase 9A	-3.31	-3.96
Pde4b	phosphodiesterase 4B	-1.52	-1.42
8. Methylglyoxal degradation			
Ldhd	lactate dehydrogenase D	-3.72	-1.63
9. Isoleucine degradation			
Bcat1	branched chain amino-acid transaminase 1	-1.13	-1.21
10. Phospholipases			
Pla2g2a	phospholipase A2 group IIA	2.15	2.79
Pla1a	phospholipase A1 member A	1.68	1.55
Plb1	phospholipase B1	-1.51	-1.49

Among thirteen genes in this category, there were four genes, *Hmgcs1*, *Dhcr24*, *Sc5d* and *Hmgcr*, which have been identified previously as differentially expressed in high producer cells. *Hmgcs1* has been reported as down-regulated gene in high producer cells (Trummer et al., 2008) while *Dhcr24* (Schaub et al., 2010) and *Sc5d* (Doolan et al., 2008) have been identified as up-regulated genes in high producer CHO cells. There was a conflicted result about the transcript level of *Hmgcr*. Schaub et al. (2010) has found down-regulation of this gene in high titre IgG producing CHO cell whereas Doolan et al. (2008) has reported up-regulation of this gene in high producer rhBMP-2 expressing CHO DUKX subclone co-expressing paired basic amino acid cleaving enzyme. However, it is quite difficult to compare previous result with current result because clone 22 which represents high producer clone exhibited the same transcript level of genes related to cholesterol biosynthesis with clone 16 which represents low producer clone. It is possible that induction of these genes indicates high demand of cholesterol of clones 16 and 22 in order to survive because clones need to be more self-sufficient than non-cloned (mixed population) which cholesterol can be obtain from other cells. Although up-regulation of cholesterol biosynthesis genes were detected in CHO-MDH II clones, they exhibited similar growth pattern with the control with slightly decreased cell density during day 1-4 (Figure 5.20).

6.3.2.2 tRNA charging

General down-regulation of genes related to aminoacyl-tRNA synthetases (ARSs) were found in clones 16 and 22 (Table 6.1). ARSs play an essential role in protein synthesis, catalyzing ligation of amino acids to their cognate tRNAs. In addition to this function, they can play a role in several biological processes including RNA processing and trafficking, apoptosis, rRNA synthesis, regulation of cellular metabolism and amino acid transport, angiogenesis and inflammation (Ko et al., 2002, Lee et al., 2004, Park et al., 2010). It has been reported that ARSs are universally expressed and their expression

levels are varied temporally in the developing mouse (Ko et al., 2002). Vishwanathan et al. (2013) found up-regulation of aminoacyl tRNA biosynthesis genes in high producer subclone which is contrary to the current result. However, there is no direct evidence explaining the reason for the down-regulation of ARSs in clones 16 and 22.

6.3.2.3 The UPR

The UPR pathway is an adaptive pathway that helps cells handle the increased load of unfolded proteins. ER stress has been reported to up-regulate the UPR pathway (Castranova et al., 2016). A down-regulation trend was observed for five genes, *Ddit3* (CHOP in Figure 6.3), *Cebpg*, *Atf4*, *Ern1* (IRE1 in Figure 6.3) and *Atf6*, involved in UPR responses for clones 16 and 22 (Table 6.1 and Figure 6.3). Such data implies that protein folding is still within the capacity of the cell and not over burdened. Additionally, it can be suggested that the selection process may select for cells that have developed cellular machineries to cope with ER stress and as a result clone 16 and clone 22 were more resistant to ER stress than the control. There was a conflict result of transcriptomic profiling of genes related to UPR pathway. Some publications have suggested a strong correlation between enhanced UPR and antibody productivity (Prashad and Mehra, 2015) and up-regulation of UPR genes have been found in subclones compared to parental cells (Doolan et al., 2008, Harreither et al., 2015). Others reported that UPR genes were unchanged when comparing high and low producer cells (Nissom et al., 2006).

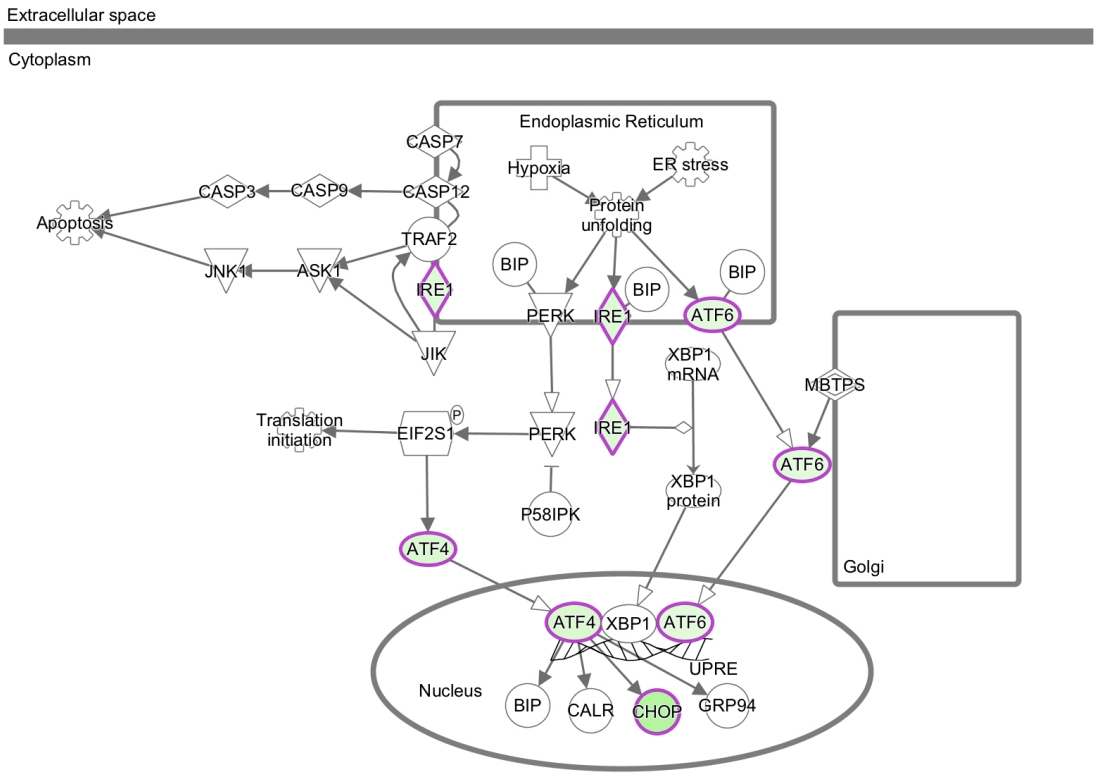

Figure 6.3 Changes in UPR signaling of CHO-MDH II clones.
Changes in gene expression are compared between CHO-MDH II clones and the control, where down-regulated genes show in green and the darker colour indicates the more downregulation. Figure was prepared in IPA®.

6.3.2.4 Serine and glycine biosynthesis

In serine and glycine biosynthesis pathway, 3-phosphoglycerate (glycolytic intermediate) is converted to serine following a four-step enzymatic reaction. Four enzymes involved in serine and glycine biosynthesis pathway: phosphoglycerate dehydrogenase (PHGDH), phosphoserine aminotransferase (PSAT1) or phosphoserine transaminase in diagram, phosphoserine phosphatase (PSPH) and serine hydroxymethyltransferase (SHMT) or glycine hydroxymethyltransferase in diagram (Figure 6.4). The result of differential expression profiles showed that the first three enzymes were repressed in clone 16 and clone 22 (Table 6.1). Down-regulation of enzymes in serine and glycine biosynthesis pathways might be link to cell proliferation because serine and glycine are

important amino acids which provides essential precursors for nucleotide biosynthesis (Amelio et al., 2014, Narkewicz et al., 1996). Jun et al. (2008) showed that expression level of human *Phgdh* transcript appeared to be up-regulated to support cellular proliferation. This report is consistent with the data presented in this thesis in which down-regulation of *Phgdh* was observed in clone 16 and clone 22 along with lower cell density than the control during day 2-4 (Figure 5.20).

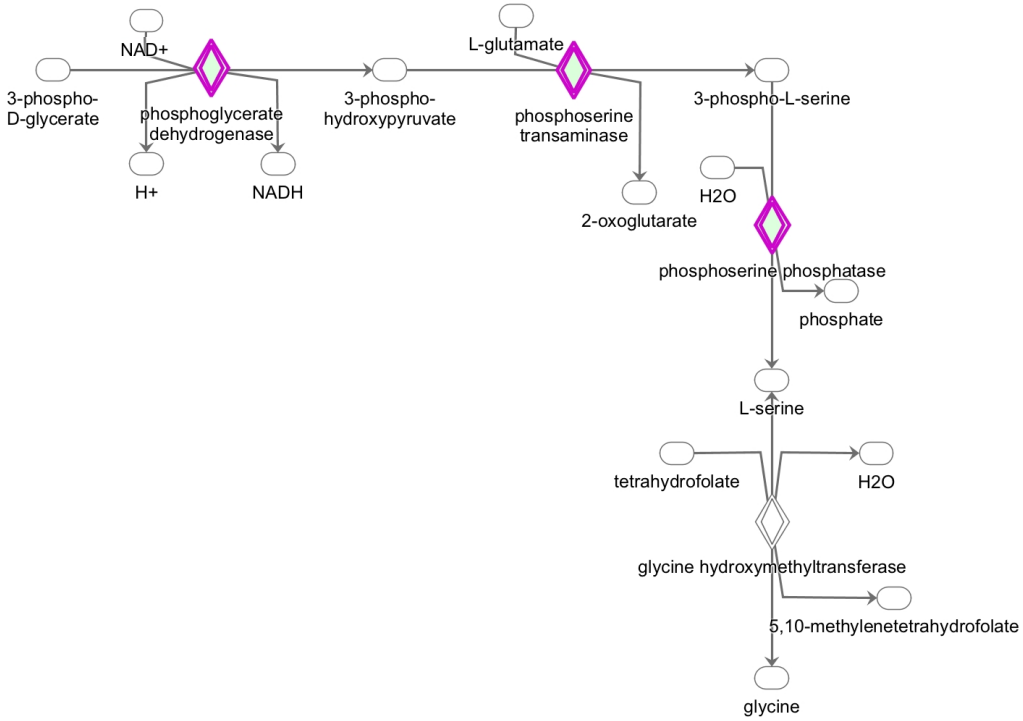

Figure 6.4 Change in serine and glycine biosynthesis pathway of CHO-MDH II clones.

Changes in gene expression are compared between CHO-MDH II clones and the control, where down-regulated genes show in green and the darker colour indicates the more downregulation. Figure was prepared in IPA®.

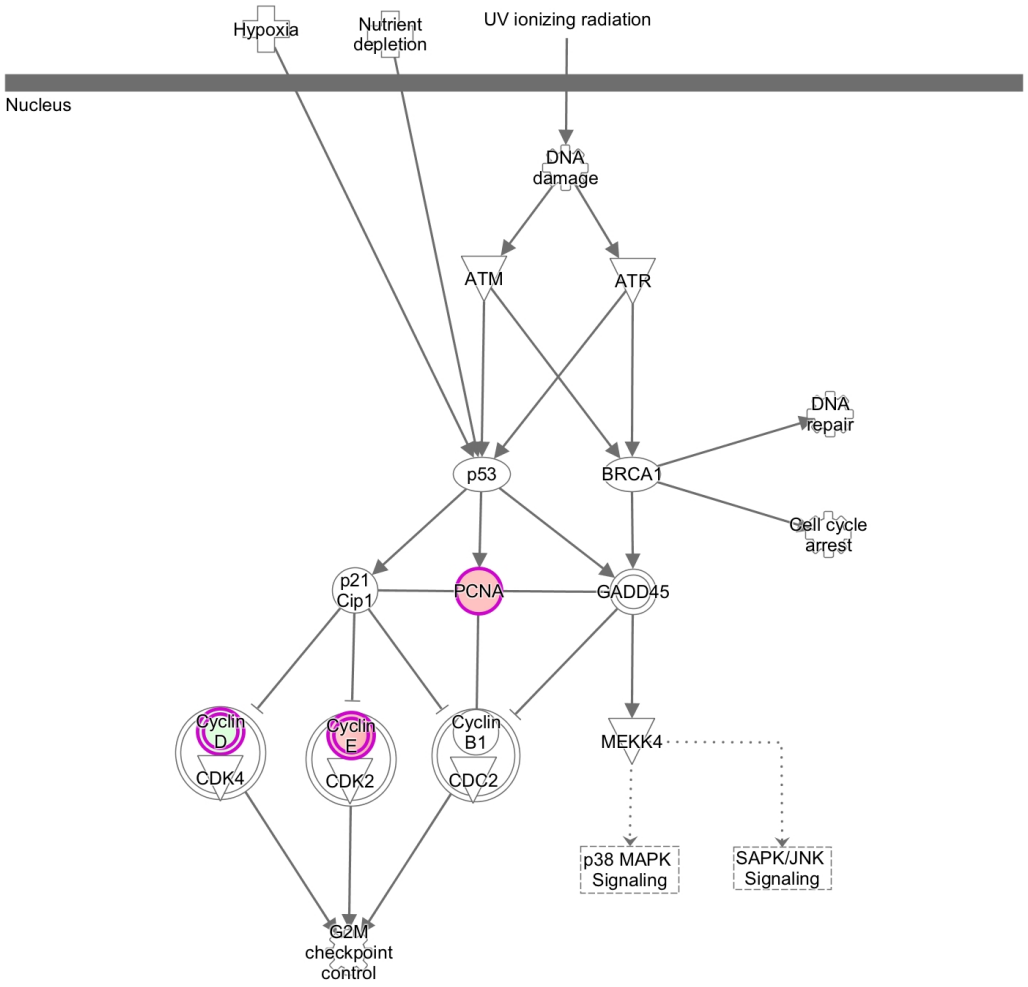

Figure 6.5 Change in cell cycle regulation of CHO-MDH II clones.
Changes in gene expression are compared between CHO-MDH II clones and the control, where up- and down-regulated genes show in red and green, respectively and the darker colour indicates the more up- and down-regulation. Figure was prepared in IPA®.

6.3.2.5 Cell cycle regulation

Cyclins are a family of proteins that control the progression of cells through the cell cycle by activating cyclin-dependent kinase (Cdk) enzymes. Cyclin D (cyclin D1, D2 and D3) and cyclin E (cyclin E1 and E2) regulate transition from G_1 to S phase. No consistent regulatory pattern was observed in transcripts related to cell cycle regulation. The expression of *Ccnd2* which encodes cyclin D2 was down-regulated while *Ccne1* and *Ccne2* which encode two homologues of cyclin E were up-regulated (Figure 6.5). This

might be because regulation of cell cycle is a homeostatic balance of many positive and negative factors. For regulatory networks involving complicated interaction of positive and negative elements, the state of the functional class may not be easily identified as up- or down-regulation (Charaniya et al., 2009, Shen et al., 2010). In addition to cyclins, *Pcna* which encode proliferating cell nuclear antigen (PCNA) was also up-regulated. PCNA is a cofactor for DNA polymerase δ in eukaryotic cells and is essential for DNA replication (Maga and Hubscher, 2003). Thus, induction of this gene is related to DNA synthesis phase of the cell cycle. Overall, the differential expression of these genes may reflect changes in growth regulation in clones 16 and 22 as seen from lower cell number than the control during day 2-4.

6.3.2.6 Retinoate biosynthesis

Adh7 and *Dhrs9* which are genes related to retinoate biosynthesis were up- and down-regulated, respectively in clones 16 and 22. *Adh7* encodes alcohol dehydrogenase 7 sigma subunit (ADH7) which is a member of the alcohol dehydrogenase family. ADH7 is inefficient in ethanol oxidation but it is involved in the metabolism of other alcohol (retinol) (Jairam and Edenberg, 2014, Kotagiri and Edenberg, 1998, Wang et al., 2014, Zgombicknight et al., 1995). Retinol is oxidized to retinal which is the precursor to retinoic acid, a signaling molecule important for cell differentiation (Jairam and Edenberg, 2014, Luo et al., 2008). *Dhrs9* encodes a member of the short-chain dehydrogenases/reductases (SDR) family. The encoded protein can perform distinct functions. It has oxidoreductase activity toward hydroxysteroids and can convert 3-α-tetrahydroprogesterone to dihydroxyprogesterone and 3-α-androstanediol to dihydroxyprogesterone in the cytoplasm. Moreover, it play a role in the biosynthesis of retinoic acid (Hu et al., 2016, Jones et al., 2007) and function as a transcriptional repressor in the nucleus (Markova et al., 2006). Although differential expression of these

genes was found between CHO-MDH II clones and the control, their relationship to cell culture performance is unclear.

6.3.2.7 Phosphodiesterases

Up-regulation of *Pde2a* and down-regulation of *Pde4a* and *Pde9a* were found in clones 16 and 22. *Pde* encodes cyclic nucleotide phosphodiesterases (PDEs) which play an important role in signal transduction by controlling the intracellular levels of cyclic nucleotides. These enzymes hydrolyze cAMP and cGMP to their respective 5' nucleoside monophosphates. PDEs consist of 11 families characterized by their substrate affinity and allosteric regulation (Sadhu et al., 1999). PDE2 hydrolyzes both cAMP and cGMP. PDE4 is a cAMP-specific PDE while PDE9 is highly specific for cGMP (Lugnier, 2006). Since PDEs can regulate various cellular functions through signal transduction, the change in transcripts of those genes could be somehow related to cell culture performance of clones 16 and 22 but the direct correlation have not yet been demonstrated.

6.3.2.8 Methylglyoxal degradation

Ldhd which encodes lactate dehydrogenase D was down-regulated in clones 16 and 22. This enzyme locates in mitochondria and involves in methylglyoxal pathway which eliminate cytotoxic methylglyoxal from glycolysis by conversion of D-lactate as a final product from methylglyoxal pathway to pyruvate in mitochondria. This enzyme has been extensively studied in *E. coli* and *Saccharomyces cerevisiae* but the role of it in mammalian cells still remains unclear.

6.3.2.9 Isoleucine degradation

Bcat1 was down-regulated in clones 16 and 22. This gene encodes cytosolic form of the enzyme branched-chain amino acid transaminase (BCATc). This enzyme catalyzes the first step in the catabolism of the branched chain amino acids leucine, isoleucine, and valine (Hutson et al., 2005). It is likely that repression of *Bcat1* could relate to change of branched-chain amino acid catabolism in clones 16 and 22. This result seems to be consistent with increased amount of leucine, isoleucine, and valine found in clones 16 and 22 at day 4 compared to the control (Figure 5.22). However, increased amount of other amino acid (such as alanine, lysine, methionine, serine and threonine) was also detected in clones 16 and 22 at day 4.

6.3.2.10 Phospholipases

Genes related to phospholipase showed a mixture of induction and repression in clones 16 and 22. *Pla1a* (phospholipase A1) and *Pla2g2a* (phospholipase A2) were induced while *Plb1* (phospholipase B1) was repressed. Phospholipases hydrolyze phospholipids into fatty acids and other lipophilic substances. There are four major classes, phospholipase A, B, C and D, distinguished by the type of reaction which they catalyze. Phospholipases may be involved in phospholipid turnover, membrane remodeling, signal transduction and apoptosis (Seth et al., 2005). However, their relationship to cell culture performance remains unclear.

Overall, it can be concluded that expression of genes related to cholesterol biosynthesis, tRNA charging, UPR responses, serine and glycine biosynthesis, cell cycle regulation, retinoate biosynthesis, phosphodiesterases, methylglyoxal degradation, isoleucine degradation and phospholipases were different between parental cells and subclones. Genes related to cholesterol biosynthesis and tRNA charging were up- and down-

regulated, respectively, in both MDH II clones comparing to the control. This implies that cells increased proliferation and decreased protein synthesis. This result is contrary to cell growth and antibody production profile of both CHO-MDH II clones which showed decreased cell density during day 2-4 (Figure 5.20A) and clone 22 also generated greater antibody titre than the control (Figure 5.20B). Moreover, there is a correlation between UPR response and tRNA charging. Han et al. (2013) reported that when ER stress is occurred, ATF4 which is a sensor to restore ER homeostasis will be activated and function to increase the expression of genes that are involved in protein synthesis such as ARSs. It implies that high expression of ATF4 could increase expression of ARSs gene. In this result, genes related to UPR response were down-regulated in clone 16 and clone 22. This was consistent with down-regulation of ARSs genes. However, these data fail to explain why clone 22 produced greater antibody yield than clone 16 when both clones displayed the same down-regulation pattern of ARSs genes. One possibility is that genes involved in ARSs might not be significant markers to identify high producer cells. Based on these results, small overlap with previous results was found. There were only four genes related to cholesterol biosynthesis pathway (Section 6.3.2.1), a group of genes related to aminoacyl tRNA biosynthesis (Section 6.3.2.2) and UPR (Section 6.3.2.3) have been reported previously as differentially expressed in high producer cells or subclones. However, our result showed mixture between consistency and inconsistency with previous results.

In this section the differences of transcriptomics profiling between parental cells and subclones was investigated. In the following section, specific genes differentially expressed in clone 16 and clone 22 compared to the control were identified in order to find out the genes that cause distinct phenotype between clones 16 and 22.

6.3.3 A series of specific genes differentially expressed in clone 16 and clone 22 compared to control

As mentioned in Section 6.3.2, a total of 561 and 536 genes were identified as differentially expressed genes between clone 16 *vs*. the control and clone 22 *vs*. the control, respectively. Besides 385 common genes between clones 16 and 22 (Section 6.3.2), 176 and 151 genes exhibited a unique differential expression for clone 16 and clone 22 compared to the control, respectively. Canonical pathways for these 176 and 151 genes were identified by IPA®. The details of top ten pathways are shown in Table 6.2 and 6.3 for unique genes of clone 16 and clone 22 compared to the control, respectively.

The result showed that most of specific genes of clone 16 and clone 22 were genes related to cell signaling pathways. There was no overlap gene with previous publications that have been reported to relate to clonal difference or high producer cells. In addition, no direct role for these genes in regulating protein synthesis or metabolism has yet been demonstrated. Therefore, based on this result, it can be suggested that distinct phenotype of both clones might result from direct or indirectly change of genes related to cell signaling pathways. However, in order to narrow down the marker genes related to high productivity and metabolic change, direct comparison of gene expression profiles between clones 16 and 22 will be undertaken in next section (Section 6.4).

Table 6.2 List of top 10 canonical pathways of unique genes differentially expressed between clone 16 and the control

Gene Symbol	Entrez Gene Name	Log2 fold change
1. Hepatic Cholestasis		
Adcy7	adenylate cyclase 7	-2.43
Insr	insulin receptor	-1.09
Lif	leukemia inhibitory factor	-1.08
Hnf4a	hepatocyte nuclear factor 4, alpha	-1.06
2. Role of Macrophages, Fibroblasts and Endothelial Cells in Rheumatoid Arthritis		
Figf	c-fos induced growth factor (vascular endothelial growth factor D)	1.79
Fn1	fibronectin 1	1.37
Pik3cg	phosphatidylinositol-4,5-bisphosphate 3-kinase catalytic subunit gamma	-1.72
Plch2	phospholipase C eta 2	-1.21
Sfrp4	secreted frizzled-related protein 4	-1.01
3. Hepatic Fibrosis / Hepatic Stellate Cell Activation		
Col6a3	collagen, type VI, alpha 3	2.61
Flt1	fms related tyrosine kinase 1	-1.63
Col11a2	collagen, type XI, alpha 2	-1.35
4. Axonal Guidance Signaling		
Figf	c-fos induced growth factor (vascular endothelial growth factor D)	1.79
Ngf	nerve growth factor (beta polypeptide)	1.16
Sema3e	semaphorin 3E	-1.25
Adamts6	ADAM metallopeptidase with thrombospondin type 1 motif 6	-1.09
Farp2	FERM, ARH/RhoGEF and pleckstrin domain protein 2	-1.05
Brcc3	BRCA1/BRCA2-containing complex subunit 3	-1.03
5. PPAR Signaling		
Fos	FBJ murine osteosarcoma viral oncogene homolog	-1.21
Insr	insulin receptor	-1.09
6. IL-Signaling		
Il1rapl2	interleukin 1 receptor accessory protein like 2	3.16
Il1rl1	interleukin 1 receptor like 1	1.45

Table 6.2 (Cont.) List of top 10 canonical pathways of unique genes differentially expressed between clone 16 and the control

Gene Symbol	Entrez Gene Name	Log2 fold change
7. p38 MAPK Signaling		
Map4k1	mitogen-activated protein kinase kinase kinase kinase 1	-1.12
Dusp10	dual specificity phosphatase 10	-1.03
8. Ephrin Receptor Signaling		
Sh2d3c	SH2 domain containing 3C	1.20
Ephb4	EPH receptor B4	-1.19
Epha2	EPH receptor A2	-1.12
9. Relaxin Signaling		
Pde1b	phosphodiesterase 1B	1.14
10. p53 Signaling		
Thbs1	thrombospodin 1	-1.17
Bbc3	BCL2 binding component 3	-1.12
Dram1	DNA damange regulated autophagy modulator 1	-1.05

Table 6.3 List of top 10 canonical pathways of unique genes differentially expressed between clone 22 and the control

Gene Symbol	Entrez Gene Name	Log2 fold change
1. IL-8 Signaling		
Vcam1	vascular cell adhesion molecule 1	1.88
Flt1	FMS-related tyrosine kinase 1	-3.13
Eif4ebp1	eukaryotic translation initiation factor 4E binding protein 1	-1.10
2. Choline Biosynthesis III		
Pcyt1b	phosphate cytidylyltransferase 1, choline, beta	1.01
Gpld1	glycosylphosphatidylinositol specific phospholipase D1	-1.06
3. HMGB1 Signaling		
Il17d	interleukin 17D	1.25
Lif	leukemia inhibitory factor	-1.13
4. ErbB Signaling		
Ereg	epiregulin	-1.68
Fos	FBJ murine osteosarcoma viral oncogene homolog	-1.32
Hbegf	heparin-binding EGF-like growth factor	-1.03
5. TGF-β Signaling		
Irf7	interferon regulatory factor 7	1.37
Smad9	SMAD family member 9	1.00
6. Nitric Oxide Signaling in the Cardiovascular System		
Pde1c	phosphodiesterase 1C	4.25
Chrm1	cholinergic receptor, muscarinic 1	1.72
Flt1	FMS-related tyrosine kinase 1	-3.13
7. Granulocyte Adhesion and Diapedesis		
Ccl17	chemokine (C-C motif) ligand 17	1.43
Cxcl3	chemokine (C-X-C motif) ligand 3	-1.67
Cldn6	claudin 6	-1.04
8. Creatine-phosphate Biosynthesis		
Ckmt1b	creatine kinase, mitochondrial 1B	1.13

Table 6.3 (Cont.) List of top 10 canonical pathways of unique genes differentially expressed between clone 22 and the control

Gene Symbol	Entrez Gene Name	Log2 fold change
9. Tetrapyrrole Biosynthesis II		
Uros	uroporphyrinogen III synthase	-1.00
10. Gαs Signaling		
Chrm3	cholinergic receptor, muscarinic 3	2.55
Ryr3	ryanodine receptor 3	1.83
Chrm1	cholinergic receptor, muscarinic 1	1.72

6.4 Transcriptomics analysis of differences between clone 16 and clone 22

In addition to comparing differential gene expression between two CHO-MDH II clones and the control (Section 6.3), data from RNA-seq was also used in a direct comparison between two CHO-MDH II clones (clone 16 and clone 12) to examine potential relationships between differences in productivity and metabolism at a clonal level. In this analysis, the same differential expression analysis raw data used in Section 6.3 was analyzed by IPA® to identify differentially expressed genes for clones 16 and 22.

The IPA® program identified a total of 27 genes with fold change ≥ 0.5, p-value <0.05 and FDR ≤0.05 as a cut-off. In previous analysis (Section 6.3), fold change > 1 was used for analysis but in this analysis we screened genes that had fold change ≥ 0.5 for two reasons. Firstly, if a fold change ≥ 1 was applied as threshold, a number of differentially expressed genes were too few (9 genes) for analysis. Secondly, change of phenotype might occur through a multitude of subtle changes rather than a small number of large changes (Dietmair et al., 2012b, Seth et al., 2007, Vishwanathan et al., 2014). Although genes with fold change ≥ 0.5 were taken into consideration, the number of differentially expressed genes identified between clone 22 and 16 was still relatively small (27 genes). Canonical pathways of 27 genes identified by IPA® appeared to fall in

three main categories: cytoskeleton-related element (9 genes), cell signaling (12 genes) and others (6 genes) as shown in Table 6.4.

Table 6.4 List of 27 differentially expressed genes between clone 22 and clone 16 identified by IPA®

Gene Symbol	Entrez Gene Name	Log2 fold change
1. Cytoskeleton-related element		
Vcam1	vascular cell adhesion molecule 1	2.52
Ctgf	connective tissue growth factor	0.86
Mapre3	microtubule-associated protein, RP/EB family, member 3	0.68
Lmo7	LIM domain 7	0.64
Actr3	ARP3 actin-related protein 3 homolog	0.54
Col6a3	collagen type VI alpha 3	-2.11
Flt1	FMS-related tyrosine kinase 1	-1.51
Fn1	fibronectin 1	-1.04
Kras	Kirsten rat sarcoma viral oncogene homolog	-0.59
2. Cell signaling		
Pde1c	phosphodiesterase 1C, calmodulin-dependent 70kDa	3.55
Nrg1	neuregulin 1	1.80
Chrm1	cholinergic receptor, muscarinic 1	1.60
Tspan7	tetraspanin 7	0.99
Nedd9	neural precursor cell expressed, developmentally down-regulated 9	0.85
Dusp4	dual specificity phosphatase 4	0.71
Lpar6	lysophosphatidic acid receptor 6	0.78
Pla2g2a	phospholipase A2, group IIA (platelets, synovial)	0.64
Flnc	filamin C, gamma	-3.70
Ereg	epiregulin	-0.70
Itpr2	inositol 1,4,5-trisphosphate receptor	-0.63
Flot1	flotillin 1	-0.56
3. Others		
Mlxipl	MLX Interacting Protein-Like	1.58
Ckmt1b	creatine kinase, mitochondrial 1B	0.57
Phldb3	Pleckstrin Homology-Like Domain, Family B	0.53
Cmas	cytidine monophosphate N-acetylneuraminic acid synthetase	-0.66
Etnk1	ethanolamine kinase 1	-0.63
Atp6v0a2	ATPase, H+ Transporting, Lysosomal V0 Subunit A2	-0.60

6.4.1. Cytoskeleton-related element

Nine genes related to cytoskeleton-related element were identified as differential expressed genes between clone 22 and clone 16. Five genes were up-regulated and four genes were down-regulated (Table 6.4).

The most up-regulated gene was *Vcam1* which was up-regulated with 2.519 log2 fold change. This gene encodes vascular cell adhesion molecule 1 which functions as cell adhesion molecule mediated leukocyte-endothelial cell adhesion and signal transduction. The most down-regulated gene was *Col6a3* which showed down-regulation with 2.11 log2 fold change. *Col6a3* encodes the alpha-3 chain, one of the three alpha chains of type VI collagen which acts as cell-binding protein. Another up- and down-regulated genes in this group were altered in rang of 0.5-1.5 log2 fold change. Among nine genes related to cytoskeleton element, only one gene, *Fn1*, has been identified previously as differentially expressed in high producer CHO DUXB11 cells (Vishwanathan et al., 2014). *Fn1* is involved in cell adhesion, migration process and protein processing.

However, no direct role is known for these genes in regulation of protein synthesis or metabolism but it has been observed previously that the change in cytoskeletal elements might be related to vesicle trafficking and protein secretion (Charaniya et al., 2009). In addition, genes linked to cytoskeleton function might play an essential role in various functions such as maintaining cell shape, exocytosis, endocytosis, mitosis and cell motility (Charaniya et al., 2009). Several researchers have also reported the change of expression of cytoskeleton element genes with increased specific productivity (Kantardjieff et al., 2010, Yee et al., 2008, Yee et al., 2009).

6.4.2 Cell signaling

Fifteen expressed differentially between clones 22 and 16 were involved in cell signaling pathways. Nine genes were up-regulated and six genes were down-regulated (Table 6.4).

Pde1c was the most up-regulated gene in this category with 3.55 log2 fold change. This gene belongs to G-protein couple receptor signaling. It is a member of PDE1 family that is stimulated by calcium-calmodulin complex. *Pde1c* encodes phosphodiesterase 1C which catalyzes hydrolysis of the cyclic nucleotide cAMP and cGMP which act as intracellular second messengers involved in many important physiological process such as gene transcription, cell proliferation and sugar and lipid metabolism (Rasmussen and Goodman, 1977). Since up-regulation of *Pde1c* might link to change the level of cyclic nucleotide which are key regulators of many cellular functions, it is quite difficult to define which pathways were changed in response to phenotype change of clone 22. It has been reported that *Pde1c* level was decreased in all conditions that inhibited cell proliferation in smooth muscle cells (Dolci et al., 2006) and increased cAMP level appeared to inhibit cell growth in CHO cells (Spence et al., 1995). However, it is likely that this observation is inconsistent with our result because up-regulation of this gene was found in clone 22 but clone 22 and 16 exhibited similar growth pattern. It is possible that up-regulation of *Pde1c* might be an adaptive responses to increase in intracellular cAMP levels (Spence et al., 1997).

Nrg1 was the second most up-regulated gene (1.799 log2 fold change). The protein encoded by this gene is a membrane glycoprotein that mediates cell-cell signaling. It is interacts with ERBB3 and ERBB4 tyrosine kinase receptor and plays an important role in the growth and development of multiple organ systems (Talmage, 2008) but the direct role of this gene in regulating protein metabolism or metabolic shift has not yet been demonstrated.

The most down-regulated gene in this category was *Flnc* which was down-regulated 3.704 log2 fold change. *Flnc* encodes Filamin C which is muscle-specific filamin. Filamin C may be involved in reorganizing the actin cytoskeleton in response to signaling events (Zhou et al., 2010). However, this gene does not seem to be directly related to change of phenotype of clone 22. Another genes in this category were up- and downregulated in range between 0.5-1.5 log2 fold change.

There were two genes in this in category, *Itpr2* and *Dusp4*, which have been found down- and up-regulated in high producer cells, respectively (Kang et al., 2014, Seth et al., 2007). *Itpr2* encodes a receptor protein for inositol 1,4,5-triphosphate which is a second messenger that mediates the release of intracellular calcium. Inositol triphosphate receptor-mediated signaling is involved in cell migration, cell division, smooth muscle contraction, and neuronal signaling. *Dusp4* which encodes dual specificity phosphatase 4 is a member of the mitogen-activated protein (MAP) kinase family which involves in the regulation of phosphorylation-mediated signaling. It acts as a critical signal for regulation of cell proliferation and differentiation.

It can be concluded that several differentially expressed transcripts between clones 16 and 22 were involved in cell signaling pathways suggesting a direct or indirect correlation between those biological functions and high productivity. Signaling molecules belong to the cascade of processes which a signal interacts with a receptor causing a change in a second messenger or other downstream target, and eventually affecting a change in the functioning of the cell (Seth et al., 2007). In addition, beyond the regulation at the transcriptional level, many cell signaling pathways are also altered at post-translational level (Shen et al., 2010). Although change of genes related to cell signaling pathway might impact phenotype of the cells, this might not cause significance to differences between high and low productive clones.

6.4.3 Others

In addition to genes related to cytoskeleton element and cell signaling, there were another seven uncategorized genes that differentially expressed between clone 22 and clone 16 as shown in Table 6.4.

MLX interacting protein-like (*Mlxipl*) or carbohydrate response element binding protein (*ChREBP*), which is a leucine zipper transcription factor, was up-regulated with 1.58 log2-fold change in clone 22. This protein mediates activation of several regulatory enzymes of glycolysis and lipogenesis including L-type pyruvate kinase, acetyl CoA carboxylase and fatty acid synthase. Overexpression of *Mlxipl* in primary cultured hepatocytes resulted in increased transcription activity of L-PK gene in response to high glucose (Kawaguchi et al., 2001). It is possible that up-regulation of this gene lead to increase the activity of glycolysis and biosynthesis of fatty acid pathway. As a result, the cells obtain high energy production for protein synthesis. However, change of expression of genes related to glycolysis and fatty acid pathway did not observe in clone 22 comparing to clone 16.

Among seven genes in this group, two genes have been reported to be associated with metabolic phenotype and high production in NS0 cells. The first gene was *Phldb3* which was upregulated with 0.53 log2 fold change in clone 22. This gene encodes pleckstrin homology-like domain, family B. This protein is a downstream transcriptional target activated by p53. It suppresses the activity of AKT1 signaling pathway. AKT1 is known to regulate glycolysis (via multiple posttranscriptional mechanisms including glucose transporter 1 surface localization, stimulation of hexokinase activity, and posttranscriptional regulation of phosphofructokinase 1 expression) (Rathmell et al., 2003) and several cellular functions including cell growth, apoptosis and survival (Song et al., 2005) . *Phlda3* has been found to have high expression in the lactate consumption

phase of mouse myeloma cell line (NS0) culture (Mulukutla et al., 2012). Mulukutla et al. (2012) suggested that AKT1 signaling plays an important role in lactate consumption and lactate consumption is a consequence of decreased glycolytic flux. Thus, it can be concluded that up-regulation of *Phldb3* led to suppress the activity of glycolysis by suppression AKT1 activity resulted in lactate consumption. However, change of AKT1 transcript was not found in clone 22. The second gene was Atp6v0a2 which encodes ATPase, H+ transporting, lysosomal V0 subunit A2. It is an enzyme transporter that functions to acidify intracellular compartments in eukaryotic cells. This gene was down-regulated with 0.6 log2 fold change in clone 22. This result is inconsistent with the report of Seth et al. (2007) who found up-regulation of this gene in high producer NS0 cells.

Overall, it can be seen that the number of differentially expressed genes between clone 22 and clone 16 were much smaller than when clone 22 or clone 16 compared to the control. It is possible that clone 22 and clone 16 were generated from the same process through transfection of the control with MDH II construction vector and were selected by limiting dilution and antibiotic selection step (Chapter 5) resulted in a relatively similar transcriptional profile. Although both clones had a relatively similar transcript profile, they still showed distinct metabolic and productivity characteristics. This finding suggests the possibility that high productivity and/or metabolic change do not require large changes at the transcripts level. This result seem to be consistent with Korke et al. (2004) who found very small number of differentially expressed genes (around 1.2% for cDNA microarray and 0.5% for Affymetrix gene chip) between mAb-producing hybridoma cells in high lactate/glucose steady state and low lactate/glucose steady state.

Based on overall transcript profiles, it can be concluded that the majority of differentially expressed genes between clone 22 and clone 16 analyzed by IPA® software could be categorised into two main functional groups: cytoskeleton-related elements and cell signaling. These two gene sub-types might have direct or indirect roles in regulation of antibody synthesis or metabolic pathways related to high production and metabolic shift

of clone 22. However, the relationship of changes of those genes detected by differential expression analysis and phenotype alteration of clone 22 remains unclear. Since decreased lactate production and increased extent of TCA cycle intermediates was a property that was found in clone 22, it was expected that there might be alteration in expression of genes related to lactate metabolism, TCA cycle, or redox shuttle in clone 22. Unexpectedly, no alteration of lactate dehydrogenase A or lactate dehydrogenase B which directly involves in L-lactate metabolism were found. In addition, the alteration of genes related to redox shuttle (malate-aspartate shuttle and glycerol phosphate shuttle) and TCA cycle that might directly related to change in metabolism of clone 22 were not found in this study. Moreover, differential expression of genes related to protein processing that might be key genes for increased productivity of clone 22 was also not found although many papers have reported correlations between induction of protein processing genes and high productive cells (O'Callaghan et al., 2010, Clarke et al., 2011, Doolan et al., 2008, Harreither et al., 2015, Nissom et al., 2006). It is possible that the scale of difference in productivity might affect the transcripts profiling (detail in Section 6.5). In addition, increased productivity and metabolic shift of clone 22 might not clearly impact at the transcriptome level and these may instead be affected at other levels (e.g. the proteome) since this behavior is a combined effect of both biochemical events at reaction level and gene expression at transcription and translation level (Korke et al., 2004). In addition, many researchers have shown that there were proteins detected as differentially expressed at protein level but not at transcript (Clarke et al., 2011, Ley et al., 2015, Nissom et al., 2006, Seth et al., 2007). This will be discussed in the next section.

6.5 Discussion

Based on the result in Chapter 5 that clone 22 possessed different metabolite profile (decreased lactate production and increased amount of TCA cycle intermediates) and produced greater antibody titre than clone 16 and the control. This Chapter focused on investigating the correlation between transcriptome, metabolome and productivity of CHO cells by using two CHO-MDH II clones, clone 16 and clone 22, as models. It was hypothesized that difference in transcript amounts offer a potential route to understand the metabolic phenotype and productivity variations. Thus, transcriptomics profiling of clone 16, clone 22 and the control at day 4 were investigated by RNA-Seq approaches. Specifically, analyses were focused on comparison of clone 16 and clone 22.

Differentially expressed genes between CHO-MDH II clones and parental cells were genes related to cholesterol biosynthesis, tRNA charging, UPR responses, serine and glycine biosynthesis, cell cycle regulation, retinoate biosynthesis, phosphodiesterases, methylglyoxal degradation, isoleucine degradation and phospholipases (Section 6.3.2). Change of genes involved in cholesterol biosynthesis (Section 6.3.2.1), tRNA charging (Section 6.3.2.2) and UPR (Section 6.3.2.3) have been identified in other studies to be associated with high productive cell or difference between parental cells and subclones but there were inconsistency of results among previous results. Therefore, in this case, it is impossible to conclude that our results are consistent or inconsistent with previous results. These variations are probably due to biological variation of cells, difference in cell culture condition or time point of samples.

The comparison of transcriptomics profiling between clones 22 and 16 showed that the majority of differentially expressed genes between clones 22 and 16 were in two main groups related to cytoskeleton element and cell signaling (Section 6.4). Thus, it can be concluded that different expression in cell signaling or cytoskeleton element found in this

result might be directly or indirectly effect translational machinery or metabolic pathways lead to increase antibody production and alteration of metabolic profiles of clone 22. However, it should be note that these findings do not clearly explain the occurrence in clone 22. In addition, there were a little overlap of genes (5 out of 27 genes) related to high productivity or metabolic alteration between this study and previous studies (Figure 6.6, indicated by *). Many researchers have reported that differential expression of genes, especially genes related to protein translation and processing, could affect productivity variation between cells (O'Callaghan et al., 2010, Clarke et al., 2011, Doolan et al., 2008, Harreither et al., 2015, Nissom et al., 2006). In addition, a general trend of down-regulation of genes related to glycolysis, pentose phosphate pathway and TCA cycle was observed in lactate consumption state of mouse myeloma cells (Korke et al., 2004, Mulukutla et al., 2012) whereas transcript levels of oxidative phosphorylation subunits was upregulated in lactate consumption state (Mulukutla et al., 2012). However, the difference in genes related to protein translation and processing, glycolysis and TCA cycle were not found between clones 22 and 16.

All in all, it seems to be that the results of transcriptomic profiles in this study do not clearly explain why clone 22 exhibited enhanced productivity and different metabolism with clone 16 and the control. There are three possible explanations for this finding. Firstly, it is possible that the scale of difference in productivity between clones 16 and 22 (1.75 times greater in antibody production) might not generate sufficient impact toward transcripts profile (Carinhas et al., 2013). Several research have compared cells which exhibited markedly difference in productivity about three-fold (Harreither et al., 2015), five-fold (Charaniya et al., 2009, Schaub et al., 2010) or 25-fold (Ley et al., 2015). In addition, Koke et al. (2002) suggested that small change in metabolism might not involve in alteration of gene expression profiles.

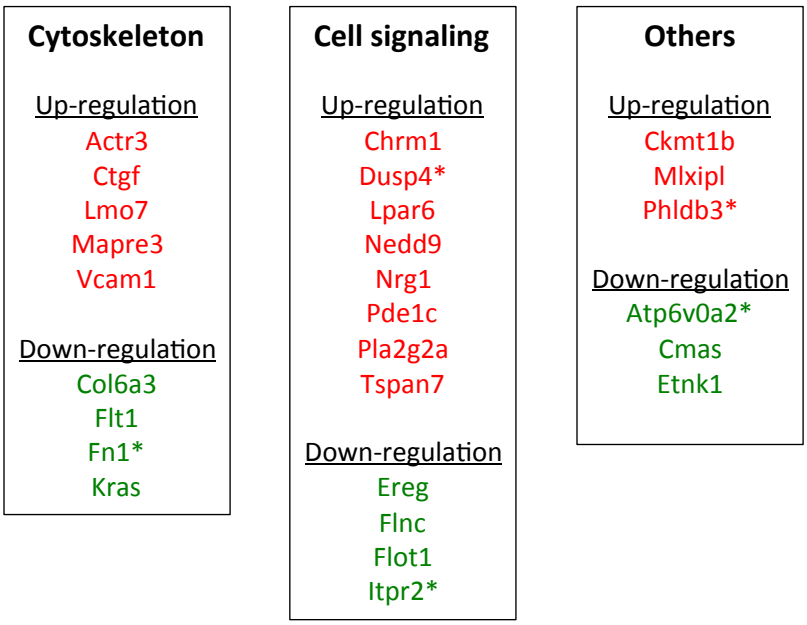

Figure 6.6 Differentially expressed genes between clone 22 and 16
Summarization of list of up-regulated (red) and down-regulated (green) genes of clone 22 compared with clone 16 (data from Table 6.4). The genes which have been reported in previous publication were indicated (*).

Secondly, it has been suggested that variation of productivity might not impacted at the transcriptome level but these may instead be affected at protein level (Clarke et al., 2011, Ley et al., 2015, Nissom et al., 2006) and using only a single omics technique might provide a limited perspective of the cellular machinery (Dietmair et al., 2012b). Nissom et al. (2006) and Seth et al. (2007) found that there were proteins detected as differentially expressed at protein level but not at transcript level. Ley et al. (2015) suggested that the bottleneck of recombinant protein production might be the step downstream of transcription including translation, translocation, protein folding, glycosylation and protein transport. Furthermore, protein synthesis rate might also be the maker for productivity determinant (Fomina-Yadlin et al., 2015). Thus, it would be interested to investigate proteomic profiles or protein synthesis rate of clone 22 and 16 to provide complementary sets of information for completely understanding of transcripts, protein and metabolite profiles of high productive cells. Finally, since we do not precisely know the time when genes will be expressed in response to intrinsic

programs lead to phenotype change and the transcripts levels change dynamically during culture process (Bort et al., 2012, Vishwanathan et al., 2014, Schaub et al., 2010), selection time point of samples is one of an important issue for experimental success. Therefore, RNA-Seq at a series of time points would be required in the future (Chapter 7). This could generate clearer correlation between genotype and phenotype change than using the sample at one time point.

In addition, based on an experience of data analysis of RNA-Seq data, there appear to be a number of limitations. Firstly, analyzing and interpreting the RNA-Seq data are substantially complex and there are multiple open source tools for analysis. It requires bioinformatics experience and it is a profound work. Although there are a number of software tools which are able to analyze and visualize transcriptomic data, the biological significance of overrepresented networks is often unclear. Secondly, one of the drawbacks of transcriptomic analysis is the selection of an appropriate threshold. The list of differentially expressed genes depends on the stringency of the statistical threshold used. More stringent criteria imply a lower risk of false positive genes but might obtain too few genes for analysis and might provide inconsistent comparison with studies on similar biological systems. Additionally, high stringency might prevent the identification of small change but phenotype significant differences. Finally, the case which a single gene may have multiple functions, which may not all be known, can make the difficult interpretation of the results.

Overall, despite clearly understanding the relationship between transcriptomic and metabolic profile of high productive clone was not obtained in this study but this experiment provides a great opportunity to learn a novel very powerful technology for transcriptomics study like RNA-Seq. The overall idea and experience attained from this study can be adapted for further work as mentioned previously.

CHAPTER 7

Discussion

7.1 Overall discussion

The results in this thesis have been presented in four chapters and the detailed discussions have been made at the end of each chapter. It was hypothesized that increased TCA cycle flux and related metabolism will enhance the growth and/or productivity of CHO cells. Therefore, the overall aim of this thesis was to clarify these relationships in recombinant CHO cells to improve the efficiency of CHO cells for recombinant protein production by optimization of nutrient feeding and cell engineering.

In order to achieve the aim, first of all, cell culture performance and metabolite profile of CHO-LB01 cells in CD OptiCHO^{TM} medium supplemented with five nutrients (Asn, Asp, Glu, Py and HB) based on the work of Sellick et al. (2011) and Donamaria (2012) was examined to understand the relationship between nutrient feeding on cell culture performance and metabolite profiles of CHO-LB cells (Chapter 3). Addition of Asn or HB improved cell culture performance and affected general metabolite profiles (decreased amount of lactate, glycerol, sorbitol and amino acids and increased amount TCA cycle intermediates). Therefore, glucose and some amino acids (leucine, isoleucine, tyrosine and valine) which were almost depleted in stationary phase were supplemented with cells fed Asn or HB in order to further enhance antibody titre by prolong stationary phase (Chapter 4). Improvement of growth and antibody yield were found in cells supplemented with Asn+Glc and HB+Glc. Addition of glucose with Asn or HB can provide anapleurotic balance to the effects of Asn or HB. Consequently, high amounts of TCA cycle intermediates were maintained until last day of culture. As a result, the cells can survive longer and increased antibody yield. Based on these finding, increased flow of carbon atoms from glycolysis to TCA cycle by decreased sorbitol production and/or increased flux in the TCA cycle at the point of malate-oxaloacetate was hypothesized to underpin the enhanced antibody yield in CHO-LB01 cells. Then, inhibition of sorbitol production by AR inhibitor and siRNA designed against *Akr1b1* approaches and/or

overexpression of *Mdh2* were undertaken in CHO-LB01 cells (Chapter 5). Unfortunately, enhance antibody production cannot be achieved by inhibition of sorbitol production and overexpression of *Mdh2* but the relationship between high productive cell and alteration of TCA cycle intermediates and related metabolites was unexpectedly found again in CHO-MDH II clone 22. Therefore, transcriptomics profiling between high and low producing clones were investigated by RNA-Seq to examine the potential correlation between transcriptome, metabolome and productivity of CHO cells (Chapter 6). The majority of differentially expressed genes between high and low producing clones were genes related to cytoskeleton-related element and cell signaling pathways.

Overall, it can be concluded that the aim of this thesis was achieved. The efficiency of CHO-LB01 cells for recombinant protein production was improved by nutrient feeding but not by cell engineering. In addition, these results proved that the hypothesis is right. High productive CHO cells showed increased amounts of TCA cycle intermediates and decreased amount of lactate, glycerol, sorbitol and amino acids. The key findings from this thesis are summarized below:

1. This result confirmed the relationship between increased the amount of TCA cycle intermediates and increased antibody production. Increased production of metabolites in the TCA cycle could result in increased the flow of TCA cycle lead to enhance energy generation and recombinant protein production.

2. Lactate profile might be another basic indicator for screening high productive CHO cells because lactate consumption event was found in cells that produced greater antibody titre (cells fed HB, Asn+HB, HB+Glc and CHO-MDH II clone 22). It can be suggested that lactate consuming CHO cells suppose to be high producer cell line. This assumption is in agreement with many previous publications (Dean and Reddy, 2013, Luo et al., 2012, Sellick et al., 2011, Sellick et al., 2015).

3. Cells fed HB enhanced antibody production. This might be due to increased the amount of TCA cycle intermediates and NADH production in mitochondria and decreased ammonia accumulation.

4. Feeding Asn caused increased maximum viable cell density and earlier death. Asn itself might have a positive effect on cell growth and Asn can generate glutamate which might be important for cell growth. Since, more rapid glucose consumption and lower amount of amino acids compared to feeding HB and the control were observed in cells fed Asn, These are probably also the reason why cells fed Asn grew and died quicker than HB-fed cells and the control.

5. Addition of HB or Asn generated similar metabolite profiles. Both decreased the amount of lactate, glycerol, sorbitol and amino acids and increased the amount of TCA cycle intermediates.

6. Cells can prolong stationary phase and maintain high titer for 3-4 days when glucose was added in cell fed Asn or HB. In addition combination of glucose with Asn or HB generated similar metabolite profiles with cell fed Asn or HB alone but the effect was more pronounced in the presence of glucose.

7. Supplementation with the combination of leucine, isoleucine, tyrosine and valine in cell fed Asn or HB did not have any effect on cell culture performance. This indicated that these amino acids were not growth-limiting nutrients.

8. Decreased sorbitol production by inhibition of AR activity and overexpression of MDH II to increase the TCA cycle flux did not have a significant effect on cell growth and antibody production of CHO-LB01 cells.

9. Transcriptomics profiling between high and low productive CHO-MDH II clones cannot provide clearly correlations between transcriptome and metabolome in relation to productivity in this study.

Based on the key findings, there are two main points that will be emphasized in the discussion below.

7.1.1 What are the factors related to metabolism that associate with enhanced efficiency of CHO cells for recombinant protein production?

As mentioned in key findings that cells fed HB, HB+Glc and Asn+Glc which antibody titre was enhanced generated the same pattern of metabolite profiles which showed increased amount of TCA cycle intermediates and decreased amount of lactate, glycerol, sorbitol and amino acids, it may be suggested that such a pattern of metabolites is a feature of highly productive cells (cells that produce more antibody per cell). Moreover, in order to prove the correlation between the amount of TCA cycle intermediates and the concentration of antibody, an analysis of this correlation was performed based on the result of antibody production and metabolite profiles of cells fed Asn or HB using the data at day 6 (Chapter 3) and cells fed Asn+Glc, HB+Glc, Glc, HB using the data at day 8 (Chapter 4) (Figure 7.1). There was a very strong positive linear correlation between the concentration of antibody and the amount of citrate (the correlation coefficient (r) = 0.98), malate (r = 0.97) and fumarate (r = 0.96) while the correlation of the amount of succinate was moderate (r = 0.63) of cells fed Asn or HB (Figure 7.1A). Similarly, cells fed Asn+Glc or HB+Glc exhibited a very strong positive linear correlation between the concentration of antibody and the amount of citrate (r = 0.85), malate (r = 0.97) and fumarate (r = 0.85) while the correlation of the amount of succinate was moderate (r = 0.57) (Figure 7.1B). In this case, r was slightly lower than cells fed Asn or HB. Together, it can be concluded that there is a strong positive correlation between the amount of TCA cycle intermediates (except for succinate) and the concentration of antibody. This finding supports the hypothesis that increased TCA cycle flux and related metabolism will enhance productivity of CHO cells.

A.

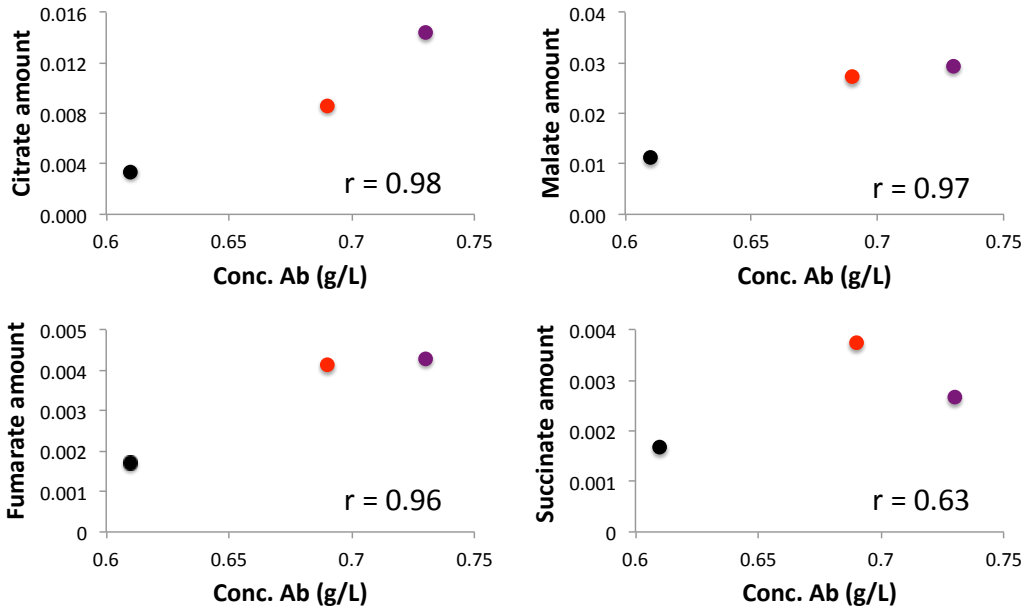

B.

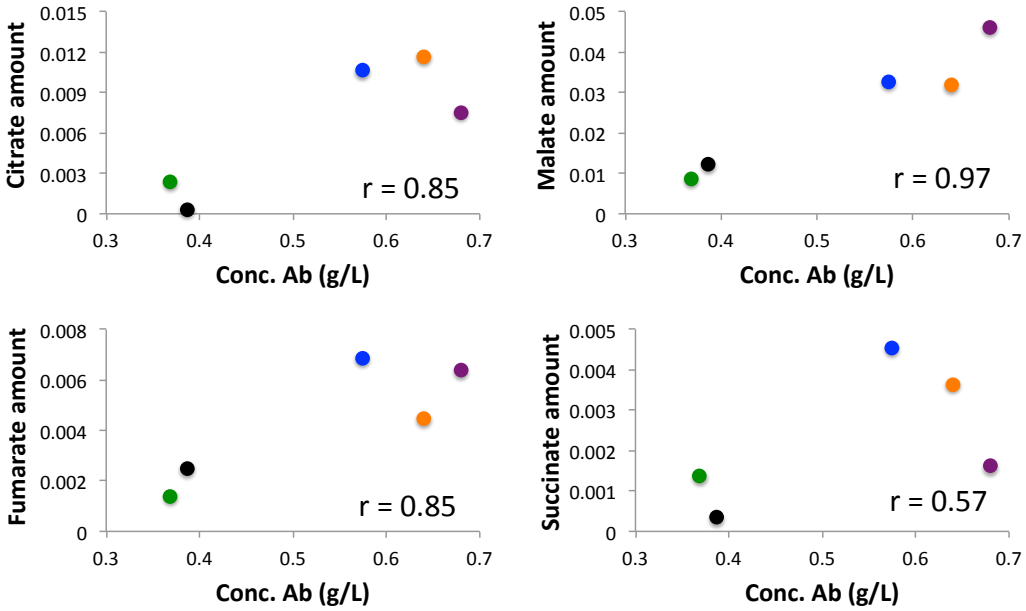

Figure 7.1 Correlations between concentration of antibody and the amount of TCA cycle intermediates.

Concentration of antibody was plotted against the amount of TCA cycle intermediate at day 6 in case of feeding Asn or HB in the absence of Glc (A) or at day 8 in case of combination of Asn or HB with Glc (B). The correlation coefficient (r) was calculated and shown in each graphs. (black = control, red = feeding Asn, purple = feeding HB, green = feeding Glc, blue = feeding Asn+Glc and orange = feeding HB+Glc)

A.

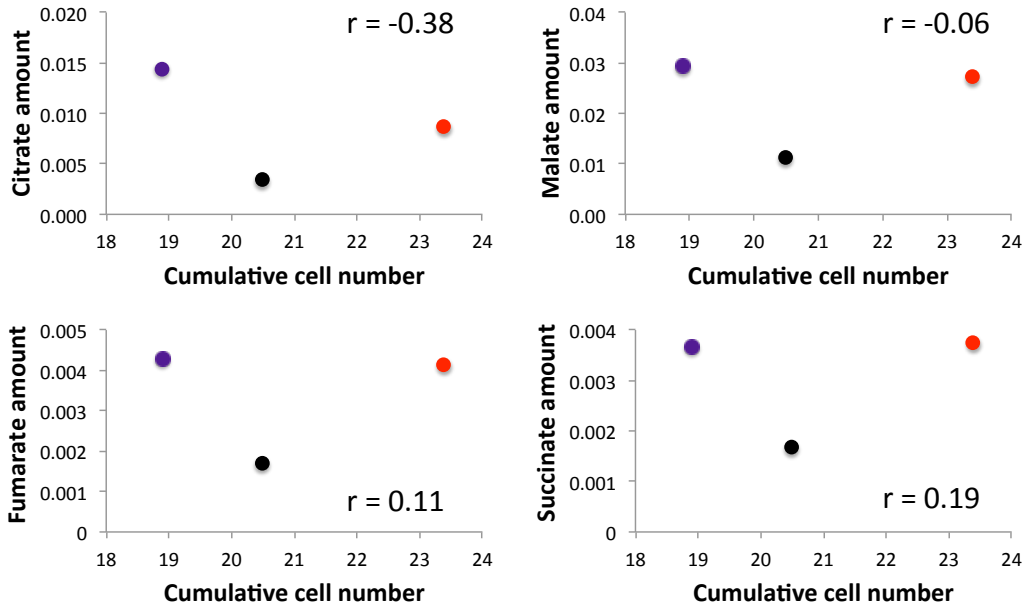

B.

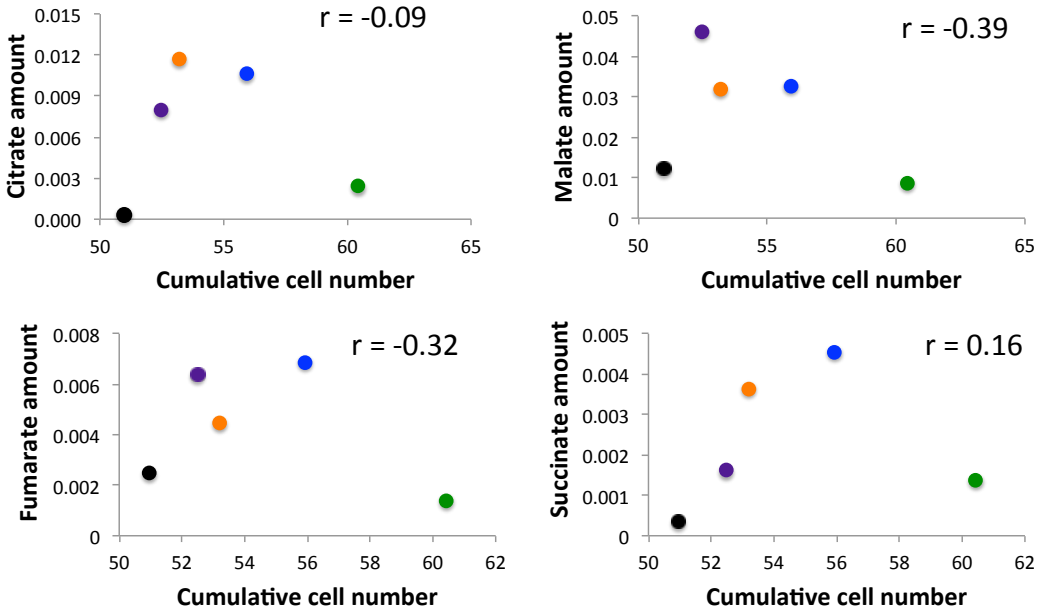

Figure 7.2 Correlations between cumulative cell number and the amount of TCA cycle intermediates.

Cumulative cell number was plotted against the amount of TCA cycle intermediate at day 6 in case of feeding Asn or HB in the absence of Glc (A) or at day 8 in case of combination of Asn or HB with Glc (B). The correlation coefficient (r) was calculated and shown in each graphs. (black = control, red = feeding Asn, purple = feeding HB, green = feeding Glc, blue = feeding Asn+Glc and orange = feeding HB+Glc)

Furthermore, in order to prove whether enhanced the amount of TCA cycle intermediates is a result of increased cell number, the correlation between the amount of TCA cycle intermediates and cumulative cell number was also analyzed in cells fed Asn, HB, Asn+Glc, HB+Glc, Glc (Figure 7.2). Contrary to the correlation between the amount of TCA cycle intermediates and the concentration of antibody, there was no correlation between the amount of TCA cycle intermediates and cumulative cell number (r ranking from 0.19 to -0.39). This indicates that greater amount of TCA cycle intermediates did not result from greater cell number. In addition, it can be said that increased amount of TCA cycle intermediates did not contribute to enhance cell number but it might help to maintain cell survival by providing more metabolic intermediates and energy for survival of cells.

Based on the positive correlation between the amount of TCA cycle intermediates and the concentration of antibody, the question is how do we assure that greater amount of TCA cycle intermediates is a result of high TCA cycle flux not result from an accumulation of those metabolites because of the restriction of some parts of TCA cycle. There are two pieces of evidence that address this conclusion. Firstly, cells fed Asn or HB exhibited greater oxygen consumption rate than the control (Section 3.5.1). It can be suggested that increased production of intermediates in the TCA cycle in the presence of Asn or HB might correlate with enhanced flux of the TCA cycle leading to enhanced oxidative metabolism and increased oxygen consumption rate. Secondly, the amount of almost all amino acids decreased when cells were fed with Asn, HB, Asn+Glc or HB+Glc. This result reflects that amino acids were consumed quicker in order to replenish the flow of the TCA cycle as a result of high TCA cycle flux or to supply more cell number and protein production. Therefore, based on this information, this indicates that increased amount of TCA metabolites is a result of more active TCA cycle flux. However, in order to confirm this explanation MFA and assessment of activity of enzymes in TCA cycle would be required (Section 7.2).

Overall, it can be concluded that increased TCA cycle flux is an important factor related to metabolism to enhance productivity of CHO cells. When TCA cycle flux is increased, less glucose is converted to sorbitol and glycerol and lactate was reutilized in order to increase the flow of carbon intermediates into the TCA cycle and maintain energy generation by TCA cycle. In addition, amino acids were consumed quicker in order to replenish the flow of the TCA cycle. Consequently, NADH and ATP production was enhanced leading to increased antibody titre.

7.1.2 Can HB be used as supplementary nutrient of CHO cells to enhance recombinant protein product yield at industrial scale?

As mentioned in Section 1.1.1, biopharmaceutical product yield has significantly increased over the past two decades due to improvements in bioprocess technology, feeds, media composition and DNA recombinant technology. However, further enhancement is still attractive to meet high demand and decrease production cost. In this thesis, supplementation with HB was found to enhance antibody yield by 50% in CHO-LB01 cell cultured in CD OptiCHO^{TM} medium (Chapter 3). This offers a promising simple strategy to increase antibody production. However, this experiment was undertaken in lab scale (20-50 mL culture). If this strategy were to be applied in industrial scale (20,000 L bioreactor), many other factors need to be considered, especially cost which will be discussed below.

In nutrient feed experiments, HB was added to culture medium at a final concentration 10 mM (1.26 g/L). Therefore, in 20,000 L bioreactor, 25,200 g of HB would be required to get a final concentration at 10 mM. Based on the price of HB from Sigma (178.50 GBP in volume of 50 g or 3.57 GBP/g), 25,200 g of HB will cost 89,964 GBP (probably get the discounts) and based on the result of feeding HB (Chapter 3), maximum concentration of antibody of cells fed HB and unfed cells were 0.9 g/L and 0.6 g/L,

respectively. This means that in 20,000 L culture, cells fed HB and unfed cells would generate 18 kg and 12 kg of antibody, respectively. It can be concluded that in 20,000 L bioreactor addition of 25,200 g of HB which cost 89,964 GBP will be required to get 18 kg of antibody or it can be said that it will cost 89,964 GBP to obtain extra 6 kg of antibody (14.99 GBP/g). At a present, the price of therapeutic antibody is about 16,410 GBP/g (Trastuzumab emtansine (Kadcyla®)). Thus, if we sell 6 kg of antibody, we will earn 98,460,000 GBP. This means that we will get a profit about 98,370,036 GBP.

In summary, it can be suggested that HB can be used as supplementary nutrient to offers a simple effective strategy to increase antibody production of CHO-LB01 in commercial scale production. However, addition of HB had positive effects on antibody production of CHO-LB01 cells but not for CHO-TRex cells as mentioned in Section 3.2 (Figure A3.1). Therefore, it should be note that the effect of HB addition might depend on cell type and culture medium used. In addition, it is important to control many factors such as mixing time, oxygen transfer, and carbon dioxide removal when scaling up a CHO cells culture process (Xing et al., 2009). Goyel et al. (2005) found that cell culture performances of CHO cells producing antibody-fusion protein B1 were decreased at production scale compared with bench scale. Thus, it can be concluded that process scale-up from laboratory to production scale remains a challenging task for CHO cells culture systems.

7.2 Future work

In order to complement the explanation of some results in this thesis, some future investigations can be suggested.

First of all, comparison of MFA between nutrient fed (Asn, HB, Asn+Glc and HB+Glc) and unfed cells would be performed in both exponential and stationary/decline phase to confirm the explanation of the metabolite profiles result that feeding nutrient could increase the flow of TCA cycle lead to increased amount of TCA cycle intermediates (Chapters 3 and 4). In addition, MFA could provide the answer why feeding the combination of Asn+Glc or HB+Glc can prolong cell stationary phase (Chapter 4) and would generate useful information to identify potential target genes to improve efficiency of CHO cells by cell engineering in the future (Chapter 5). Moreover, the result of lactate metabolism showed the reutilization of lactate in culture fed with nutrients. Thus, with a hypothesis that lactate entered the TCA cycle to maintain energy generation when glucose was depleted (Chapters 3 and 4), feeding ^{13}C lactate into the culture medium will track the molecule of lactate throughout the central metabolism of CHO-LB01 cells. The results from this experiment would provide useful confirmatory information about regulation of metabolism in CHO cells.

In addition to MFA, analysis of activity of enzymes in TCA cycle (citrate synthase, aconitase, iso-citrate dehydrogenase, αKG dehydrogenase, succinate dehydrogenase, fumarase and MDH II) could be conducted in order to suggest rate-limiting steps of the TCA cycle. However, the kinetic behavior of these enzymes might be different from their behavior when they are bound to the inner surface of the mitochondrial inner membrane or when they are coupled with each other (Robinson et al., 1987, Velot et al., 1997).

Since it was suggested that generation of NADH inside mitochondria (from the conversion of HB to acetoacetate) could provide a reason to explain why feeding HB significantly increased antibody production. Thus, it would be helpful to examine intracellular ATP, NAD^+ and NADH in cells fed nutrients to determine their concentration in response to nutrients addition (Chapters 3 and 4). Furthermore, it was hypothesized that increased glutamate production inside mitochondria (from transamination of aspartate to oxaloacetate) might be the main reason to increased maximum cell density of cells fed Asn (Chapter 3). However, from the result of glutamate profile, both cells fed Asn and cells fed HB increased the amount of glutamate inside the cells. It is possible that glutamate was generated in different compartments inside the cells. Therefore, measurement the concentration of glutamate inside mitochondria of cells fed Asn compared to cells fed HB would be required in the future.

Based on the result of cell size, cells exhibited larger size in the presence of HB (Chapter 3). Changing of cell size might be associated with a linked activity of mTORC1 pathway (Laplante and Sabatini, 2012, Meyuhas and Dreazen, 2009) or changing of osmolarity. Thus, the effects of HB at the molecular level on the mTORC1 pathway (the phosphorylation degree of downstream targets of mTORC1) by immunoblotting and measurement of solution osmolality by osmometer could be undertaken.

The final aspect for the future work would be comparing transcriptomics profiling between high and low producing CHO-MDH II clones at a series of time points because transcripts are changes dynamically during culture process (Vishwanathan et al., 2014, Schaub et al., 2010) (Chapter 6). This study would generate clearer correlation between transcriptome and metabolome in relation to productivity.

7.3 Final remarks

Improving the efficiency of CHO cells for protein production requires an understanding of how recombinant protein production is related to cell growth and metabolism because metabolism is central for cellular energy generation and links to protein production including biopharmaceuticals. In this study, supplementation with HB, Asn, HB+Glc or Asn+Glc resulted in enhanced antibody titre (except for feeding Asn alone) and the additions all resulted in similar changes to metabolite profiles. These findings support a conclusion that increased the amount of TCA cycle intermediates could relate to enhanced antibody production. In addition, reutilization of lactate, decreased sorbitol and glycerol production and decreased amount of amino acids occurred in parallel to increased amounts of TCA cycle intermediates. Furthermore, this work represents the first study to illustrate that addition of HB offers a simple effective strategy to increase recombinant protein production.

REFERENCES

AHN, W. S. & ANTONIEWICZ, M. R. 2011. Metabolic flux analysis of CHO cells at growth and non-growth phases using isotopic tracers and mass spectrometry. *Metabolic Engineering,* 13**,** 598-609.

AHN, W. S. & ANTONIEWICZ, M. R. 2012. Towards dynamic metabolic flux analysis in CHO cell cultures. *Biotechnology Journal,* 7**,** 61-74.

AHN, W. S. & ANTONIEWICZ, M. R. 2013. Parallel labeling experiments with 1,2-C-13 glucose and U-C-13 glutamine provide new insights into CHO cell metabolism. *Metabolic Engineering,* 15**,** 34-47.

ALLEN, G. C., SPIKER, S. & THOMPSON, W. F. 2000. Use of matrix attachment regions (MARs) to minimize transgene silencing. *Plant Molecular Biology,* 43**,** 361-376.

ALTAMIRANO, C., BERRIOS, J., VERGARA, M. & BECERRA, S. 2013. Advances in improving mammalian cells metabolism for recombinant protein production. *Electronic Journal of Biotechnology,* 16.

ALTAMIRANO, C., CAIRO, J. J. & GODIA, F. 2001. Decoupling cell growth and product formation in Chinese hamster ovary cells through metabolic control. *Biotechnology and Bioengineering,* 76**,** 351-360.

ALTAMIRANO, C., ILLANES, A., BECERRA, S., CAIRO, J. J. & GODIA, F. 2006a. Considerations on the lactate consumption by CHO cells in the presence of galactose. *Journal of Biotechnology,* 125**,** 547-556.

ALTAMIRANO, C., ILLANES, A., CANESSA, R. & BECERRA, S. 2006b. Specific nutrient supplementation of defined serum-free medium for the improvement of CHO cells growth and t-PA production. *Electronic Journal of Biotechnology,* 9**,** 61-67.

ALTAMIRANO, C., PAREDES, C., CAIRO, J. J. & GODIA, F. 2000. Improvement of CHO cell culture medium formulation: Simultaneous substitution of glucose and glutamine. *Biotechnology Progress,* 16**,** 69-75.

AMELIO, I., CUTRUZZOLA, F., ANTONOV, A., AGOSTINI, M. & MELINO, G. 2014. Serine and glycine metabolism in cancer. *Trends in Biochemical Sciences,* 39**,** 191-198.

BAIDOO, E. E. K., BENKE, P. I. & KEASLING, J. D. 2012. Mass spectrometry-based microbial metabolomics. *Methods in molecular biology (Clifton, N.J.),* 881**,** 215-78.

BAIK, J. Y., LEE, M. S., AN, S. R., YOON, S. K., JOO, E. J., KIM, Y. H., PARK, H. W. & LEE, G. M. 2006. Initial transcriptome and proteome analyses of low culture temperature-induced expression in CHO cells producing erythropoietin. *Biotechnology and Bioengineering,* 93**,** 361-371.

BARNES, L. M., BENTLEY, C. M. & DICKSON, A. J. 2000. Advances in animal cell recombinant protein production: GS-NS0 expression system. *Cytotechnology,* 32**,** 109-123.

BARRON, J. T., GU, L. P. & PARRILLO, J. E. 1998. Malate-aspartate shuttle, cytoplasmic NADH redox potential, and energetics in vascular smooth muscle. *Journal of Molecular and Cellular Cardiology,* 30**,** 1571-1579.

BEBBINGTON, C. R., RENNER, G., THOMSON, S., KING, D., ABRAMS, D. & YARRANTON, G. T. 1992. HIGH-LEVEL EXPRESSION OF A RECOMBINANT ANTIBODY FROM MYELOMA CELLS USING A GLUTAMINE-SYNTHETASE GENE AS AN AMPLIFIABLE SELECTABLE MARKER. *Bio-Technology,* 10**,** 169-175.

BECKER, E., FLORIN, L., PFIZENMAIER, K. & KAUFMANN, H. 2008. An XBP-1 dependent bottle-neck in production of IgG subtype antibodies in chemically defined serum-free Chinese hamster ovary (CHO) fed-batch processes. *Journal of Biotechnology,* 135**,** 217-223.

BEHJOUSIAR, A., KONTORAVDI, C. & POLIZZI, K. M. 2012. In Situ Monitoring of Intracellular Glucose and Glutamine in CHO Cell Culture. *Plos One,* 7.

BERG, J., TYMOCZKO, J. & STRYER, L. 2002. Many Shuttles Allow Movement Across the Mitochondrial Membranes. *Biochemistry, 5th edition.* New York: W H Freeman.

BERGMAN, L. W. & KUEHL, W. M. 1979. FORMATION OF INTER-MOLECULAR DISULFIDE BONDS ON NASCENT IMMUNOGLOBULIN POLYPEPTIDES. *Journal of Biological Chemistry,* 254**,** 5690-5694.

BETTS, Z. & DICKSON, A. J. 2015. Assessment of UCOE on Recombinant EPO Production and Expression Stability in Amplified Chinese Hamster Ovary Cells. *Molecular Biotechnology,* 57**,** 846-858.

BETTS, Z. & DICKSON, A. J. 2016. Ubiquitous Chromatin Opening Elements (UCOEs) effect on transgene position and expression stability in CHO cells following methotrexate (MTX) amplification. *Biotechnology Journal,* 11**,** 554-564.

BIRCH, J. R. & RACHER, A. J. 2006. Antibody production. *Advanced Drug Delivery Reviews,* 58**,** 671-685.

BOGHIGIAN, B. A., SETH, G., KISS, R. & PFEIFER, B. A. 2010. Metabolic flux analysis and pharmaceutical production. *Metabolic Engineering,* 12**,** 81-95.

BOLLATI FOGOLIN, M., WAGNER, R., ETCHEVERRIGARAY, M. & KRATJE, R. 2004. Impact of temperature reduction and expression of yeast pyruvate carboxylase on hGM-CSF-producing CHO cells. *Journal of Biotechnology,* 109**,** 179-191.

BORT, J. A. H., HACKL, M., HOEFLMAYER, H., JADHAV, V., HARREITHER, E., KUMAR, N., ERNST, W., GRILLARI, J. & BORTH, N. 2012. Dynamic mRNA and miRNA profiling of CHO-K1 suspension cell cultures. *Biotechnology Journal,* 7**,** 500-515.

BORTH, N., MATTANOVICH, D., KUNERT, R. & KATINGER, H. 2005. Effect of increased expression of protein disulfide isomerase and heavy chain binding protein on antibody secretion in a recombinant CHO cell line. *Biotechnology Progress,* 21**,** 106-111.

BORTNER, C. D. & CIDLOWSKI, J. A. 2002. Apoptotic volume decrease and the incredible shrinking cell. *Cell Death and Differentiation,* 9**,** 1307-1310.

BUTLER, M. 2005. Animal cell cultures: recent achievements and perspectives in the production of biopharmaceuticals. *Applied Microbiology and Biotechnology,* 68**,** 283-291.

BUTLER, M. & JENKINS, H. 1989. NUTRITIONAL ASPECTS OF THE GROWTH OF ANIMAL-CELLS IN CULTURE. *Journal of Biotechnology,* 12**,** 97-110.

CAIN, K., PETERS, S., HAILU, H., SWEENEY, B., STEPHENS, P., HEADS, J., SARKAR, K., VENTOM, A., PAGE, C. & DICKSON, A. 2013. A CHO cell line engineered to express XBP1 and ERO1-L has increased levels of transient protein expression. *Biotechnology Progress,* 29**,** 697-706.

CARINHAS, N., DUARTE, T. M., BARREIRO, L. C., CARRONDO, M. J. T., ALVES, P. M. & TEIXEIRA, A. P. 2013. Metabolic Signatures of GS-CHO Cell Clones Associated With Butyrate Treatment and Culture Phase Transition. *Biotechnology and Bioengineering,* 110**,** 3244-3257.

CARLAGE, T., HINCAPIE, M., ZANG, L., LYUBARSKAYA, Y., MADDEN, H., MHATRE, R. & HANCOCK, W. S. 2009. Proteomic Profiling of a High-Producing Chinese Hamster Ovary Cell Culture. *Analytical Chemistry,* 81**,** 7357-7362.
CASTRANOVA, D., DAVIS, A. E., LO, B. D., MILLER, M. F., PAUKSTELIS, P. J., SWIFT, M. R., PHAM, V. N., TORRES-VAZQUEZ, J., BELL, K., SHAW, K. M., KAMEI, M. & WEINSTEIN, B. M. 2016. Aminoacyl-Transfer RNA Synthetase Deficiency Promotes Angiogenesis via the Unfolded Protein Response Pathway. *Arteriosclerosis Thrombosis and Vascular Biology,* 36**,** 655-662.
CHANG, M., LIU, R., JIN, Q., LIU, Y. & WANG, X. 2014. Scaffold/matrix attachment regions from CHO cell chromosome enhanced the stable transfection efficiency and the expression of transgene in CHO cells. *Biotechnology and Applied Biochemistry,* 61**,** 510-516.
CHARANIYA, S., KARYPIS, G. & HU, W.-S. 2009. Mining Transcriptome Data for Function-Trait Relationship of Hyper Productivity of Recombinant Antibody. *Biotechnology and Bioengineering,* 102**,** 1654-1669.
CHEN, K. Q., LIU, Q., XIE, L. Z., SHARP, P. A. & WANG, D. I. C. 2001. Engineering of a mammalian cell line for reduction of lactate formation and high monoclonal antibody production. *Biotechnology and Bioengineering,* 72**,** 55-61.
CHEN, P. F. & HARCUM, S. W. 2005. Effects of amino acid additions on ammonium stressed CHO cells. *Journal of Biotechnology,* 117**,** 277-286.
CHIANG, G. G. & SISK, W. P. 2005. Bcl-x(L) mediates increased production of humanized monoclonal antibodies in chinese hamster ovary cells. *Biotechnology and Bioengineering,* 91**,** 779-792.
CHONG, W., REDDY, S., YUSUFI, F., LEE, D., WONG, N., HENG, C., YAP, M. & HO, Y. 2010. Metabolomics-driven approach for the improvement of Chinese hamster ovary cell growth: Overexpression of malate dehydrogenase II. *Journal of Biotechnology,* 147**,** 116-121.
CHUNG, M. I., LIM, M. H., LEE, Y. J., KIM, I. H., KIM, I. Y., KIM, J. H., CHANG, K. H. & KIM, H. J. 2003. Reduction of ammonia accumulation and improvement of cell viability by expression of urea cycle enzymes in Chinese hamster ovary cells. *Journal of Microbiology and Biotechnology,* 13**,** 217-224.
CHUSAINOW, J., YANG, Y. S., YEO, Y. H. M., TOH, P. C., ASVADI, P., WONG, N. S. C. & YAP, M. G. S. 2009. A Study of Monoclonal Antibody-Producing CHO Cell Lines: What Makes a Stable High Producer? *Biotechnology and Bioengineering,* 102**,** 1182-1196.
CLARKE, C., DOOLAN, P., BARRON, N., MELEADY, P., O'SULLIVAN, F., GAMMELL, P., MELVILLE, M., LEONARD, M. & CLYNES, M. 2011. Large scale microarray profiling and coexpression network analysis of CHO cells identifies transcriptional modules associated with growth and productivity. *Journal of Biotechnology,* 155**,** 350-359.
COLEMAN, P. S. & LAVIETES, B. B. 1981. MEMBRANE CHOLESTEROL, TUMORIGENESIS, AND THE BIOCHEMICAL PHENOTYPE OF NEOPLASIA. *Crc Critical Reviews in Biochemistry,* 11**,** 341-393.
COST, G. J., FREYVERT, Y., VAFIADIS, A., SANTIAGO, Y., MILLER, J. C., REBAR, E., COLLINGWOOD, T. N., SNOWDEN, A. & GREGORY, P. D. 2010. BAK and BAX Deletion Using Zinc-Finger Nucleases Yields Apoptosis-Resistant CHO Cells. *Biotechnology and Bioengineering,* 105**,** 330-340.
CRONWRIGHT, G. R., ROHWER, J. M. & PRIOR, B. A. 2002. Metabolic control analysis of glycerol synthesis in Saccharomyces cerevisiae. *Applied and Environmental Microbiology,* 68**,** 4448-4456.

CROWELL, C. K., GRAMPP, G. E., ROGERS, G. N., MILLER, J. & SCHEINMAN, R. I. 2007. Amino acid and manganese supplementation modulates the glycosylation state of erythropoietin in a CHO culture system. *Biotechnology and Bioengineering,* 96**,** 538-549.
DADEHBEIGI, N. & DICKSON, A. J. 2015. Chemical manipulation of the mTORC1 pathway in industrially relevant CHOK1 cells enhances production of therapeutic proteins. *Biotechnology Journal,* 10**,** 1041-1050.
DANNA, J. A., VALDEZ, J. G., HABBERSETT, R. C. & CRISSMAN, H. A. 1997. Association of G(1)/S-phase and late S-phase checkpoints with regulation of cyclin-dependent kinases in Chinese hamster ovary cells. *Radiation Research,* 148**,** 260-271.
DATTA, P., LINHARDT, R. J. & SHARFSTEIN, S. T. 2013. An 'omics approach towards CHO cell engineering. *Biotechnology and Bioengineering,* 110**,** 1255-1271.
DAVIS, R., SCHOOLEY, K., RASMUSSEN, B., THOMAS, J. & REDDY, P. 2000. Effect of PDI overexpression on recombinant protein secretion in CHO cells. *Biotechnology Progress,* 16**,** 736-743.
DAWSON, A. G. 1979. OXIDATION OF CYTOSOLIC NADH FORMED DURING AEROBIC METABOLISM IN MAMMALIAN-CELLS. *Trends in Biochemical Sciences,* 4**,** 171-176.
DEAN, J. & REDDY, P. 2013. Metabolic analysis of antibody producing CHO cells in fed-batch production. *Biotechnology and Bioengineering,* 110**,** 1735-1747.
DEROUAZI, M., MARTINET, D., SCHMUTZ, N. B., FLACTION, R., WICHT, M., BERTSCHINGER, M., HACKER, D. L., BECKMANN, J. S. & WURM, F. M. 2006. Genetic characterization of CHO production host DG44 and derivative recombinant cell lines. *Biochemical and Biophysical Research Communications,* 340**,** 1069-1077.
DESHPANDE, R., YANG, T. H. & HEINZLE, E. 2009. Towards a metabolic and isotopic steady state in CHO batch cultures for reliable isotope-based metabolic profiling. *Biotechnology Journal,* 4**,** 247-263.
DESHPANDE, R. R. & HEINZLE, E. 2004. On-line oxygen uptake rate and culture viability measurement of animal cell culture using microplates with integrated oxygen sensors. *Biotechnology Letters,* 26**,** 763-767.
DIETMAIR, S., HODSON, M. P., QUEK, L.-E., TIMMINS, N. E., CHRYSANTHOPOULOS, P., JACOB, S. S., GRAY, P. & NIELSEN, L. K. 2012a. Metabolite profiling of CHO cells with different growth characteristics. *Biotechnology and Bioengineering,* 109**,** 1404-1414.
DIETMAIR, S., NIELSEN, L. K. & TIMMINS, N. E. 2012b. Mammalian cells as biopharmaceutical production hosts in the age of omics. *Biotechnology Journal,* 7**,** 75-89.
DINNIS, D. M., STANSFIELD, S. H., SCHLATTER, S., SMALES, C. M., ALETE, D., BIRCH, J. R., RACHER, A. J., MARSHAL, C. T., NIELSEN, L. K. & JAMES, D. C. 2006. Functional proteomic analysis of GS-NS0 murine myeloma cell lines with varying recombinant monoclonal antibody production rate. *Biotechnology and Bioengineering,* 94**,** 830-841.
DOLCI, S., BELMONTE, A., SANTONE, R., GIORGI, M., PELLEGRINI, M., CAROSA, E., PICCIONE, E., LENZI, A. & JANNINI, E. A. 2006. Subcellular localization and regulation of type-1C and type-5 phosphodiesterases. *Biochemical and Biophysical Research Communications,* 341**,** 837-846.
DONAMARIA, P. 2012. Optimisation of the Expression of Therapeutic Proteins in Mammalian Cell Lines: Novel Nutrient Feeds to Enhance Antibody Titre and Cell Biomass. Faculty of Life Sciences The University of Manchester.

DOOLAN, P., MELEADY, P., BARRON, N., HENRY, M., GALLAGHER, R., GAMMELL, P., MELVILLE, M., SINACORE, M., MCCARTHY, K., LEONARD, M., CHARLEBOIS, T. & CLYNES, M. 2010. Microarray and Proteomics Expression Profiling Identifies Several Candidates, Including the Valosin-Containing Protein (VCP), Involved in Regulating High Cellular Growth Rate in Production CHO Cell Lines. *Biotechnology and Bioengineering,* 106**,** 42-56.

DOOLAN, P., MELVILLE, M., GAMMELL, P., SINACORE, M., MELEADY, P., MCCARTHY, K., FRANCULLO, L., LEONARD, M., CHARLEBOIS, T. & CLYNES, M. 2008. Transcriptional profiling of gene expression changes in a PACE-transfected CHO DUKX cell line secreting high levels of rhBMP-2. *Molecular Biotechnology,* 39**,** 187-199.

DORAI, H., KYUNG, Y. S., ELLIS, D., KINNEY, C., LIN, C., JAN, D., MOORE, G. & BETENBAUGH, M. J. 2009. Expression of Anti-Apoptosis Genes Alters Lactate Metabolism of Chinese Hamster Ovary Cells in Culture. *Biotechnology and Bioengineering,* 103**,** 592-608.

DORAI, H. & MOORE, G. P. 1987. THE EFFECT OF DIHYDROFOLATE REDUCTASE-MEDIATED GENE AMPLIFICATION ON THE EXPRESSION OF TRANSFECTED IMMUNOGLOBULIN GENES. *Journal of Immunology,* 139**,** 4232-4241.

DORNER, A. J., WASLEY, L. C. & KAUFMAN, R. J. 1992. OVEREXPRESSION OF GRP78 MITIGATES STRESS INDUCTION OF GLUCOSE REGULATED PROTEINS AND BLOCKS SECRETION OF SELECTIVE PROTEINS IN CHINESE-HAMSTER OVARY CELLS. *Embo Journal,* 11**,** 1563-1571.

DUARTE, T. M., CARINHAS, N., BARREIRO, L. C., CARRONDO, M. J. T., ALVES, P. M. & TEIXEIRA, A. P. 2014. Metabolic Responses of CHO Cells to Limitation of Key Amino Acids. *Biotechnology and Bioengineering,* 111**,** 2095-2106.

DUVAL, D., DEMANGEL, C., MUNIERJOLAIN, K., MIOSSEC, S. & GEAHEL, I. 1991. FACTORS CONTROLLING CELL-PROLIFERATION AND ANTIBODY-PRODUCTION IN MOUSE HYBRIDOMA CELLS .1. INFLUENCE OF THE AMINO-ACID SUPPLY. *Biotechnology and Bioengineering,* 38**,** 561-570.

ECKER, D. M., JONES, S. D. & LEVINE, H. L. 2015. The therapeutic monoclonal antibody market. *Mabs,* 7**,** 9-14.

EDROS, R., MCDONNELL, S. & AL-RUBEAI, M. 2014. The relationship between mTOR signalling pathway and recombinant antibody productivity in CHO cell lines. *Bmc Biotechnology,* 14.

FANN, C. H., GUIRGIS, F., CHEN, G., LAO, M. S. & PIRET, J. M. 2000. Limitations to the amplification and stability of human tissue-type plasminogen activator expression by Chinese hamster ovary cells. *Biotechnology and Bioengineering,* 69**,** 204-212.

FIEHN, O. 2002. Metabolomics - the link between genotypes and phenotypes. *Plant Molecular Biology,* 48**,** 155-171.

FIGUEROA, B., JR., AILOR, E., OSBORNE, D., HARDWICK, J. M., REFF, M. & BETENBAUGH, M. J. 2007. Enhanced cell culture performance using inducible anti-apoptotic genes E1B-19K and Aven in the production of a monoclonal antibody with chinese hamster ovary cells. *Biotechnology and Bioengineering,* 97**,** 877-892.

FINGAR, D. C., SALAMA, S., TSOU, C., HARLOW, E. & BLENIS, J. 2002. Mammalian cell size is controlled by mTOR and its downstream targets S6K1 and 4EBP1/eIF4E. *Genes & Development,* 16**,** 1472-1487.

FOMINA-YADLIN, D., MUJACIC, M., MAGGIORA, K., QUESNELL, G., SALEEM, R. & MCGREW, J. T. 2015. Transcriptome analysis of a CHO cell line expressing a

recombinant therapeutic protein treated with inducers of protein expression. *Journal of Biotechnology,* 212**,** 106-115.
FUSSENEGGER, M., MAZUR, X. & BAILEY, J. E. 1997. A novel cytostatic process enhances the productivity of Chinese hamster ovary cells. *Biotechnology and Bioengineering,* 55**,** 927-939.
GATTI, M. D. L., WLASCHIN, K. F., NISSOM, P. M., YAP, M. & HU, W.-S. 2007. Comparative transcriptional analysis of mouse hybridoma and recombinant Chinese hamster ovary cells undergoing butyrate treatment. *Journal of Bioscience and Bioengineering,* 103**,** 82-91.
GENZEL, Y., RITTER, J. B., KONIG, S., ALT, R. & REICHL, U. 2005. Substitution of glutamine by pyruvate to reduce ammonia formation and growth inhibition of mammalian cells. *Biotechnology Progress,* 21**,** 58-69.
GILBERT, A., MCELEARNEY, K., KSHIRSAGAR, R., SINACORE, M. S. & RYLL, T. 2013. Investigation of Metabolic Variability Observed in Extended Fed Batch Cell Culture. *Biotechnology Progress,* 29**,** 1519-1527.
GIROD, P. A. & MERMOD, N. 2003. Use of scaffold/matrix-attachment regions for protein production. *Gene Transfer and Expression in Mammalian Cells,* 38**,** 359-379.
GLACKEN, M. W., FLEISCHAKER, R. J. & SINSKEY, A. J. 1986. REDUCTION OF WASTE PRODUCT EXCRETION VIA NUTRIENT CONTROL - POSSIBLE STRATEGIES FOR MAXIMIZING PRODUCT AND CELL YIELDS ON SERUM IN CULTURES OF MAMMALIAN-CELLS. *Biotechnology and Bioengineering,* 28**,** 1376-1389.
GODIA, F. & CAIRO, J. J. 2006. Cell metabolism. *Cell Culture Technology for Pharmaceutical and Cell-Based Therapies***,** 81-112.
GOYAL, M., RANK, D. L., GUPTA, S. K., BOOM, T. V. & LEE, S. S. 2005. Effects of elevated pCO(2) and osmolality on growth of CHO cells and production of antibody-fusion protein B1: A case study. *Biotechnology Progress,* 21**,** 70-77.
HAMMOND, S., KAPLAREVIC, M., BORTH, N., BETENBAUGH, M. J. & LEE, K. H. 2012. Chinese hamster genome database: An online resource for the CHO community at www.CHOgenome.org. *Biotechnology and Bioengineering,* 109**,** 1353-1356.
HAMMOND, S., SWANBERG, J. C., KAPLAREVIC, M. & LEE, K. H. 2011. Genomic sequencing and analysis of a Chinese hamster ovary cell line using Illumina sequencing technology. *Bmc Genomics,* 12.
HAN, J., BACKA, S. H., HUR, J., LIN, Y.-H., GILDERSLEEVE, R., SHAN, J., YUAN, C. L., KROKOWSKI, D., WANG, S., HATZOGLOU, M., KILBERG, M. S., SARTOR, M. A. & KAUFMAN, R. J. 2013. ER-stress-induced transcriptional regulation increases protein synthesis leading to cell death. *Nature Cell Biology,* 15**,** 481-+.
HAN, Y., LIU, X.-M., LIU, H., LI, S.-C., WU, B.-C., YE, L.-L., WANG, Q.-W. & CHEN, Z.-L. 2006. Cultivation of recombinant Chinese hamster ovary cells grown as suspended aggregates in stirred vessels. *Journal of Bioscience and Bioengineering,* 102**,** 430-435.
HANSEN, H. A. & EMBORG, C. 1994a. EXTRA AND INTRACELLULAR AMINO-ACID-CONCENTRATIONS IN CONTINUOUS CHINESE-HAMSTER OVARY CELL-CULTURE. *Applied Microbiology and Biotechnology,* 41**,** 560-564.
HANSEN, H. A. & EMBORG, C. 1994b. INFLUENCE OF AMMONIUM ON GROWTH, METABOLISM, AND PRODUCTIVITY OF A CONTINUOUS SUSPENSION CHINESE-HAMSTER OVARY CELL-CULTURE. *Biotechnology Progress,* 10**,** 121-124.
HARREITHER, E., HACKL, M., PICHLER, J., SHRIDHAR, S., AUER, N., LABAJ, P. P., SCHEIDELER, M., KARBIENER, M., GRILLARI, J., KREIL, D. P. & BORTH, N.

2015. Microarray profiling of preselected CHO host cell subclones identifies gene expression patterns associated with in-creased production capacity. *Biotechnology Journal,* 10**,** 1625-1638.
HAYES, N. V. L., SMALES, C. M. & KLAPPA, P. 2010. Protein Disulfide Isomerase Does Not Control Recombinant IgG4 Productivity in Mammalian Cell Lines. *Biotechnology and Bioengineering,* 105**,** 770-779.
HAYTER, P. M., CURLING, E. M. A., BAINES, A. J., JENKINS, N., SALMON, I., STRANGE, P. G. & BULL, A. T. 1991. CHINESE-HAMSTER OVARY CELL-GROWTH AND INTERFERON-PRODUCTION KINETICS IN STIRRED BATCH CULTURE. *Applied Microbiology and Biotechnology,* 34**,** 559-564.
HE, L., WINTERROWD, C., KADURA, I. & FRYE, C. 2012. Transgene copy number distribution profiles in recombinant CHO cell lines revealed by single cell analyses. *Biotechnology and Bioengineering,* 109**,** 1713-1722.
HINTERKOERNER, G., BRUGGER, G., MUELLER, D., HESSE, F., KUNERT, R., KATINGER, H. & BORTH, N. 2007. Improvement of the energy metabolism of recombinant CHO cells by cell sorting for reduced mitochondrial membrane potential. *Journal of Biotechnology,* 129**,** 651-657.
HU, L., CHEN, H.-Y., HAN, T., YANG, G.-Z., FENG, D., QI, C.-Y., GONG, H., ZHAI, Y.-X., CAI, Q.-P. & GAO, C.-F. 2016. Downregulation of DHRS9 expression in colorectal cancer tissues and its prognostic significance. *Tumor Biology,* 37**,** 837-845.
HUTSON, S. M., SWEATT, A. J. & LANOUE, K. F. 2005. Brached-chain amino acid metabolism: Implications for establishing safe intakes'. *Journal of Nutrition,* 135**,** 1557S-1564S.
JAIRAM, S. & EDENBERG, H. J. 2014. Single-Nucleotide Polymorphisms Interact to Affect ADH7 Transcription. *Alcoholism-Clinical and Experimental Research,* 38**,** 921-929.
JAYAPAL, K. R., WLASCHIN, K. F., HU, W.-S. & YAP, M. G. S. 2007. Recombinant protein therapeutics from CHO cells - 20 years and counting. *Chemical Engineering Progress,* 103**,** 40-47.
JEONG, D. W., KIM, T. S., LEE, J. W., KIM, K. T., KIM, H. J., KIM, I. H. & KIM, I. Y. 2001. Blocking of acidosis-mediated apoptosis by a reduction of lactate dehydrogenase activity through antisense mRNA expression. *Biochemical and Biophysical Research Communications,* 289**,** 1141-1149.
JIANG, Z., HUANG, Y. & SHARFSTEIN, S. T. 2006. Regulation of recombinant monoclonal antibody production in Chinese hamster ovary cells: A comparative study of gene copy number, mRNA level, and protein expression. *Biotechnology Progress,* 22**,** 313-318.
JOHARI, Y. B., ESTES, S. D., ALVES, C. S., SINACORE, M. S. & JAMES, D. C. 2015. Integrated cell and process engineering for improved transient production of a "difficult-to-express" fusion protein by CHO cells. *Biotechnology and Bioengineering,* 112**,** 2527-2542.
JONES, R. J., DICKERSON, S., BHENDE, P. M., DELECLUSE, H.-J. & KENNEY, S. C. 2007. Epstein-Barr virus lytic infection induces retinoic acid-responsive genes through induction of a retinol-metabolizing enzyme, DHRS9. *Journal of Biological Chemistry,* 282**,** 8317-8324.
JUN, D. Y., PARK, H. S., LEE, J. Y., BAEK, J. Y., PARK, H.-K., FUKUI, K. & KIM, Y. H. 2008. Positive regulation of promoter activity of human 3-phosphoglycerate dehydrogenase (PHGDH) gene is mediated by transcription factors Sp1 and NF-Y. *Gene,* 414**,** 106-114.

KANG, S., MULLEN, J., MIRANDA, L. P. & DESHPANDE, R. 2012. Utilization of tyrosine- and histidine-containing dipeptides to enhance productivity and culture viability. *Biotechnology and Bioengineering,* 109**,** 2286-2294.
KANG, S., REN, D., XIAO, G., DARIS, K., BUCK, L., ENYENIHI, A. A., ZUBAREV, R., BONDARENKO, P. V. & DESHPANDE, R. 2014. Cell Line Profiling to Improve Monoclonal Antibody Production. *Biotechnology and Bioengineering,* 111**,** 748-760.
KANTARDJIEFF, A., JACOB, N. M., YEE, J. C., EPSTEIN, E., KOK, Y.-J., PHILP, R., BETENBAUGH, M. & HU, W.-S. 2010. Transcriptome and proteome analysis of Chinese hamster ovary cells under low temperature and butyrate treatment. *Journal of Biotechnology,* 145**,** 143-159.
KAO, F. T. & PUCK, T. T. 1968. GENETICS OF SOMATIC MAMMALIAN CELLS .7. INDUCTION AND ISOLATION OF NUTRITIONAL MUTANTS IN CHINESE HAMSTER CELLS. *Proceedings of the National Academy of Sciences of the United States of America,* 60**,** 1275-&.
KAWAGUCHI, T., TAKENOSHITA, M., KABASHIMA, T. & UYEDA, K. 2001. Glucose and cAMP regulate the L-type pyruvate kinase gene by phosphorylation/dephosphorylation of the carbohydrate response element binding protein. *Proceedings of the National Academy of Sciences of the United States of America,* 98**,** 13710-13715.
KHOO, S. H. G. & AL-RUBEAI, M. 2009. Metabolic characterization of a hyper-productive state in an antibody producing NS0 myeloma cell line. *Metabolic Engineering,* 11**,** 199-211.
KILDEGAARD, H. F., BAYCIN-HIZAL, D., LEWIS, N. E. & BETENBAUGH, M. J. 2013. The emerging CHO systems biology era: harnessing the 'omics revolution for biotechnology. *Current Opinion in Biotechnology,* 24**,** 1102-1107.
KIM, J. Y., KIM, Y.-G. & LEE, G. M. 2012. CHO cells in biotechnology for production of recombinant proteins: current state and further potential. *Applied Microbiology and Biotechnology,* 93**,** 917-930.
KIM, N. S. & LEE, G. M. 2001. Overexpression of bcl-2 inhibits sodium butyrate-induced apoptosis in Chinese hamster ovary cells resulting in enhanced humanized antibody production. *Biotechnology and Bioengineering,* 71**,** 184-193.
KIM, N. S. & LEE, G. M. 2002. Inhibition of sodium butyrate-induced apoptosis in recombinant Chinese hamster ovary cells by constitutively expressing antisense RNA of caspase-3. *Biotechnology and Bioengineering,* 78**,** 217-228.
KIM, S. H. & LEE, G. M. 2007a. Down-regulation of lactate dehydrogenase-A by siRNAs for reduced lactic acid formation of Chinese hamster ovary cells producing thrombopoietin. *Applied Microbiology and Biotechnology,* 74**,** 152-159.
KIM, S. H. & LEE, G. M. 2007b. Functional expression of human pyruvate carboxylase for reduced lactic acid formation of Chinese hamster ovary cells (DG44). *Applied Microbiology and Biotechnology,* 76**,** 659-665.
KIM, T. K., CHUNG, J. Y., SUNG, Y. H. & LEE, G. M. 2001. Relationship between Cell Size and Specific Thrombopoietin Productivity in Chinese Hamster Ovary Cells during Dihydrofolate Reductase-mediated Gene Amplification. *Biotechnology Bioprocess,* 6**,** 332-336.
KIM, Y.-G., KIM, J. Y., MOHAN, C. & LEE, G. M. 2009. Effect of Bcl-x(L) Overexpression on Apoptosis and Autophagy in Recombinant Chinese Hamster Ovary Cells Under Nutrient-Deprived Condition. *Biotechnology and Bioengineering,* 103**,** 757-766.

KISHISHITA, S., KATAYAMA, S., KODAIRA, K., TAKAGI, Y., MATSUDA, H., OKAMOTO, H., TAKUMA, S., HIRASHIMA, C. & AOYAGI, H. 2015. Optimization of chemically defined feed media for monoclonal antibody production in Chinese hamster ovary cells. *Journal of Bioscience and Bioengineering,* 120**,** 78-84.

KLEIN, T., NIKLAS, J. & HEINZLE, E. 2015. Engineering the supply chain for protein production/secretion in yeasts and mammalian cells. *Journal of Industrial Microbiology & Biotechnology,* 42**,** 453-464.

KO, Y. G., PARK, H. & KIM, S. 2002. Novel regulatory interactions and activities of mammalian tRNA synthetases. *Proteomics,* 2**,** 1304-1310.

KORKE, R., GATTI, M. D., LAU, A. L. Y., LIM, J. W. E., SEOW, T. K., CHUNG, M. C. M. & HU, W. S. 2004. Large scale gene expression profiling of metabolic shift of mammalian cells in culture. *Journal of Biotechnology,* 107**,** 1-17.

KORKE, R., RINK, A., SEOW, T. K., CHUNG, M. C. M., BEATTIE, C. W. & HU, W. S. 2002. Genomic and proteomic perspectives in cell culture engineering. *Journal of Biotechnology,* 94**,** 73-92.

KOTAGIRI, S. & EDENBERG, H. J. 1998. Regulation of human alcohol dehydrogenase gene ADH7: Importance of an AP-1 site. *DNA and Cell Biology,* 17**,** 583-590.

KREMKOW, B. G., BAIK, J. Y., MACDONALD, M. L. & LEE, K. H. 2015. CHOgenome.org 2.0: Genome resources and website updates. *Biotechnology Journal,* 10**,** 931-938.

KU, S. C. Y., NG, D. T. W., YAP, M. G. S. & CHAO, S.-H. 2008. Effects of overexpression of X-box binding protein 1 on recombinant protein production in Chinese hamster ovary and NS0 myeloma cells. *Biotechnology and Bioengineering,* 99**,** 155-164.

KU, S. C. Y., TOH, P. C., LEE, Y. Y., CHUSAINOW, J., YAP, M. G. S. & CHAO, S.-H. 2010. Regulation of XBP-1 Signaling During Transient and Stable Recombinant Protein Production in CHO Cells. *Biotechnology Progress,* 26**,** 517-526.

KURANO, N., LEIST, C., MESSI, F., KURANO, S. & FIECHTER, A. 1990. GROWTH-BEHAVIOR OF CHINESE HAMSTER OVARY CELLS IN A COMPACT LOOP BIOREACTOR .2. EFFECTS OF MEDIUM COMPONENTS AND WASTE PRODUCTS. *Journal of Biotechnology,* 15**,** 113-128.

LANOUE, K. F. & WILLIAMS.JR 1971. INTERRELATIONSHIPS BETWEEN MALATE-ASPARTATE SHUTTLE AND CITRIC ACID CYCLE IN RAT HEART MITOCHONDRIA. *Metabolism-Clinical and Experimental,* 20**,** 119-&.

LAPLANTE, M. & SABATINI, D. M. 2012. mTOR Signaling in Growth Control and Disease. *Cell,* 149**,** 274-293.

LAY, J. O., JR., BORGMANN, S., LIYANAGE, R. & WILKINS, C. L. 2006. Problems with the "omics". *Trac-Trends in Analytical Chemistry,* 25**,** 1046-1056.

LEE, H. W., CHRISTIE, A., STARKEY, J. A., READ, E. K. & YOON, S. 2015. Intracellular metabolic flux analysis of CHO cells supplemented with wheat hydrolysates for improved mAb production and cell-growth. *Journal of Chemical Technology and Biotechnology,* 90**,** 291-302.

LEE, M. S., KIM, K. W., KIM, Y. H. & LEE, G. M. 2003. Proteome analysis of antibody-expressing CHO cells in response to hyperosmotic pressure. *Biotechnology Progress,* 19**,** 1734-1741.

LEE, S. W., CHO, B. H., PARK, S. G. & KIM, S. 2004. Aminoacyl-tRNA synthetase complexes: beyond translation. *Journal of Cell Science,* 117**,** 3725-3734.

LEWIS, N. E., LIU, X., LI, Y., NAGARAJAN, H., YERGANIAN, G., O'BRIEN, E., BORDBAR, A., ROTH, A. M., ROSENBLOOM, J., BIAN, C., XIE, M., CHEN, W., LI, N., BAYCIN-HIZAL, D., LATIF, H., FORSTER, J., BETENBAUGH, M. J., FAMILI, I., XU, X.,

WANG, J. & PALSSON, B. O. 2013. Genomic landscapes of Chinese hamster ovary cell lines as revealed by the Cricetulus griseus draft genome. *Nature Biotechnology,* 31**,** 759-+.

LEY, D., SERESHT, A. K., ENGMARK, M., MAGDENOSKA, O., NIELSEN, K. F., KILDEGAARD, H. F. & ANDERSEN, M. R. 2015. Multi-omic profiling of EPO-producing Chinese hamster ovary cell panel reveals metabolic adaptation to heterologous protein production. *Biotechnology and Bioengineering,* 112**,** 2373-2387.

LI, J., WONG, C. L., VIJAYASANKARAN, N., HUDSON, T. & AMANULLAH, A. 2012. Feeding lactate for CHO cell culture processes: Impact on culture metabolism and performance. *Biotechnology and Bioengineering,* 109**,** 1173-1186.

LI, J. H., HUANG, Z., SUN, X. M., YANG, P. Y. & ZHANG, Y. X. 2006. Understanding the enhanced effect of dimethyl sulfoxide on hepatitis B surface antigen expression in the culture of Chinese hamster ovary cells on the basis of proteome analysis. *Enzyme and Microbial Technology,* 38**,** 372-380.

LIM, S. F., CHUAN, K. H., LIU, S., LOH, S. O. H., CHUNG, B. Y. F., ONG, C. C. & SONG, Z. 2006. RNAi suppression of Bax and Bak enhances viability in fed-batch cultures of CHO cells. *Metabolic Engineering,* 8**,** 509-522.

LIU, Y., ZHOU, J. & WHITE, K. P. 2014. RNA-seq differential expression studies: more sequence or more replication? *Bioinformatics,* 30**,** 301-304.

LIU, Z., DAI, S., BONES, J., RAY, S., CHA, S., KARGER, B. L., LI, J. J., WILSON, L., HINCKLE, G. & ROSSOMANDO, A. 2015. A quantitative proteomic analysis of cellular responses to high glucose media in Chinese hamster ovary cells. *Biotechnology Progress,* 31**,** 1026-1038.

LLOYD, D. R., HOLMES, P., JACKSON, L. P., EMERY, A. N. & AL-RUBEAI, M. 2000. Relationship between cell size, cell cycle and specific recombinant protein productivity. *Cytotechnology,* 34**,** 59-70.

LOH, W. P., LOO, B., ZHOU, L., ZHANG, P., LEE, D.-Y., YANG, Y. & LAM, K. P. 2014. Overexpression of microRNAs enhances recombinant protein production in Chinese hamster ovary cells. *Biotechnology Journal,* 9**,** 1140-1151.

LOVATT, D., SONNEWALD, U., WAAGEPETERSEN, H. S., SCHOUSBOE, A., HE, W., LIN, J. H. C., HAN, X., TAKANO, T., WANG, S., SIM, F. J., GOLDMAN, S. A. & NEDERGAARD, M. 2007. The transcriptome and metabolic gene signature of protoplasmic Astrocytes in the adult murine cortex. *Journal of Neuroscience,* 27**,** 12255-12266.

LU, S. B., SUN, X. M., SHI, C. O. & ZHANG, Y. X. 2003. Determination of tricarboxylic acid cycle acids and other related substances in cultured mammalian cells by gradient ion-exchange chromatography with suppressed conductivity detection. *Journal of Chromatography A,* 1012**,** 161-168.

LU, S. B., SUN, X. M. & ZHANG, Y. X. 2005. Insight into metabolism of CHO cells at low glucose concentration on the basis of the determination of intracellular metabolites. *Process Biochemistry,* 40**,** 1917-1921.

LUGNIER, C. 2006. Cyclic nucleotide phosphodiesterase (PDE) superfamily: A new target for the development of specific therapeutic agents. *Pharmacology & Therapeutics,* 109**,** 366-398.

LUO, J., VIJAYASANKARAN, N., AUTSEN, J., SANTURAY, R., HUDSON, T., AMANULLAH, A. & LI, F. 2012. Comparative metabolite analysis to understand lactate metabolism shift in Chinese hamster ovary cell culture process. *Biotechnology and Bioengineering,* 109**,** 146-156.

LUO, X., KRANZLER, H. R., ZUO, L., ZHANG, H., WANG, S. & GELERNTER, J. 2008. ADH7 variation modulates extraversion and conscientiousness in substance-

dependent subjects. *American Journal of Medical Genetics Part B-Neuropsychiatric Genetics,* 147B**,** 179-186.
MA, N., ELLET, J., OKEDIADI, C., HERMES, P., MCCORMICK, E. & CASNOCHA, S. 2009. A Single Nutrient Feed Supports Both Chemically Defined NS0 and CHO Fed-Batch Processes: Improved Productivity and Lactate Metabolism. *Biotechnology Progress,* 25**,** 1353-1363.
MAGA, G. & HUBSCHER, U. 2003. Proliferating cell nuclear antigen (PCNA): a dancer with many partners. *Journal of Cell Science,* 116**,** 3051-3060.
MARKOVA, N. G., PINKAS-SARAFOVA, A. & SIMON, M. 2006. A metabolic enzyme of the short-chain dehydrogenase/reductase superfamily may moonlight in the nucleus as a repressor of promoter activity. *Journal of Investigative Dermatology,* 126**,** 2019-2031.
MARTINEZ, V. S., DIETMAIR, S., QUEK, L.-E., HODSON, M. P., GRAY, P. & NIELSEN, L. K. 2013. Flux balance analysis of CHO cells before and after a metabolic switch from lactate production to consumption. *Biotechnology and Bioengineering,* 110**,** 660-666.
MASTRANGELO, A. J. & BETENBAUGH, M. J. 1998. Overcoming apoptosis: new methods for improving protein-expression systems. *Trends in Biotechnology,* 16**,** 88-95.
MASTRANGELO, A. J., HARDWICK, J. M., BEX, F. & BETENBAUGH, M. J. 2000a. Part I. Bcl-2 and Bcl-x(L) limit apoptosis upon infection with alphavirus vectors. *Biotechnology and Bioengineering,* 67**,** 544-554.
MASTRANGELO, A. J., HARDWICK, J. M., ZOU, S. F. & BETENBAUGH, M. J. 2000b. Part II. Overexpression of bcl-2 family members enhances survival of mammalian cells in response to various culture insults. *Biotechnology and Bioengineering,* 67**,** 555-564.
MCCRACKEN, N. A., KOWLE, R. & OUYANG, A. 2014. Control of galactosylated glycoforms distribution in cell culture system. *Biotechnology Progress,* 30**,** 547-553.
MCGETTIGAN, P. A. 2013. Transcriptomics in the RNA-seq era. *Current Opinion in Chemical Biology,* 17**,** 4-11.
MEYUHAS, O. & DREAZEN, A. 2009. Ribosomal Protein S6 Kinase: From TOP mRNAs to Cell Size. *Translational Control in Health and Disease,* 90**,** 109-153.
MOHAN, C. & LEE, G. M. 2010. Effect of Inducible Co-Overexpression of Protein Disulfide Isomerase and Endoplasmic Reticulum Oxidoreductase on the Specific Antibody Productivity of Recombinant Chinese Hamster Ovary Cells. *Biotechnology and Bioengineering,* 107**,** 337-346.
MOHAN, C., PARK, S. H., CHUNG, J. Y. & LEE, G. M. 2007. Effect of doxycycline-regulated protein disulfide isomerase expression on the specific productivity of recombinant CHO cells: Thrombopoietin and antibody. *Biotechnology and Bioengineering,* 98**,** 611-615.
MORRIS, J., DORNER, A., EDWARDS, C., HENDERSHOT, L. & KAUFMAN, R. 1997. Immunoglobulin Binding Protein (BiP) Function Is Required to Protect Cells from Endoplasmic Reticulum Stress but Is Not Required for the Secretion of Selective Proteins. *The Journal Of Biological Chemistry,* 272**,** 4327-4334.
MULUKUTLA, B. C., GRAMER, M. & HU, W.-S. 2012. On metabolic shift to lactate consumption in fed-batch culture of mammalian cells. *Metabolic Engineering,* 14**,** 138-149.
MULUKUTLA, B. C., KHAN, S., LANGE, A. & HU, W.-S. 2010. Glucose metabolism in mammalian cell culture: new insights for tweaking vintage pathways. *Trends in Biotechnology,* 28**,** 476-484.

NARKEWICZ, M. R., SAULS, S. D., TJOA, S. S., TENG, C. & FENNESSEY, P. V. 1996. Evidence for intracellular partitioning of serine and glycine metabolism in Chinese hamster ovary cells. *Biochemical Journal,* 313**,** 991-996.
NEERMANN, J. & WAGNER, R. 1996. Comparative analysis of glucose and glutamine metabolism in transformed mammalian cell lines, insect and primary liver cells. *Journal of Cellular Physiology,* 166**,** 152-169.
NEUHOFER, W. & BECK, F. X. 2005. Response of renal medullary cells to osmotic stress. *Cellular Stress Responses in Renal Diseases,* 148**,** 21-34.
NEWSHOLME, P., LIMA, M. M. R., PORCOPIO, J., PITHON-CURI, T. C., DOI, S. Q., BAZOTTE, R. B. & CURI, R. 2003. Glutamine and glutamate as vital metabolites. *Brazilian Journal of Medical and Biological Research,* 36**,** 153-163.
NISHIMIYA, D. 2014. Proteins improving recombinant antibody production in mammalian cells. *Applied Microbiology and Biotechnology,* 98**,** 1031-1042.
NISHIMIYA, D., MANO, T., MIYADAI, K., YOSHIDA, H. & TAKAHASHI, T. 2013. Overexpression of CHOP alone and in combination with chaperones is effective in improving antibody production in mammalian cells. *Applied Microbiology and Biotechnology,* 97**,** 2531-2539.
NISSOM, P., SANNY, A., KOK, Y., HIANG, Y., CHUAH, S., SHING, T., LEE, Y., WONG, K., HU, W., SIM, M. & PHILP, R. 2006. Transcriptome and proteome profiling to understanding the biology of high productivity CHO cells. *Molecular Biotechnology,* 34**,** 125-140.
NOLAN, R. P. & LEE, K. 2011. Dynamic model of CHO cell metabolism. *Metabolic Engineering,* 13**,** 108-124.
O'CALLAGHAN, P. M., BERTHELOT, M. E., YOUNG, R. J., GRAHAM, J. W. A., RACHER, A. J. & ALDANA, D. 2015. Diversity in host clone performance within a Chinese hamster ovary cell line. *Biotechnology Progress,* 31**,** 1187-1200.
O'CALLAGHAN, P. M., MCLEOD, J., PYBUS, L. P., LOVELADY, C. S., WILKINSON, S. J., RACHER, A. J., PORTER, A. & JAMES, D. C. 2010. Cell Line-Specific Control of Recombinant Monoclonal Antibody Production by CHO Cells. *Biotechnology and Bioengineering,* 106**,** 938-951.
OHYA, T., HAYASHI, T., KIYAMA, E., NISHII, H., MIKI, H., KOBAYASHI, K., HONDA, K., OMASA, T. & OHTAKE, H. 2008. Improved production of recombinant human antithrombin III in Chinese hamster ovary cells by ATF4 overexpression. *Biotechnology and Bioengineering,* 100**,** 317-324.
OLDIGES, M., LUETZ, S., PFLUG, S., SCHROER, K., STEIN, N. & WIENDAHL, C. 2007. Metabolomics: current state and evolving methodologies and tools. *Applied Microbiology and Biotechnology,* 76**,** 495-511.
OMASA, T., TAKAMI, T., OHYA, T., KIYAMA, E., HAYASHI, T., NISHII, H., MIKI, H., KOBAYASHI, K., HONDA, K. & OHTAKE, H. 2008. Overexpression of GADD34 Enhances Production of Recombinant Human Antithrombin III in Chinese Hamster Ovary Cells. *Journal of Bioscience and Bioengineering,* 106**,** 568-573.
ORR, A. L., ASHOK, D., SARANTOS, M. R., NG, R., SHI, T., GERENCSER, A. A., HUGHES, R. E. & BRAND, M. D. 2014. Novel Inhibitors of Mitochondrial sn-Glycerol 3-phosphate Dehydrogenase. *Plos One,* 9.
OWEN, O. E., MORGAN, A. P., KEMP, H. G., SULLIVAN, J. M., HERRERA, M. G. & CAHILL, G. F. 1967. BRAIN METABOLISM DURING FASTING. *Journal of Clinical Investigation,* 46**,** 1589-&.
PARK, H. S., KIM, I. H., KIM, I. Y., KIM, K. H. & KIM, H. J. 2000. Expression of carbamoyl phosphate synthetase I and ornithine transcarbamoylase genes in

Chinese hamster ovary dhfr-cells decreases accumulation of ammonium ion in culture media. *Journal of Biotechnology,* 81**,** 129-140.
PARK, S. G., CHOI, E.-C. & KIM, S. 2010. Aminoacyl-tRNA Synthetase-Interacting Multifunctional Proteins (AIMPs): A Triad for Cellular Homeostasis. *Iubmb Life,* 62**,** 296-302.
PASCOE, D. E., ARNOTT, D., PAPOUTSAKIS, E. T., MILLER, W. M. & ANDERSENI, D. C. 2007. Proteome analysis of anti body-producing CHO cell lines with different metabolic profiles. *Biotechnology and Bioengineering,* 98**,** 391-410.
PENG, R.-W., ABELLAN, E. & FUSSENEGGER, M. 2011. Differential Effect of Exocytic SNAREs on the Production of Recombinant Proteins in Mammalian Cells. *Biotechnology and Bioengineering,* 108**,** 611-620.
PEREZ, A. & FERRARIS, J. 1995. Aldose Reductase Gene Expression and Osmoregulation in Mammalian Renal Cells. *In:* STRANGE, K. (ed.) *Cellular and Molecular Physiology of Cell Volume Regulation.* United States of America: CRC Press, Inc.
PRASHAD, K. & MEHRA, S. 2015. Dynamics of unfolded protein response in recombinant CHO cells. *Cytotechnology,* 67**,** 237-254.
PYBUS, L. P., DEAN, G., WEST, N. R., SMITH, A., DARAMOLA, O., FIELD, R., WILKINSON, S. J. & JAMES, D. C. 2014. Model-Directed Engineering of "Difficult-to-Express'' Monoclonal Antibody Production by Chinese Hamster Ovary Cells. *Biotechnology and Bioengineering,* 111**,** 372-385.
QUEK, L.-E., DIETMAIR, S., KROEMER, J. O. & NIELSEN, L. K. 2010. Metabolic flux analysis in mammalian cell culture. *Metabolic Engineering,* 12**,** 161-171.
RAO, K. N. 1995. THE SIGNIFICANCE OF THE CHOLESTEROL BIOSYNTHETIC-PATHWAY IN CELL-GROWTH AND CARCINOGENESIS (REVIEW). *Anticancer Research,* 15**,** 309-314.
RASMUSSEN, H. & GOODMAN, D. B. P. 1977. RELATIONSHIPS BETWEEN CALCIUM AND CYCLIC NUCLEOTIDES IN CELL ACTIVATION. *Physiological Reviews,* 57**,** 421-509.
RATHMELL, J. C., FOX, C. J., PLAS, D. R., HAMMERMAN, P. S., CINALLI, R. M. & THOMPSON, C. B. 2003. Akt-directed glucose metabolism can prevent Bax conformation change and promote growth factor-independent survival. *Molecular and Cellular Biology,* 23**,** 7315-7328.
REICHERT, J. M. 2014. Antibodies to watch in 2014 Mid-year update. *Mabs,* 6**,** 799-802.
REINHART, D., DAMJANOVIC, L., KAISERMAYER, C. & KUNERT, R. 2015. Benchmarking of commercially available CHO cell culture media for antibody production. *Applied Microbiology and Biotechnology,* 99**,** 4645-4657.
REITZER, L., WICE, B. & KENNELL, D. 1979. Evidence That Glutamine, Not Sugar, Is the Major Energy Source for
Cultured HeLa Cells* *Journal of Biological Chemistry,* 254**,** 2669-2676.
ROBINSON, J. B., INMAN, L., SUMEGI, B. & SRERE, P. A. 1987. FURTHER CHARACTERIZATION OF THE KREBS TRICARBOXYLIC-ACID CYCLE METABOLON. *Journal of Biological Chemistry,* 262**,** 1786-1790.
ROCHFORT, S. 2005. Metabolomics reviewed: A new "Omics" platform technology for systems biology and implications for natural products research. *Journal of Natural Products,* 68**,** 1813-1820.
ROUX, A., LISON, D., JUNOT, C. & HEILIER, J.-F. 2011. Applications of liquid chromatography coupled to mass spectrometry-based metabolomics in clinical chemistry and toxicology: A review. *Clinical Biochemistry,* 44**,** 119-135.

RYAN, D. & ROBARDS, K. 2006. Metabolomics: The Greatest Omics of Them All? *Analytical Chemistry,* 78**,** 7954-7958.
SADHU, K., HENSLEY, K., FLORIO, V. A. & WOLDA, S. L. 1999. Differential expression of the cyclic GMP-stimulated phosphodiesterase PDE2A in human venous and capillary endothelial cells. *Journal of Histochemistry & Cytochemistry,* 47**,** 895-905.
SAUERWALD, T. M., BETENBAUGH, M. J. & OYLER, G. A. 2002. Inhibiting apoptosis in mammalian cell culture using the caspase inhibitor XIAP and deletion mutants. *Biotechnology and Bioengineering,* 77**,** 704-716.
SAUERWALD, T. M., OYLER, G. A. & BETENBAUGH, M. J. 2003. Study of caspase inhibitors for limiting death in mammalian cell culture. *Biotechnology and Bioengineering,* 81**,** 329-340.
SCHAUB, J., CLEMENS, C., SCHORN, P., HILDEBRANDT, T., RUST, W., MENNERICH, D., KAUFMANN, H. & SCHULZ, T. W. 2010. CHO Gene Expression Profiling in Biopharmaceutical Process Analysis and Design. *Biotechnology and Bioengineering,* 105**,** 431-438.
SCHMIDT, E. V. 1999. The role of c-myc in cellular growth control. *Oncogene,* 18**,** 2988-2996.
SCHNEIDER, M., MARISON, I. W. & VONSTOCKAR, U. 1996. The importance of ammonia in mammalian cell culture. *Journal of Biotechnology,* 46**,** 161-185.
SCHRODER, M. & KAUFMAN, R. J. 2005a. ER stress and the unfolded protein response. *Mutation Research-Fundamental and Molecular Mechanisms of Mutagenesis,* 569**,** 29-63.
SCHRODER, M. & KAUFMAN, R. J. 2005b. The mammalian unfolded protein response. *Annual Review of Biochemistry,* 74**,** 739-789.
SELLICK, C. A., CROXFORD, A. S., MAQSOOD, A. R., STEPHENS, G., WESTERHOFF, H. V., GOODACRE, R. & DICKSON, A. J. 2011. Metabolite Profiling of Recombinant CHO Cells: Designing Tailored Feeding Regimes That Enhance Recombinant Antibody Production. *Biotechnology and Bioengineering,* 108**,** 3025-3031.
SELLICK, C. A., CROXFORD, A. S., MAQSOOD, A. R., STEPHENS, G. M., WESTERHOFF, H. V., GOODACRE, R. & DICKSON, A. J. 2015. Metabolite profiling of CHO cells: Molecular reflections of bioprocessing effectiveness. *Biotechnology Journal,* 10**,** 1434-1445.
SELVARASU, S., HO, Y. S., CHONG, W. P. K., WONG, N. S. C., YUSUFI, F. N. K., LEE, Y. Y., YAP, M. G. S. & LEE, D.-Y. 2012. Combined in silico modeling and metabolomics analysis to characterize fed-batch CHO cell culture. *Biotechnology and Bioengineering,* 109**,** 1415-1429.
SENGUPTA, N., ROSE, S. T. & MORGAN, J. A. 2011. Metabolic Flux Analysis of CHO Cell Metabolism in the Late Non-Growth Phase. *Biotechnology and Bioengineering,* 108**,** 82-92.
SETH, G., PHILP, R. J., DENOYA, C. D., MCGRATH, K., STUTZMAN-ENGWALL, K. J., YAP, M. & HU, W. S. 2005. Large-scale gene expression analysis of cholesterol dependence in NSO cells. *Biotechnology and Bioengineering,* 90**,** 552-567.
SETH, G., PHILP, R. J., LAU, A., JIUN, K. Y., YAP, M. & HU, W.-S. 2007. Molecular portrait of high productivity in recombinant NS0 cells. *Biotechnology and Bioengineering,* 97**,** 933-951.
SHAPIRO, H. M. 2000. Membrane potential estimation by flow cytometry. *Methods-a Companion to Methods in Enzymology,* 21**,** 271-279.
SHEN, D., KIEHL, T. R., KHATTAK, S. F., LI, Z. J., HE, A., KAYNE, P. S., PATEL, V., NEUHAUS, I. M. & SHARFSTEIN, S. T. 2010. Transcriptomic Responses to

Sodium Chloride-Induced Osmotic Stress: A Study of Industrial Fed-Batch CHO Cell Cultures. *Biotechnology Progress,* 26**,** 1104-1115.
SOLAINI, G., SGARBI, G., LENAZ, G. & BARACCA, A. 2007. Evaluating mitochondrial membrane potential in cells. *Bioscience Reports,* 27**,** 11-21.
SONG, G., OUYANG, G. L. & BAO, S. D. 2005. The activation of Akt/PKB signaling pathway and cell survival. *Journal of Cellular and Molecular Medicine,* 9**,** 59-71.
SPENCE, S., RENA, G., SULLIVAN, M., ERDOGAN, S. & HOUSLAY, M. D. 1997. Receptor-mediated stimulation of lipid signalling pathways in CHO cells elicits the rapid transient induction of the PDE1B isoform of Ca2+/calmodulin-stimulated cAMP phosphodiesterase. *Biochemical Journal,* 321**,** 157-163.
SPENCE, S., RENA, G., SWEENEY, G. & HOUSLAY, M. D. 1995. INDUCTION OF CA2+/CALMODULIN-STIMULATED CYCLIC-AMP PHOSPHODIESTERASE (PDE1) ACTIVITY IN CHINESE-HAMSTER OVARY CELLS (CHO) BY PHORBOL 12-MYRISTATE 13-ACETATE AND BY THE SELECTIVE OVEREXPRESSION OF PROTEIN-KINASE-C ISOFORMS. *Biochemical Journal,* 310**,** 975-982.
STEIN, L. R. & IMAI, S.-I. 2012. The dynamic regulation of NAD metabolism in mitochondria. *Trends in Endocrinology and Metabolism,* 23**,** 420-428.
STEINMEYER, D. E. & MCCORMICK, E. L. 2008. The art of antibody process development. *Drug Discovery Today,* 13**,** 613-618.
STEPHANOPOULOS, G., ARISTIDOU, A. & NIELSON, J. 1998. *Metabolomic Engineering: Principles and Methodologies,* San Diego, Academic Press.
SUNG, Y. H., HWANG, S. J. & LEE, G. M. 2005. Influence of down-regulation of caspase-3 by siRNAs on sodium-butyrate-induced apoptotic cell death of Chinese hamster ovary cells producing thrombopoietin. *Metabolic Engineering,* 7**,** 457-466.
SUNG, Y. H. & LEE, G. M. 2005. Enhanced human thrombopoietin production by sodium butyrate addition to serum-free suspension culture of Bcl-2-overexpressing CHO cells. *Biotechnology Progress,* 21**,** 50-57.
SUNG, Y. H., LEE, J. S., PARK, S. H., KOO, J. & LEE, G. M. 2007. Influence of co-down-regulation of caspase-3 and caspase-7 by siRNAs on sodium butyrate-induced apoptotic cell death of Chinese hamster ovary cells producing thrombopoietin. *Metabolic Engineering,* 9**,** 452-464.
TAIT, S. W. G. & GREEN, D. R. 2012. Mitochondria and cell signalling. *Journal of Cell Science,* 125**,** 807-815.
TALMAGE, D. A. 2008. Mechanisms of neuregulin action. *Novartis Foundation symposium,* 289**,** 74-84; discussion 84-93.
TANG, W. H., MARTIN, K. A. & HWA, J. 2012. Aldose reductase, oxidative stress, and diabetic mellitus. *Frontiers in Pharmacology,* 3.
TEMPLETON, N., DEAN, J., REDDY, P. & YOUNG, J. D. 2013. Peak antibody production is associated with increased oxidative metabolism in an industrially relevant fed-batch CHO cell culture. *Biotechnology and Bioengineering,* 110**,** 2013-+.
TEMPLETON, N., LEWIS, A., DORAI, H., QIAN, E. A., CAMPBELL, M. P., SMITH, K. D., LANG, S. E., BETENBAUGH, M. J. & YOUNG, J. D. 2014. The impact of anti-apoptotic gene Bcl-2 Delta expression on CHO central metabolism. *Metabolic Engineering,* 25**,** 92-102.
TEY, B. T., SINGH, R. P., PIREDDA, L., PIACENTINI, M. & AL-RUBEAI, M. 2000. Influence of Bcl-2 on cell death during the cultivation of a Chinese hamster ovary cell line expressing a chimeric antibody. *Biotechnology and Bioengineering,* 68**,** 31-43.

TIGGES, M. & FUSSENEGGER, M. 2006. Xbp1-based engineering of secretory capacity enhances the productivity of Chinese hamster ovary cells. *Metabolic Engineering,* 8**,** 264-272.
TJIO, J. H. & PUCK, T. T. 1958. GENETICS OF SOMATIC MAMMALIAN CELLS .2. CHROMOSOMAL CONSTITUTION OF CELLS IN TISSUE CULTURE. *Journal of Experimental Medicine,* 108**,** 259-&.
TOUSSAINT, C., HENRY, O. & DUROCHER, Y. 2016. Metabolic engineering of CHO cells to alter lactate metabolism during fed-batch cultures. *Journal of Biotechnology,* 217**,** 122-131.
TRUMMER, E., ERNST, W., HESSE, F., SCHRIEBL, K., LATTENMAYER, C., KUNERT, R., VORAUER-UHL, K., KATINGER, H. & MUELLER, D. 2008. Transcriptional proflling of phenotypically diffierent Epo-Fc expressing CHO clones by cross-species microarray analysis. *Biotechnology Journal,* 3**,** 924-937.
TSUJIMOTO, Y. 1998. Role of Bcl-2 family proteins in apoptosis: apoptosomes or mitochondria. *Genes to Cells,* 3 697-707.
URLAUB, G. & CHASIN, L. A. 1980. ISOLATION OF CHINESE-HAMSTER CELL MUTANTS DEFICIENT IN DIHYDROFOLATE-REDUCTASE ACTIVITY. *Proceedings of the National Academy of Sciences of the United States of America-Biological Sciences,* 77**,** 4216-4220.
URLAUB, G., KAS, E., CAROTHERS, A. M. & CHASIN, L. A. 1983. DELETION OF THE DIPLOID DIHYDROFOLATE-REDUCTASE LOCUS FROM CULTURED MAMMALIAN-CELLS. *Cell,* 33**,** 405-412.
VAN DYK, D. D., MISZTAL, D. R., WILKINS, M. R., MACKINTOSH, J. A., POLJAK, A., VARNAIL, J. C., TEBER, E., WALSH, B. J. & GRAY, P. P. 2003. Identification of cellular changes associated with increased production of human growth hormone in a recombinant Chinese hamster ovary cell line. *Proteomics,* 3**,** 147-156.
VELOT, C., MIXON, M. B., TEIGE, M. & SRERE, P. A. 1997. Model of a quinary structure between Krebs TCA cycle enzymes: A model for the metabolon. *Biochemistry,* 36**,** 14271-14276.
VISHWANATHAN, N., LE, H., JACOB, N. M., TSAO, Y.-S., NG, S.-W., LOO, B., LIU, Z., KANTARDJIEFF, A. & HU, W.-S. 2014. Transcriptome Dynamics of Transgene Amplification in Chinese Hamster Ovary Cells. *Biotechnology and Bioengineering,* 111**,** 518-528.
VISHWANATHAN, N., YONGKY, A., JOHNSON, K. C., FU, H.-Y., JACOB, N. M., LE, H., YUSUFI, F. N. K., LEE, D. Y. & HU, W.-S. 2015. Global Insights Into the Chinese Hamster and CHO Cell Transcriptomes. *Biotechnology and Bioengineering,* 112**,** 965-976.
WAGNER, R. 1997. Metabolic control of animal cell culture processes. *Mammalian Cell Biotechnology in Protein Production***,** 193-232.
WALSH, G. 2010. Biopharmaceutical benchmarks 2010. *Nature Biotechnology,* 28**,** 917-924.
WALSH, G. 2014. Biopharmaceutical benchmarks 2014. *Nature Biotechnology,* 32**,** 992-1000.
WANG, J., WEI, J., XU, X., PAN, W., GE, Y., ZHOU, C., LIU, C., GAO, J., YANG, M. & MAO, W. 2014. Replication Study of ESCC Susceptibility Genetic Polymorphisms Locating in the ADH1B-ADH1C-ADH7 Cluster Identified by GWAS. *Plos One,* 9.
WANG, W. W., WU, Z. L., DAI, Z. L., YANG, Y., WANG, J. J. & WU, G. Y. 2013. Glycine metabolism in animals and humans: implications for nutrition and health. *Amino Acids,* 45**,** 463-477.

WANG, Z., GERSTEIN, M. & SNYDER, M. 2009. RNA-Seq: a revolutionary tool for transcriptomics. *Nature Reviews Genetics,* 10**,** 57-63.
WILKENS, C. & GERDTZEN, Z. 2015. Comparative Metabolic Analysis of CHO Cell Clones Obtained through Cell Engineering, for IgG Productivity, Growth and Cell Longevity. *Plos One,* 10.
WILKENS, C. A., ALTAMIRANO, C. & GERDTZEN, Z. P. 2011. Comparative Metabolic Analysis of Lactate for CHO Cells in Glucose and Galactose. *Biotechnology and Bioprocess Engineering,* 16**,** 714-724.
WLASCHIN, K. F. & HU, W.-S. 2007. Engineering cell metabolism for high-density cell culture via manipulation of sugar transport. *Journal of Biotechnology,* 131**,** 168-176.
WLASCHIN, K. F., NISSOM, P. M., GATTI, M. D., ONG, P. F., ARLEEN, S., TAN, K. S., RINK, A., CHAM, B., WONG, K., YAP, M. & HU, W. S. 2005. EST sequencing for gene discovery in Chinese hamster ovary cells. *Biotechnology and Bioengineering,* 91**,** 592-606.
WONG, D. C. F., WONG, K. T. K., LEE, Y. Y., MORIN, P. N., HENG, C. K. & YAP, M. G. S. 2006. Transcriptional profiling of apoptotic pathways in batch and fed-batch CHO cell cultures. *Biotechnology and Bioengineering,* 94**,** 373-382.
WORTON, R. G., HO, C. C. & DUFF, C. 1977. CHROMOSOME STABILITY IN CHO CELLS. *Somatic Cell Genetics,* 3**,** 27-45.
WURM, F. M. 2004. Production of recombinant protein therapeutics in cultivated mammalian cells. *Nature Biotechnology,* 22**,** 1393-1398.
WURM, F. M. & HACKER, D. 2011. First CHO genome. *Nature Biotechnology,* 29**,** 718-720.
XIE, L. Z. & WANG, D. I. C. 1994. STOICHIOMETRIC ANALYSIS OF ANIMAL-CELL GROWTH AND ITS APPLICATION IN MEDIUM DESIGN. *Biotechnology and Bioengineering,* 43**,** 1164-1174.
XING, Z., KENTY, B., KOYRAKH, I., BORYS, M., PAN, S.-H. & LI, Z. J. 2011. Optimizing amino acid composition of CHO cell culture media for a fusion protein production. *Process Biochemistry,* 46**,** 1423-1429.
XING, Z. Z., KENTY, B. N., LI, Z. J. & LEE, S. S. 2009. Scale-Up Analysis for a CHO Cell Culture Process in Large-Scale Bioreactors. *Biotechnology and Bioengineering,* 103**,** 733-746.
XU, P., DAI, X.-P., GRAF, E., MARTEL, R. & RUSSELL, R. 2014. Effects of Glutamine and Asparagine on Recombinant Antibody Production Using CHO-GS Cell Lines. *Biotechnology Progress,* 30**,** 1457-1468.
XU, X., NAGARAJAN, H., LEWIS, N. E., PAN, S., CAI, Z., LIU, X., CHEN, W., XIE, M., WANG, W., HAMMOND, S., ANDERSEN, M. R., NEFF, N., PASSARELLI, B., KOH, W., FAN, H. C., WANG, J., GUI, Y., LEE, K. H., BETENBAUGH, M. J., QUAKE, S. R., FAMILI, I., PALSSON, B. O. & WANG, J. 2011. The genomic sequence of the Chinese hamster ovary (CHO)-K1 cell line. *Nature Biotechnology,* 29**,** 735-U131.
YANG, M. & BUTLER, M. 2000. Effects of ammonia on CHO cell growth, erythropoietin production, and glycosylation. *Biotechnology and Bioengineering,* 68**,** 370-380.
YEE, J. C., GATTI, M. D. L., PHILP, R. J., YAP, M. & HU, W.-S. 2008. Genomic and proteomic exploration of CHO and hybridoma cells under sodium butyrate treatment. *Biotechnology and Bioengineering,* 99**,** 1186-1204.
YEE, J. C., GERDTZEN, Z. P. & HU, W.-S. 2009. Comparative Transcriptome Analysis to Unveil Genes Affecting Recombinant Protein Productivity in Mammalian Cells. *Biotechnology and Bioengineering,* 102**,** 246-263.

YING, W. 2008. NAD(+)/ NADH and NADP(+)/NADPH in cellular functions and cell death: Regulation and biological consequences. *Antioxidants & Redox Signaling,* 10**,** 179-206.
YIP, S. S. M., ZHOU, M., JOLY, J., SNEDECOR, B., SHEN, A. & CRAWFORD, Y. 2014. Complete Knockout of the Lactate Dehydrogenase A Gene is Lethal in Pyruvate Dehydrogenase Kinase 1, 2, 3 Down-Regulated CHO Cells. *Molecular Biotechnology,* 56**,** 833-838.
YU, M., HU, Z., PACIS, E., VIJAYASANKARAN, N., SHEN, A. & LI, F. 2011. Understanding the Intracellular Effect of Enhanced Nutrient Feeding Toward High Titer Antibody Production Process. *Biotechnology and Bioengineering,* 108**,** 1078-1088.
YUN, C. Y., LIU, S., LIM, S. F., WANG, T., CHUNG, B. Y. F., TEO, J. J., CHUAN, K. H., SOON, A. S. C., GOH, K. S. & SONG, Z. 2007. Specific inhibition of caspase-8 and-9 in CHO cells enhances cell viability in batch and fed-batch cultures. *Metabolic Engineering,* 9**,** 406-418.
ZAGARI, F., JORDAN, M., STETTLER, M., BROLY, H. & WURM, F. M. 2013. Lactate metabolism shift in CHO cell culture: the role of mitochondrial oxidative activity. *New Biotechnology,* 30**,** 238-245.
ZAGARI, F., STETTLER, M., BALDI, L., BROLY, H., WURM, F. & JORDAN, M. 2013 High expression of the aspartate-glutamate carrier Aralar1 favors lactate consumption in CHO cell culture. *Pharmaceutical Bioprocessing,* 1 19-27.
ZGOMBICKNIGHT, M., FOGLIO, M. H. & DUESTER, G. 1995. GENOMIC STRUCTURE AND EXPRESSION OF THE ADH7 GENE ENCODING HUMAN CLASS-IV ALCOHOL-DEHYDROGENASE, THE FORM MOST EFFICIENT FOR RETINOL METABOLISM IN-VITRO. *Journal of Biological Chemistry,* 270**,** 4305-4311.
ZHANG, F., SUN, X., YI, X. & ZHANG, Y. 2006. Metabolic characteristics of recombinant Chinese hamster ovary cells expressing glutamine synthetase in presence and absence of glutamine. *Cytotechnology,* 51**,** 21-28.
ZHANG, Y. 2009. Approaches to Optimizing Animal Cell Culture Process: Substrate Metabolism Regulation and Protein Expression Improvement. *Biotechnology in China I: from Bioreaction to Bioseparation and Bioremediation,* 113**,** 177-215.
ZHOU, A.-X., HARTWIG, J. H. & AKYUREK, L. M. 2010. Filamins in cell signaling, transcription and organ development. *Trends in Cell Biology,* 20**,** 113-123.
ZHOU, M., CRAWFORD, Y., NG, D., TUNG, J., PYNN, A. F. J., MEIER, A., YUK, I. H., VIJAYASANKARAN, N., LEACH, K., JOLY, J., SNEDECOR, B. & SHEN, A. 2011. Decreasing lactate level and increasing antibody production in Chinese Hamster Ovary cells (CHO) by reducing the expression of lactate dehydrogenase and pyruvate dehydrogenase kinases. *Journal of Biotechnology,* 153**,** 27-34.
ZHU, C. 2013 Aldose Reductase Inhibitors as Potential Therapeutic Drugs of Diabetic Complications. *In:* OGUNTIBEJU, O. O. (ed.) *Diabetes Melitus-Insights and Perspectives.* Croatia.
ZIELKE, H. R., ZIELKE, C. L. & OZAND, P. T. 1984. GLUTAMINE - A MAJOR ENERGY-SOURCE FOR CULTURED MAMMALIAN-CELLS. *Federation Proceedings,* 43**,** 121-125.
ZUSTIAK, M. P., JOSE, L., XIE, Y., ZHU, J. & BETENBAUGH, M. J. 2014. Enhanced transient recombinant protein production in CHO cells through the co-transfection of the product gene with Bcl-x(L). *Biotechnology Journal,* 9**,** 1164-1174.

APPENDICIES

Appendix 1 Suppliers of materials and equipment

Mammalian cell lines

Dickson Lab, University of Manchester, UK

CHO-LB01, CHO-S, CHO-TRex

Media and supplements

Life technologies ™, USA

CD OptiCHO medium

CD CHO medium

Geneticin® selective antibiotic (G418 sulfate)

Sigma-Aldrich Company Ltd, UK

L-methionine sulfoximine

Chemicals and solvents

Abnova

mouse anti-MDH II (M01)

BDH Chemical Ltd., UK

Potassium phosphate

Sodium acetate

Sodium carbonate

Sodium fluoride

Sodium phosphate

Bioline, UK

BIOTAQ™ DNA polymerase

cDNA synthesis kit

dNTP set

HyperLadder™ 25 bp

HyperLadder™ 1 kb

SensiMix™ SYBR No-Rox kit

BOC Industrial, UK

Helium (GC grade)

Cell signaling

rabbit anti-MDH II (#8610)

Eurofins MWG operon, Germany

Oligonucleotide primers

siRNA

Jackson ImmunoResearch Laboratories, Inc., USA

Goat Anti-Human IgG Fcγ capture antibody

Licor

Licor IRDye® 800CW goat anti-mouse

Licor IRDye® 800CW goat anti-rabbit

Life technologies™, USA

Lipofectamine™ RNAiMAX Reagent

TRIzol® reagent

National Diagnostics, USA

Protogel solution

New England Biolabs®, UK

2x RNA loading dye

Restriction endonucleases

ColorPlus™ Prestained Protein Ladder, Broad Range (10-230 kDa)

Qiagen Ltd., UK

QIAprep Spin Miniprep kit

Santa Cruz Biotechnology Inc, USA

mouse anti-AR

mouse anti-ERK

rabbit anti-MDH II (A-22)

Sigma-Aldrich Company Ltd, UK

- 3,3',5,5'-Tetramethylbensidine (TMB) tablets
- 4-Amino antipyrene (Fluka)
- Adenosine triphosphate (ATP)
- Agarose
- Ammonium bicarbonate
- Ammonium chloride
- Ammonium persulphate
- L-Asparagine
- L-Aspartate
- b-mercaptoethanol
- Bovine Serum Albumin (BSA)
- Bromophenol blue
- Calcium chloride
- Deoxycholic acid
- Dithiothreitol (DTT)
- Dimethyl sulphoxide (DMSO)
- DNaseI kit
- EBPC (2,5-Dihydro-4-hydroxy-5-oxo-1-(phenylmethyl)-1H-pyrrole-3-carboxylic acid ethyl ester)
- Glucose
- Glucose oxidase
- L-Glutamic acid
- Glycerol-3-phosphate dehydrogenase
- Glycerokinase
- Glycine
- Horse radish peroxidase
- Hydrazine monohydrate
- Hydrogen peroxide
- Imidazole
- Isoleucine
- Lactate dehydrogenase
- Leucine
- Magnesium chloride
- Methoxyamine hydrochloride (MOX)
- Myristic acid-d27
- β-Nicotinamide adenine dinucleotide hydrate (NAD^+)
- PBS (phosphate buffered saline) tablets

Phenol

Phosphoric acid

Polyethlene glycol (PEG)

Potassium dihydrogen phosphate (KH_2PO_4)

Potassium phosphate dibasic trihydrate ($K_2HPO_4.3H_20$)

Propidium iodine

Pyridine

Sodium bicarbonate

Sodium citrate

Sodium chloride

Sodium dithionite (Sodium hydrosulfite)

Sodium 3-hydroxybutyrate

Sodium L-lactate

Sodium nitroprusside

Sodium hypochlorite

Sodium orthovanadate

Sodium pyrophosphate

Sodium pyruvate

TEMED (N,N,N,N',N'-Tetramethyl-Ethylenediamine)

Triton x-100

TrizmaTM

Tween-20

Tyrosine

Valine

Thermo Fisher Scientific Inc, USA

Chloroform

Ethanol

EDTA (Ethylenediaminetetra-acetic acid [di-sodium salt]) Glycerol

Glycine

Isopropanol

Methanol (HPLC grade)

MSTFA + 1 % TCMS (1 mL ampoules)

Orthoboric acid

Sodium chloride

SDS (Sodium dodecyl sulphate)

di-Sodium hydrogen orthophosphate

Sodium hydroxide pellets

SYBR® Safe DNA Gel Stain

Milk powder (Marvel™) can be bought from most supermarkets

Apparatus

All general and disposable glassware and plasticware were obtained from standard suppliers, specialised equipment was purchased from the following companies:

Agilent Technologies, UK

7890A gas chromatograph

5975C Inert XL MSD mass spectrometer with triple-axis detector

7683B series autosampler

7683B series sample injector

BD Biosciences, UK

BD Accuri™

BDH Chemicals Ltd., UK

Haemocytometer (Improved Neubauer)

Beckman Coulter Inc., USA

J2-21 centrifuge with JA-20 rotor

L8-70 centrifuge with SW41 rotor

Bio-Rad Laboratories Ltd, UK

Chromo4 thermal cycler

Clear plastic caps for MJ white plates

Gene Pulser XcellTM Electroporation system

Mini-PROTEAN Tetra system

MJ white 96 well plate for q-RT-PCR

Thick filter paper

Trans-blot Semi-dry Transfer Cell

Boeco, Germany

U-32 centrifuge

S-22 UV/Vis spectrophotometer

Corning Inc. Life Sciences, USA

120 Digital pH meter

125 mL Erlenmeyer flask, vented cap

250 mL Erlenmeyer flask, vented cap

50 mL Mini Bioreactors, centrifuge tube with vent cap

Dynex Technologies Inc., UK

Dias System Plate Reader

Eppendorf, UK

Concentrator-Plus vacuum centrifuge

Wolf Laboratories, UK

Galaxy R CO_2 incubator

Grant Instruments Ltd, UK

Water bath

Kuhner Shaker Inc., Switzerland

Lab-Therm LT-X incubator shaker

Labcaire systems Ltd., UK

Re-circulating class II microbiological safety cabinet

Life TechnologiesTM, USA

Horizontal electrophoresis gel tank

iBlot® Western Blotting System

Mini iBlot® Transfer Stack

Millipore, USA

Milli-Q Synthesis A10 Water Purification System

MJ Research, UK

Opticon Monitor real-time PCR software version 3

Tetrad PTC-225 Thermo Cycler

New Brunswick Scientific Ltd., UK

- Innova 2100 platform shaker
- Innova 4000 shaking incubator

Olympus Ltd. UK

- Olympus BX51 upright microscope

Prestige Medical, UK

- Classic portable autoclave

Rank Brothers, UK

- Clark-type oxygen cell

Schleicher and Schuell, Germany

- Nitrocellulose membrane

Sigma-Aldrich Company Ltd, UK

- Nalgene® Mr Frosty freezing container
- Benchtop microcentrifuge

Thermo Fisher Scientific Inc, USA

- Countess Automated Cell Counter
- Cryovials
- NanoDrop® 1000 UV-Vis Spectrophotometer
- Nunc-immuno plates (MaxiSorp® F96)
- Reach-In CO_2 Incubator
- Techne TC-3000X PCR Thermal Cycler

Appendix 2 Cell growth of CHO-S cells in response to nutrient feeding

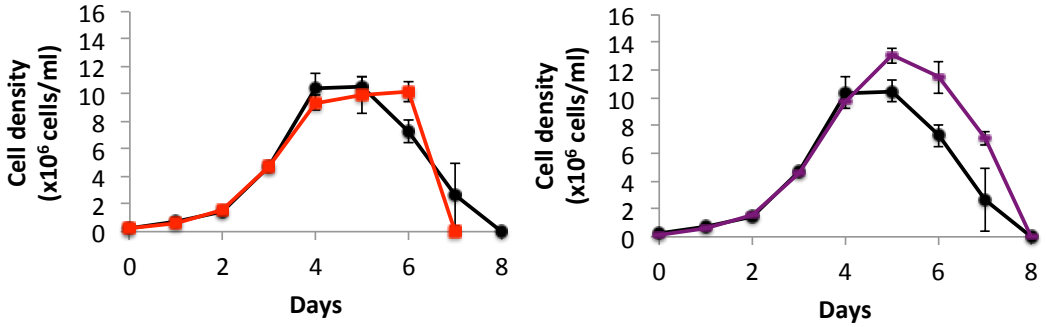

Figure A2.1 Cell growth of CHO-S cells in response to Asn and HB.

Viable cell density were measured for CHO-S cells throughout batch culture in CD OptiCHO™ (control, black symbols) or with supplemention at day 4 of culture with Asn (1.5 mM, red) or HB (10 mM, purple) (Section 2.2.1 and 2.2.4). Medium samples were collected for cell counts (Section 2.2.2). Values presented are mean ± SEM for three replicates for Asn and HB.

Appendix 3 Cell growth and antibody production of CHO-TRex cells in response to nutrient feeding

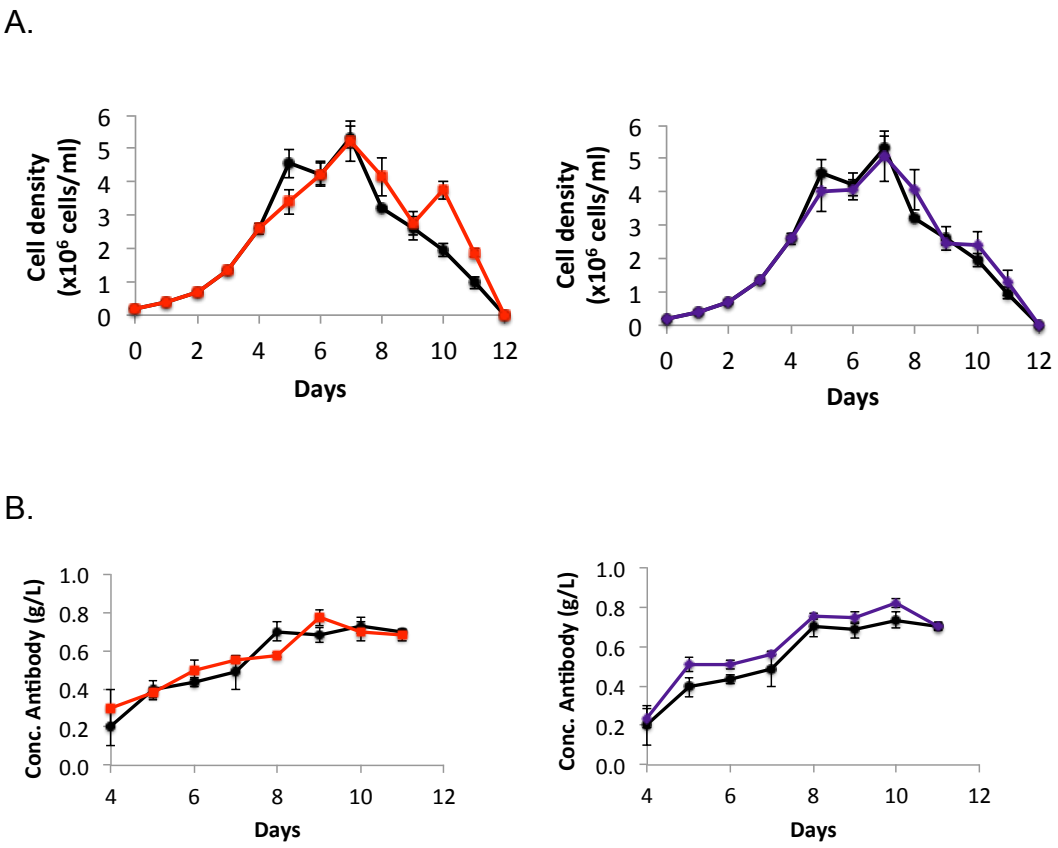

Figure A3.1 Cell growth of CHO-TRex cells in response to Asn and HB.
Viable cell density (A) and antibody production (B) were measured for CHO-TRex cells throughout batch culture in CD CHO (control, black symbols) or with supplemention at day 4 of culture with Asn (1.5 mM, red) or HB (10 mM, purple) (Section 2.2.1 and 2.2.4). Medium samples were collected for cell counts (Section 2.2.2) and ELISA (Section 2.4.1). Values presented are mean ± SEM for three replicates for Asn and HB.

Appendix 4 Verification of nucleotide sequence of MDH II + pcDNA3.1 construct by double digestion

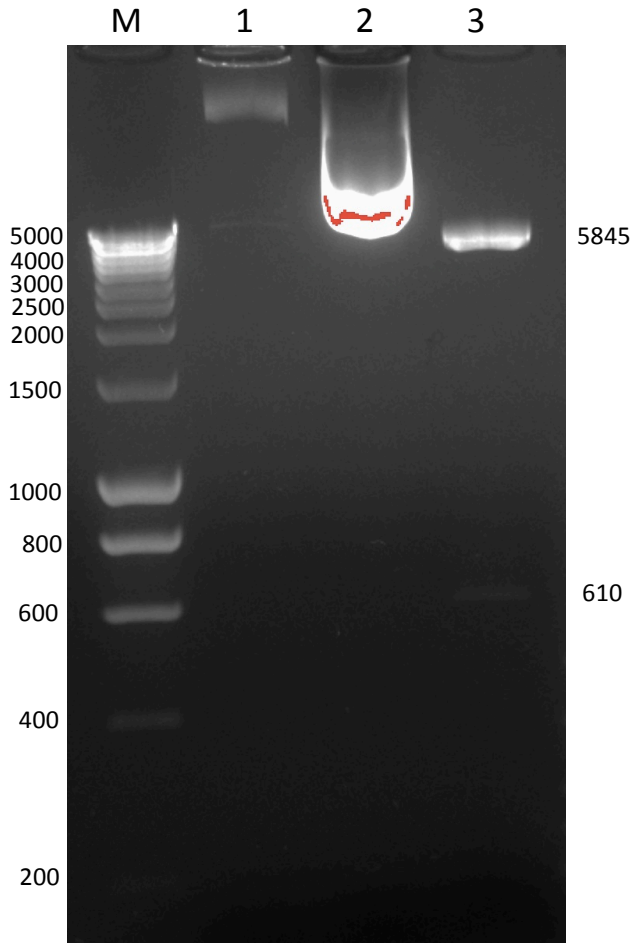

Figure A4.1 Double digestion of MDH II + pcDNA3.1 construct.

MDH II + pcDNA3.1 construct from GeneArt® Gene Synthesis (1), purified MDH II + pcDNA3.1 plasmid that was transformed into *E. coli* (2) and double digestion of MDH II + pcDNA3.1 plasmid with *Hin*dIII and *Bam*HI were separated by 1% (w/v) gel electrophoresis with HyperLadder™ 1kb (M). The image was taken by UV transillumination. The digestion product size was around 610 and 5845 bp.

Appendix 5 Sequencing result of MDH II + pcDNA3.1 construct

Figure A5.1 Sequence alignment of MDH II + pcDNA3.1 construct and *Mdh2* nucleotide sequence.

MDH II + pcDNA3.1 construct in forward (T7) and reverse (BGH) direction and *Mdh2* nucleotide sequence (*Cricetulus griseus Mdh2*, accession XM_007641683.1) (MDH) were aligned using ClustalW2 software. * indicates a single fully conserved residue.

```
BGH       ------------------------------------------------------------    0
MDH       ------------------------------ATGTTGTCCGCCCTCGCCCGACCGGCCGGC    30
T7        NNNNNNNNNNNNNNNNNNTTAACTTAAGCTTATGTTGTCCGCCCTCGCCCGACCGGCCGGC    60


BGH       ---------------------------------------CANNNATGCTAAGTANCGTGCT    22
MDH       GCCGCTCTCCGCCGCAGCTTCAGCACTTCGGCCCAGAACAATGCTAAAGTAGCCGTGCTC    90
T7        GCCGCTCTCCGCCGCAGCTTCAGCACTTCGGCCCAGAACAATGCTAAAGTAGCCGTGCTC    120
                                              **    *

BGH       CGAGCATCTGGGGGCATTGGGCAGC-CCTTTCCCTCCTCTTGAAGAACA--GCCCNNAGT    79
MDH       GGAGCATCTGGGGGCATTGGGCAGCCCCTTTCCCTCCTCCTGAAGAACAGCCCCCTAGTG    150
T7        GGAGCATCTGGGGGCATTGGGCAGCCCCTTTCCCTCCTCCTGAAGAACAGCCCCCTAGTG    180
           ************************ ************* *********   ***

BGH       GAGCGCCTGACCCTCTACGATATTGCTCATACACCTGGTGTGGCGGCGGATCTGAGTCAC    139
MDH       AGCCGCCTGACCCTCTACGATATTGCTCATACACCTGGTGTGGCGGCGGATCTGAGTCAC    210
T7        AGCCGCCTGACCCTCTACGATATTGCTCATACACCTGGTGTGGCGGCGGATCTGAGTCAC    240
             ************************************************************

BGH       ATCGAGACCAGAGCAAATGTGAAAGGCTACCTCGGACTGAGCA-GCTGCC-AGACTGCTG    197
MDH       ATCGAGACCAGAGCAAATGTGAAAGGCTACCTCGGACCTGAGCAGCTGCCAGACTGCCTG    270
T7        ATCGAGACCAGAGCAAATGTGAAAGGCTACCTCGGACCTGAGCAGCTGCCAGACTGCCTG    300
          ************************************       ******       ***

BGH       AAAGGTTGTGATGTGGTGGTGATCCCAGCTGGAGTGCCCAGGAAGCCAGGAATGACACGA    257
MDH       AAAGGTTGTGATGTGGTGGTGATCCCAGCTGGAGTGCCCAGGAAGCCAGGAATGACACGA    330
T7        AAAGGTTGTGATGTGGTGGTGATCCCAGCTGGAGTGCCCAGGAAGCCAGGAATGACACGA    360
          ************************************************************

BGH       GATAGAAACATAGAAACAGGCTCTTTTACAAAGTACAGATCACATGGCATGGCCATCTTG    317
MDH       GATAGAAACATAGAAACAGGCTCTTTTACAAAGTACAGATCACATGGCATGGCCATCTTG    390
T7        GATAGAAACATAGAAACAGGCTCTTTTACAAAGTACAGATCACATGGCATGGCCATCTTG    420
          ************************************************************

BGH       CCTTGCAGATGGCTCACAGTTATTGACAGGGCCTGTTGCTGGTCTCCACCCTCAGCTGAC    377
MDH       CCTTGCAGATGGCTCACAGTTATTGACAGGGCCTGTTGCTGGTCTCCACCCTCAGCTGAC    450
T7        CCTTGCAGATGGCTCACAGTTATTGACAGGGCCTGTTGCTGGTCTCCACCCTCAGCTGAC    480
          ************************************************************

BGH       ATCTGTCTCATGGTTTTCCCAGTTAACTCCACCATCCCCATCACAGCTGAAGTTTTTAAG    437
MDH       ATCTGTCTCATGGTTTTCCCAGTTAACTCCACCATCCCCATCACAGCTGAAGTTTTTAAG    510
T7        ATCTGTCTCATGGTTTTCCCAGTTAACTCCACCATCCCCATCACAGCTGAAGTTTTTAAG    540
          ************************************************************

BGH       AAGCATGGAGTGTACAACCCCAACAAGATCTTCGGTGTGACAACCCTTGACATCGTCAGA    497
MDH       AAGCATGGAGTGTACAACCCCAACAAGATCTTCGGTGTGACAACCCTTGACATCGTCAGA    570
T7        AAGCATGGAGTGTACAACCCCAACAAGATCTTCGGTGTGACAACCCTTGACATCGTCAGA    600
          ************************************************************

BGH       GCGAACACATTCGTGGCAGAGCTGAAGGGTTTGGATCCCTCTCGAGTCAATGTGCCTGTC    557
MDH       GCGAACACATTCGTGGCAGAGCTGAAGGGTTTGGATCCCTCTCGAGTCAATGTGCCTGTC    630
T7        GCGAACACATTCGTGGCAGAGCTGAAGGGTTTGGATCCCTCTCGAGTCAATGTGCCTGTC    660
          ************************************************************
```

```
BGH       ATTGGTGGCCACGCTGGGAAGACCATCATCCCATTGATCTCTCAGTGTACCCCCAAGGTT    617
MDH       ATTGGTGGCCACGCTGGGAAGACCATCATCCCATTGATCTCTCAGTGTACCCCCAAGGTT    690
T7        ATTGGTGGCCACGCTGGGAAGACCATCATCCCATTGATCTCTCAGTGTACCCCCAAGGTT    720
          ************************************************************

BGH       GACTTTCCCCAAGACCAGCTGACCGCACTCACCGGGAGAATCCAGGAGGCTGGCACGGAA    677
MDH       GACTTTCCCCAAGACCAGCTGACCGCACTCACCGGGAGAATCCAGGAGGCTGGCACGGAA    750
T7        GACTTTCCCCAAGACCAGCTGACCGCACTCACCGGGAGAATCCAGGAGGCTGGCACGGAA    780
          ************************************************************

BGH       GTCGTGAAGGCCAAGGCTGGAGCAGGTTCTGCCACTCTGTCCATGGCTTACGCTGGAGCC    737
MDH       GTCGTGAAGGCCAAGGCTGGAGCAGGTTCTGCCACTCTGTCCATGGCTTACGCTGGAGCC    810
T7        GTCGTGAAGGCCAAAGCTGGAGCA-GTTCTGCCACTCTGTCCATGGCTTACGCTGGAGCC    839
          ************** ******** **********************************

BGH       CGTTTTGTCTTCTCCCTTGTGGACGCCATGAATGGGAAGGAAGGTGTCGTTGAGTGTTCT    797
MDH       CGTTTTGTCTTCTCCCTTGTGGACGCCATGAATGGGAAGGAAGGTGTCGTTGAGTGTTCT    870
T7        CGTTTTGTCTTCTCCCTTGTGGACGCCATGAATGGGAAGGAAGGTGTCGTTGAGTGTTCT    899
          ************************************************************

BGH       TTTGTTCAGTCCAAAGAGACAGAGTGCACTTACTTCTCCACACCCTTGCTGTTGGGGAAA    857
MDH       TTTGTTCAGTCCAAAGAGACAGAGTGCACTTACTTCTCCACACCCTTGCTGTTGGGGAAA    930
T7        TTTGTTCAGTCCAAAGAGACAGAGTGCACTTACTTCTCCACACCCTTGCTGTTGGGGAAA    959
          ************************************************************

BGH       AAAGGCCTGGAGAAGAACCTGGGCATTGGCAAAATCACTCCTTTTGAGGAGAAGATGATT    917
MDH       AAAGGCCTGGAGAAGAACCTGGGCATTGGCAAAATCACTCCTTTTGAGGAGAAGATGATT    990
T7        AAANNCTGNNAAGAA----CCTGGCATTGGCAAATCACTCCTTTTGAGGAGAAGATGATT    1015
          ***  *    *  *        *   * *  ****************************

BGH       GCCGAGGCCATCCCTGAGCTAAAAGCCTCCATCAAGAAAGGCGAGGACTTTGTCAAGAAC    977
MDH       GCCGAGGCCATCCCTGAGCTAAAAGCCTCCATCAAGAAAGGCGAGGACTTTGTCAAGAAC    1050
T7        GCCGAGGCCATCCCTGAGCTAAAAGCTCNTCAAGA-------------------------    1050
          **************************       *

BGH       ATGAAGTGAGAATTCTGCAGATATCCAGCACAGTGGCGGCCGCTCGAGTCTAGAGNCCCC    1037
MDH       ATGAAGTGA---------------------------------------------------    1059
T7        ------------------------------------------------------------    1050


BGH       GTNNNNNNNNNNC     1050
MDH       -------------     1059
T7        -------------     1050
```